



Characteristics and mechanisms of phosphorus removal by dewatered water treatment sludges and the recovery

THIS THESIS IS SUBMITTED IN PARTIAL FULFILMENT OF THE
REQUIREMENTS FOR THE DEGREE OF
DOCTOR OF PHILOSOPHY (PhD)

By

Talib Al Tahmazi

B.Sc., M.Sc.

Cardiff School of Engineering

Cardiff, Wales, UK

2017

DECLARATION

This work has not been submitted in substance for any other degree or award at this or any other university or place of learning, nor is being submitted concurrently in candidature for any degree or other award.

Signed:..... (candidate): **Talib Al Tahmazi** Date:

STATEMENT 1

This thesis is being submitted in partial fulfillment of the requirements for the degree of PhD (insert MCh, MD, MPhil, PhD etc, as appropriate)

Signed:..... (candidate): **Talib Al Tahmazi** Date:

STATEMENT 2

This thesis is the result of my own independent work/investigation, except where otherwise stated, and the thesis has not been edited by a third party beyond what is permitted by Cardiff University's Policy on the Use of Third Party Editors by Research Degree Students. Other sources are acknowledged by explicit references. The views expressed are my own.

Signed:..... (candidate): **Talib Al Tahmazi** Date:

STATEMENT 3

I hereby give consent for my thesis, if accepted, to be available online in the University's Open Access repository and for inter-library loan, and for the title and summary to be made available to outside organisations.

Signed:..... (candidate): **Talib Al Tahmazi** Date:

Characteristics and mechanisms of phosphorus removal by dewatered water treatment sludges and the recovery

Abstract

The use of novel industrial by-products (IBPs) to remove phosphorus (P), instead of high-cost P removal techniques, is one of the sustainable solutions to protect aquatic life from excessive P discharges. One of such IBPs is dewatered drinking water treatment works sludges generating from using aluminium or iron salts as coagulant during the drinking water treatment process. Previous studies have shown that the sludges hold promise as a novel adsorbent for the removal of P from wastewaters; however, comprehensive investigation into factors affecting the P removal and the recovery is lacking. Therefore, the main aim of this study is to contribute to a mechanistic understanding of P removal and retention by dewatered water treatment sludge (DWTS), and the associated coagulant recycling and P recovery from the P-saturated sludge used as substrate in a constructed wetland system. Seventeen DWTSs were collected from different areas in the UK to study the combined effect of sludge inherent properties and solution chemistry; and the P equilibrium and kinetic adsorption behaviour using batch experiments. Results revealed that the metal content (Al, Fe, Al_{oxalate} and Fe_{oxalate}) and specific surface area components had the most significant explanation for the variance of: (i) P-uptake at different initial P concentrations; (ii) the adsorption maxima; and (iii) the Freundlich constant. Overall, giving the combined effect of intrinsic sludge properties and solution chemistry, dewatered waterworks sludges with high reactive metal content (Al and Fe), Ca and SO₄²⁻ ions, and total specific surface area, would be the best choice for P retention in practical applications.

Phosphorus retention by two Al- and two Fe-DWTS were modelled under various operation conditions of hydraulic retention time and influent P concentration, using a continuous feeding system. Four design equations for P retention were developed and these successfully predicted discrete P retention, maximum P loaded to the sludge, accumulative amount of P retention, and lifespan at the required P saturation degree. The model results revealed that the lifespan of ferric sludge is about four years to reach its saturation point, if the flow rate of 190 (l/capita.d) and inflow P concentration of 5 mg/l are used.

With regards to coagulant recycling and P recovery using electro dialysis (ED) technology, P saturation degree influenced negatively on Fe and P recovery where their percentages dropped from $70 \pm 8\%$, $49 \pm 3\%$ to 17 ± 2 , $6 \pm 1\%$ when P saturated sludge increase from 0% to 100% respectively. The normalised values of recovered Fe to permeated dissolved organic carbon (DOC) were between 29 and 290. Most of the recovered coagulants were comparable in performance with commercial coagulant in term of DOC removal (42 to 59%), Turbidity, and UV254 absorbance.

Overall, the results have shown that DWTS has great potential not only for P removal but also for coagulant and P recovery. However, further research is needed before the developed models can be applied at field scale, and also to enhance the ED recovery for further benefits.

Dedication

This thesis work is dedicated to my family for their unconditional love, continuous support, and encouragement during the preparation of this research.

Acknowledgements

I would like to express my thanks and sincerest gratitude to the Iraqi Ministry of Higher Education and Scientific Research for awarding me a PhD scholarship to continue my postgraduate education and make a difference in my life.

With my deepest gratitude, I would like to thank my main supervisor, Dr Akintunde Babatunde for giving me the opportunity to undertake this research project under his supervision and guidance. I would not be the researcher I am today without his support, suggestions, valuable discussions and continuous provisions that benefited me much in completion and success of this study.

I would like to thank Cardiff University technical staff, who helped me during my PhD journey. In particular, I would like to thank Jeffrey Rowlands and Marco Santonastaso for their efforts with me in laboratory work, and also providing the required apparatus and advises for experimental setup. I would like to thank Harry, Gary, Pual and Steffan from the soil laboratory for their help and contribution towards completing my experimental setup.

I am particularly thankful to Benjamin for helping in many aspects of my research. I am also thankful to those special people who we worked together in the same laboratory for the past three years of my life at Cardiff University, for their support and all those nice moments we have spent together: Abdulla, Mishari, Alya, Yi, Kris, Mohammed, Khabeer, Safaa and Ban. I apologise to those whose names I did not mention, but who should also be here.

Finally, special thanks to my dearest and most precious father, mother, brothers and sisters for their support, encouragement and love. My greatest thanks go to my wife (Zainab) and my kids (Mohammed, Afnan, and Ali) who make everything and every moment in my life shine brighter, and for their continuous support and prayers and love; my life has no meaning without you since you are the largest part of it. Thank you and I love you all very much

Talib Al-Tahmazi

June 2017

List of Publications

Publication and conference presentation:

1. Al-Tahmazi, T. and Babatunde, A.O. 2016. Mechanistic study of P retention by dewatered waterworks sludges. *Environmental Technology & Innovation* 6, pp. 38–48.
2. Mohammed, A., Al-Tahmazi, T. and Babatunde, A.O. 2016. Attenuation of metal contamination in landfill leachate by dewatered waterworks sludges. *Ecological Engineering* 94, pp. 656–667.
3. Al-Tahmazi, T. and Babatunde, A.O. 2016. Modelling phosphorus uptake by dewatered water treatment sludges under continuous feeding conditions. Submitted to *J. Environmental modelling & Software*.
4. Al-Tahmazi, T. and Babatunde, A.O. 2016. Coagulant and phosphorus recovery from three levels of P saturated sludge using electro dialysis process. Submitted to *J. Environmental Science & technology journal*.
5. Al-Tahmazi, T. and Babatunde, A.O. 2016. Characteristics and mechanisms of phosphorus retention by 17 dewatered waterworks sludges and the influence of source. IWA World Water Congress. Accepted for presentation.
6. Al-Tahmazi, T. and Babatunde, A.O. 2016. Key factors for modelling phosphorus retention by dewatered water treatment sludges. International Water Association Conference. Accepted for presentation.
7. Al-Tahmazi, T. and Babatunde, A.O. 2017. Influence of P – saturation residual sludge on the purity and performance of recovered coagulants. International Resource Recovery Conference. Accepted for presentation.

Table of contents

Abstract	III
Acknowledgements	VI
List of Publications	VII
Table of contents	VIII
List of figures	XIII
List of tables	XVIII
1 Chapter 1 Introduction	1
1.1 Background	1
1.2 Aims and objectives	4
1.3 Thesis Structure	6
2 Chapter 2: Literature review	9
2.1 Introduction	9
2.2 Role of Phosphorus in Eutrophication.....	9
2.3 State of the art review for phosphorus removal.....	10
2.3.1 Chemical phosphorus precipitation.....	10
2.3.1.1 Phosphorus precipitation by Al.....	11
2.3.1.2 Phosphorus Precipitation by Fe	11
2.3.1.3 Phosphorus Precipitation by Ca	13
2.3.2 Biological phosphorus removal.....	13
2.3.2.1 Factors Affecting Biological Phosphorus Removal.....	16
2.3.3 Adsorption.....	18
2.3.3.1 Phosphorus Adsorption	18
2.3.3.2 Adsorbents	19
2.3.3.2.1 Natural materials	19
2.3.3.2.2 Industrial by-products.....	20
2.3.3.2.3 Man-Made Products	27

2.4	Dewatered water treatment sludges.....	29
2.4.1	Production, disposal and associated cost	30
2.4.2	Characteristics of water treatment works sludges	32
2.4.3	P adsorption characteristics and influencing factors	34
2.4.4	Equilibrium and kinetics of phosphorus adsorption	36
2.4.5	Phosphorus adsorption of DWTS under long-term experiments	41
2.5	Coagulant and phosphorus recovery	41
2.5.1	Coagulants usage and associated costs	41
2.5.2	Phosphorus importance and future needs.....	42
2.5.3	Chemical separation technologies.....	42
2.5.3.1	Electrodialysis technology.....	43
2.5.4	Coagulant recovery	48
2.5.5	Phosphorus recovery	48
2.6	Summary	49
3	Chapter 3 Mechanistic study of P retention by dewatered waterworks sludges ..	51
3.1	Introduction	51
3.2	Material and Methods.....	52
3.2.1	General Physicochemical characterization	52
3.2.2	Adsorption isotherm study	54
3.2.3	P retention – Mechanism and linkage with inherent properties.....	54
3.2.3.1	Exchangeable ions and Precipitation tests	54
3.2.3.2	Linkage with inherent properties.....	55
3.3	Results and discussion.....	56
3.3.1	General physicochemical characterization.....	56
3.3.2	Adsorption isotherm study	59
3.3.3	P retention – Mechanisms	61
3.3.4	P retention –Linkage with inherent properties	66

3.4	Summary	70
4	Chapter 4 Experimental and theoretical investigation of P adsorption by dewatered waterworks sludges.....	72
4.1	Introduction	72
4.2	Material and Methods.....	72
4.2.1	Physical and chemical characteristics	72
4.2.2	Adsorption isotherm experiments	72
4.2.2.1	Langmuir isotherm	73
4.2.2.2	Freundlich isotherm	74
4.2.2.3	Temkin isotherm	74
4.2.2.4	Harkins–Jura (H-J) isotherm	75
4.2.3	Adsorption kinetics and rate constants.....	75
4.2.4	Competing ions test.....	77
4.3	Results and discussion.....	77
4.3.1	Physical and chemical properties	77
4.3.2	Adsorption characteristics differentiation	78
4.3.2.1	Behaviour of dewatered sludges for P uptake.....	78
4.3.2.2	Adsorption isotherms.....	80
4.3.2.2.1	Langmuir model	80
4.3.2.2.2	Freundlich model	83
4.3.2.2.3	Temkin and H-J model	85
4.3.3	Phosphorus adsorption kinetics differentiation	88
4.3.4	Effect of competing anions on P uptake by Al- and Fe-based sludge ...	93
4.4	Summary	94
5	Chapter 5: Modelling phosphorus uptake by dewatered water treatment sludges under continuous feeding conditions	96
5.1	Introduction	96
5.2	Materials and methods.....	97
5.2.1	Characterisation of dewatered water treatment sludge	97

5.2.2	Continuous feeding system, setup and experiment conditions	97
5.2.3	Phosphorus adsorption – batch experiments	99
5.2.4	Data analysis and P removal modelling	100
5.3	Results and discussion	102
5.3.1	Comparison of P adsorption under continuous feeding and batch experiments	102
5.3.2	Combined effect of hydraulic retention time and inflow P concentration on P uptake	104
5.3.3	P adsorption modelling	107
5.3.4	Predicting life expectancy of dewatered treatment sludge for P uptake	113
5.4	Summary	117
6	Chapter 6: Coagulant and phosphorus recovery from P saturated sludge	119
6.1	Introduction	119
6.2	Materials and method	120
6.2.1	P saturation iron-based sludge and solubilization	120
6.2.2	Electrodialysis cells	121
6.2.2.1	Design and operation	121
6.2.2.2	Chemical analysis	125
6.2.3	Evaluation of recovered coagulants for water treatment	125
6.3	Results and discussion	127
6.3.1	Solubilization of coagulant and P	127
6.3.2	Soluble iron and P in dilution compartment and electrochemistry characteristics	130
6.3.3	Effect of P-saturation degree on:	132
6.3.3.1	P and coagulant recovery	132
6.3.3.2	Recovered coagulant purity	134
6.3.3.3	Recovered coagulant performance with respect water treatment	136

6.4 Summary	140
Chapter 7: Conclusions and recommendations	142
7.1 Conclusions	142
7.2 Recommendations for further work.....	145
References	147
Appendices	167
Appendix A - Supporting Data for Chapter 4	167
Appendix B –Support data for Chapter 5.....	181
Appendix C – Supporting data for Chapter 6	184

List of figures

Figure 1.1 Study concept and structure of PhD.	8
Figure 2.1 Typical mainstream biological phosphorus removal type Phoredox (A/O) (Metcalf and Eddy 2003).	14
Figure 2.2 Typical mainstream biological phosphorus removal type A ² O (Metcalf and Eddy 2003).	14
Figure 2.3 Typical mainstream biological phosphorus removal type UCT (Metcalf and Eddy 2003).	15
Figure 2.4 Typical side-stream biological phosphorus removal type PhoStrip (Metcalf and Eddy 2003).	16
Figure 2.5 Global water treatment sludge production. Data extracted from Babatunde and Zhao (2007); Fujiwara (2011); Goldbold et al. (2003); Prakash and Sengupta (2003); and Pan et al. (2004).	30
Figure 2.6 Final disposal routes for water treatment works sludges. Data extrapolated from Fujiwara (2011)-Japan; McCormick et al. (2009)-US; and Simpson et al. (2002)-UK.	31
Figure 2.7 Schematic diagram of electro dialysis process explaining the theoretical recovery process of cation and anion ions.	44
Figure 3.1 XRD patterns of three Al-based sludges (a-c) and three Fe-based sludges (d-f).	59
Figure 3.2 Isotherms of P uptake by the seventeen dewatered water sludges (at initial pHs of 4, 7 and 9; t=48 hours; plots on the left and right refer to, respectively aluminium- and iron-based sludges). (Y-axes are amended to maximum scale of 35).	60
Figure 3.3 P adsorption capacities of Al- and Fe-based sludges calculated from fitting Langmuir model at three initial pH solution values.	62
Figure 3.4 FTIR spectra of (a) Fe-based sludge and (b) Al-based sludge before and after adsorption test with 10 mg/l initial P concentration at pH 4 and 7.	67
Figure 4.1 P-uptake of Al-based sludges (a-c) and Fe-based sludges (d-f) at three pH values with seven levels of initial P concentration; and their corresponding fitting with the Langmuir isotherm model. (Exp = experimental data; Model = Langmuir model data).	81

Figure 4.2 Maximum P loadings (calculated from Langmuir model) for different Al- and Fe- based sludges. a1, a2, and a3 represent, respectively the mean results obtained in the current study at initial pH solution 4, 7 and 9 for five Al-based and eight Fe-based sludges. Only sludges fitted well with the Langmuir model were used. b represents values of two Al- and one Fe-based sludges at initial pH 6.2 (Gibbons and Gagnon 2011). c represents mean values of 21 Al-based sludge (Dayton et al. 2003). d1, d2 and d3 represent, respectively mean values at three initial pH solution 5, 7 and 9 for three Al-based and two Fe-based sludges (Bai et al. 2014). e represents mean values of thirteen sands with mainly iron content and with initial pH equal to equilibrium pH (Del Bubba et al. 2003)..... 83

Figure 4.3(a-f) P-uptake of three Al-based (a-c) and Fe-based (d-f) dewatered sludges at three pH values with seven initial P concentration; and their corresponding fitting with the Freundlich isotherm model. (Exp = experimental adsorption data; Model = Freundlich model data). 84

Figure 4.4 Kinetics of P adsorption onto dewatered water treatment sludges with initial P concentration = 10 mg/L and initial pH solution of 4, 7 and 9. Lines represent modelled results using pseudo-first-order (model1) and pseudo-second-order (model 2) models. (a = Al-based sludges and b = Fe-based sludges). 88

Figure 4.5 Effect of coexisting anions (Cl^- and SO_4^{2-}) on the phosphorus uptake of Al-based (a) and Fe-based (b) sludges with initial P concentration = 10 mg/L and 1g of sludge. 93

Figure 5.1 Schematic and laboratory setup of the continuous feeding system used to obtain P uptake at various combination of hydraulic retention time and influent concentration. a, b, c, d, e and f refers to the Mariotte bottle, vent tube, supplying tube, column, peristaltic pump and samples collection respectively. 99

Figure 5.2 Elemental dissolution at different initial P concentration in the batch experiments for two iron- and aluminium based sludges with contact time 48h..... 103

Figure 5.3 Leached ions and P uptake of: (a) iron- and (b) aluminium based sludge with retention time of 4 h and inflow P concentration of 5 mg/l under short-term continuous feeding system. 105

Figure 5.4 Accumulative P uptake after 48 h operation time for two iron- (FO and MO) and two aluminium (GU and WD) based sludges at different conditions of five inlet P concentrations and four hydraulic retention times..... 106

Figure 5.5 Effect of HRT on P uptake for (a) Fe- (MO) and (b) Al- (WD) based sludges at influent P concentration of 10 (mg/l).	107
Figure 5.6 Modelling steps of P uptake for iron- (a to c) (MO) and aluminium- (d to f) (WD) based sludges at inflow P concentration of 10 mg/l. a & d represents the exponential correlation between the P uptakes and P loaded to the sludge at inlet P concentration of 10 mg/l and HRT of 0.5, 1,2 and 4 h; b & e represent the experimental P uptake and the modelled P uptake curve at HRT of 2 h and inlet P concentration of 10 mg/l; c & f represent the experimental cumulative and modelled cumulative data of P uptake at HRT of 2 h and inlet P concentration of 10 mg/l.	110
Figure 5.7 Predicted lifespan and the treated wastewater volume at a range of P saturation levels from 0% to 95% for Fe- sludge (FO). a and b refer to flow rates of 190 and 460 (l/c.d), with influent P dry mass weight of 17.3 and 7.2 (g/c.d).....	115
Figure 6.1 Schematic diagram of three compartments (a- mode 1), five compartments electro dialysis (b- mode 2) cells, and their lab setup.	124
Figure 6.2 Schematic diagram of the experimental processes for P loading, extraction, and recovery.	126
Figure 6.3 Mean value of soluble iron and P, and current profile with acidity and electrical conductivity changes in the dilution compartment (DC) in the 3ED and 5ED modes at three levels of P-saturated dewatered water treatment sludge (0%-P, 50%-P, and 100%-P).....	131
Figure 6.4 Mean values of sulphate ion reduction in dilution compartment for both ED mode at two different initial concentrations (n=3).....	132
Figure 6.5 Mean values of the mobilised Fe and P ions between DC and CC\CCC of three levels of solubilized P-saturation sludge, with low concentration (LC) and high concentration (HC) applied in two operation modes of electro dialysis cell.	134
Figure 6.6 Optimisation steps of coagulant dose for commercial coagulant (a) and pH (b) for remaining turbidity, remaining DOC and zeta potential (n=4).....	137
Figure A.1 Fitting P adsorption data of alum-based sludges at three different pH values to the linearized form of Langmuir model.	167
Figure A.2 Fitting P adsorption data of iron-based sludges at three different pH values to the linearized form of Langmuir model.	168
Figure A.3 Fitting P adsorption data of alum-based sludges at three different pH values to the linearized form of Freundlich model.	169

Figure A.4 Fitting P adsorption data of iron-based sludges at three different pH values to the linearized form of Freundlich model.....	170
Figure A.5 Fitting P adsorption data of alum-based sludges at three different pH values to the linearized form of Temkin model.	171
Figure A.6 Fitting P adsorption data of iron-based sludges at three different pH values to the linearized form of Temkin model.	172
Figure A.7 Fitting P adsorption data of alum-based sludges at three different pH values to the linearized form of Harkins–Jura (H-J) model.....	173
Figure A.8 Fitting P adsorption data of iron-based sludges at three different pH values to the linearized form of Harkins–Jura (H-J) model.	174
Figure A.9 Fitting P adsorption kinetic data of alum-based sludges at three different pH values and 10 mg/l initial P concentration to the linearized form of Pseudo-first order kinetic model.	175
Figure A.10 Fitting P adsorption kinetic data of iron-based sludges at three different pH values and 10 mg/l initial P concentration to the linearized form of Pseudo-first order kinetic model.	176
Figure A.11 Fitting P adsorption kinetic data of alum-based sludges at three different pH values and 10 mg/l initial P concentration to the linearized form of Pseudo-second order kinetic model.	177
Figure A.12 Fitting P adsorption kinetic data of iron-based sludges at three different pH values and 10 mg/l initial P concentration to the linearized form of Pseudo-second order kinetic model.	178
Figure A.13 Fitting P adsorption kinetic data of alum-based sludges at three different pH values and 10 mg/l initial P concentration to the intraparticle diffusion model.....	179
Figure A.14 Fitting P adsorption kinetic data of iron-based sludges at three different pH values and 10 mg/l initial P concentration to the intraparticle diffusion model.....	180
Figure B.1 The exponential relationship between P uptake and amount of P loaded to Fe-sludges (FO-DWTS left side figures, MO-DWTS right side figures). Data obtained from continuous feeding system.	181
Figure B.2 The exponential relationship between P uptake and amount of P loaded to Al-sludges (GU-DWTS left side figures, WD-DWTS right side figures). Data obtained from continuous feeding system.	182

Figure C.1 Breakthrough curves showing the P saturation degrees of 50% and 100% of Fe-based sludge.....	184
Figure C.2 The extractability of Fe and P and leachability of DOC from the iron-based sludge of three levels of P saturation (0%, 50%, 100%) at two steps of the extraction process.....	185
Figure C.3 Profile of pH and electrical conductivity in dilution compartment (DC), anodic compartment (AC), and cathodic compartment (CC) using high concentration (HC) of acid-solubilized sludge 0%, 50%, and 100% P-saturation degrees in 3ED. Please note that pH readings in DC in case 0% P-saturation are lost. (n=3)	186
Figure C.4 Profile of pH and electrical conductivity in dilution compartment (DC), anodic concentrated compartment (ACC), and cathodic concentrated compartment (CCC) using high concentration (HC) of acid-solubilized sludge 0%, 50%, and 100% P-saturation degrees in 5ED. (n=3).....	187
Figure C.5 Current profile of 3ED mode 1 (a) and 5ED mode 2 (b) using high concentration of acid-solubilized of 0%, 50%, and 100% P-saturated sludge. (n=3).	188
Figure C.6 Mass balance of the reduction percentages of Fe and P in DC, and the lost and recovered percentages in DC and CC/CCC respectively.	189

List of tables

Table 2.1 Natural materials used for phosphorus removal	21
Table 2.2 Application of industrial by-products for phosphorus removal.....	23
Table 2.3 The applied man-made adsorbents for P removal.....	28
Table 2.4 General properties of aluminium and iron-based water treatment sludge. ...	33
Table 2.5 Rate and adsorption capacity of P for DWTS under different conditions of batch experiments and P adsorption behaviour under continuous feeding systems. ...	38
Table 2.6 Summary of chemical separation technologies (after Keeley et al. 2014a).	45
Table 3.1 Physicochemical properties of the seventeen dewatered waterworks sludges.	58
Table 3.2 Equilibrium pH and the released concentrations of aluminium, iron, calcium, magnesium and phosphorus after agitating 1g of each sludge in 100 ml of deionized water with three initial pH values for 48 h (n=2).	63
Table 3.3 Precipitation test with different initial pH values and Ca and p concentrations.	65
Table 3.4 Principal component analysis of the physicochemical characteristics of the seventeen dewatered waterworks sludges; and linear regression analysis between the three principal components scores and initial pH solution as predictors, and the amount of P-uptake at different initial P concentration, P adsorption capacity maxima and Freundlich P bonding energy-related constant as outcomes variables.....	69
Table 4.1 Mean and standard deviation of chemical and physical characteristics of Al- and Fe-based sludges.....	79
Table 4.2 Adsorption isotherm model equations and their linearized expression.	82
Table 4.3 Constant parameters, adsorption capacity and correlation coefficients calculated for the five-adsorption models at three different pHs.	86
Table 4.4 Adsorption rate constants and correlation coefficients for adsorption of phosphorus on dewatered waterworks sludges at initial P concentrations of 10 mg/L in three levels of initial pH solution.	91
Table 5.1 The intercept (b_0), slope (b_1) and correlation coefficient at different operation conditions of HRT and inlet P concentrations obtained from fitting P uptake with P loading exponentially for two iron-(FO and MO) and two aluminium- (GU and WD) based sludge.	111

Table 5.2 Model coefficients for intercept and slope resulted from multiple linear regressions model, where intercept and slope of exponential correlations as dependent variables and HRTs and inlet P concentrations as independent variables.	112
Table 5.3 Parameters for estimation of life expectancy of DWTSSs at inlet concentrations of 5 and 10 mg/l and hydraulic retention times of 0.5, 1, 2 and 4 h. .	116
Table 6.1 Mass balance of dewatered water treatment sludge constituents before and after P loading, and after acid extraction and the amount of the solubilized elements in the acid solution of three levels of P saturation degree.....	129
Table 6.2 Characterization of recovered coagulant in terms of Fe and DOC concentrations, and Fe/DOC ratios	136
Table 6.3 Purified water quality and percentage removals obtained by commercial and recovered coagulants (n=3).	139
Table B.1 Masses of acid-washed sand and sludge for two iron (FO and MO) - and aluminium (GU and WD) based sludges at different operation conditions of hydraulic retention time and influent P concentration.	183

1 Chapter 1 Introduction

1.1 Background

Wastewater industry discharges are regarded as the primary source of the increasing P concentration in water sources like oceans, rivers, lakes and lagoons (Smith et al. 1999). Phosphorus is a vital element for algae growth, and with increasing P loads discharged into water sources, an extraordinary growth of algae and aquatic plants occur. As the algae and aquatic plants die and decompose, the decomposing organisms deplete the dissolved oxygen. This causes a phenomenon called eutrophication which involves water degradation. To overcome this problem in the UK, £15 million pounds is spent annually by the water industry (Heal et al. 2003).

Eutrophication has now become a global environmental concern, particularly with waters worldwide experiencing major increases in P concentrations leading to additional drinking water treatment, decreased biodiversity and loss of recreational value. For example, P fluxes to oceans have increased approximately 2.8-fold since the industrial revolution, and over 400 coastal dead zones can be found at the mouths of rivers discharging P (Diaz and Rosenberg 2008). Surveys in the United States and the European Union (EU) estimates that 78% and 65% of their coastal areas, respectively, exhibit symptoms of eutrophication (Mayer et al. 2013), whilst inland waters are equally at risk. According to the US Environmental Protection Agency, eutrophication is the biggest overall source of impairment of the nation's rivers and streams, lakes and reservoirs, and estuaries; while in the EU, approximately 50% of all lakes have total P (TP) at levels which pose a risk of eutrophication (Bogestrand 2004). In the UK, the Technical Advisory Group has advised that 65% of England's rivers fail current P limits with lakes being more sensitive to contamination (Wood et al. 2007).

Therefore, the legislation has become stricter on P discharges into the water environment. The European Union Directive on Urban Wastewater Treatment (91/271/EEC) established the limits of phosphorus discharge into water bodies between 1 to 2 mg P/l. On the other hand, the US Environmental Protection Agency (EPA) have noted that total effluent P concentrations between 0.009 to 0.05 mg/L are required to solve water quality problems (Ragsdale 2007).

Conventional and advanced P removal technologies mainly involve biological P uptake, chemical precipitation using either aluminium or iron salts, adsorption, and several innovative engineering solutions such as crystallisation and ion exchange (de-Bashan and Bashan 2004; Mayer et al. 2013; Morse et al. 1998). However, these technologies are either expensive, generate secondary sludge which needs to be disposed of, or they cannot be relied upon in certain cases. Such cases can include when aiming for low P concentration in final effluents, or when dealing with wastewater with highly variable characteristics. Moreover, most of the technologies do not lend themselves to P recovery, and this is becoming a significant issue. Consequently, P removal technologies which also lend themselves to P recovery, are gaining increasing attention. Adsorption is one of such technologies, and a number of materials have been used as an adsorbent for P removal (Johansson Westholm 2006; Mayer et al. 2013).

Dewatered water treatment sludge (DWTS) is another novel material which can be used as an adsorbent for P removal, and which can also enable P recovery. DWTS is a by-product of drinking water purification processes. It is generated when chemical coagulant (alum or iron salt) is added to the raw water during water treatment process (including coagulation, flocculation, clarification and filtration) to remove particle, colour and impurities especially from raw waters with high turbidity. Afterwards, the sidestream effluent from the water treatment processes is dewatered by a process to generate the DWTS.

A vast amount of DWTS sludge is produced every year. In the USA alone, more than 2 million tonnes per year of dewatered aluminium-coagulated treatment residual is produced (Sengupta and Prakash 2004), while in the UK, Simpson et al. (2002) reported that the production of dry solids of waterworks sludge is about 131,000 tonnes. These sludge quantities increase with the global population growth, leading to large quantities of coagulant in water and wastewater treatment plants to meet the demands. In the UK, the annual commercial coagulant used exceeds 330 thousand tonnes (Henderson et al. 2009), costing about £40m (Keeley et al. 2016). The waterworks sludge generated is typically disposal by landfilling or through land application. However, the increasing production of waterworks sludges, together with the increasingly stringent environmental regulations on their disposal, has led to

increased research to find other alternative disposal routes or beneficial reuses. Other ways in which waterworks sludge have been reused include its use in building and construction, coagulant recovery and incorporation into the activated sludge process (Babatunde and Zhao 2007).

The waterworks sludges which are mainly aluminium or iron-based, contain either aluminium or iron hydroxides usually in amorphous forms. These forms generally have larger surface areas available for P binding than the corresponding crystalline forms. In addition to these metal oxides, the DWTS also contains calcium, magnesium, chloride, sulphate ions and organic matter (OM), all of which might play a role in P retention through precipitation and/or ion exchange. The characteristics of DWTS depend on the treated water properties (may be affected by geology, vegetation or microclimate), coagulant type, coagulant dose, and sludge dewatering process (Skerratt and Anderson 2003). This variation in sludge characteristics might induce differences in P adsorption capacities, consequently, it is unclear which inherent sludge characteristics and chemical solution conditions impact on P adsorption mechanisms (Huang and Chiswell 2000; Kim et al. 2003; Yang et al. 2006a; Mortula et al. 2007; Song et al. 2011).

In most cases, short-term evaluation of potential adsorbent for P removal is usually conducted using batch experiments (Yang et al. 2006a; Song et al. 2011). Data extracted from these batch tests are utilised in constructing isotherms and kinetics equations describing the P adsorption behaviour (Cooney 1998). These short-term tests are affected by adsorbent properties and experimental conditions such as adsorbent particle size, surface area, initial pH, P concentration, solid to liquid ratio, agitation time, and temperature (Ippolito et al. 2003; Makris et al. 2004a; Dayton and Basta 2005; Babatunde et al. 2008). In addition, the maximum P adsorption capacities obtained from these isotherm models are either an over or under estimation of the actual values, particularly in a continuous feed system (Stoner et al. 2012), thereby making the prediction of system lifespan to be difficult. Long-term P adsorption column experiments are another useful procedure to estimate the lifespan of a system (Drizo et al. 2002; Drizo et al. 2006; Babatunde and Zhao 2009; Bowden et al. 2009). These studies examined the long-term operation of different mediums in constructed wetland for P adsorption performance. The operating

conditions closely simulate those that are commonly used in real life such as constant inflow P concentration, and hydraulic loading rate (HLR) or hydraulic retention time (HRT). As an example, a continuous flow column study was conducted to evaluate dewatered treatment sludge as wetland substrate for P removal. It was reported that a 92% P removal efficiency was achieved at an HLR of 0.36 m³/m².d (Zhao et al., 2009). Similarly, Babatunde et al. (2009) conducted column experiments with different proportion of Al-based sludge. Results obtained showed that significant P removal was obtained at 3 and 4 hours hydraulic retention time. However, the time required to reach the saturation point; and the associated costs regarding installation, and long-term analysis necessitates the need for rapid small-scale column tests to mitigate the cost and the time constraints.

The feasibility of P and coagulant recovery after adsorption was also investigated in this study. This could be a novel approach for reusing the P saturated sludge (Mejia Likosova et al. 2013; Mejia Likosova et al. 2014). Phosphorus is an important and unique non-renewable natural source; and the sources of inexpensive P in the world are predicted to be diminished in the next 50 – 100 years (Duley 2001; Conley et al. 2009). The demand for P will increase in the future as the global population increases. Therefore, a cyclic use of coagulants and P would offer a cost reduction for coagulant and a new source of a finite element, P. Furthermore, coagulant recovery can potentially promise a reduction in the cost of coagulant usage. About £2.5m would be saved annually with a 10% reduction in coagulant consumption across the UK water industry (Henderson et al. 2009). Therefore, a particular focus of this study will be on investigating the influence of the P saturated degree of DWTS on the recovery of both P and coagulant efficiency, and the purity. The major challenge for reusing the recovered coagulant in water treatment is the dissolved organic carbon (DOC) contamination that might impose disinfection by-products potential formation (DBPs) after final step of disinfection process in water treatment (Sengupta and Prakash 2004; Ulmert and Särner 2005; Keeley et al. 2016). Therefore, this is also investigated in the study.

1.2 Aims and objectives

The overall aim of this thesis is to understand the mechanisms of P removal by DWTS, and the influence of source and other properties; and to investigate the

recovery of P and coagulants from the P-saturated sludge. The following objectives are set to meet these aims.

The first objective is to characterise the physical and chemical properties of seventeen DWTSs, and determine the physical and chemical characteristics, and to investigate the mechanism of their P adsorption. The hypothesis is that water treatment processes purify different raw water sources using various types of coagulants, softeners, chemicals for pH regulation, and polymers. Therefore, this would generate DWTS with varying characteristics and also this would impact on the adsorption mechanisms.

The second objective is to investigate P uptake and adsorption capacities of the DWTSs relative to their specific physical and chemical properties; and to determine the capacity and dynamics of P adsorption. The hypothesis is that the P kinetics and adsorption would be affected by the local characteristics of DWTS, which involves raw water characteristics, type of flocculants, and sludge dewatering processes.

The third objective is to find out the key factors for modelling P retention of DWTS using a short-term continuous flow system. Together with the applied conditions of initial P concentrations and retention times, design P retention curves and a model for predicting the P removal performance of the DWTS are generated. The hypothesis is that P retention of DWTS varies under different continuous flow conditions; and that the generalised model of various inflow characteristics can predict the lifespan of DWTS.

The fourth objective is to quantify the level of P and coagulant recovery from the DWTS at different degrees of P-saturation, using ion exchange membrane process (electrodialysis technology). The hypothesis is that P and coagulant recovery from P-saturated DWTS are P- saturation degree dependent, feasible with low DOC contamination achievable, and be reused in the water purification process.

1.3 Thesis Structure

After the background introduction to the research in Chapter 1, Chapter 2 gives an extensive literature review that includes three main parts. The first part focuses on the fundamental understanding of the current P removal processes and influencing factors; the second part is about DWTS production, associated cost, characterization, short- and long-term experiment of P adsorption; and the third part is about P and coagulant separation technology.

Chapter 3 describes in details the material and experimental methods used to characterise DWTS and understand the mechanism of P adsorption. After physiochemical and P adsorption characterization of 17 DWTSs, the variation of these characteristics and its relationship to the line of water treatment, and the linking of the effect of these characteristics to the P retention behaviour are discussed. Leachability and precipitation test, Fourier transform infrared (FTIR) spectroscopy before and after adsorption test, and P selectivity were used to study P retention mechanisms. The combined effect of solution chemistry and the sludge's inherent properties on P retention was statistically investigated to improve understanding of the properties that regulate P retention by the DWTSs using principal component analysis and a multiple linear regression model.

Chapter 4 describes the material and methods used to characterise and examine the equilibrium and kinetic P adsorption behaviour of the DWTSs; and it explores the theoretical adsorption isotherm models of Langmuir, Freundlich and Temkin; and the kinetic models of pseudo- first and second order and intraparticle diffusion models. Error functions and correlation coefficients were used to find the best fitting model for P adsorption equilibrium and P kinetics in the fast and slow stages.

Chapter 5 includes experimental setup details of the continuous feeding system (CFS), P adsorption differences under CFS and batch experiments, and statistical-mathematical construction steps for P removal modelling. Phosphorus adsorption comparison between CFS and batch experiments, combined effect of hydraulic retention time and inlet P concentration, P removal modelling, and life expectancy were discussed.

Chapter 6 describes in details preparation of different degree of P saturated DWTS and their acid solubilization, design and setup of electrodialysis cells, sampling and chemical analysis procedure, and evaluation the recovered coagulant for water treatment performance. The results were presented to investigate the interaction and solubilization degree of P and coagulant with continuous and recirculation acid feeding in a fixed bed column, P and coagulant permeation and the electrochemistry characteristics in ED cell, and influence of P saturation degree on the recovery efficiency and the purity. The performance of the recovered coagulant for water treatment in comparison with commercial coagulant is also discussed.

Chapter 7 presents a summary of the key conclusions of the thesis and gives recommendations for future work. The overall structure of the thesis is provided in Figure 1.1.

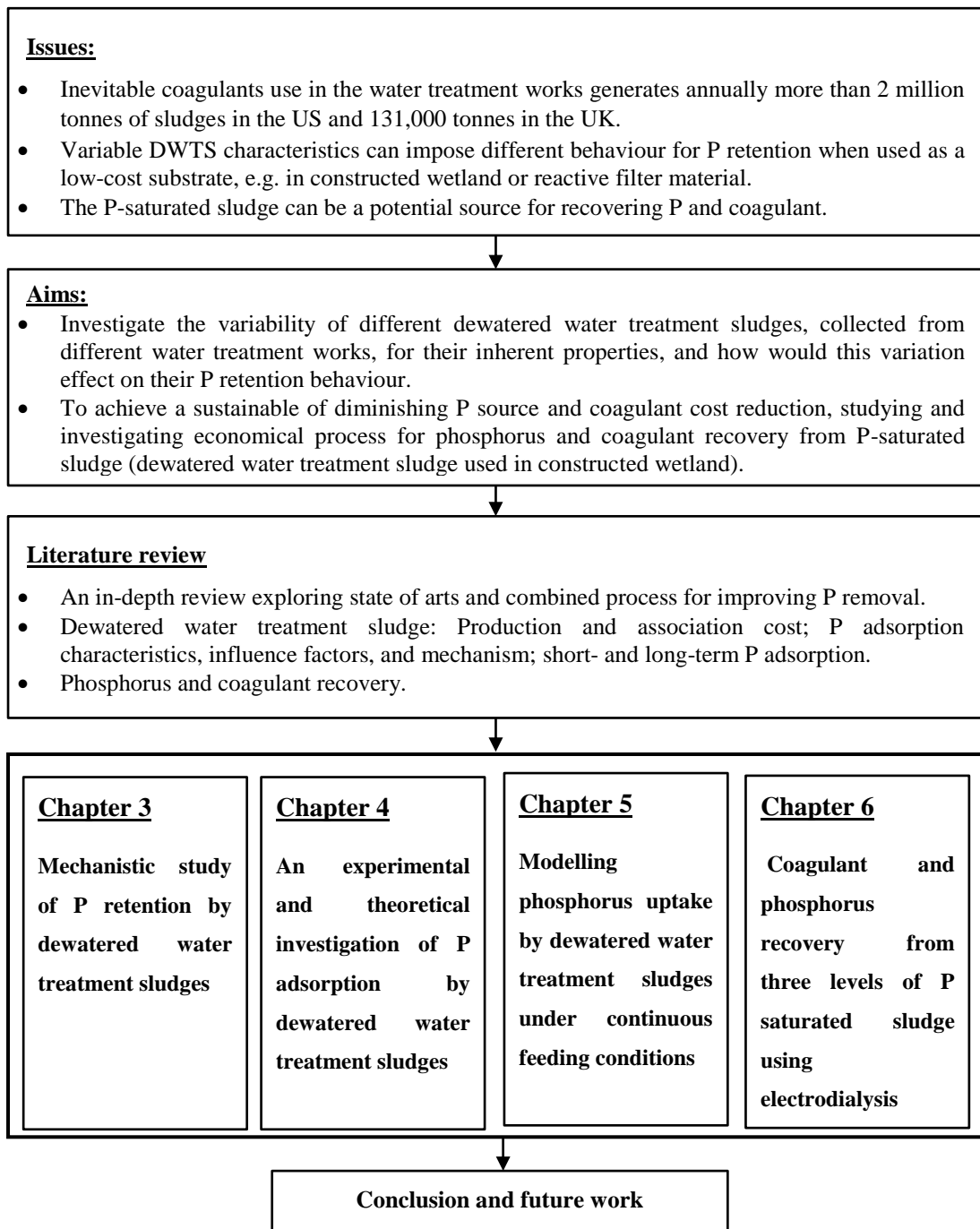


Figure 1.1 Study concept and structure of PhD.

2 Chapter 2: Literature review

2.1 Introduction

This chapter reviews previous undertaken research to verify the background issues for the work presented in this thesis. These issues derive from the pressure faced by the water industry in terms of P removal and the disposal of DWTS. The purposes of this review are:

- To explore and discuss in-depth, the state of art for P removal;
- To review the process of DWTS production, disposal and possible reuse options;
- To identify the gap in knowledge regarding DWTS characteristics, and factors affecting its use as a reactive material for P adsorption;
- To explore coagulant and P separation technologies, and their constraints and shortcomings to meet the purification requirements for use in recovery application;

2.2 Role of Phosphorus in Eutrophication

Eutrophication as defined by the European legislation concerning wastewater treatment (Council of the European Union 1991), is the enrichment of water by nutrients (mainly nitrogen (N) and P), resulting in an excessive growth of algae or floating plant mats and higher forms of plant life, thereby generating an undesirable disturbance to the balance of organisms present in the water and to the quality of the water concerned.

During the algal bloom, floating thick mat of algae prevents light from reaching plants under the surface. When algal organisms die, they settle to the bottom, where they are digested by bacteria which live in the sediments. This mechanism leads to bacteria blooms in conjunction with an algal bloom, and thus oxygen consumption is increased leading to anoxia in poorly mixed bottom water. Over time, sediments release P that reinforces the eutrophication (Kagalou et al. 2008).

Phosphorus is regarded as the important and limiting nutrient for aquatic plant populations, and the primary sources of P loads into water resources are municipal and industrial drainages (point sources), and agricultural runoff (non-point or diffuse sources, Smith et al. 1999). Mainston and Parr (2002) and Jarvie et al. (2006) found that the most significant risk for river eutrophication, even in rural areas, is the release of P from point sources. Therefore, legislation on the effluent from WWTPs has been created to restrict P discharges into the surrounding environment. For instance, the European Union Directive on Urban Wastewater Treatment (91/271/EEC) has consented the following discharge limits: for medium WWTPs (10000-100000 population equivalent (PE)), the annual average effluent of TP concentration is 2 mg/L and reduction of 80% of the TP influent is required; for large WWTPs (>100000 PE), the annual average effluent of TP concentration is 1 mg/L and reduction of 80% of the TP influent is required.

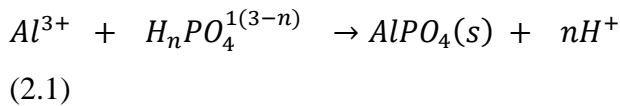
2.3 State of the art review for phosphorus removal

2.3.1 Chemical phosphorus precipitation

Phosphorus removal by chemical precipitation is achieved by the addition of multivalent metal salts that form precipitates of sparingly soluble phosphates. The mechanisms of converting the dissolved P species into particulate form include chemical precipitation of metal-hydroxo-complexes of low solubility, selective adsorption of dissolved P species onto freshly precipitated metal-hydroxo-complex surface, and flocculation and co-precipitation of the finely dispersed colloidal matter. The latter mechanism depends on the size and surface chemical properties of the P-containing colloids. These mechanisms occur simultaneously when precipitants are added (Maurer and Boller 1999). The main multivalent metal salts commonly used are aluminium (Al), iron (Fe) and calcium (Ca) (Metcalf and Eddy 2003). Chemical P removal has many advantages over biological P removal: it is less sensitive to variation in influent characteristic, loading rate, and temperature changes. In addition, less time is required to achieve the chemical treatment, unlike the biological P removal in which the performance slowly improves with time as the microbial community matures.

2.3.1.1 Phosphorus precipitation by Al

Aluminium is used to precipitate a wide range of phosphate species in wastewater. These species include orthophosphate, polyphosphates, pyrophosphate, metaphosphate and tripolyphosphate. The stoichiometric of the Al and P reaction is presented in Equation 2.1. Thus, 1 mole of Al is essential to precipitate 1 mole of phosphorus. This reaction cannot be used to calculate the necessary chemical dosages because it is affected by alkalinity, pH, trace elements and ligands found in wastewater (McGhee and Steel 1991; Metcalf and Eddy 2003). Therefore, bench-scale tests and sometimes full-scale tests, particularly if polymers are used, are used to determine the dosages.

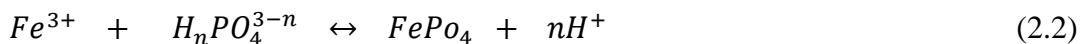


When Al concentration is less than the stoichiometric value, $AlPO_4$ forms colloids that are not ready to settle, while precipitation occurs when the Al concentration is equal to the stoichiometric amount (Hendricks 2010).

Aluminium hydroxide has a significant adsorptive capacity for orthophosphate, condensed phosphate and organic phosphate; this was found through batch adsorption tests under pH values between 5 and 6 (Hendricks 2010). However, organic phosphate precipitates as aluminium-organic phosphate form at pH 3.6 (Galarneau and Gehr 1997). Orthophosphate removal occurs via co-precipitation of a mixed aluminium hydroxide phosphate. This was demonstrated by a theoretical analysis of $Al(OH)_3$ and $Al(PO_4)$. Aluminium oxide can act as an adsorbent with high adsorption capacity for a long period.

2.3.1.2 Phosphorus Precipitation by Fe

Equation 2.2 represents the basic reaction of P precipitation with iron. As mentioned previously, this equation cannot be used to estimate chemical dosages for phosphorus removal, laboratory scale and occasionally full scale experiments are used (Metcalf and Eddy 2003).



When iron is added to wastewater in concentrated or acidic form, neutralisation of the alkalinity of wastewater to the acidic ferric solution occurs. This leads to rapid precipitation of hydrous ferric oxides. Soluble phosphate is removed continuously with hydrous ferric oxides by co-precipitation and by adsorption of phosphate onto hydrous ferric oxides particles. Sorbent to sorbate (Fe/P) ratio, mean velocity gradient (G-value) and reaction time are factors necessary for the design of chemical P removal systems. Here, reaction time is essential for improving P removal via slower diffusion reactions, and it reduces active surface sites of the adsorbent for P removal through ageing of metal flocs (Smith et al. 2007).

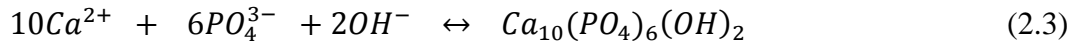
Initial pH, Fe-dose and initial P concentration have a significant effect on P removal. Fytianos et al. (1998) investigated three factors affecting ferric chloride - P removal from aqueous and wastewater using batch experiments. They found that 63% optimum P removal is achievable at a 1:1 molar ratio of iron (III) and pH of 4.5, with slightly higher removal observed when using real wastewater than that obtained using aqueous solution; and with 155% excess Fe dose required to complete P removal.

Iron (II) and Iron (III) are mostly used as precipitants for P removal. Iron (III) readily forms settleable flocs within a short time, while this settling ability is dependent on conversion of iron (II) to iron (III) when the former is used as a coagulant (Maurer and Boller 1999). In a detailed study investigating the effect of pH, redox potential and dissolved oxygen concentration on the conversion rate of ferrous (Fe^{2+}) to ferric (Fe^{3+}), Thistleton et al. (2001) observed that the average conversion rate of 68.7% was achieved at optimum conditions of high DO (1.0–5.7 mg/l), mid-range redox potential (57–91 mV), and high pH (7.5–8.0); and that the most significant variables were pH and dissolved oxygen.

The majority of wastewater treatment plants in the UK used iron salts for chemical P removal. Iron salts are dosed in one or a combination of wastewater treatment stages to remove P and suspended solids. The stages include dosing ferric salts to raw wastewater (precipitation), ferrous salts into aeration basin of activated sludge process (co-precipitation), iron salts into secondary sedimentation process (post-precipitation) (Carliell-Marquet et al. 2010)

2.3.1.3 Phosphorus Precipitation by Ca

Lime $\text{Ca}(\text{OH})_2$ is added as a source of calcium ion to react with the phosphate as shown in Equation 2.3 to precipitate hydroxyapatite ($\text{Ca}_{10}(\text{PO}_4)_6(\text{OH})_2$) (Metcalf and Eddy 2003).



The presence of carbonates inhibits hydroxyapatite (calcium phosphate) formation (Battistoni et al. 1997; Cao and Harris 2008). Solution pH is the key factor influencing the precipitation process. At pH 8, the rate of phosphate precipitation is significantly lessened by carbonates, and this effect disappears when pH solution rises to 9; this confirms that precipitation of calcium phosphate is decreased by the carbonates. This reduction rate is due to the formation of ion pairs between carbonate and calcium, thereby diminishing the free calcium ions. In the pH range 9 to 11, co-precipitation occurs for carbonate with calcium phosphate solution, thereby resulting in relatively low P content in the precipitate (Cao and Harris 2008).

2.3.2 Biological phosphorus removal

Phosphorus removal by biological treatment depends on the ability to take up excessive P by polyphosphate-accumulating microorganisms (PAOs), via the process called enhanced biological phosphorus removal (EBPR). The stored P in the cells is removed from the liquid by sludge wasting. This process of P uptake leads to cost reduction of chemical addition and reduces the generated sludge in comparison with chemical P removal. The microorganisms are exposed to anaerobic and aerobic conditions in the mainstream, and the process is called Phoredox (A/O) as shown in Figure 2.1 (Metcalf and Eddy 2003).

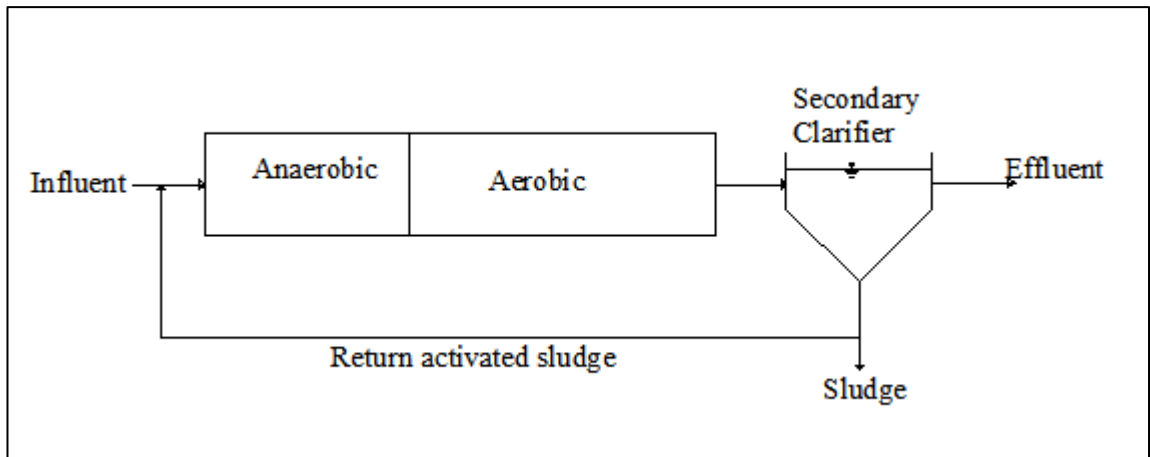


Figure 2.1 Typical mainstream biological phosphorus removal type Phoredox (A/O) (Metcalf and Eddy 2003).

This configuration can be combined with nitrogen removal unit by using anaerobic, anoxic and aerobic zones (A²O or Bardenpho process), where another recycling step from aerobic region to anoxic region is added as shown in Figure 2.2 (Metcalf and Eddy 2003).

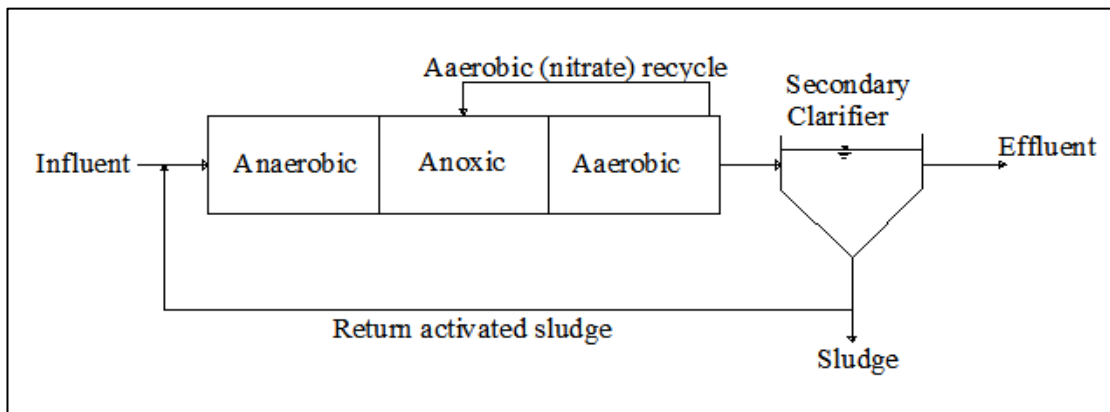


Figure 2.2 Typical mainstream biological phosphorus removal type A²O (Metcalf and Eddy 2003).

The University of Cape Town (UCT) modified the A²O process because the return sludge in the A²O process contains nitrate and oxygen that encourage heterotrophic bacteria, instead of PAOs, to consume readily biodegradable chemical oxygen demand in the anaerobic zone. In UCT, the recycling mixed liquor to the anaerobic zone is drawn from the effluent of the anoxic zone (where the nitrate concentration is minimal) while the underflow of the secondary clarifier is recycled to the anoxic zone as in Figure (2.3) (Metcalf and Eddy 2003).

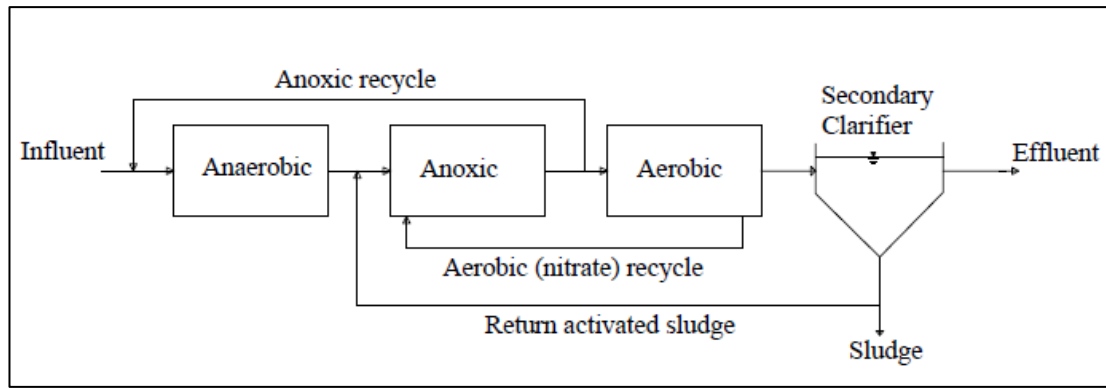


Figure 2.3 Typical mainstream biological phosphorus removal type UCT (Metcalf and Eddy 2003).

The PhoStrip process is a side stream process, which takes a portion of phosphorus – rich return activated sludge from secondary clarifier to the anaerobic tank as in Figure (2.4). The stripped supernatant is settled by chemical addition, and a part of the stripped biomass is returned to the aeration tank. A number of configurations have been derived from this including the modified Bardenpho (5-stage), UCT (modified), VIP, Johannesburg process, and sequence batch reactor (Rofe 1994; Metcalf and Eddy 2003).

Under anaerobic conditions, PAOs obtain energy by breaking up polyphosphate (that is stored in their cell) to consume the organic matter and carbon source from wastewater, accumulate storage polyhydroxyalkanoate (PHA) and glycogen, and release soluble orthophosphate from the sludge. Under aerobic conditions, the microorganisms take up a significant amount of orthophosphate greater than this released in anaerobic phase. PAOs utilise intracellular PHA molecules as a source of energy and carbon.

The nature of the anaerobic phosphate release, and how this may be metabolically associated with PHA formation, was investigated by Bond and Blackall (1999). Iodoacetate inhibited the formation of PHA and phosphate release in the anaerobic phase. It was found that phosphate release depends on the intercellular pH. When intercellular pH rose, the essential phosphate release in EBPR was caused without volatile fatty acids uptake (Bond and Blackall 1999). The influence of initial pH of anaerobic condition on EBPR from wastewater containing acetic and propionic acids

was also studied. The optimal pH for higher orthophosphate released was in the range of 6.4 to 7.2 (Liu et al. 2007).

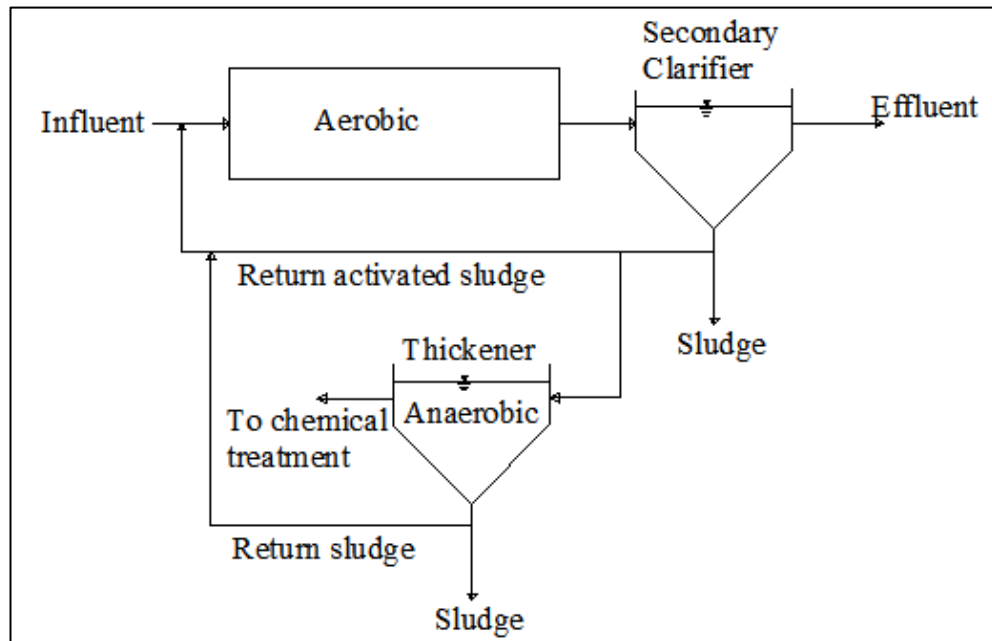


Figure 2.4 Typical side-stream biological phosphorus removal type PhoStrip (Metcalf and Eddy 2003).

2.3.2.1 Factors Affecting Biological Phosphorus Removal

For the design of biological nutrient removal system (BNR), many considerations are taken into account that include wastewater characteristics, anaerobic contact time, temperature, solid retention time (SRT), waste sludge processing method, and capability of chemical addition (de-Bashan and Bashan 2004; Mulkerrins et al. 2004).

For efficient P removal in BNR, the fluctuation in influent wastewater characteristic should be inhibited. In particular, excessive loading, excessive aeration, shortage of potassium, and excessive nitrate loading in the anaerobic zone can lead to an inefficient operation of BNR or its collapse (Mulkerrins et al. 2004). Changing the composition of influent organic such as volatile fatty acids (VFAs) to sugar (glucose) stimulates glycogen accumulating organisms (GAO) growth. GAOs have a very similar metabolism to PAOs, except that they use glycogen as a major source of energy, and they do not hydrolyze polyphosphate for energy (Mulkerrins et al. 2004). Such disturbances may cause competition between PAOs and GAOs.

The anaerobic process depends mostly on the available amount and quality of organic substances in the wastewater that includes VFAs, especially short chain volatile acids, such as acetic and propionic acids, and, to a lesser extent, glucose. It is noted that 7:1 on a weight basis is the minimum organic to phosphate ratio that should be available for P release from breaking up stored polyphosphate in the anaerobic region and P uptake by PAOs in the aerobic region. If organic acids are not sufficient, supplementation by chemical addition and fermenter options can be considered (Kang et al. 2007). Chen et al. (2004) also confirmed that high propionic acid content leads to improving EBPR efficiency in long-term cultivation. Organic carbon to P ratio in the influent is an important factor for efficient P uptake. GAOs are encouraged to grow instead of PAOs when wastewater feed with high COD/P ratio (> 50 mg COD/ mg P). When this ratio is lowered (10 – 20 mg COD/ mg P), the growth of PAOs is accumulating (Mino et al. 1998).

Temperature is a critical factor for assessing the overall efficiency of BNR. In addition to its influences on the metabolic activities, it affects gas transfer rates and settling characteristics of the biological solids (Metcalf and Eddy 2003). There are contradicting reports on temperature influence on BNR. Some reports recorded that BNR efficiency improves at a higher temperature (20-37°C) (McClintock et al. 1993; Converti et al. 1995), while, in contrast, better removal efficiency was reported at low temperature (5-15°C) (Mulkerrins et al. 2004). Erdal et al. (2003) indicated less competition for the organic substance in the non-oxic zones at low temperature (5 °C), which resulted in increasing of PAOs population. Panswad et al. (2003) found that the dominant bacteria was GAOs as the temperature rose from 20 to 33.5 °C. Meanwhile, PAOs became the dominating microorganisms and P uptake increased when the temperature was less than 20 °C. In general, by increasing the temperature until the optimum is reached, generally causes an increase in growth rate (Metcalf and Eddy 2003).

The main metal components of polyphosphate granules within the cells are Ca, Mg and K. The ratios of Ca, Mg and K in polyphosphate granules are likely to control biological P removal (BPR). When the magnesium concentration is doubled from 15 to 30 mg/L in the influent, P removal efficiency improved from 85% to 97% (de-Bashan and Bashan 2004). The effect of P precipitation in the BPR was studied via

applying different influent calcium concentration in a sequence batch reactor (Barat et al. 2008). The concentration of influent calcium ranged from 10 to 90 mg-Ca/l. Barat et al. (2008) found that calcium phosphate precipitation controls the calcium behaviour, and that the precipitation mechanisms involves precipitation of amorphous calcium phosphate and crystallisation of hydroxyapatite. They also found that PAOs can change their metabolism pathway by depending on the external condition, and that P precipitation process within BPR can affect the PAOs metabolism.

2.3.3 Adsorption

Adsorption refers to the process by which substances or solute molecules (adsorbate) adhere to the solid surface (adsorbent) under the attracting influence of surface forces (van der waals force. Casey and Casey 1997). Adsorption may occur by physical or chemical properties of the adsorbent and/or the adsorbate. Physical adsorption results from the molecular concentration of adsorbate in the capillaries of the adsorbent. Meanwhile, chemical adsorption is likely dependent on the formation of a large monomolecular of the adsorbate on the surface of the adsorbent through remaining valence forces of the adsorbent (Eckenfelder 1989).

2.3.3.1 Phosphorus Adsorption

The primary mechanisms of P adsorption are ligand exchanges for surface OH groups, with the formation of inner-sphere complexes and adsorption on the surface of the substrate (Chitrakar et al. 2006; Yang et al. 2006b; Wu and Sansalone 2013).

Replacing the anion exchange groups of the adsorbent with phosphate ion occurs when the adsorbent is in contact with the aqueous phosphate solution (Blaney et al. 2007). However, the presence of competing anions such as chloride, nitrate and sulphate, which are commonly found in wastewater, may limit the efficiency of P removal.

Sansalone et al. (2009) studied the effect of mono and divalent ions on the capacity of P adsorption. They found that divalent ions (such as SO_4^{2-}) inhibit P adsorption, while monovalent ions (such as NO_3^-) had minor to negligible effects on the adsorption. This effect of divalent ions is due to the competition of these ions with divalent phosphate ions for available adsorption sites. Wu and Sansalone (2013) used

actual runoff to compare the kinetics of the studied media. Their results showed that the adsorption was slower that due to competitive effect of SO_4^{2-} with phosphate ions, and this effect was reduced when the Ca^{2+} concentration increased. Similarly, in their investigation on Ca^{2+} effect; Sansalone et al. (2009) found that Ca^{2+} enhance P adsorption by forming ternary complexes.

The major factor that affects P adsorption behaviour is pH, where the adsorption capacity decreases with increasing pH value. By using dewatered alum sludge from water treatment, Yang et al. (2006b) found that the phosphorus adsorption capacity of alum sludge decreased from 3.5 to 0.7 mg P/ g sludge when the pH increased from 4.3 to 9. Also, Sansalone and Ma (2011) found that pH is the vital factor influencing P adsorption capacity of aluminium oxide coated media. It was found that when pH increased from 5 to 9, the adsorption capacity decreased.

2.3.3.2 Adsorbents

Recently, P removal via adsorption using materials that have a high affinity for P binding have been studied extensively. This method of P removal is considered to be more useful and efficient than biological and chemical precipitation methods (Ugurlu and Salman 1998). Common materials which have been used as filter substrates (such as sand and gravel) have limited P removal capacity (Arias et al. 2001). Therefore, searching for alternative materials as P adsorbents, in particular for use in treatment systems such as filters and constructed wetlands have become a priority. In recent times, there have been increased testing of a large number of potential materials for use as P adsorbents. These materials can be grouped into three main categories according to their origin: natural materials, industrial by-products, and man-made products (Johansson Westholm 2006).

2.3.3.2.1 Natural materials

Natural adsorbents material includes minerals and rocks (dolomite, limestone, bauxite, zeolite, opoka), soils (laterite, marl, spodosols) and sediments (maerl, shell sand). Most of these materials have a high affinity for P binding because they are rich in aluminium, iron or calcium (Johansson Westholm, 2006). Table 2.1 shows the application of natural materials for P adsorption from synthetic or real wastewater using batch and column experiments.

Natural materials are seen as readily available, cheap and safe for final disposal which makes using them as a reactive medium for P removal attractive. Despite the fact that many studies have investigated these materials in short and long-term experiments for P retention, it is difficult to compare their efficiency because of the differences in their inherent chemical and physical properties, particle size, solid to liquid ratio, agitation speed and time, temperature, pH, retention time, hydraulic conductivity, initial P concentration, and P loading rate. Most of these materials retain P via precipitation as calcium phosphate precipitates which depends on the Ca concentration availability, initial P concentration, solution pH, and contact time. It can be noted from Table 2.1 that the P adsorption capacities vary between 0.1 mg/g (Opoka) and 9.6 mg/g (shell sand). These values of P removal are affected by the chemical composition of the natural materials. It is reported that the chemical composition can inhibit the adsorption capacity (Drizo et al. 1999; Johansson Westholm 2006). The large particle sizes of these materials might restrict the required interaction between the phosphate ions and their chemical composition.

2.3.3.2 Industrial by-products

Constituents of industrial by-products which gives them high adsorption capacities are metal oxides of aluminium, iron and calcium. This makes these industrial by-products attractive to use as alternative adsorbents in wastewater processes. In addition, reusing by-products is also an important element of green engineering and sustainable design. When the by-products used as adsorbents are relatively inexpensive compared to commercial adsorbents. Table 2.2 lists the industrial by-products that have been examined for their ability for P adsorption using either batch or column experiments.

Using industrial by-products is attractive due to their high capacity for P retention. Their physical properties of small particle sizes and/or high porosity helps phosphate ions to fully contact with reactive surfaces of metals oxides. Adsorption capacities vary between 0.469 mg/g for cement kiln dust material and 113.9 mg/g for red mud. This variation in P removal is mostly due to the variation in the experimental conditions, and the physical and chemical characteristics of the media.

Chapter 2: Literature review

Table 2.1 Natural materials used for phosphorus removal

Material	Study type	Particle size (mm)	Mass (g)	Experiment conditions	Initial concentration mg/l	Main findings and shortcomings	reference
Dolomite (mainly contains Ca and Mg)	Batch	<0.425 and >0.180	0.2	-100 ml of P solution - 20, 40, and 60 °C at pH 7 -10, 15, 30, and 60 min contact time -90 to 150 rpm stirring speed	10 – 100 increased by 10	- Temperature affected negatively on P removal. -Slight increase in P removal with increase in pH. -15 to 30 min contact time was enough to reach adsorption equilibrium at high and low initial P concentration respectively. - Removal mechanism was physical interaction. - Structure and pore size distribution change with increasing temperature, leading to decrease its ability to retain P.	(Karaca et al. 2006)
Bauxite (Al and Fe oxides)	Batch	Mostly between 6.8 and 12.6	20	-60 rpm shaking speed for 24 h at 21°C	Five different concentrations ranging from 2.5 to 40	- Adsorption capacity was 0.61 mg/g.	(Drizo et al. 1999)
	Column			-12 h retention time -25 g-P/m ³ .d at first 40 d -100 g-P/m ³ .d used for an operation period	-5 used firstly. -35 to 45 used to reach saturation.	- Maximum P uptake was 0.335 mg/g.	
Zeolite (hydrated aluminium silicate)	Batch	Mostly between 6.8 and 12.6	20	-60 rpm shaking speed for 24 h at 21°C	Five different concentrations ranging from 2.5 to 40	-Maximum adsorption capacity was 0.46 mg/g. - Its large particle size effect considerably on P diffusion.	(Drizo et al. 1999)
Maerl (calcified seaweed)	Batch	---	4	-100 ml of P solution -200 rpm shaking speed for 72 h	0, 5, 50, 500, and 5000	- Adsorption capacity was 1.2 mg/ g of material. - Less effective for nitrogen removal.	(Gray et al. 2000)
Wollastonite	Batch	---	2	-40 ml of P stock solution.	5, 10	- 90 % removal was obtained in the first 21h	(Brooks et al.

Chapter 2: Literature review

Material	Study type	Particle size (mm)	Mass (g)	Experiment conditions	Initial concentration mg/l	Main findings and shortcomings	reference
(calcium metasilicate mineral)				- agitation time from 0.1 to 71 h		- 98% to 100% removal was obtained after 72 hrs.	2000)
	columns	---	---	-Secondary wastewater feeding solution -vertical upflow system - 15 to 180 h residence times (RTs)	---	-RT was a significant factor. The highest percentage removal was achieved at RT >40h. - 39% removal efficiency obtained with decreasing residence time - In long-term operation, the high residence time is required which is inappropriate with high inflow conditions.	
Apatite	Batch	2.5–10	35	-700 of P solution of 8.0 pH and 1000 μ s/cm conductivity - 160 rpm stirring speed at 22 °C for 42 h	-A range from 5 to 150	- P adsorption capacity was 0.3 mg p/g apatite. - P removal via forming hydroxyapatite is depending on the dissolved calcium. Therefore, it is spent within short time of operation.	(Bellier et al. 2006)
	Column	2.5–10	---	- 7.5 pH of P solution -0.7 l/d flow rate with upflow system -1.5 d retention time	30	- Complete P removal during first 15 days (mixture of apatite and limestone 1:1) and the removal declined to 65% until end of 39 days.	
Opoka (mainly contain CaCO ₃)	Batch	0 - 2	1	-50 ml of P solution with pH 7 -70 rpm shaking speed for 20 h at room temperature	5, 10, 15, 20, and 25	- P uptakes were between 0 and 0.1 mg/g. - CaCO ₃ inhibits the removal efficiency. - Hydroxyapatite formation is the dominant mechanism which is depending on Ca dissolution, resulting poor P removal efficiency.	(Johansson and Gustafsson 2000)
Shell sand	Batch	3 - 7	3	-90 ml of P solution -24 h shaking time	0 - 480	- Maximum P removal was 9.6 mg/g of shell sand at initial concentration 480 mg-P/l.	(Ádám et al. 2007)

Chapter 2: Literature review

Table 2.2 Application of industrial by-products for phosphorus removal

IBP	Study type	Particle Size mm	Mass (g)	Experiment conditions	Initial concentration mg/L	Main findings and shortcomings	Reference
Steel slag (mainly contains Ca)	Batch	< 2	2	- 50 ml of P stock solution and initial pH 5.2. - 200 rpm stirring speed for 2 h. -pH is ranging from 3.5 to 11.5 to study its effect. - to study the effect of adsorbent dose, 2, 4, 8, 16, 20, 40, 60, 80, and 100 g/l were used	- 5, 10, 30, 50, 75, 100, 125, 150, and 200 to study adsorption isotherm - 22.79 to study pH and adsorbent dose effect	-5.3 mg P/g slag of maximum adsorption capacity. - P removal increased with increasing temperature and adsorbent dose; and decreased with increasing initial P concentration. - P adsorption data fitted with Langmuir and Freundlich models. - P retention depends on Ca dissolution; making long-term experiments are necessitated to evaluate the material for future applications.	(Xiong et al. 2008)
	columns	< 2	6029	-Secondary effluent from WWTP with TP (1-3.4) mg/L. - 8.37 ml/min flow rate	1 – 3.4	- TP removal rate was 62 – 79 % while dissolved P removal was 71 – 82 %	
	Full-scale active filter	10 - 20	---	-2883 m ² Filter area with 0.5 m depth - 2000 m ³ /d average flowrate of effluent from pond system. -3 days retention time	-8.2 (± 7.6) for period from 1993 to 1994 -8.6 (± 0.6) from 2002 to 2003.	- 77% TP removal at first 5 years operation. - 22.4 tonnes of P was removed over the 11 years, mostly in the first 5 years. - after 5 years monitoring, P removal declined to 1.23 kg TP/tonne of sludge material as a result of Ca depletion. - Failure to regenerate the saturated slag - Further research is required to determine the longevity and understand the removal mechanisms under long-term operation condition.	(Shilton et al. 2006)

Chapter 2: Literature review

IBP	Study type	Particle Size mm	Mass (g)	Experiment conditions	Initial concentration mg/L	Main findings and shortcomings	Reference
Basic oxygen steel slag	Batch	< 0.3 mm	0.05	- P solution contained 2% of slag. - initial pH 7 and conductivity of 1410 μm . 150 rpm shaking speed for 24 h. -Range 2 to 12 of pH to study its effect	---	-P removal capacity increased from 5.9 to 9.62 mg/g with increasing PH from 2 to 12 respectively. - The removal was affected by initial concentration and slag size, and there was no effect on ionic strength. - Adsorption to metal hydroxides at $\text{pH} < 7.5$ and calcium phosphate precipitation at $\text{pH} \geq 8$.	(Bowden et al. 2009)
	columns	20		Two set of columns were used, set A with HRT (4-22) h conducting for 406 d and set B with HRT 8 h conducting for 306.	-Set A (1, 5, 15, 25, and 50) -Set B (100 - 300)	- P removal was up to 63% in set A columns and 8.39 mg/g in Set B columns. -It is needed to understand the leachate composition.	
Blast furnace slag (mainly contain Ca and Si)	Batch	0.02-0.03	0.07 to 3.5	-50 ml of P stock solution. - diff temperatures 25, 45, and 65 °C and pHs -60 min equilibrium time and pH of 8.5.	180	-P removal influenced by pH, temperature, agitation rate, adsorbent dose. - 99% of P removal was achieved, and mechanism of removal was chemical precipitation. Adsorption capacity was 6.37 mg/g. - The weak physical interaction between adsorbent and phosphate ions makes P desorbed easily.	(Oguz 2004)
	Batch	< 0.1	0.5- 1	-100 ml of P solution - Mixture shook for 1 min and then hold for 150 h at room temperature.	50-500	-Adsorption isotherm followed Langmuir model. -Kinetic adsorption was described by Pseudo-second-order reaction. - 18.94 mg/g maximum adsorption capacity. - Grain size impacts significantly on the removal.	(Kostura et al. 2005)
Activated red mud	Batch	---	0.1	- 50 ml of P solution at pH of 5.2 -shaking for 1 h	30-100	- An 80% to 90% removal of P was achieved. - P adsorption fitted to Langmuir and Freundlich isotherm models.	(Pradhan et al. 1998)

Chapter 2: Literature review

IBP	Study type	Particle Size mm	Mass (g)	Experiment conditions	Initial concentration mg/L	Main findings and shortcomings	Reference
						<ul style="list-style-type: none"> - P adsorption capacity increased with increasing pH and adsorbent dose and decreased with increasing P concentration. - Process of activating with acid increases the cost and also increases the effluent solution pH. 	
Red mud	Batch	< 0.149	0.1	<ul style="list-style-type: none"> - 20 ml of P stock solution and pH range of 1 to 11. - 180 rpm shaking speed for 4 h. 	0.31, 3.1, 15.5, 155, 775, 1550, and 3100	<ul style="list-style-type: none"> - 99% maximum removal efficiency. - Langmuir fitted better than other models. - 113.9 mg/g maximum adsorption capacity. - Optimum pH for maximum adsorption capacity was 7. - Activating process with acid or heat increases the cost. 	(Li et al. 2006)
Dried alum sludge	batch	1.25		Two types were used, one was synthetic solution and the second was secondary effluent from WWTP	First one was 2.5 The second one was 2.5 to 3.0	<ul style="list-style-type: none"> - Reduce P concentration from 2.5 to 1.0, 0.8, 0.4, 0.2, and 0.1 mg/l by using alum sludge concentration 4, 8, 12, and 10 g/l respectively. - 0.674 mg/g maximum adsorption capacity. - with secondary effluent, 16 mg/l of alum residual reduced TP from 3.0 to 0.5 mg/l. - In long-term experiments, clogging is a major problem that needs further research. - Metals leachability can be an issue to limit using it in specific applications. 	(Mortula et al. 2007)
Cement Kiln Dust	batch	< 0.1 mm	---	<ul style="list-style-type: none"> - 0, 4, 8, 12, and 16 g/l adsorbent doses - synthetic P solution and secondary effluent from WWTP - for equilibrium, 12 d contact time and 16 g/l adsorbent dose 	-2.5 for stock solution -The second effluent solution was 2.5 to 3	<ul style="list-style-type: none"> - Reduce P concentration 2.5 mg/l to 1.2, 0.25, 0.1 and 0.05 mg/l by using concentration of 4, 8, 12, and 16 g/l of cement kiln dust respectively. - 0.469 mg/g maximum adsorption capacity. - with secondary effluent, 16 g/l of cement kiln dust reduced TP from 3.7 to 1.8 mg/l. - Clogging problem and shortcutting are the main issues if it is used in field applications. 	(Mortula et al. 2007)

Chapter 2: Literature review

IBP	Study type	Particle Size mm	Mass (g)	Experiment conditions	Initial concentration mg/L	Main findings and shortcomings	Reference
Fly ash	column	0.125 – 0.063	0.2	-50 ml of stock solution. -4, 10, 20 g/l of adsorbent with initial P concentration of 20 mg/l - contact times were 5, 10, 15, 20, 25, and 30 min	20, 50, and 100	- Insignificant of adsorbent dose on the removal. -significant effect of temperature on the removal. - > 99% P removal was achieved at 40°C and PH 4, and P concentration at equilibrium was 0.02 mg/l.	(Ugurlu and Salman 1998)
Iron oxide tailings	batch	0.069	0.2	-100 ml of stock solution with constant pH range of 6.6 to 6.8. -180 rpm shaking speed for 24 h at room temperature.	5, 10, 20, 40, 70, 100, and 150	- Adsorption capacity decreased from 8.6 mg/g at pH 3.2 to 4.6 at pH 9.5. - 8.21 mg/g maximum adsorption capacity. -The metals composition include a high percentage weight of heavy metals that may be leach under long-term operation.	(Zeng et al. 2004)
Oil shale ash	batch	1 - 2	1 and 5	-100 ml of stock solution. -75 rpm shaking speed for 48 h	1.6 to 98	-A 65 mg P adsorption capacity of 1 g oil shale in a solution containing 98 mg-P/l. - Removal efficiency was between 67 – 85% at diff loadings (5-300 mg/l of P per 1 and 5 g of ash. - High P removal explained by the high ratio of reactive calcium minerals. -Containing a considerable trace elements and heavy metals that may limit its field application.	(Kaasik et al. 2008)

2.3.3.2.3 Man-Made Products

Different synthetic materials have been studied regarding their P adsorption capacity. These adsorbent materials include lightweight expanded aggregate, obtained by heating to a temperature up to 1000 °C e.g. Filtralite®, LECA, Polonite® and ion exchange fibers such as hybrid anion exchange (HAIX)-PhosXnp, granular ferric hydroxide (GFH), and hydrated ferric oxide (HFO)-coated sand. Most of the manufactured adsorbents contain a high content of Ca, Mg and metal hydroxide (Johansson Westholm 2006; Ádám et al. 2007; Li et al. 2009; Mayer et al. 2013). Table 2.3 shows some of these synthetic materials applied for P removal and recovery in different experiments conditions.

Anion exchangers are manufactured by the synthesis of poly-styrene matrices with amino groups to produce polymers with hydrophilic characteristics. They have a strong affinity for P binding in the presence of competing ions such as bicarbonate, chloride and nitrate (Blaney et al. 2007; Awual et al. 2011). These polymeric anion exchangers usually combine with the monovalent (H_2PO_4^-) and divalent (HPO_4^{2-}) phosphate forms (Kadlec and Wallace 2009).

There is an environmentally sound argument against using man-made products as the production of the substrates requires a large amount of energy (Johansson Westholm 2006). Other disadvantages of using these products are expense and commercial availability. However, the lack of P adsorption and selectivity, weak adsorption mechanisms, unable to regenerate the exhausted adsorbent or low regeneration performance, poor P recovery efficiency, and high operation cost have been the predominant reasons for continuing using the synthetic materials instead the other adsorbents types.

Chapter 2: Literature review

Table 2.3 The applied man-made adsorbents for P removal.

Material	Study type	Particle size (mm)	Mass (g)	Experiment conditions	Initial concentration mg/l	Main findings and shortcomings	reference
Filtralite®	Batch	0.5-4 Effective porosity 40%	3	- A 90 ml of P solution shook for 24h.	- A range of 0 - 480	-Adsorption data did not fit Langmuir and Freundlich models. -At initial P concentration of 10 mg/l, P retention capacity was about 1.3 mg/g. -The adsorption behaviour became worse when the initial P concentration increased.	(Ádám et al. 2007)
	Column	Particle porosity 68% for two columns	1- 10660 2- 10340	1- Loading rate 5.5 l/day with RT of 3.5d. 2- Loading rate 4.9l/day with RT of 3.8d.	1- 10 stock solution 2-4.9 secondary wastewater	-54% and 91% average P removal for column1 and 2 up to effluent of 1 mg-P/l, respectively. -High Ca and Mg concentrations release from both column combined with raising pH of effluent, especially at the first days of P loading. -With cost associated with manufacturing process, making using it for long-term operation undesirable.	
Polonite	Column	2-5.6	---	-A 10 cm diameter column filled with 50cm. - Loading rate of 530 L/m ² .d, hydraulic conductivity 226 m/d, RT from 4 to 5 h.	Synthetic solution containing 10 mg/l.	-High percentage of phosphate removal with no sign of breakthrough point over 68 weeks of operation. -After the media saturated with P, it needs to replace with another fresh one, meaning that it is unable for regenerating.	(Renman and Renman 2010)
Hybrid anion exchange (HAIX)	Fixed-bed column	---	---	-Glass column with 11mm diameter and 250mm length. -Superficial liquid velocity of 2.5 m/h.	0.25	-P breakthrough occurred after 4000 pore volume with effluent P concentration of 0.05 mg/l. High P selectivity over other anions of sulphate, chloride, and bicarbonate. -It is applicable for regenerating and P recovery (90%) in less than 10 pore volumes. -Constant P removal performance during the seasonal fluctuation in temperature.	(Blaney et al. 2007)

2.4 Dewatered water treatment sludges

Until now, sludge is an inevitable by-product of drinking water treatment process. The sludge normally contains mineral and humic matter which are removed from the raw water, together with residues of any treatment chemical used as a coagulant (commonly aluminium and iron salts) and coagulant aids (mostly organic polymers).

Alum- and iron- water treatment sludges are generated when aluminium sulphate and iron are used as coagulants. Aluminium sulphate is the most widely used coagulant in drinking water treatment. The processes in water treatment works include coagulation, flocculation, and sedimentation, followed by filtration and disinfection. Negative charge neutralisation of stable particles carried in water is achieved by adding a coagulant. After coagulant addition to water, they dissociate leading to series of hydrolysis reaction products such as $\text{Al}(\text{OH})^{2+}$ and $\text{Al}_{13}\text{O}_4(\text{OH})_{12}^{7+}$ (in the case using aluminium sulphate as a coagulant). The hydrolysis products can actively attract and adsorb on the negative charge particles (Sincero and Sincero 2002; Parsons and Jefferson 2006).

Through coagulation and flocculation processes in water treatment, these complexes adsorb inorganic contaminants and natural organic matter which may include humic and fulvic acids, microorganisms (bacteria, protozoa, and algae) and organic substances (fine soil particles, Stumm and Morgan 2012). During the flocculation, sedimentation and filtration processes, the colloidal particles, including the hydrolytic aluminium or iron species, are transferred to the sludge stream.

Because of the variation of the natural contaminants loaded to the water treatment plant, sludges with variable characteristic are produced. The fluctuating characteristics are water source dependent. For example, rivers can contain a high percentage of suspended clay colloids, while elevated concentration of natural organic matter can be found in water sources of upland and peaty areas (Parsons and Jefferson 2006). In addition, the seasonal growth of algae can impact on the performance of coagulation-flocculation processes that uses either clay colloids or natural organic matters to determine the optimum coagulant dose. Therefore, higher

coagulant doses are needed, leading to increased sludge volumes (Matilainen et al. 2010).

2.4.1 Production, disposal and associated cost

Several million tonnes of waterworks sludge are generated every year in Europe, and this may increase twofold by the next decade (Basibuyuk and Kalat 2004). These have led to increased concerns about their disposal and associated costs. The amount of generated sludge varies with the drinking water production rate, dosage of coagulant or other treatment chemicals used, and suspended solids concentration and other carry-over contaminants in the raw water source. The quantity of water treatment works sludge generated in the UK is more than 180 thousand tonnes (Goldbold et al. 2003), while in Ireland the sludge generated has been estimated to increase double fold by the end of next decade, from a current estimate of 15 to 18 thousand tonnes per annum of the dried solid (Zhao et al. 2000). The yearly quantity of water sludge production in selected countries is presented in Figure 2.5.

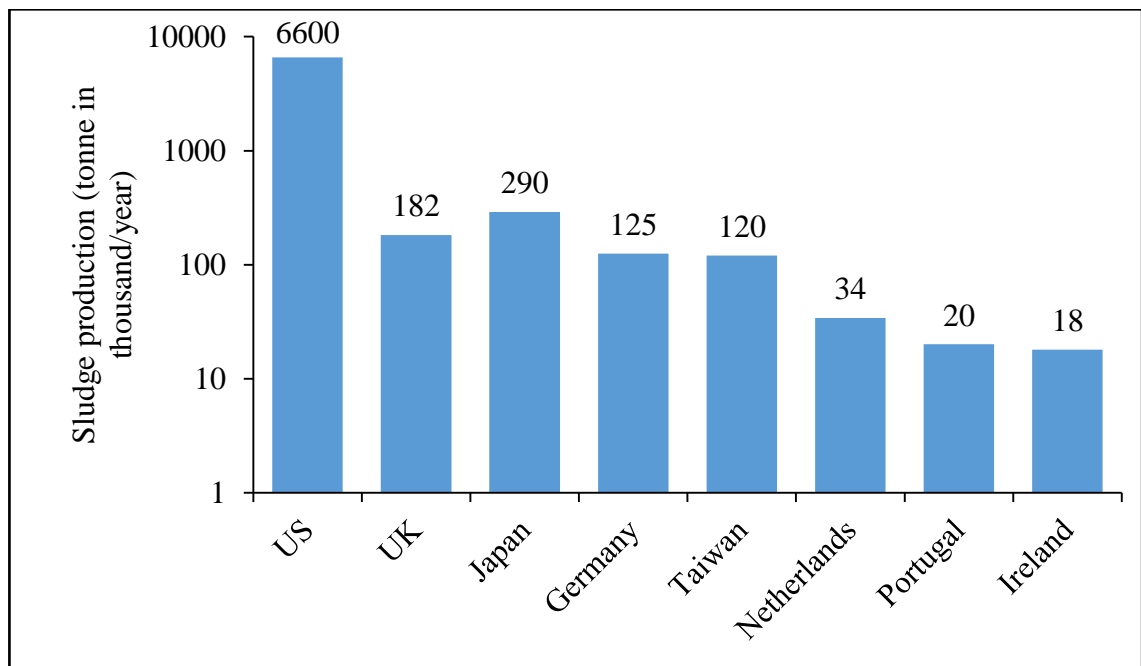


Figure 2.5 Global water treatment sludge production. Data extracted from Babatunde and Zhao (2007); Fujiwara (2011); Goldbold et al. (2003); Prakash and Sengupta (2003); and Pan et al. (2004).

The costs of handling the waterworks sludge increases the overall operating cost of water treatment works, and these costs are likely to rise due to increasingly stringent environmental requirements. Horth et al. (1994) reported that water sludge disposal in Netherlands costs between 30 to 40 million pounds per year. The sludge disposal cost depends on the chosen waste management technique. In the UK, the mean cost is £41 per tonne of sludge and the highest is £323 per tonne of sludge (Simpson et al. 2002). The predicted increase in sludge production can be explained by the population growth, regulatory changes, and the combined raw water characteristics changing with climatic conditions (Arnell 1998; Hurst et al. 2004; Delpla et al. 2009).

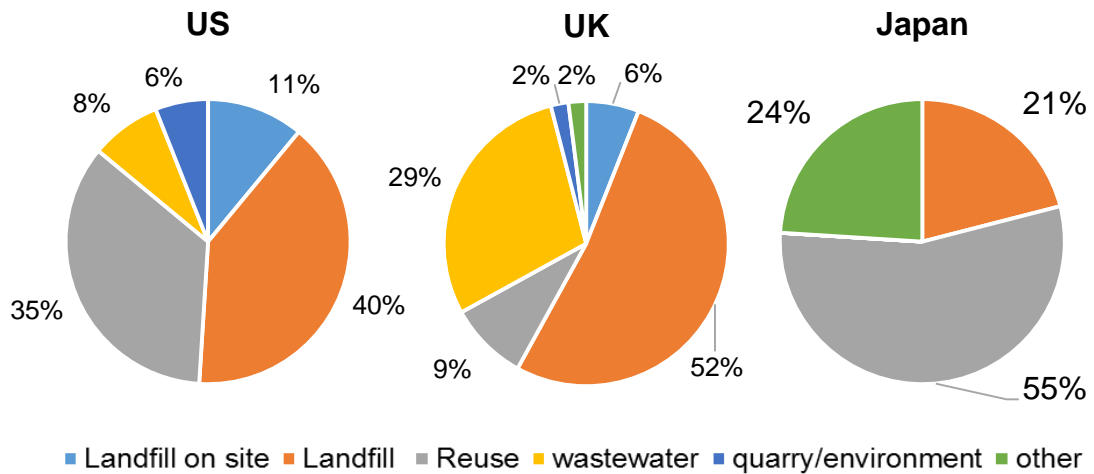


Figure 2.6 Final disposal routes for water treatment works sludges. Data extrapolated from Fujiwara (2011)-Japan; McCormick et al. (2009)-US; and Simpson et al. (2002)-UK.

Before 1946, water sludges were discharged into the nearest water body (Proudfit 1968). However, this is now forbidden in many locations. Waterworks has a number of options for handling the produced sludge. These options are recycling, discharging to landfills, land application, and other applications such as ceramics, bricks, tiles production and disposal with sewage (Owen 2002; Pan et al. 2004; U.S. Epa 2011). Land application water sludge can be used for soil pH neutralisation instead of commercial products, while alum or iron sludge are used as filler material. The different management routes for water sludges in the US, UK and Japan are presented in Figure 2.6. It should be noted that the recycling option might increase

soil metal content, reduce phosphorus availability, and impair groundwater quality (U.S. 2011).

2.4.2 Characteristics of water treatment works sludges

The dominant constituents of water sludges are the primary coagulant used (aluminium and iron (hydr)oxides), chemical additives either for pH adjustment or water softening, natural organic matter, the separated colloids of clay, and minerals. Aluminium sulphate ($\text{Al}_2(\text{SO}_4)_3 \cdot 14\text{H}_2\text{O}$) (the Al content ranging from 7.4 to 9.5 percentage by mass or traditionally from 9 to 17 percent as equivalent alumina), and ferric sulphate (40 to 42% $\text{Fe}_2(\text{SO}_4)_3$ and 11.5% Fe^{3+} by mass, in liquid form) or ferric chloride (43% FeCl_3 , by mass) are the most popular coagulant used in coagulation-flocculation water treatment process. Polymers are added to enhance flocculation of the mixture and also to accelerate the separation of particles from the water (Bratby 2015).

The general characteristics of Al- and Fe- based water sludges are presented in Table 2.4. These figures represent the mean and standard deviation of values extrapolated from previous studies. The main chemical compositions of water sludges are Al, Fe, Ca and TC. The content of Al, Fe and Ca in the sludges reflects the coagulants used, while the other chemical characteristics originate from the raw water source properties. The water source can be classified into upland surface water, lowland surface water, groundwater, brackish well water, and seawater. Low mineral concentrations, low solids content, and a significant amount of dissolved organic matter are found with upland surface water. A mixture of groundwater, upland surface water, and effluent from municipal wastewater treatment works and industrial outfalls contributes to lowland surface water characteristics. Moreover, the properties of these water sources can vary significantly from season to season (Parsons and Jefferson 2006).

The water treatment levels are determined based on the water source characteristics. From Table 2.4, high variation in most of the major and minor water sludge constituents can be explained by the change of water source characteristics, coagulant type and applied dose, and water treatment level. For example, elevated turbidity may increase coagulant dosages during the treatment, leading to increased sludge quantity. Organic matters including fulvic and humic acids cause yellowish or

brown colour, taste and odour in water. Drinking water standard legislation obligate water treatment companies to reduce metals and organic matter, and avoid or reduce the potential for disinfection by-product formation.

Table 2.4 General properties of aluminium and iron-based water treatment sludge.

Element	Unit	Al-based		Fe-based ^a	
		Average	STDV	Average	STDV
Al	mg/g	79.19	36.09	23.59	23.83
Fe	mg/g	24.81	58.64	229.22	82.39
P	mg/g	1.68	1.05	3.53	3.42
Aloxa	mg/g	57.69	29.60	4.28	2.24
Feoxa	mg/g	19.25	49.83	135.84	55.24
Poxa	mg/g	1.69	1.20	1.37	1.23
Ca	mg/g	12.53	13.25	21.45	15.47
Mg	mg/g	0.89	0.96	3.69	5.05
Mn	mg/g	0.56	0.39	3.85	4.17
K	mg/g	3.33	1.26	---	---
Ca soluble	mg/g	0.96	1.08	---	---
Zn	mg/kg	83.5	75.66	---	---
Cd	mg/kg	45.9	0.06	---	---
Cr	mg/kg	8.65	0.01	---	---
Cu	mg/kg	2655	2057.7	---	---
Ni	mg/kg	1251.3	1751.9	---	---
Pb	mg/kg	536.8	903.4	---	---
As	mg/kg	18.4	40.1	50	70.7
Hg	mg/kg	0.3	0.3	---	---
Total N	mg/g	6.2	2.1	8.3	2.2
TC	mg/g	131.4	74.2	147.2	40.0
OC	mg/g	72.5	21.9	---	---
pH	---	6.7	0.9	6.1	1.2
EC	ds/m	2.6	2.9	8.2	---

^a data of average and standard deviation of Al-and Fe-based sludges were extracted from Agyin-Birikorang et al. (2001); Babatunde et al. (2009); Codling (2008); Dayton et al. (2003); Elliott et al. (2002); Gibbons and Gagnon (2011); Ippolito et al. (2003); Mahdy et al. (2008); Makris et al. (2004a, 2006, 2005b); Ramirez et al. (2008); Rew (2006); Stoner et al. (2012); Wang et al. (2011b); Yang et al. (2006b).

2.4.3 P adsorption characteristics and influencing factors

Numerous studies have been conducted to examine the effectiveness of water treatment sludges (especially alum residuals) for P (and other contaminants) removal from aqueous solution (Drizo et al. 1999; Huang and Chiswell 2000; Zhao et al. 2000; Kim et al. 2002; Dayton et al. 2003; Ippolito et al. 2003; Makris et al. 2005b; Yang et al. 2006a; Zhao et al. 2007; Babatunde et al. 2009; Babatunde et al. 2011; Sansalone and Ma 2011). Phosphorus adsorption onto water treatment sludges can be defined by the availability of the amorphous forms of aluminium and iron oxides or hydroxides. These reactive metals have been demonstrated to improve physical and chemical adsorption characteristics (Kumar et al. 2014a; Kumar et al. 2014b). However, the adsorption characteristics of metals hydr(oxide)s in water treatment sludges are influenced by two factors. The first factor refers to the physiochemical properties such as surface area, particle size, elemental content of Al, Fe, Ca and OC, the reactive metals (Al or Fe), and pH_{pzc} (Dayton and Basta 2005; Makris et al. 2005a; Babatunde et al. 2009). The second factor relates to the chemical properties of the treated water source including pH, temperature, dissolved organic carbon, low molecular weight organic acids, initial P concentration and P species (Razali et al. 2007; C. Wang et al. 2011a; Wang et al. 2012; Gao et al. 2013; Wang et al. 2013).

In a previous study, seven water treatment sludges (four alum-based and three iron-based sludges) were used to demonstrate the effect of specific surface area (SSA), porosity, and carbon content on P immobilisation in long-term P adsorption experiments (Makris et al. 2005a). They found that TC content reduced P adsorption per unit pore volume or surface area, and that the TC and SSA measured by N_2 and CO_2 methods explained 82% of the long-term P adsorption variability. While in another study using hydrolysis and P adsorption batch tests, a positive correlation was observed between P removal in solution and the increased concentration of the released OC (Yang et al. 2006b). This discrepancy in the results might be explained by the differences in experimental conditions and sludge characteristics. Knowing the amorphous aluminium or iron oxide content in water sludge can give a meaningful estimation of P adsorption. Dayton and Basta (2005) found that the amorphous Al extracted with ammonium oxalate explains significantly 91% of maximum P adsorption which was calculated using the Langmuir isotherm model.

However, a significant water sludge characteristics is particle size; reducing the particle size of alum-based sludge from < 2 mm to < 150 μm increases the maximum P adsorption capacity from 3.93 to 9.68 mg/g using equilibration time of 17 h.

To investigate the effect pH on P adsorption, several studies have been conducted using batch experiments with different initial pH conditions. Results have shown that P adsorption capacity increases with decreasing pH (Kim et al. 2002; Yang et al. 2006b; Babatunde et al. 2009). Yang et al. (2006b) used a range of pH solution from 4.3 to 9.0 to identify the P adsorption behaviour of alum-based sludge. It was found that the P adsorption capacity decreased when the solution pH changed from acid to alkali condition. Babatunde et al. (2009) explained that the effect of solution pH could be contributed to the surface charge of alum sludge, and the P competing with hydroxyl ions when the pH solution is larger than the pH at the point of zero charge (pHpzc). The alkali P solution causes the sludge surface to be predominantly negatively charged, and this then leads to fewer places available for P adsorption, due to the competition with hydroxyl ions. The effect of solution pH and temperature on P adsorption by Al-Fe-based sludge were demonstrated (Wang et al. 2011b). They found that P adsorption decreases with increasing pH, and it is elevated with increasing temperature, thus describing adsorption characteristics of the studied sludge as endothermic. In another study, Wang et al. (2012) studied the effect of low molecular weight organic acids (such as citric acid, tartaric acid, and oxalic acid) on P immobilisation by Al-Fe-based sludge using batch and column experiments. It was found that these organic acids inhibit P adsorption and this inhibitory effect becomes weaker with time. Solution chemistry may also contain a range of P species which can affect the P adsorption. Kim et al. (2002) investigated alum sludge for P adsorption using a range of P species. It was found that maximum adsorption capacity in batch experiments was 25 mg/g for ortho-P and followed the order: ortho-P > pyro-P > tri-P > organic-P at a pH range of 4 to 6. In another study by Razali et al. (2007), it was also reported that the adsorption capacities of alum sludge were in the order of ortho-P > poly-P > organic-P.

2.4.4 Equilibrium and kinetics of phosphorus adsorption

In the previous section, details about the factors that can effect the P adsorption characteristics of DWTS were discussed. The P adsorption properties can be defined based on adsorption isotherms and kinetics models. Using these models can enable the determination of the maximum amount of P that can be removed until the point of saturation, and the P adsorption rate onto the DWTS. Usually, batch tests are used for adsorption characteristics. These are easy, cheap and require short time to obtain the data. However, batch experiments are arbitrary due to the variety of applied conditions, despite DWTS characteristics which can be influenced by the source. Table 2.5 shows different conditions used in batch tests to study P adsorption characteristics of DWTS. It can be seen from the table that variable adsorption capacities were obtained from the previous studies. This variability can be explained by the varying particle sizes, different mass of DWTS to liquid ratio, initial pH solution, range of initial P concentration, mixing time and shaking speed. Furthermore, Al-DWTS showed higher P adsorption rate than Fe-DWTS. The batch experiment conditions and type of DWTS used in the experiments have a significant effect on the adsorption capacity. For example, Babatunde and Zhao (2010) used 1 g of Al-DWTS, particle size less than 2 mm, 100 ml of P solution with concentration ranging from 0 to 360 mg/l, three levels of initial pH solution 4, 7 and 9; 200 rpm shaking speed and 48h stirring time. They found that the maximum adsorption capacities calculated using the Langmuir model were 31.9, 23.9, and 1.2 mg of P/g-sludge obtained at pH 4, 7, and 9, respectively. In another study using 0.15 g of Fe-DWTS, particle size less than 0.098 mm, 120 rpm shaking speed, 24 h shaking time, 5.5 initial pH, solution of 50 ml and P concentration ranging from 5 to 50 mg/l, the maximum P adsorption capacity was determined as 25.5 mg-P/g (Song et al. 2011).

Kinetic of P adsorption to the surface of DWTS has been found to be fast and well described by pseudo second order kinetic model (Babatunde and Zhao 2010; Bal Krishna et al. 2016). Coefficients calculated from the different kinetic models depend on initial P concentration, incubation pH, the amount of sludge used, and other batch experimental conditions. 100% P removal was obtained within 30 min of shaking 2 g of Fe-sludge in 20 ml of 100 mg/l P solution (Leader et al. 2008); this indicates the rapid P binding to the sludge surface. In a similar study, 1 g of Al-sludge was mixed

with 25 ml of 10 mg/l P solution for up to 24 h. Wagner et al. (2008) noticed that a 50 percent P removal was achieved within 2 min, 90 percent and almost 100% in 15 min and after 24 h, respectively. Babatunde and Zhao (2010) observed the interparticle rate constant increased from 0.0075 mg/g.min to 0.1795 mg/g.min when the initial P concentration increased from 5 mg/l to 60 mg/l. Kinetic P adsorption onto the DWTS can be classified into two phases: the fast phase of P adsorption into the accessible pores on the surface of the particle such as macropores (size > 50nm) and exteriors (between 2 and 50 nm); and slow phase of P diffusion into the micropores (size < 2nm) (Makris et al. 2005a). Phosphorus adsorption by DWTS can be described through P diffusion into micropores for long-term stabilisation and immobilisation (Makris et al. 2004a). In an attempt to desorb P from Fe-sludge loaded with 0.95 mg-P/g, via shaking in 20 ml of 0.01 mol/l KCl for 24 h, Leader et al. (2008) measured less than 0.01 mg/g of P released, suggesting that the previously adsorbed P in DWTS is irreversible. In a similar study, Al-sludge loaded with 12.5 mg-P/g was subjected to P desorption experiment for 211d by agitation in 0.01 mol/l CaCl₂ (Ippolito et al. 2003). The authors observed that the initially released P was re-adsorbed chemically to Al-sludge as the agitation time increased

From all previous studies on DWTS, it has been proven that DWTS has excellent potential for P removal. However, more investigation is required to verify the differences in their adsorption capacities and how their inherent physical and chemical properties can regulate P removal.

Table 2.5 Rate and adsorption capacity of P for DWTS under different conditions of batch experiments and P adsorption behaviour under continuous feeding systems.

Sludge type	Study type	Particle Size (mm)	Mass (g)	Experiment condition	Initial concentration mg/L	Adsorption capacity	Reference
Al-based	batch	< 2	1	- pH of 7.1. - 24h shaking time. - 30 ml of P solution used.	100,200, 400, 800, 1000, 2000, and 4000 of P species mixture (ortho-P, pyro-P, tri-P, and adenosin-P).	-Higher inorganic P removal than organic P. -Maximum adsorption capacities were 25, 16.6, 14.3, and 12.5 mg/g for ortho-P, pyro-P, tri-P, and adenosin-P respectively.	(Kim et al. 2003)
	column	< 2	130	- 3.0 ml/min of flowrate - pH of 3, 4, 5, and 12. - 32 min residence time. - 96 ml pore volume. - Up flow with continuous feeding.	- 30 mg-PO ₄ ³⁻ /l.	- The effluent P concentration was less than 1 mg/l after passing 250 pore volume at pH 4 and 200 pore volume at pH 5.	
Al-based	batch	< 2.36	0.1 – 0.5	- pH of 4, 5.5, 7, and 9. - 17, 24, 48 h and 6, and 80 d of shaking time. - 200 rpm mixing speed - 21 ± 2 °C room temperature.	- 5 to 3500 of P range which consisted of ortho-P, poly-P, and organic-P.	- At pH 4 and 24 h equilibrium time, maximum adsorption capacities for ortho-P, poly-P, and organic-P were 10.2, 7.4, and 4.8 mg/g to be decreased to 6.3, 3.2, and 2.6 mg/g respectively at pH 9.	(Razali et al. 2007)
	column	< 2.36	500	- 2.79 m ³ /m ² .d of hydraulic loading rate. - 210.5 g-PO ₄ ³⁻ /m ² .d of P loading rate. - pH range of 6.8 to 7.2 - 60 d continuous down flow feeding.	- A mixture of ortho-P (50.8), poly-P (18.1), and organic-P (6.5).	- P removal > 80% of influent P within the first 30 d operation. - P saturation point did not reach with 60 d.	

Chapter 2: Literature review

Sludge type	Study type	Particle Size (mm)	Mass (g)	Experiment condition	Initial concentration mg/L	Adsorption capacity	Reference
Al-based	batch	< 2	1	For isotherm experiments: - 48 h shaking time. - 200 rpm shaking speed. - pH levels of 4, 7, and 9.	- P concentrations from 0 to 360. - 100 ml volume of P solution	- Isotherm fitting order; Langmuir, Freundlich, Temkin, Frumkin, Dubinin–Radushkevich (D-R), and Harkins–Jura (H-J). - Maximum adsorption capacities were 31.9, 23.0, and 1.2 mg/g at pH 4, 7, and 9 respectively.	(Babatunde and Zhao 2010)
				For kinetic experiments: - pH of 7. - 200 rpm shaking speed. - A range of 10 to 120 min shaking time.	- Four initial P concentration of 5, 15, 30, and 60. - 100 ml volume of P solution.	- Intraparticle diffusion rate constant increased with increasing initial P concentration. - Rapid phosphate molecules transfer into the Al-sludge.	
Fe-based	Batch	< 0.098	0.15	- 24 h shaking time. - 120 rpm shaking speed. - pH of 5.5. - 25°C temperature.	- The initial range for isotherm experiment ranged from 5 to 50. - 50 ml of P volume.	- Highest adsorption was obtained at pH 5.5 and sludge dose 3 g/l. - maximum adsorption capacity was 25.5 mg/g. - In the kinetic study, P adsorption reached 25.5 mg/g after a contact time of 1000 min. - M Langmuir and Pseudo-second order were well describing the adsorption and kinetic characteristics.	(Song et al. 2011)
	column	< 0.098	- Sludge: sand ratio (1:1). - 4, 6, and 8g of sludge with depth of 20, 30,	- 10 ml/min flow rate. - pH of 5.5 - Down flow continuous feeding system.	- 30 mg/l of influent P concentration.	- 30 mg/g maximum P adsorption joined with using 6 and 8 g.	

Chapter 2: Literature review

Sludge type	Study type	Particle Size (mm)	Mass (g)	Experiment condition	Initial concentration mg/L	Adsorption capacity	Reference
			and 40 mm respectively				
Al-Fe-based	batch	< 0.18	0.3	- Initial adjusted pH of 7. - shaking speed 100 rpm. - shaking time 24h	- 155, 310, 620, 930, 1550, 2170, and 3100 of initial P concentrations used for isotherm study.	- Maximum adsorption capacity was 28.5 mg/g for sludge without pretreatment. - after thermal-acid activation treatment (600°C for 6h, cooling, 0.1- 0.3M of HCl for 2h), adsorption maxima was 49.1 mg/g.	Wang et al. 2011a)
four Al-based One Al-Fe-based	Batch	0.15-0.6 mm	---	- Initial pH of 7 - Shaking speed 150 rpm. - shaking time 24h. Temperature 25°C.	- A range of initial P concentration. - 100 ml of P solution volume	- Maximum adsorption capacities were 15.625, 4.167, 90.909, 15.385, and 20.41 mg/g.	(Li et al. 2013)
Fe-based 3Al-based	Batch	15 – 600 μm	2.5	For isotherm experiments: - Initial pH 6. - Shaking speed 200 rpm. - shaking time 48h.	- synthetic and secondary effluent wastewater - P range for both type: 0, 50, 100, 150, 200, 300, 400, and 600. - 250 ml of P solution volume.	- Maximum adsorption capacity for Fe-sludge was 30.3 mg/g, and for Al-sludges were 41.67, 34.48, and 32.26 mg/g with synthetic wastewater. With secondary effluent, 32.6 mg/g for Fe-sludge and 47.62, 40.00, and 41.67 mg/g for Al-sludges.	(Bal Krishna et al. 2016)
			5	For kinetic experiments: - Initial pH 6. - Shaking speed 100 rpm. - shaking time 24h.	- Synthetic and secondary effluent wastewater. - 50 mg-P/l - 500 ml of P solution volume.	- P adsorption kinetic fitted with a Pseudo-second order for all sludges. - Al-sludges had higher P removal rate than Fe-sludge.	

2.4.5 Phosphorus adsorption of DWTS under long-term experiments

Despite the fact that batch experiments are useful for characterizing P adsorption capacity of potential adsorbents, it has been observed that several factors associated with these adsorption tests impacts on their accuracy in predicting long-term P adsorption. These aspects include initial P concentration, pH, material to solution ratio, shaking time and temperature (Drizo et al. 2002; Søvik and Kløve 2005; Ádám et al. 2007; Cucarella and Renman 2009). As a result of this, long-term of P adsorption using flow-through experiments is used to overcome some of the disadvantages associated with the batch tests. In many cases, several studies have used long-term experiments to mimic the operational conditions used in constructed wetlands. DWTS is one of the reactive substrates that is rich in aluminium, iron and calcium metals, which are used for the removal of certain inorganic nutrients such as phosphorus and nitrogen. The P adsorption behaviour of water sludges under continuous flow systems using laboratory-scale columns is represented in Table 2.5.

Data obtained from these studies showed that stark differences in the P removal efficiencies over time, and in different experiments conditions. This leads to difficulties in comparing the results.

2.5 Coagulant and phosphorus recovery

Coagulant and phosphorus recovery from P-saturated water treatment sludge offers a sustainable approach to coagulant reuse in drinking water treatment plants and P recycling.

2.5.1 Coagulants usage and associated costs

The coagulation-flocculation process is a widely used technique in drinking water purification processes for removing turbidity, natural organic matter and other impurities. Chemical coagulants of iron and aluminium salts are usually applied during the purification process, with more than 70% of water treatment plants using these salts (Betancourt and Rose 2004). This annual coagulant usage costs more than £28m (Keeley et al. 2014b). The costs and quantity of coagulant used depend on the raw water quality, site location and grade of coagulant used. For instance, the

average alum usage and its cost per water utility in Australia is about 1,700 tonnes per year and US\$ 374,000 per year, respectively (Maiden et al. 2015).

2.5.2 Phosphorus importance and future needs

P is an essential element in common life activities, through incorporation as a major constituent of deoxyribonucleic acid (DNA) and adenosine triphosphate (ATP), making about 1% of body mass. It is also a vital ingredient in many products such as detergents, toothpaste, plastics stabilisers and corrosion inhibitors (Cisse and Mrabet 2004).

Phosphorus is mainly produced from rock which is a non-sustainable natural source originating from sedimentary and igneous deposits, and relatively low-cost sources. Most of the phosphate rock production is used to manufacture fertilisers, animal feeds, and pesticides; and this contributes to 95% of total phosphate rock consumption. Whilst the importance of P compounds for everyday life activity is well known; it has been estimated that these P sources will be largely depleted in less than 50 to 100 year at the current utilisation rate (Isherwood 2000; Duley 2001; Conley et al. 2009). Therefore, finding alternative P sources is a crucial need to meet life necessities. One of these sources can be from water sludges used as a reactive adsorbent in CWs that is saturated with P.

2.5.3 Chemical separation technologies

The first stage of coagulant and P recovery from P-saturated water sludge is to convert these elements from undissolved phase to dissolved phase via solubilization process. This unavoidable process is not selective and other contaminants are released from the sludge, including heavy metals and OMs. Recent studies have focused on finding efficient recycling processes to separate the beneficial elements with high purity from the metal-contaminated solution. However, these processes could elevate the risk of DOC accumulation with the recovered coagulant. If the recovered coagulant contaminated with DOC is recycled, the potential for the formation of DBPs would be elevated in treated water (Keeley et al. 2014a).

Metal recovery technologies such as pressure driven membrane, ion exchange and electrochemical systems have been used after acidified sludge in previous studies

(Prakash and Sengupta 2003; Mejia Likosova et al. 2014; Keeley et al. 2016). These technologies offer coagulant recovery via two steps of extraction and stripping, or simultaneous coagulants recovery in one-step through ion exchange membrane. However, there are many issues reported regarding using these technologies; these include: (i) the fouling, energy demand and limited selectivity for pressure driven membrane; (ii) the required volume of extractor, resin or membrane areas at full scale in order to satisfy industry requirements for fast kinetics, sufficient capacity and high yields (Keeley et al. 2014a). Furthermore, many obstacles are facing coagulant recovery from DWTS; these can be classified into: (i) failure of controlling process to manage the variability of DWTS, (ii) accumulation of acid-soluble impurities, particularly manganese, and (iii) recycling the recovered coagulant for water purification poses a particular risk of recycling DOC alongside with the recovered coagulant. Table 2.6 presents a summary of the recovery technologies.

2.5.3.1 Electro dialysis technology

Electrodialysis is one of the Ion-exchange processes that had been described to be highly selective for trivalent coagulant metals, Al and Fe, whilst rejecting the vast majority of DOC in addition to its reliance on a diffusive transport mechanism and reducing the potential for membrane fouling (Prakash and Sengupta 2003; Keeley et al. 2014a).

In an electro dialysis system, alternative arrangement of cation exchange membrane (CEM) and anion exchange membrane (AEM) with according to the anode and cathode electrodes is constructed to form cell. Feeding solution is pumped through the cells while the electrical potential is applied and maintained across the electrodes. The cation ions (with positive charge) in solution migrate through CEM toward the cathode and anion ions (with negative charge) migrate through AEM toward the anode. The positive charge ions can easily pass through CEM (negative charge) but they are retained by AEM (positive charge). Similarly, the negative charge ions pass through AEM and they are retained by CEM. The result of this process is that recovery stream becomes rich with ions while the feeding stream becomes depletion of ions. The process of recovery using electro dialysis technology is illustrated in Figure 2.7.

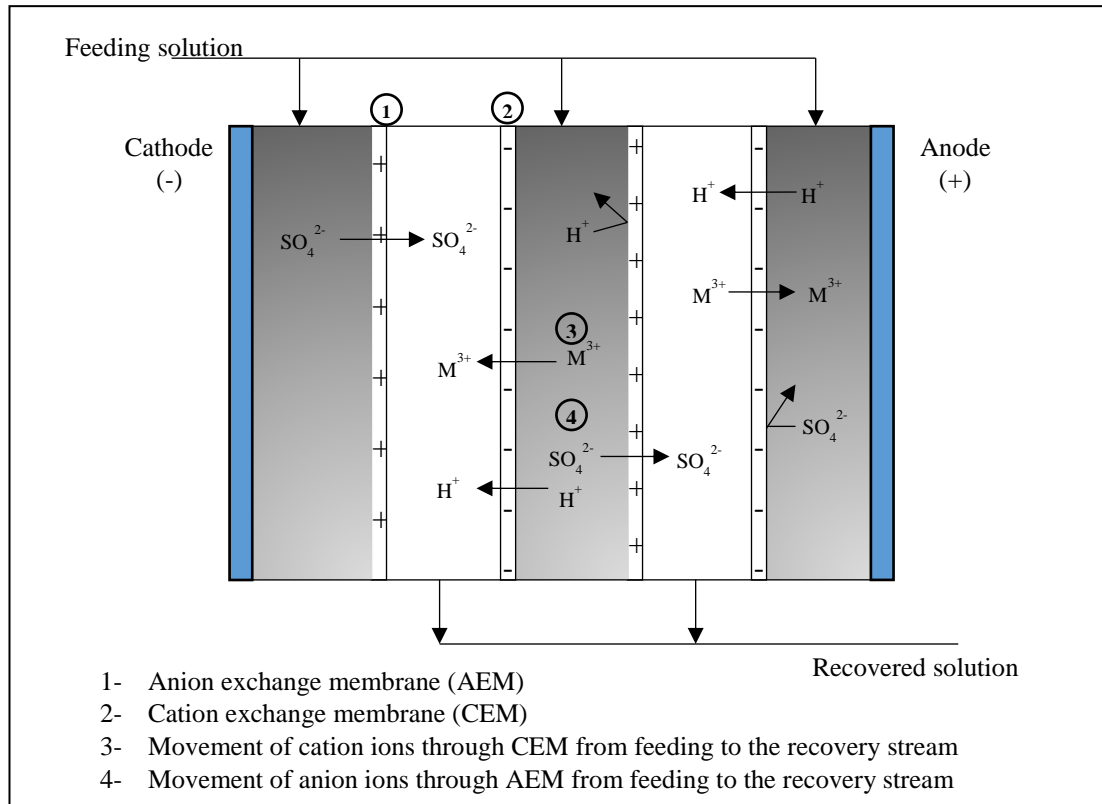


Figure 2.7 Schematic diagram of electrodedialysis process explaining the theoretical recovery process of cation and anion ions.

Table 2.6 Summary of chemical separation technologies (after Keeley et al. 2014a)

Classification	Technology	Principle of operation	Target	Advantages	Disadvantages
	Liquid ion exchange	Mixing organic based extractor with impure acidified sludge. After saturation with metal, the mixture is exposed to dissolution and removing step using an organic solvent (hydrophobic). Finally, metal recovery and organic extractor generating via using acid stripping solution.	- Al recovery - organic matter and heavy metal rejection - the high quality of recovered coagulant	- more than 90% alum recoveries at concentration and quality comparable with a commercial coagulant - Recovered coagulant also has similar water treatment performance in term turbidity and colour removal. - Offering cost reduction	- Possible contamination with organic solvent during the stripping step. - Risk of DBPs formation
Charge-Based Separation	Ion exchange resins	Ion-exchange media with selective adsorption for either anions or cations contaminants. After saturation, stripping attacked ions and generating the resin using sodium hydroxide, forming precipitates of metal hydroxide.	- Manufactured to adsorb cationic contaminants leaving anions in solution stream and vice versa.	- Less toxic to minimise the risk of treatment stream contamination and more simple in comparison with liquid ion extraction. - more than 90% of Al recovery can be achieved - comparable recovered metal purity	- Extraction and stripping are characterised by slow diffusion kinetics, making a limit practical application. - The stoichiometry cost of excess NaOH used for stripping and generating step exceeds the value of recovered coagulant.

Chapter 2: Literature review

Classification	Technology	Principle of operation	Target	Advantages	Disadvantages
	Donnan membrane processes	Ion selectivity in Donnan membrane is driven by the electrochemical difference between the feeding and the recovered side. The recovery side contains a higher concentration of H ⁺ ion than the other side, making differential gradient across the membrane	One-step process to extract and strip the aiming ions simultaneously through the membrane.	<ul style="list-style-type: none"> - fouling minimised on the membrane due to the lack of transmembrane pressure - Possible implementation with plug-flow operation system. - OMs are rejected with mono- and divalent heavy metals by the cation-selective membrane. 	<ul style="list-style-type: none"> - Ions flux through the membrane limits by chemical gradient and the membrane characteristics. - Ionic diffusion rate declines as the process reached equilibrium. - based on diffusion time of 24 h and membrane area of 120 cm²/l, the cost benefit is questionable. - generate acidified waste stream due to the movement direction of acid to the opposite of recovered metal.
	Electrodialysis	The flowing electric current through stacks of the cell containing different solution including the impure acidified solution causes movement of cationic ions away from other ions through cationic membrane toward the cathode.	Providing greater control over process kinetics and process cost, control the applied potential.	<ul style="list-style-type: none"> - Lager than 90% metal recovery. - Organic fouling on the membrane can be managed by ED polarity reversal. - The recovered metals purity and selectivity are comparable to the process used a similar ion-exchange membrane. 	<ul style="list-style-type: none"> - Energy consumption, which can be reduced using high ions concentrations.

Chapter 2: Literature review

Classification	Technology	Principle of operation	Target	Advantages	Disadvantages
				- Acid recovery can be achieved with using less porous membrane (> 90%).	
Pressure-driven membrane	Ultrafiltration (UF), nanofiltration (NF)	Applying high pressure on membrane from acidified feeding side to force trivalent ion to permeate to the recovery side and in same time reject the OM. NF is used to concentrate the recovered coagulant through water permeation only, cooling the retained coagulant to 0°C, forming Al hydroxide, and finally filtering washing alum crystals with cold water to remove OM.	- Achieving high recovered coagulant purity. - offering the lowest cost in comparison with other options.	- Larger than 90% coagulant recovery and total rejected.	- Unavoidable fouling on the pressure driven membrane. - Relatively recovered coagulant contains high organic contaminants.

2.5.4 Coagulant recovery

Several studies have been conducted to investigate coagulant recovery from water treatment sludges. Iron and P separation from P-saturated ferric sludge was successfully conducted by forming ferric sulphide precipitates through adding different molar ratios of S/Fe (Mejia Likosova et al. 2013). A new electrochemical process was proposed to recover and recycle ferric and sulphide from the separated ferric sulphide precipitated (Mejia Likosova et al. 2014). It was found that the novel recovery approach can recover about 40% to 60% of Fe on feeding real and synthetic suspensions respectively.

Due to the potential of raising the level of DBPs in treated water using recovered coagulants, recent studies have focused on the purity and evaluation of the recovered coagulant for use in water treatment, in comparison with commercial coagulant (Keeley et al. 2016). The authors used UF and Donnan dialysis (DD) technologies for coagulant recovery. DOC extraction with alkalization as an initial step before acidification, and additional tertiary polishing step using powder activated carbon (PAC) was suggested. The alkali-acidified Fe sludge provides ferric concentration (874 mg/l) to DOC contaminant concentration (61 mg/l) ratio 14:1, which is the same as from the UF process. DD process provided higher Fe selectivity with concentration of 2555 mg/l and lower DOC contamination (29 mg/l). Dosing 80 mg/l of PAC in the polishing step enabled the DOC content to be reduced to less than 1 mg/l in UF or alkali pre-treatment sludge (Keeley et al. 2016). Also, the authors found that in terms of the Fe recovered; it provided the same water treatment performance in comparison to commercial coagulant.

2.5.5 Phosphorus recovery

Phosphorus is a vital element for agriculture and a number of industrial processes. However, it is a non-renewable resource and its removal via adsorption and subsequent recovery has become a very attractive alternative to chemical addition and biological methods (Gray et al. 2015).

After the adsorbent is saturated with P, physical treatment or chemical treatment can be used to desorb the P desorption from the P-saturated substrates. Drying, agitation

and crushing of P-saturated substrates are the suggested physical techniques for substrate regeneration and P desorption (Drizo et al., 2002; Drizo et al., 2008; Pratt et al., 2009), whilst solvent extraction using acids or bases is suggested as the chemical method (Zhao et al., 2011; Zhao and Zhao, 2009). The physical treatments are mainly aimed at rejuvenating steel slag (Pratt et al. 2009). Zhao and Zhao (2009) investigated the efficiency of P extraction from P-saturated alum water sludge used as a substrate in CWs. The P extraction technique involved 1 to 6 h agitation time for a mixture of 0.8 g of P saturated sludge, and 150 ml of different acids (HCl, HNO₃, and H₂SO₄) or bases (NaOH and KOH) solution with concentration of up to 1 M. They found that both solvent types are efficient for P extraction with extraction, percentage of 98% and the most suitable solvent was sulfuric acid for efficiency, price and safety. However, the extracted P contains significant concentration of metals such as Al, Ca, Fe and Mg, and OC released alongside with P under acid or alkali condition. This makes the reuse of the extracted P for different activities like fertiliser application undesirable. A recent study was conducted aiming at optimising the P and ferric separation conditions, from the P saturated ferric sludge using sulphide to form iron sulphide precipitates. Mejia Likosova et al. (2013) observed that faster iron sulphide separation and higher P recovery were achieved at pH 4, and P recovery increased from 70% to 90% when the S/Fe molar ratio increased from 1.5 to 2.5. Whilst successful results for P and Fe separation has been achieved, no information about other metals and OC contaminants usually present in water sludge, have been reported or investigated.

2.6 Summary

Technologies for P removal from polluted water by various treatment processes have been developed over time to achieve discharge consents, and in order to prevent eutrophication. These processes include chemical-precipitation, biological uptake, chemical-biological removal, and adsorption. Using reactive adsorbents for P removal has advantages over other conventional methods. This is because of their simplicity, high performance and possible nutrient recovery. A wide range of adsorbents have been investigated for their P adsorption capacity. Moreover, looking for low-cost reactive materials makes adsorption process more attractive. Dewatered water treatment sludge is a by-product generated from the use of aluminium and iron

salts in the coagulation-flocculation process during drinking water treatment. DWTS is produced in vast quantities that increases with increasing population growth. DWTS is regarded a reactive material because it is mainly composed of the coagulant used during the water purification. However, the chemical and physical characteristics of DWTS mostly depends on coagulant, polymer and other chemical dosages, and the characteristics of the water source. Several studies have been demonstrated that DWTS has a high affinity for P adsorption, showing variable P adsorption capacity over short and long-term experiments. Whilst this variation in P removal is explained by influence of solution pH, initial P concentration, surface charge of sludge, solid to liquid ratio, HRT, and sludge characteristics, it is noted that considerable research is still needed to investigate the combined effect of solution chemistry and the inherent sludge properties on the P adsorption behaviour.

Long-term experiments have been utilised for characterising P adsorption, and it is also useful to estimate DWTS life expectancy. However, these tests require long time operation to reach the saturation point; they are expensive due to the continuous chemical analysis, and more importantly, they are limited to specific operation conditions of HRT and influent P concentrations. Therefore, short-term evaluation mimicking the long-term is required to consider the variability in inflow wastewater characteristics, and to be able to construct models that can predict the DWTS lifespan under different operational conditions.

The cost of chemical consumption in water treatment, and the disposal of produced sludge is constantly increasing. Finding a new approach for coagulant recovery with comparable characteristics with commercial coagulant, and then recycling the recovered coagulants would reduce the cost of the chemical and the generated sludge volume. If DWTS is utilised as a substrate in CWs system, a beneficial final usage from P-saturated sludge can be as a source for coagulant and P. To recover both resources, one-step separation technology is proposed.

3 Chapter 3 Mechanistic study of P retention by dewatered waterworks sludges¹

3.1 Introduction

Phosphorus removal via adsorption on novel materials and by-products is gaining increased attention as an environmentally friendly and cost-effective means of removing and reducing P in wastewater streams, and enabling its recovery. This chapter focuses on one of such novel by-products, DWTS which is a widely available by-product of drinking water purification processes, and which has been shown to be an effective adsorbent for P (Babatunde et al. 2009). However, while the sludges can retain P and therefore be used as an adsorbent for P removal, there is a need to further investigate the factors that influence their P retention behaviour. This is because drinking water treatment plants use different water sources, and different coagulants and polyelectrolytes; and therefore, they produce sludges with variable elemental compositions and characteristics. Whilst some studies have examined the influence of either solution chemistry or physicochemical characteristics of the sludges on their P retention, an investigation into their combined effects over a wide range of samples from various sources has been limited. This is however crucial for improving our mechanistic understanding of their P retention behaviour, and for their effective use for P removal.

Therefore, the specific objectives of this chapter are (i) to evaluate the physicochemical properties of seventeen DWTSs collected from different sources; and together with the solution chemistry effects, relate these to their P retention behaviour; (ii) to probe the characteristics of P retention by the DWTSs; and (iii) to investigate and determine the mechanisms involved in P retention by the sludges.

¹ This chapter has been published as “Al-Tahmazi, T. and Babatunde, A.O. 2016. Mechanistic study of P retention by dewatered waterworks sludges. *Environmental Technology & Innovation* 6, pp. 38–48”.

3.2 Material and Methods

3.2.1 General Physicochemical characterization

DWTSs were collected from seventeen drinking water treatment works located in the United Kingdom. The date of samples collection was in February 2014. The treatment plant locations are kept anonymous on request, and samples obtained were simply labelled using a sequential alphabetic code generated from the location names. Samples of DWTSs were spread on trays and left to air dry for 3 to 4 weeks. The air-dried samples were then grounded to particle size less than 2 mm. The author did all the analyses procedures followed in this thesis.

To determine the chemical composition, approximately 0.1000 g of air-dried samples was microwaved and acid-digested using an Anton Paar Multiwave 3000 Microwave digester system. The weighted amount of sludge was dissolved in a mixture of 6 ml of hydrochloric acid and nitric acid with volume ratio 1:1 (HCl:HNO₃), and then digested in a microwave for 30 min with a temperature 200 °C. The vessel content was left to cool down and then diluted with deionized water up to 50 ml. The diluted sample was analysed using inductively coupled plasma atomic emission spectroscopy (ICP-AES) (Perkin Elmer Optima 2100D). The mass of metal to the mass of sludge in unit of mg/g was calculated from the final volume after dilution (50 ml), measured concentration (mg/l) from ICP, and used amount of sludge sample (g).

Chloride, sulphate and dissolved calcium ions were determined by the extracted amount of air-dried sludge with deionized water at 1:10 solid:liquid ratio for 4 hours, followed by filtration using 0.45 µm membrane filters. The chloride and sulphate ions were measured using Ion Chromatography (ICS – 2000 Ion Chromatography system), while Ca concentration was measured using ICP-AES. The mass of the measured elements to the mass of sludge used was calculated using the same procedure as for the acid digestion samples.

Total carbon (TC) and OC were determined by Total Organic Carbon Analyzer (TOC-V CSH (Shimadzu)). A pre-weighed amount of air-dried sludge was put in 1000°C burned ceramic vessel (to ensure no carbon source). Total carbon and

inorganic carbon (IC) were measured, and the difference between these two readings was taken as the OC.

The pH of the sludges was determined following the British Standards Institution method (British Standards Institution 1990). Thirty gram of air-dried sludge with particle size < 2 mm was stirred for few minutes with 75 ml deionized water. The mixture was covered and allowed to stand for at least 8 h. Thereafter, the pH was taken using a three-point calibration pH meter.

The SSA represents the area of cation exchange capacity in the mass of soil, expressed in units of m^2/g . SSA values depend on the minerals content, organic content and particle size distribution of soil, leading to varying values between soils. SSA was measured in the sludges in a wet condition using Ethylene Glycol Monoethyl Ether (EGME) method following the procedures of Cerato and Lutenegger (2002). Firstly, a mass of sludge passed through the 420 μ m sieve size was oven dried at 110 °C for 24 h to remove any water content. About 1g of the oven-dried sludge was placed in aluminium tare. An electronic balance with an accuracy of 0.001 g was used throughout the experimental procedure. Two millilitre of EGME was added to the sludge using a pipette; and this was enough to form a uniform slurry after gently mixing by a hand swirling motion. The tare was placed inside a standard laboratory glass sealed vacuum desiccator which contains calcium chloride and EGME desiccant. A lid was placed on top of each tare with about 2mm air cap to prevent soil from being pulled out of the tare during the evacuation process. The vacuum pressure of 630 mm Hg was provided using a vacuum pump. The tare was removed after 8 to 10 h to determine sludge-EGME mixture. After 18, 24 and 28 h, the weighing step was repeated again until the variation in the weight was less than or equal to 0.001 g. After achieving a constant weight, the SSA was calculated using Equation 3.1.

$$SSA = \frac{W_a}{0.000286 * W_s} \quad 3.1$$

where: SSA is specific surface area (m^2/g), W_a is the weight of ethylene glycol monoethyl ether (EGME) retained by the sample in grammes, and calculated based on the difference between the final slurry weight and weight of soil added initially

(W_s) in grammes. The factor of 0.000286 is the weight of EGME required to form a monomolecular layer on a square meter of surface (g/ m^2).

The morphological structure of the sludges was examined via X-ray diffraction (XRD) analysis using a Phillips PW3830 X-ray generator with a Phillips Pw1710 controller; the scattering angles ranged from 2° to 80° 2θ with scanning speed at 0.02° 2θ per 0.5 seconds.

To quantify the amorphous Al and Fe oxides of the sludges, ammonium oxalate-extractable Al and Fe were measured according to the method described by McKeague and Day (1966). 0.25 g of DWTS was solubilized in 10 ml of 0.2 M acidified ammonium oxalate using 50 ml conical centrifuge tubes. After the tubes were stoppered, they were then wrapped with aluminium foil to prevent light passing through them. They were then placed horizontally in a shaker at 50 rpm shaking speed for 4 h. Thereafter, the tubes were centrifuged at 1800 rpm for 20 min. An aliquot was then taken and analysed for Al, Fe and P using ICP after destroying the OM through digestion with drops of HNO_3 and sulfuric acid (H_2SO_4).

3.2.2 Adsorption isotherm study

Adsorption test procedure using short-term batch experiments is described in chapter four (Section 4.2.1). Phosphorus adsorption maxima and the adsorption constants calculated are also detailed in Chapter 4 - Section 4.2.1.

3.2.3 P retention – Mechanism and linkage with inherent properties

3.2.3.1 Exchangeable ions and Precipitation tests

In order to investigate the possible mechanism of P retention by the sludges, through calcium phosphate precipitation and/or adsorption to the precipitated aluminium and iron oxides, exchangeable ions and precipitation tests were carried out. For the exchangeable ions test, the leachability of Ca, Al and Fe from the sludges was determined by shaking 1g each of the sludge samples in 100 ml of deionized water at three initial pH solutions (4, 7 and 9), and for 48 h at room temperature. The pH at the time of equilibrium was determined using a pH meter, and the samples were then filtered using $0.45 \mu\text{m}$ membrane filters. The supernatants were analysed for Al, Ca,

Fe, magnesium (Mg) and P using ICP-AES; and then these leached concentrations were used as background concentration for the precipitation test before adding P.

A precipitation test was then conducted to determine at which pH and Ca and P concentrations, the calcium phosphate precipitation might occur. The tests were performed in conditions simulating the P adsorption experiments. Aliquots of 100 ml of deionized water were placed in 200 ml acid-washed polyethylene bottles and then agitated with different concentration of Ca and/or Fe (the concentration of Ca and/or Fe was determined based on the result of the exchangeable test, wherein some sludges leached Ca while some leached both Ca and Fe). Thereafter, pH was adjusted using hydrochloric acid (0.01M) and potassium hydroxide (0.1M), prior to adding the P stock solution. The mixtures were then agitated on a rotary shaker for 48h before being filtered using 0.45 μm membrane filter, and then analysed for Ca, Fe and P. Any reduction in the concentrations of Ca, Fe and P after the reaction time would indicate a reaction is taking place. To further probe the reaction taking place and the possible mechanism, samples of the sludges before and after reaction with the P stock solution were examined using Fourier transform infrared spectroscopy (FTIR); the spectrum was scanned from 500 to 4000 cm^{-1} .

3.2.3.2 Linkage with inherent properties

To identify which of the measured sludge properties gives the most explanation of variance in P retention (uptake and maximum), a multiple linear regression analysis was conducted. Pearson's correlation coefficients were computed to find out if there is a high correlation between the physicochemical properties of the dewatered sludges. Due to the high correlations found between the measured physicochemical properties of the seventeen dewatered sludges, rotated principal component analysis (PCA) was performed using varimax rotation method, in order to reduce the number of predictor variables which are highly correlated (multicollinearity) from eleven single variables to three uncorrelated linearly principal components. The produced component scores were then used as predictors (independent variables) in addition to the initial pH of the solution in a multiple linear regression model (entry method was applied). P uptake at seven initial P concentrations, Phosphorus adsorption maxima and Freundlich constant were chosen as the outcome (dependent) variables.

IBM SPSS statistic software (version 20) was used for statistical analyses. The Shapiro-Wilk's test and data visualisation by histograms, normal Q-Q plots and box plots were used to assess the normal distribution of the experimental data. Where data were not normally distributed, a transformation was performed in order to obtain a normal distribution.

3.3 Results and discussion

3.3.1 General physicochemical characterization

The dewatered waterworks sludges had highly variable physicochemical properties (see Table 3.1). The main constituent of the sludges by percentage weight was either aluminium (0.39 – 15.2) % or iron (0.59 – 29.8) %. It was evident that the Al and Fe contents of the sludges were dependent on the primary coagulant used during the water treatment process. Ten of the sludges were Fe-based, and the rest (including one sludge which contains both Al and Fe) were Al-based. The SSA of the sludges ranged from 97 to 468 m²/g (see Table 3.1).

TC and OC of the Al- and Fe-based sludges ranged from 53.7 to 177.4 and 53.1 to 177.4 mg/g, respectively, as shown in Table 3.1. In addition, it can be seen that there was negligible difference between the TC and OC content of the sludges. This implies that the content of most common inorganic carbon in the sludges, i.e. calcium carbonate and calcium magnesium carbonate is minimal. TC has an adverse impact on the P adsorption capacity of dewatered sludges by retarding P diffusion into the micropores, as reported elsewhere (Makris et al. 2005a). However, Yang et al. (2006b) found that during the adsorption process, OC exchanges with P which replaces it on the surface of the sludges, thus implying that more exchangeable OC can enhance P retention by the sludges. In our study, it was not possible to isolate the effect of TC and OC on P retention; however, results of the FTIR test shows that the carboxyl group bands were changed after the sludges reacted with P, indicating the replacement of OC with phosphate ions on the surface of the sludge.

The morphological structure of the seventeen sludges did not show any sharp peak of aluminium and iron metals in the XRD spectrums as shown in Figure 3.1. However, the XRD diffraction patterns reveal sharp diffraction characteristic (peaks) for GU,

BS, HO, CA, AR, HU, SF and CF sludges; and these were defined as quartz for HO, HU and CF; graphite and iron-molybdenum for GU; Lithium phosphate and calcium manganese oxide for CA; cronosite and lavendulan for AR, graphite for SF and mica and nimitite-1 in addition to quartz for CF (see Figure 3.1 and Table 3.1). Interestingly, the two mineral peaks (mica and nimitite-1) of CF, which is a Fe-based sludge, contain iron and aluminium ions. This indicates that the iron and aluminium metals alloys are in crystalline form. This might impact on the adsorption behaviour of the CF sludge via reduction of the available reactive surfaces for P retention. In addition, the two crystalline peaks of graphite from carbon for GU and SF, which are both Al-based sludges, would suggest reducing cation and anion ions leachability from these sludges, and this could restrict the adsorption process into aluminium oxide, especially for the SF sludge which has a high TC content.

In general, XRD patterns for the sludges showed apparent poorly ordered particle distribution of Al and Fe minerals within the Al- and Fe-based sludges (except CF); this implies that the Al and Fe sludges are in the amorphous phases. Amorphous oxide phases are assumed to be extracted with acidified ammonium oxalate and associated with the non-crystalline phase of metal oxides. Thus, the quantity of Al_{oxa} and Fe_{oxa} in the sludges was determined using this method. Results show that the amorphous Al and Fe oxides represent 61.9 to 97.6% of total Al for the Al-based sludges, and 39.2 to 65.3% of total Fe for the Fe-based sludges (see Table 3.1). Phosphorus uptake is strongly linked to amorphous Al and Fe concentrations and the variation in oxalate extractable Al and Fe has been shown to account for differences in P retention by dewatered waterworks sludges (Elliott et al. 2002; Dayton and Basta 2005).

Chapter 3: Mechanistic study of P retention by dewatered waterworks sludges

Table 3.1 Physicochemical properties of the seventeen dewatered waterworks sludges.

Properties	Iron-based sludges										Aluminium-based sludges							
	BS	MO	CA	FO	HH	AR	WY	BU	CF	BG	GU	HO	WD	OS	HU	WA	SF	
Al	4.59	3.89	6.80	21.16	5.16	5.87	4.84	5.80	50.05	7.71	112.81	65.35	104.22	105.34	151.88	108.78	122.29	
Ca	6.83	2.65	3.33	3.17	3.06	24.87	0.89	1.47	12.56	6.67	1.16	1.90	1.80	0.88	3.21	0.93	0.63	
Fe	298.10	257.80	255.46	241.69	193.85	277.72	287.34	212.09	245.79	257.99	17.00	143.29	9.75	28.73	8.25	5.94	13.91	
P	0.61	0.39	0.29	0.43	0.44	0.35	0.77	0.61	3.19	1.70	0.24	0.65	0.70	0.60	4.78	0.68	0.47	
Mg	0.47	0.20	0.43	0.25	0.81	0.28	0.23	0.31	9.15	0.47	0.66	1.38	0.44	0.79	0.97	0.57	0.20	
Mn	0.94	0.79	0.45	2.32	0.37	0.52	1.28	0.17	1.55	1.27	0.33	0.57	0.29	0.40	0.66	0.43	0.42	
Zn	0.19	0.40	0.09	0.09	1.85	0.08	0.16	1.74	0.28	0.50	1.02	1.71	0.47	1.71	0.12	1.22	0.84	
Al_{oxa}	1.14	1.85	1.02	17.36	1.36	2.99	3.46	4.67	2.62	4.14	110.12	58.63	95.28	88.26	105.51	96.02	75.68	
Fe_{oxa}	143.08	149.52	144.48	121.33	121.38	113.63	146.37	138.48	118.09	101.10	13.35	72.41	3.68	14.42	2.52	4.64	6.96	
P_{oxa}	0.23	0.24	0.28	0.23	0.30	0.21	0.34	0.25	0.24	0.52	0.22	0.34	0.28	0.27	0.69	0.30	0.28	
Cl⁻	0.22	0.16	0.21	0.30	0.33	0.59	0.27	0.22	0.76	0.48	0.11	0.16	0.24	0.11	0.22	0.14	0.56	
SO₄	4.06	6.93	7.45	4.26	4.51	6.32	8.55	2.81	0.71	0.22	0.81	3.86	1.88	1.19	2.72	0.33	0.26	
TC	110.8	117.4	115.9	137.	161.9	88.62	113.7	154	53.7	144.4	119.6	105.2	119.6	170.6	75.21	154.4	177.4	
OC	110.8	117.4	115.9	137	161.9	88.62	113.7	153.6	53.1	144.4	118.9	105.2	119.1	170.1	74.2	154	177.4	
SSA	m ² /g	203.4	186.4	219.8	120.3	131.9	97.02	132.3	157.2	296.3	125.2	364.1	414.5	468	206.9	390.4	210.1	181.8
EC	μs/cm	522.8	488.3	410.7	378	375.8	1239.3	843.4	828	1073.1	471.1	455.5	665.7	723.1	421.3	541.5	688	329.2
PH	---	5.47	4.48	4.09	5.49	4.55	6.64	4.3	4.75	6.99	5.89	6.26	5.49	6.27	6.05	7.06	6.31	6.13
Crystalline minerals		Lithium boride	---	Lithium phosphate, Calcium	---	---	Cronusite, Lavendulen	---	---	Quartz, Mica, Nimite-1	---	Graphite, Iron Molybdenum	Quartz	---	---	Quartz	---	Graphite

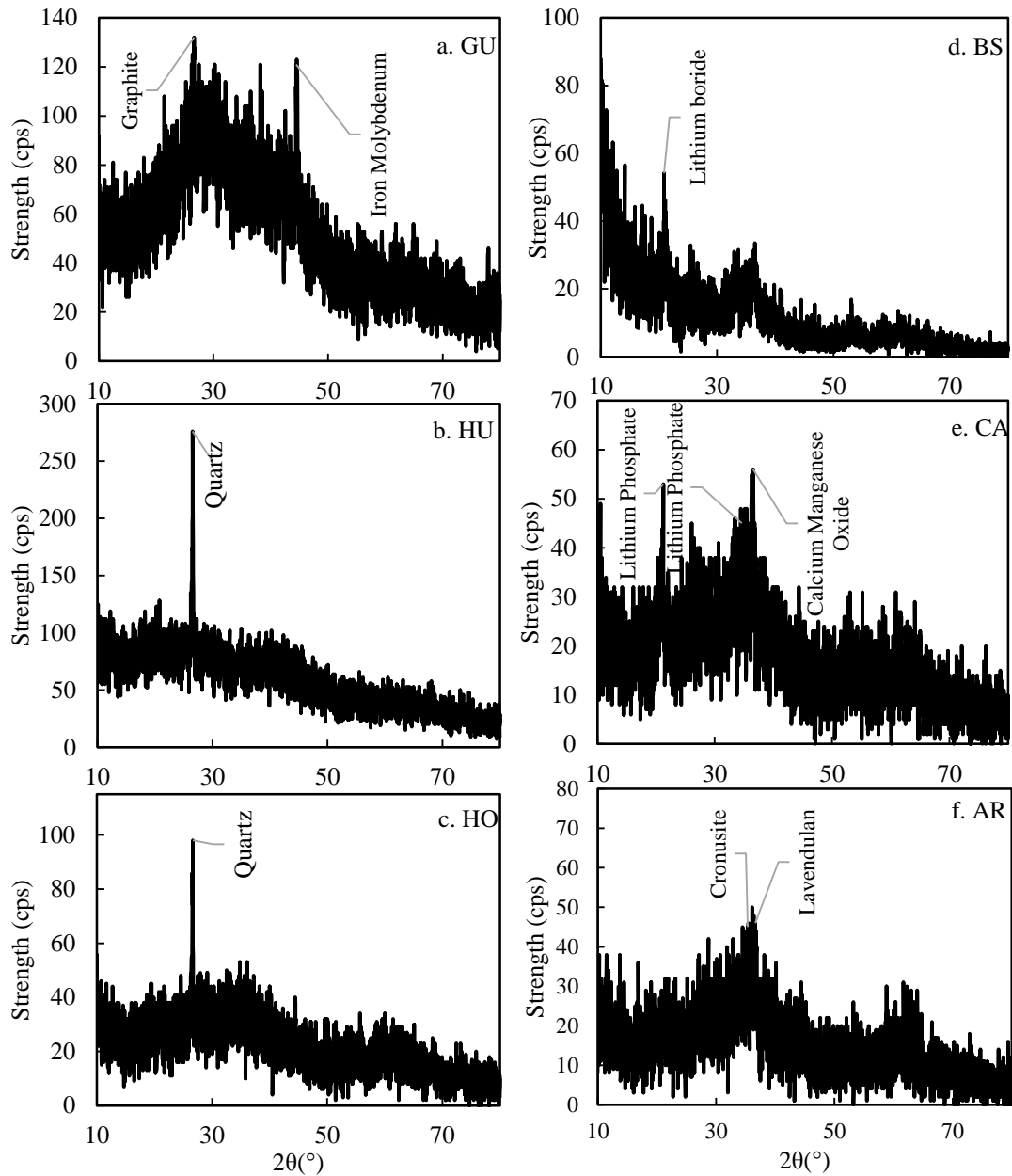


Figure 3.1 XRD patterns of three Al-based sludges (a-c) and three Fe-based sludges (d-f).

3.3.2 Adsorption isotherm study

Figure 3.2 shows the isotherms of P uptake by the sludges. For ease of comparison, the Al- and Fe-based sludges were grouped separately. To determine if there was any significant difference in P uptake between the sludges, a one-way ANOVA test was conducted. The results revealed significant differences in P uptake between the sludges ($p=0.002$), with higher P uptake values obtained for the Al-based sludges. These findings are consistent with those of Makris et al. (2005b) who studied the P

sorption/desorption characteristics and kinetics for seven dewatered waterworks sludges, and found that the Al-based sludges had higher adsorption capacity than the Fe-based sludges.

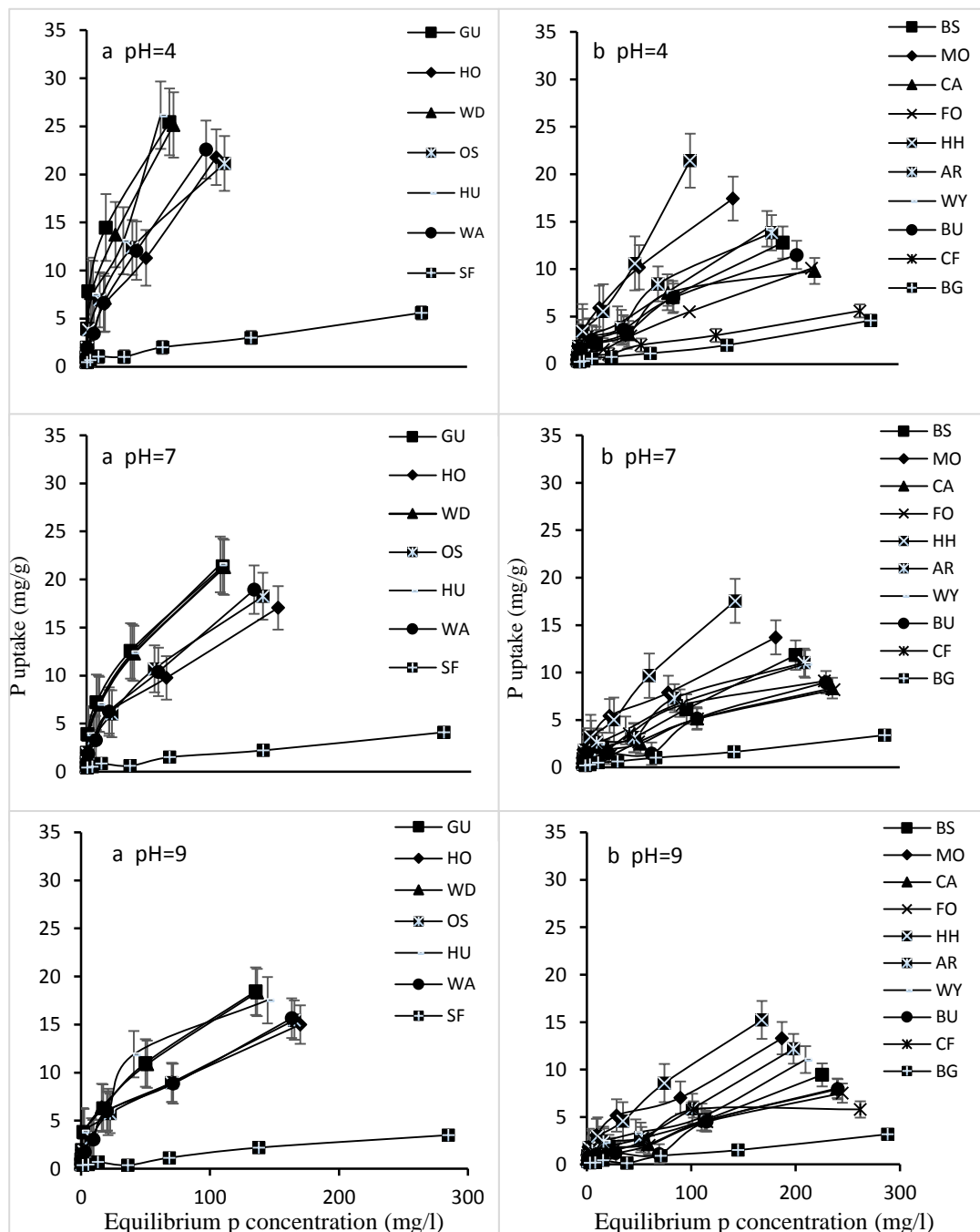


Figure 3.2 Isotherms of P uptake by the seventeen dewatered water sludges (at initial pHs of 4, 7 and 9; $t=48$ hours; plots on the left and right refer to, respectively aluminium- and iron-based sludges). (Y-axes are amended to maximum scale of 35).

Further data analyses show that the P adsorption data were well fitted with the Freundlich model, and that the adsorption density value for all the sludges was > 1 and ranged from 1.40 to 2.79. For most sludges, the bonding energy-related constant decreased as the adsorption density increased, in accordance with preferential adsorption occupying surface sites, in order from strongest to weakest binding strength (Apak 2013).

Phosphorus adsorption capacities obtained from the fitting of the Langmuir model (Figure 3.3) generally showed that the sludges had variable adsorption capacities which increased with decrease initial pH solution. This suggests that P adsorption by the sludges is favourable under acidic conditions. To compare the P adsorption capacity (as determined by the Langmuir model for those sludges with good fitting); a one-way ANOVA analysis was used. The results of the test showed that there was a significant difference in adsorption capacities between the Al- and Fe-based sludges ($P < 0.001$). This is in agreement with Makris et al. (2005b), who showed higher P adsorption capacity for Al-based sludge than Fe-based sludges. Elliott et al. (2002) also reported similar findings in P adsorption between Al- and Fe-based sludges. In addition, the adsorption capacity is related with SSA, which, in turn, depends on the metal oxide. Makris et al. (2004a) found that Al-based sludges have higher SSA than Fe-based sludges, resulting in differences in their adsorption capacities. In our study, higher SSA and P adsorption capacity were found for Al-based sludges with the exception of SF sludge. The SF sludge has the highest carbon content (crystalline – graphite) which restricts the contact surfaces available for P retention.

3.3.3 P retention – Mechanisms

Table 3.2 presents results of the exchangeable ions test. Results show that the cation concentrations decreased as the initial solution pH increased. The pH at equilibrium was either increased or decreased relative to the initial pH. This could be explained by the fact that during agitation, the hydroxyl groups on the surface of the sludge, and also the cations and anions (as Ca, Mg, Cl⁻, SO₄²⁻, TOC) released into the solution, influence the increase or decrease of the pH from its initial value. The P released from the sludges was low across the three initial pHs. This P originates from the raw water and becomes part of the structure of the dewatered sludges, and it is

minimally released over time (Makris 2004). The concentration of Ca released across the three initial pHs was generally higher than that observed for the other cations, and it ranged from 3.0 mg/l to 34.5 mg/l at initial pH 4. The amount of exchangeable Ca was proportional to the Ca content of the sludges with the exception of GU and SF, both of which contain carbon as graphite (crystalline), resulting in low exchangeable ions. In addition, significant Fe concentrations were observed for BS, CA, HH and WY sludges with 1.38; 3.73; 2.36 and 1.54 mg/l of Fe respectively at initial pH 4. The pHs were acidic for most of the sludges except for AR, HU and CF which all had approximately neutral equilibrium pH. The neutral pH of the three sludges results from the combination of the initial pH and pH at equilibrium, combined with increased Ca concentration which might then encourage calcium phosphate precipitation (Del Bubba et al., 2003).

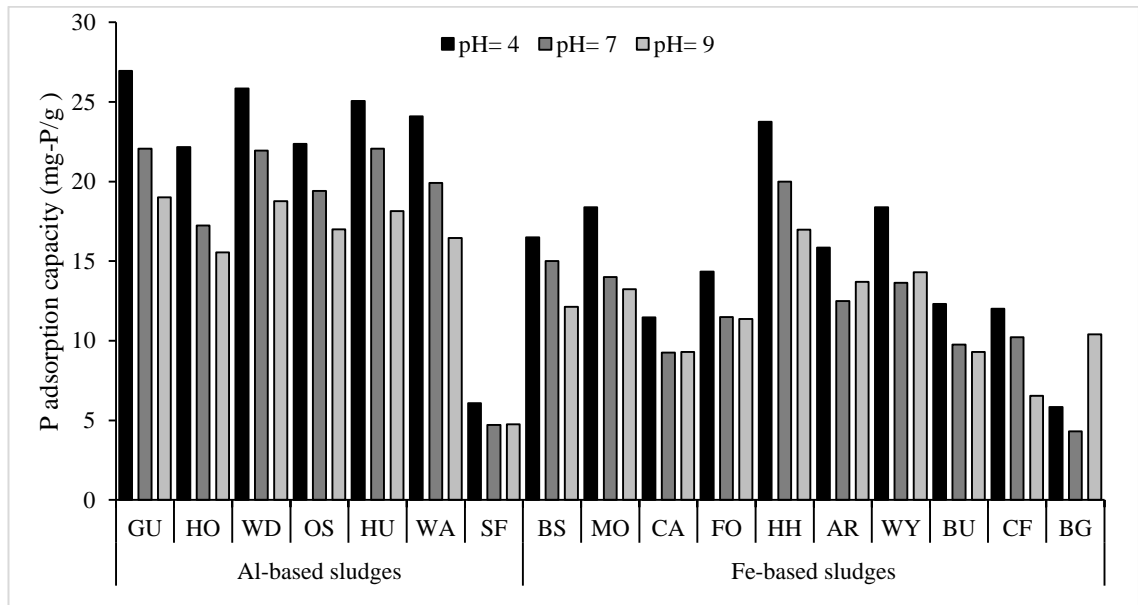


Figure 3.3 P adsorption capacities of Al- and Fe-based sludges calculated from fitting Langmuir model at three initial pH solution values.

Table 3.2 Equilibrium pH and the released concentrations of aluminium, iron, calcium, magnesium and phosphorus after agitating 1g of each sludge in 100 ml of deionized water with three initial pH values for 48 h (n=2).

sludge	pH* 4						pH* 7						pH* 9						
	pH**	Al mg/l	Ca mg/l	Fe mg/l	Mg mg/l	P mg/l	PH**	Al mg/l	Ca mg/l	Fe mg/l	Mg mg/l	P mg/l	PH**	Al mg/l	Ca mg/l	Fe mg/l	Mg mg/l	P mg/l	
Iron-based sludges	BS	5.15	0.024	13.17	1.381	1.251	0.413	5.23	0.038	11.95	1.31	1.179	0.407	5.25	0.028	11.3	1.167	1.127	0.381
	MO	4.28	0.346	6.679	0.909	0.709	0.384	4.35	0.259	6.141	0.892	0.701	0.378	4.38	0.235	6.072	0.889	0.714	0.373
	CA	4.25	0.554	12.28	3.734	1.068	0.355	4.28	0.442	11.58	3.526	1.035	0.354	4.29	0.43	11.73	3.567	1.03	0.334
	FO	5.35	0.032	8.923	0.035	0.724	0.402	5.52	0.031	7.541	0.068	0.72	0.395	5.53	0.029	6.494	0.086	0.593	0.379
	HH	4.93	0.319	4.596	2.363	0.594	0.382	5.05	0.222	3.138	2.161	0.425	0.376	5.06	0.291	3.707	2.619	0.488	0.366
	AR	7.33	0.033	34.50	1.081	0.524	0.388	7.41	0.021	33.88	0.959	0.504	0.379	7.42	0.007	33.21	0.612	0.5	0.375
	WY	3.85	0.669	6.495	1.541	0.581	0.392	3.96	0.657	6.028	1.497	0.561	0.342	3.96	0.542	5.823	1.357	0.521	0.334
	BU	4.15	0.635	5.841	0.400	0.718	0.351	4.25	0.425	5.459	0.33	0.706	0.347	4.29	0.349	5.444	0.303	0.699	0.312
	CF	7.46	0.045	13.64	0.195	0.938	0.396	7.58	0.032	10.14	0.065	0.761	0.395	7.59	0.026	9.388	0.051	0.692	0.371
Aluminium-based sludges	BG	6.50	0.04	3.431	0.098	0.423	0.378	6.64	0.032	2.361	0.094	0.332	0.378	6.66	0.029	2.325	0.047	0.327	0.356
	GU	5.93	0.027	4.345	0.003	0.447	0.549	6.07	0.018	3.228	0.001	0.428	0.441	6.08	0.016	2.939	0.001	0.411	0.402
	HO	5.36	0.121	11.94	0.146	0.928	0.391	5.49	0.095	11.21	0.095	0.875	0.375	5.47	0.075	10.11	0.064	0.888	0.357
	WD	5.76	0.045	7.778	0.0012	0.919	0.377	5.98	0.015	6.929	0.0011	0.92	0.353	6.11	0.017	7.299	0.001	0.911	0.352
	OS	5.37	0.072	3.955	0.009	0.704	0.38	5.74	0.028	2.709	0.008	0.601	0.371	5.75	0.027	2.822	0.0075	0.597	0.326
	HU	7.08	0.011	12.06	0.001	0.944	0.4	7.10	0.01	11.43	0.001	0.981	0.398	7.15	0.01	10.9	0.001	0.981	0.392
	WA	4.75	1.58	5.257	0.006	0.489	0.346	4.81	0.932	5.049	0.005	0.497	0.344	4.81	0.916	4.736	0.003	0.463	0.299
SF	4.87	0.051	2.964	0.003	0.938	0.621	5.89	0.042	2.404	0.002	0.227	0.548	5.99	0.04	2.213	0.001	0.215	0.401	

* initial pH solution, ** pH at equilibrium time (after 48 hrs agitation)

Furthermore, a precipitation test was conducted to determine the conditions of pH, Ca, Fe and P concentrations, which might cause phosphate precipitation. To decide which equilibrium pH, and Ca and Fe concentrations across the three initial pHs should be used in the precipitation test; a one-way ANOVA analysis was performed to find out if there are any significant differences in these values across the initial pHs. The results showed that there were no significant differences in the variation of the pH at equilibrium and at the Ca and Fe concentrations ($p > 0.05$). Thus, different samples with different pH values and Ca and Fe concentrations were used depending on the exchangeable ions test results; while the P concentration values used were based on the change in P uptake over the range of initial P concentrations. Results obtained (Table 3.3) indicate that no significant changes between the initial and final concentration of both Ca and P to precipitate calcium phosphate minerals occurred at pH less than 7.3. Whereas at $\text{pH} > 7.3$, preliminary phosphate retention via precipitation mechanism was found at high initial P concentrations. Based on the molar ratio of Ca to P (0.5), it can be proposed that monocalcium phosphate was the precipitated metal. The formation of monocalcium phosphate metal is dependent on the availability of phosphoric acid (H_3PO_4), which is one of the orthophosphate species; in addition to calcium at the alkaline condition. The amount of H_3PO_4 is minimal at neutral to alkaline pH solution. Thus, the calcium phosphate precipitation in this study can be considered to be minimal. The P precipitation retention mechanism as calcium phosphate minerals will spontaneously occur, and it is the dominant mechanism at $\text{pH} > 8$ (Khelifi et al. 2002; Sjøvik and Kløve 2005). In this study, high equilibrium pH (> 7.3) was observed for AR and CF sludges, both of which also have the highest Ca content (Table 3.1) and exchangeable Ca (Table 3.2). In these conditions, P retention by calcium phosphate precipitation is minimal, and P adsorption by Al and Fe oxides are the possible primary mechanisms for the AR and CF sludges.

For samples that contained Fe ions, prior to reaction with the phosphate ions; the initial Fe precipitated as iron oxides when the dissolved Fe had reacted with sodium hydroxide ions which had been added for pH adjustment. Thus, the final Fe concentrations were minimal and below the limit of detection. After adding the P stock solution, the iron precipitates have the ability to adsorb phosphate ions via

surface complexation mechanism through the formation of inner-sphere and/or outer sphere complexes with the iron precipitates.

Table 3.3 Precipitation test with different initial pH values and Ca and p concentrations.

PH	Initial Ca (mg/l)	Final Ca (mg/l)	Initial Fe (mg/l)	Final Fe (mg/l)	Initial p (mg/l)	Final P (mg/l)	Molar ration (Ca/p)
5.115	14.53	13.54	1.167	0	85.6	77.4	0.09
5.247	12.44	10.14	1.381	0	171.2	143	0.06
5.37	12.97	12.67	---	---	42.8	39.3	0.07
4.267	13.44	12.47	3.734	0	85.6	75.1	0.07
4.328	12.89	8.528	3.567	0	322.1	287.2	0.10
6.159	8.23	6.561	---	---	171.2	152	0.07
5.431	10.13	9.009	---	---	42.8	39.2	0.24
4.905	2.596	2.683	4.596	0	42.8	37.4	0.00
7.361	34.61	29.2	---	---	85.6	77.3	0.50
7.156	33.57	26.27	---	---	171.2	152	0.29
7.05	13.58	11.03	---	---	171.2	152	0.10
3.911	6.361	5.429	---	---	171.2	152	0.04
4.741	5.334	3.51	---	---	322.1	276.7	0.03
7.626	11.82	8.95	---	---	42.8	38.5	0.52
6.715	2.585	2.594	---	---	42.8	40.5	0.00

The P retention mechanism was further investigated by analysing the FTIR spectra of the sludges before and after reaction with the phosphate ions (Figure 3.4). Results reveal that without phosphate adsorption, the FTIR spectra of the sludges had a strong hydroxyl stretching (e.g. 3200 cm⁻¹ for BS and HU), and bending (1558 cm⁻¹ for BS and HU) vibrations, which are due to physically adsorbed water molecules; while the band at 1413 and 1386 cm⁻¹ could be assigned to stretching vibration of C-O and deformation vibration of C-H for carboxyl functional groups (Izquierdo et al. 2012). In addition, deformation vibrations of multi-centred hydroxyl groups of iron and aluminium oxides (Fe-OH, Al-OH) of the sludges were observed at 1028 cm⁻¹ bands for the Fe-based sludge, and two bands of 1066 and 977 cm⁻¹ for the Al-based sludges (Zhang et al., 2007). After reaction with phosphate ions, the FTIR spectrums

of the sludges showed noticeable changes. The peaks of physically adsorbed water and stretching and deformation of carboxyl groups became broad and intensive, and this is attributed to replacement of H₂O, C-O and C-H during the phosphate adsorption. Moreover, the peaks of bending vibration of multi-centred hydroxyl groups for Fe-OH and Al-OH completely disappeared, while a new broad and intensive peak appeared at 1018 and 1004 cm⁻¹ for Fe and Al oxides, respectively. This peak could be attributed to the formation of inner-sphere surface complexation between phosphate ions and oxides (Persson et al. 1996), and outer sphere surface by exchanging phosphate ions with a hydroxyl group on the surface of dewatered sludge. The FTIR results indicate that the surface complexation of inner and outer sphere played a key role in the adsorption mechanism.

3.3.4 P retention –Linkage with inherent properties

The results of the principal component analysis are presented in Table 3.4. The properties which combine in the same principal component (PC) could be identified as: PC1- metal content and SSA - related component (high loadings for Al, Fe, Al_{oxa}, Fe_{oxa} and SSA, total variance = 42.75%); PC2- Ca content, dissolved Ca (Ca_{ex}), TC, total organic carbon (TOC) related component (total variance = 34.56%); and PC3 - SO₄²⁻ content and sludge pH related component (total variance = 16.48%). Combined, the three PCs could explain 93.8% of the total variance in the physicochemical characteristics. The scores of the three PCs and initial pH of the incubation solution were then used as predictors in multiple regression analysis, where the outcome variable was the amount of P removed at different initial P concentrations. The largest and most significant explanation for the variability of P removal was found at initial P concentration of 80 mg/l. When PC1 was entered first, it accounted for 52.9% of the variance in P-uptake ($p < 0.001$). When PC2 was entered next to the model, an additional 4.5% significant P removal was recorded ($p < 0.05$); and when PC3 and the initial pH of incubation solution were entered, a 2.9% and 4.4% explanation, respectively, of significant variability in P-uptake ($p < 0.05$) was obtained.

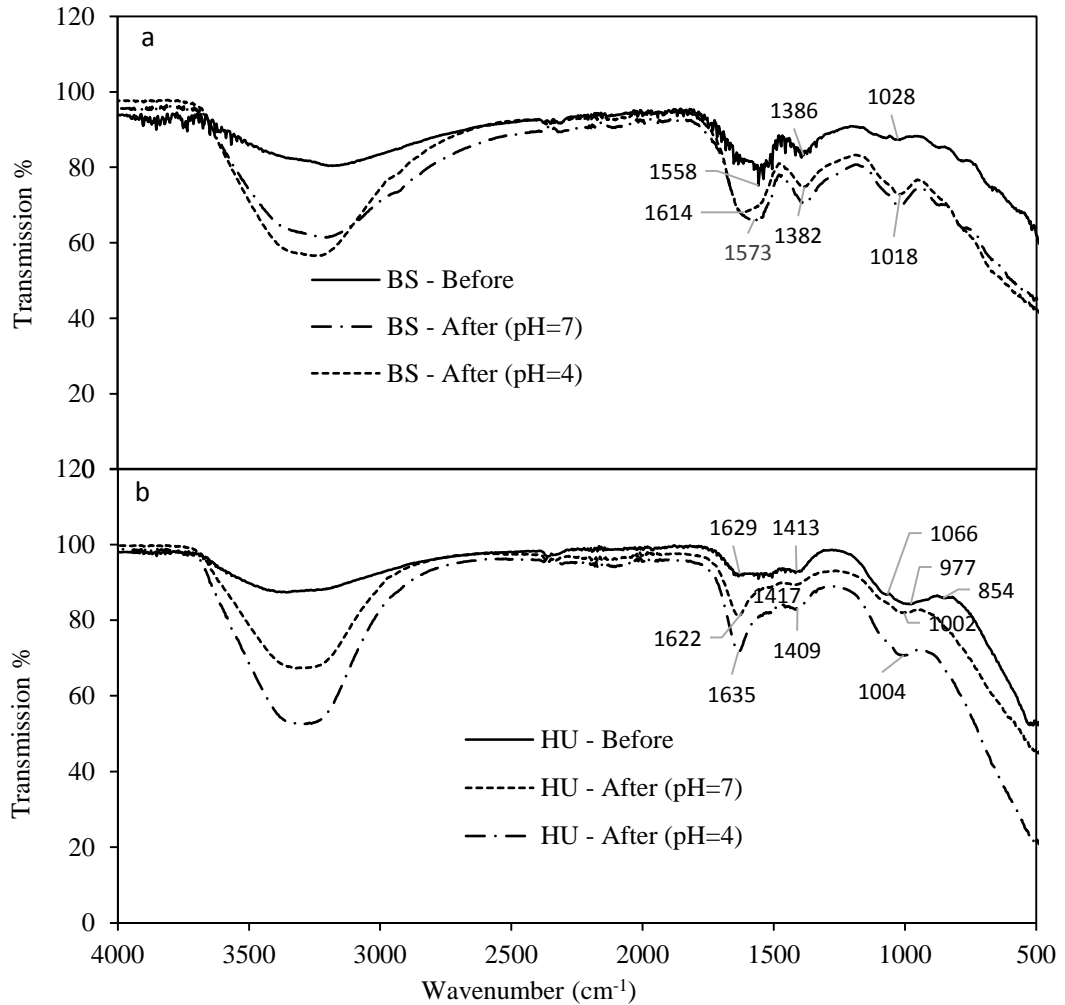


Figure 3.4 FTIR spectra of (a) Fe-based sludge and (b) Al-based sludge before and after adsorption test with 10 mg/l initial P concentration at pH 4 and 7.

Thus, the total significant variance in P-uptake in the linear regression model that could be explained by these characteristics of the sludges and initial pH solution was 64.6% ($p < 0.001$). In the case of 160 mg/l and 320mg/l initial P concentrations, the multiple linear regression analysis exhibited a similar pattern, but the total explainable variance in P-uptake became less by excluding the effect of sulphate content and pH related component (PC3). By following the same procedure for the lower initial P concentration, the total explainable variance in P-uptakes by the three predictors (initial pH solution was excluded) increased with increasing initial P concentration except for the P-uptake at 5 mg/l initial P concentration. At 5 mg/l, PC3 and initial pH solution were not significantly linked to the P-uptake and the metal content related factor; and the Ca, Ca_{ex}, TC and TOC related factor combined

together, explained 55.9% in the variance in P-uptake. The metal content related component (PC1) was the most significant predictor in explaining the variance in P-uptakes across the initial P concentration.

The same procedure above was used to determine the physicochemical characteristics of the sludges which had the most effect on the maximum P adsorption capacity, as calculated by the Langmuir model. The scores of the three PCs and the initial solution pH were used as predictors in multiple linear regression analysis, where the calculated P adsorption capacity was used as the outcome variable. Combined together, PC1 and initial solution pH accounted for 44.8% significant variability of calculated P adsorption maxima, while PC2 and PC3 were not significantly correlated with the P adsorption maxima. As discussed previously, the best fit for adsorption data for all the sludges at the three pHs was given by Freundlich model. Therefore, to identify which of the physicochemical properties of the sludges had the most effect on the Freundlich bonding energy-related parameter (K_f), the same procedure above was used. The metal content and SSA related component (PC1); Ca content, exchangeable Ca, TC and OC related component (PC2), and initial solution pH were significantly related to K_f Freundlich parameter. A total 78.4% of variability in K_f ($p < 0.001$) was explained by these predictors at significant levels < 0.001 , < 0.01 , and < 0.01 , respectively. The significant variances in P-uptakes and adsorption parameters explained by the physicochemical properties of the sludges and initial pH solution are presented in Table 3.4.

Chapter 3: Mechanistic study of P retention by dewatered waterworks sludges

Table 3.4 Principal component analysis of the physicochemical characteristics of the seventeen dewatered waterworks sludges; and linear regression analysis between the three principal components scores and initial pH solution as predictors, and the amount of P-uptake at different initial P concentration, P adsorption capacity maxima and Freundlich P bonding energy-related constant as outcomes variables.

Principal component	PC1	PC2	PC3	Independent variable	PC1	PC2	PC3	pH	TV%
Eigenvalue	5.626	3.668	1.023		Percentage of explainable variance				
Proportion of variance (%)	42.745	34.563	16.477	q ₁ ^a	45.3***	6.1*	NOT Sig.	NOT Sig.	55.9***
Cumulative proportion of variance (%)	72.745	77.308	93.785	q ₂ ^a	28.9***	9.3**	NOT Sig.	NOT Sig.	38.2**
Rotated factor loading				q ₃ ^a	30.8***	10.1**	6.1*	NOT Sig.	46.9***
Variable	PC1	PC2	PC3	q ₄ ^a	36.9***	8.1**	8.2**	NOT Sig.	53.2***
Al	0.925	-0.044	0.33	q ₅ ^a	52.9***	4.5*	2.9*	4.4*	64.6***
Fe	-0.918	0.255	-0.256	q ₆ ^a	46.4***	6.5**	NOT Sig.	6.9*	59.8***
Al _{oxa}	0.953	-0.083	0.259	q ₇ ^a	42.3***	4*	NOT Sig.	9.5**	55.8***
Fe _{oxa}	-0.881	0.168	-0.402	Q _o ^b	34.4***	NOT Sig.	NOT Sig.	10.4*	44.8***
Ca	-0.596	0.691	0.337	K _f ^c	66.4***	6.2**	NOT Sig.	5.8**	78.4***
Ca _{ex}	-0.154	0.915	-0.081	* explainable variance is significant at the 0.05 level					
SO ₄ ²⁻	-0.419	0.271	-0.801	** explainable variance is significant at the 0.01 level					
TC	0.019	-0.969	0.012	*** explainable variance is significant at the 0.001 level					
TOC	0.013	-0.969	0.009	^a P-uptakes ranged q ₁ , q ₂ , q ₃ , q ₄ , q ₅ , q ₆ , and q ₇ at initial P concentrations ranged 5, 10, 20, 40, 80, 160 and 320 mg/l; ^b calculated P adsorption maxima determined from fitting the linearized Langmuir model; ^c bonding energy-related constant calculated from fitting the linearized Freundlich model; For the principal component table, variable with high component loading are shown in bold					
TSA	0.756	0.563	0.027						
pH	0.438	0.343	0.805						

3.4 Summary

The main findings from this chapter are summarized in this section. Chemical and physical characterization showed that the sludges mainly contained Al, Fe and OC. The Al and Fe contents reflect the chemical coagulant used in the coagulant-flocculation process, while the OC depends on the source of the treated water and polymers' usage during the treatment process and sludge conditioning. The morphology structure of the sludges, graphite peaks for two Al-based sludge (GU and SF) and another peak characterised as Fe and Al alloys for Fe-based (CF) sludge were noticed. Al-sludges showed statistically higher reactivity for P uptake than Fe-sludges. The higher percentages of amorphous oxides and SSA combined with Al-sludges rather than Fe-sludges, might be the main factors responsible for the differences in P adsorption.

Phosphorus adsorption mechanisms showed that the exchangeable ions between the sludge and deionized water at three initial pHs increased as the pH decreased. The released ions and the hydroxyl groups on the surface of the sludge caused an increase or decrease of pH at equilibrium relative to the initial pH. The sludges with least ions released were GU and SF, both of which contain carbon as graphite. Results from the precipitation test of the initial and final Ca and P concentrations (molar ratio of Ca to P (0.5)) revealed that a preliminary calcium phosphate precipitation as monocalcium phosphate might occur at initial pH > 7.3. Furthermore, it is noted that P is also adsorbed into the precipitates of Fe hydroxides. FTIR spectra for the sludge before and after P adsorption test showed remarkable changes in hydroxyl and carboxyl groups.

The Al, Fe, Al_{oxa}, Fe_{oxa}, SSA, Ca content, dissolved Ca (Ca_{ex}), TC, OC, SO₄²⁻ content and sludge pH explained 94.5% of the variance in the sludge characteristic resulting from the principal component analysis. Multiple linear regression analysis showed that Al, Fe, Al_{oxa}, Fe_{oxa} and SSA are the most significant properties that influence P uptake, adsorption maxima and Freundlich constant, followed by Ca content, dissolved Ca (Ca_{ex}), TC and OC.

Next chapter will explain in details the average differences between the two main sludge types and their variation in the P adsorption equilibrium and kinetic through applying adsorption isotherm and kinetic models.

4 Chapter 4 Experimental and theoretical investigation of P adsorption by dewatered waterworks sludges

4.1 Introduction

In Chapter 3, the combined effect of physicochemical properties of dewatered waterworks sludges and solution chemistry on the P uptake and adsorption capacities of the sludges was investigated. In addition, the underlying mechanisms of P adsorption by the sludges was investigated. In the current chapter, fitting of theoretical models of adsorption with experimental data are presented for fourteen DWTSSs. Competing anions such as Cl^- and SO_4^{2-} are found in wastewater, and they might interfere with P adsorption onto the surface of dewatered waterworks sludges during competitive adsorption. Therefore, the impacts of these competing anions at six concentrations and three initial solution pH were also investigated. The objectives were to provide and compare the P equilibrium and kinetic data for DWTSSs derived from various sources; to study their adsorption behaviour including the effect of competing ions, and to characterise their adsorption equilibrium and kinetics using different theoretical models. Being that the study covers sludges from a variety of different sources, the findings would contribute to advancing the understanding of equilibrium and kinetics of P adsorption by DWTSSs; and therefore, enhance their practical application for P removal.

4.2 Material and Methods

4.2.1 Physical and chemical characteristics

The sludges were analysed for their chemical and physical characteristics as described in Chapter 3 –Section 3.2.1.

4.2.2 Adsorption isotherm experiments

P adsorption maxima of the DWTSSs was determined by equilibrating 1g each of the dewatered sludges samples in 200 ml acid-washed polyethylene bottles. The bottles contain 100 ml solution at three pH values (4, 7 and 9); and seven initial P

concentrations (5, 10, 20, 40, 80, 160 and 320 mg-P/l). Hydrochloric acid (0.01M) and potassium hydroxide (0.1M) were used for pH adjustment. The pH values were chosen to mimic the range of extreme (<5.5) and typical hydrogen ion concentration (6-9), while the P concentrations corresponded with typical ranges for domestic, dairy parlour, and livestock wastewaters as reported in similar studies. Analytic grade of potassium dihydrogen phosphate (KH_2PO_4) was used to prepare the P stock solution. After 48-hours pre-determined equilibration time, samples were filtered using a 0.45 μm membrane filter (GE-Whatman) and analysed for P using a HACH DR-3900 spectrophotometer. The mass of P adsorbed per mass of adsorbent (q) in mg/g was calculated using Equation (4.1).

$$q_e = \frac{(C_o - C_e)}{m} V \quad (4.1)$$

where C_o and C_e are the initial and equilibrium P concentrations, respectively in the solution (mg/l), V represents the volume of the solution (l), and m is the mass of the adsorbent (g).

The adsorption data obtained was fitted with the Langmuir, Freundlich, Temkin and Harkins-Jura (H-J) adsorption isotherm models.

4.2.2.1 Langmuir isotherm

The Langmuir isotherm is the most widely used adsorption isotherm model for the sorption of a pollutant from a liquid solution. It is based on three fundamental assumptions: (1) a homogeneous adsorption surface that each adsorbate molecule occupies one type of binding site; (2) the adsorbent is saturated with adsorbate by forming monolayer of one-molecule-thick when all binding sites are occupied with no further binding; and (3) surface coverage and interaction of adjacent adsorbed molecules do not impact on the adsorption energy (Metcalf and Eddy 2003). It is expressed as in Equation 4.2 (Cooney 1998):

$$q_e = \frac{Q_o b C_e}{1 + b C_e} \quad (4.2)$$

where C_e is the equilibrium concentration of P in solution (mg/L), q_e is the mass of P adsorbed on the adsorbent (dewatered sludge) at equilibrium (mg/g), b is the

Langmuir adsorption constant (l/mg), which is related to the energy of adsorption, and Q_0 is the maximum adsorption capacity (mg/g). Physically, b is a measure of the affinity of the adsorbate for the adsorbent.

4.2.2.2 Freundlich isotherm

Freundlich isotherm is an empirical equation and often used for heterogeneous surface energy systems, which are not restricted to the formation of monolayer from the adsorbate on the surface of the adsorbent. The Freundlich adsorption isotherm is mostly applied in systems with highly interactive species or organic compounds on activated carbon (Foo and Hameed 2010). It can be expressed as in Equation 4.3 (Metcalf 2003):

$$q_e = K_F C_e^{1/n} \quad (4.3)$$

where K_F is the Freundlich constant (L/g) related to the bonding energy; and $1/n$ is a measure of surface heterogeneity which ranges from 0 to 1. The adsorbent surface becomes more heterogeneous as the value of $1/n$ reaches to zero.

4.2.2.3 Temkin isotherm

The Temkin isotherm takes into consideration the interactions between adsorbent and adsorbate, and it assumes that the heat of adsorption is a function of the surface coverage with proportional linearly (Chen et al. 2008). The Temkin isotherm has been used in the following form (Equation 4.4) (Choy et al. 1999; Ozacar and Sengil 2005):

$$q_e = \frac{RT}{b} \ln(K_T C_e) \quad (4.4)$$

where $RT/b = B_I$; R is the gas constant (8.31 J/mol K), q_e is as defined before and T is the absolute temperature in K. K_T is the equilibrium binding constant (L/mg) corresponding to the maximum binding energy, and B_I is related to the heat of adsorption.

4.2.2.4 Harkins–Jura (H-J) isotherm

The Harkins–Jura adsorption isotherm is also important model used for characterising the multilayer adsorption and the existence of heterogeneous pore distribution on the adsorbent surface (Harkins and Jura 1944). It can be expressed as in Equation 4.5 (Başar 2006):

$$q_e = \left(\frac{A}{B - \log C_e} \right)^{1/2} \quad (4.5)$$

4.2.3 Adsorption kinetics and rate constants

To delineate the rate of P uptake and control the required time for the whole adsorption process, the dynamics of P adsorption was investigated using short-time batch test. The test involved agitating 1.0 g each of the sludge samples with 100 ml solution of 10 mg-P/l at three pH values (4, 7 and 9); and at different contact times of 5, 15, 30, 60, 90, 120, 360, 1440 and 2880 minutes. After the set contact times, the mixtures were withdrawn, filtered and analysed for P to determine the uptake. Thereafter, the data fitted to kinetic models as described below:

Firstly, the kinetic data was fitted to the pseudo first-order model which is given as in Equation (4.6) (Gupta et al. 2001):

$$\log(q_e - q_t) = \log q_e - \frac{k_1}{2.303} t \quad (4.6)$$

where q_t is the amount of adsorbate adsorbed at time t (mg/g), q_e is the adsorption capacity at equilibrium (mg/g), k_1 is the pseudo-first-order rate constant (min^{-1}), and t is the contact time (mins). The value of k_1 was calculated from the slope of the linear plot of $\log(q_e - q_t)$ versus t .

Secondly, the kinetic data fitted with the pseudo-second-order model. It describes the rate of adsorption as chemisorption process (Ho and McKay 1999). It has the linear form as in Equation 4.7 (Ho and McKay 1999).

$$\frac{t}{q_t} = \frac{1}{k_2 q_e^2} + \left(\frac{1}{q_e} \right) t \quad (4.7)$$

where k_2 is the pseudo-second-order rate constant (g/mg.min), and all other variables are as previously defined. The constant (k_2) was obtained from the intercept of plotting (t/q_e) against t .

To quantitatively compare the goodness of the model's fit in addition to correlation coefficient (R^2), normalized standard deviation (NSD) and sum of square of the error (SSE) were utilized and calculated using Equation 2.8 and 4.9, respectively (Behnamfard and Salarirad 2009; Demirbas et al. 2009).

$$NSD = 100 \sqrt{\frac{1}{N-1} \sum_{i=1}^N \left[\frac{q_t^{exp} - q_e^{cal}}{q_e^{exp}} \right]^2} \quad (4.8)$$

$$SSE = \sqrt{\frac{1}{N} \sum_{i=1}^N (q_e^{exp} - q_e^{cal})^2} \quad (4.9)$$

where q_t^{exp} and q_t^{cal} (mg/g) are the experimental and calculated amount of P adsorbed on the sludge at time t , and N is the number of sampling points. The more accurate model fitting measured, the smaller the values of NSD and SSE and the higher the value of R^2 .

However, although these two models have been applied widely in studying adsorption kinetics, their inherent limitation is that they cannot identify the diffusion mechanism (Wu et al. 2005). Therefore, the intraparticle diffusion model was also used (Equation 4.10).

$$q_t = k_d t^{1/2} + C \quad (4.10)$$

where k_d (mg /g. min^{1/2}) is the rate constant for intraparticle diffusion, and all other variables are as previously defined. The fractional approach to equilibrium will change according to a function of $(D_t/r^2)^{1/2}$, where r is the average particle radius of the adsorbent particles and D_t is the diffusivity of solutes within the particle. From Equation 4.10, plotting of q_t versus $t^{1/2}$ should be a straight line with a slope of k_d and

intercept of C when the adsorption mechanism is a case of intraparticle diffusion. The intercept value gives an idea about the thickness of boundary layer where the larger the intercept is, the greater the boundary layer effect (Dizge et al. 2008).

4.2.4 Competing ions test

Chloride (Cl^-) and sulphate (SO_4^{2-}) are anions that are typically present in wastewater. To investigate their competitive effect on the selective adsorption of P by the sludges, a competing ions test was conducted. The same procedure for the equilibrium adsorption experiments was followed (Section 4.2.2); however, the initial P concentration was 10 mg/L to mimic the average concentration in wastewater whilst concentrations of 0, 20, 50, 100, 200 and 300 mg/L were used for both Cl^- and SO_4^{2-} . The initial solution pHs were 4, 7 and 9; and the contact time was 48 h. After the set contact time, the samples were filtered, and the supernatant was analysed for P to determine the P uptake (calculated from the amount of P removed from the initial P concentration of particular volume per mass of sludge). The experimental conditions of P, Cl^- and SO_4^{2-} concentrations for each sludge were replicated ($n=2$). One-way ANOVA was used to compare the mean values of P uptake with and without the competing anions.

4.3 Results and discussion

4.3.1 Physical and chemical properties

Table 4.1 shows the chemical and physical characteristics of the five Al-based and nine Fe-based sludges as compared with other sludges. Generally, the physicochemical characteristics of the UK sludges were higher than those reported for other sludges. For the Al-based sludges, the mean total Al content was 118.6 mg/g; whilst for the Fe-based sludges, the mean total iron content was 240.82 mg/g. The high mean and standard deviation of Fe content could be explained by the fact that the efficiency of iron salts coagulant for removing impurities (turbidity, solid, colour, OM, and other inorganic contaminants) from water are less than that for the aluminium coagulants (Parsons and Jefferson 2006). Therefore, high doses of iron salts are used to meet the consent of drinking water standards.

The mean values of TC and OC for both sludge types were equal; this indicates that calcium carbonate and calcium magnesium (inorganic carbon) contents are negligible in the sludges. However, the mean and the variation in OC content were found to be remarkably high in Al-sludges in the current study, while high values of OC joined with the Fe-sludges were reported by previous researchers (Table 4.1). This might be explained by variation in characteristics of water sources, or due to using polymers during the treatment process. Mean P content was 1.4 and 0.51 mg-P/g respectively, for the Al and Fe-based sludges. For both sludge types, the mean value for the cations (Ca, Mg, Mn and Zn) and anions (Cl^- and SO_4^{2-}) were in the range of 0.42 – 5.93 mg/g and 0.14 – 5.43 mg/g, respectively; and the highest deviation from the mean value was observed for the Ca content of the Fe-based sludges. The mean specific surface area was found to be higher for Al-based sludges (327.9 m^2/g) than Fe-based sludges (184.76 m^2/g). Makris et al. (2005b) also found that Al-based sludges had higher SSA than Fe-based sludges. Where, Brunauer Emmett Teller-Nitrogen gas method was used in that study (Makris et al. 2005b). Nonetheless, the results show that Al-based sludges generally have higher total surface areas compared to Fe-based sludges.

4.3.2 Adsorption characteristics differentiation

4.3.2.1 Behaviour of dewatered sludges for P uptake

The characteristic adsorption behaviour of the sludges is presented in Figure 4.1 (a-f), showing the plot for three selected Al-based and Fe-based sludges. For the Al-based sludges, an increase in P-uptake with increasing initial P concentration was observed. A similar trend was observed for the Fe-based sludges. However, a higher variance in P uptake was found, and this can be adduced to the highly variable characteristics of the Fe-sludges. The maximum P-uptakes by Al- and Fe-based sludges were, respectively, 17 to 26 mg-P/g and 13 to 21 mg-P/g. These differences confirm that the sludges exhibit different P removal behaviour.

Chapter 4: Experimental and theoretical investigation of P adsorption by DWTSSs

Table 4.1 Mean and standard deviation of chemical and physical characteristics of Al- and Fe-based sludges.

Sludge source	Sludge Type (n = number)	Chemical and physical properties (mean \pm standard deviation)												Reference
		Al	Ca	Fe	P	Mg	Mn	Zn	Cl ⁻	SO ₄ ²⁻	TC	OC	Surface area	
		mg/g											m ² /g	
United Kingdom	Al-based(5)	118.60	1.60	13.94	1.40	0.68	0.42	0.90	0.14	1.38	127.88	127.26	327.9 ^a	Current study
		\pm	\pm	\pm	\pm	\pm	\pm	\pm	\pm	\pm	\pm	\pm	\pm	
	22.56	0.97	9.23	1.91	0.19	0.16	0.62	0.05	0.94	36.88	37.09	115.50		
	\pm	\pm	\pm	\pm	\pm	\pm	\pm	\pm	\pm	\pm	\pm	\pm		
Fe-based(9)	13.73	5.93	240.82	0.51	0.49	0.83	0.71	0.28	5.43	122.72	122.68	184.76 ^a		
	\pm	\pm	\pm	\pm	\pm	\pm	\pm	\pm	\pm	\pm	\pm	\pm		
USA & Canada	Al-based(2)	20.09	7.83	49.80	0.17	0.39	0.64	0.80	0.13	1.95	23.68	23.62	95.21	
		\pm	\pm	\pm	\pm	\pm	\pm	\pm	\pm	\pm	\pm	\pm	\pm	
USA	Al-based(2)	112.00	5.95	7.60	0.80	1.15	0.70	NA	NA	NA	NA	NA	NA	(Gibbons and Gagnon 2011)
		\pm	\pm	\pm	\pm	\pm	\pm	\pm	\pm	\pm	\pm	\pm	\pm	
	20.08	6.58	0.99	0.28	1.48	0.42	NA	NA	NA	NA	NA	NA		
	\pm	\pm	\pm	\pm	\pm	\pm	\pm	\pm	\pm	\pm	\pm	\pm		
Al-based(21)	90.31	43.65	28.08	1.57	NA	NA	NA	NA	NA	NA	74.01	NA	(Dayton et al. 2003)	
	\pm	\pm	\pm	\pm	\pm	\pm	\pm	\pm	\pm	\pm	\pm	\pm		
Al-based(4)	44.36	69.01	11.49	1.14	NA	NA	NA	NA	NA	NA	44.85	61.2 ^b		
	\pm	\pm	\pm	\pm	\pm	\pm	\pm	\pm	\pm	\pm	\pm	\pm		
Fe-based(3)	79.75	NA	10.33	1.45	NA	NA	NA	NA	NA	124.25	NA	33.8	(Makris et al. 2005)	
	\pm	\pm	\pm	\pm	\pm	\pm	\pm	\pm	\pm	\pm	\pm	\pm		
Al-based(4)	29.27	NA	7.04	1.11	NA	NA	NA	NA	NA	85.73	NA	25.5		
	\pm	\pm	\pm	\pm	\pm	\pm	\pm	\pm	\pm	\pm	\pm	\pm		
Fe-based(3)	4.40	NA	268.00	1.40	NA	NA	NA	NA	NA	147.00	NA	37.3		
	\pm	\pm	\pm	\pm	\pm	\pm	\pm	\pm	\pm	\pm	\pm	\pm		
Al-based(3)	4.70	NA	37.51	1.57	NA	NA	NA	NA	NA	56.24	NA	35.67		
	\pm	\pm	\pm	\pm	\pm	\pm	\pm	\pm	\pm	\pm	\pm	\pm		
China ^c	Al-based(3)	63.85	61.45	31.09	1.99	NA	NA	NA	NA	NA	44.2	37.05 ^d	15.57	(Bai et al. 2014)
		\pm	\pm	\pm	\pm	\pm	\pm	\pm	\pm	\pm	\pm	\pm		
	26.56	63.31	7.43	0.83	NA	NA	NA	NA	NA	17.1	9.56	67.50		
	\pm	\pm	\pm	\pm	\pm	\pm	\pm	\pm	\pm	\pm	\pm	\pm		
Fe-based(2)	58.23	12.38	88.60	1.36	NA	NA	NA	NA	NA	107.0	66.98 ^d	9.19		
	\pm	\pm	\pm	\pm	\pm	\pm	\pm	\pm	\pm	\pm	\pm	\pm		
Al-based(3)	22.66	5.89	12.02	0.07	NA	NA	NA	NA	NA	1.0	1.78	9.19		
	\pm	\pm	\pm	\pm	\pm	\pm	\pm	\pm	\pm	\pm	\pm	\pm		

^a surface area measured using EGME method. ^b mean value and standard deviation for three Al-based sludges. ^c sludge type was classified according to the main constituent element. ^d organic content measured as organic matter.

4.3.2.2 Adsorption isotherms

To compare the P adsorption characteristics of the fourteen dewatered sludges based on the theoretical adsorption models, four adsorption isotherm models were used. Table 4.2 gives the adsorption isotherm models and their corresponding linear forms employed in this study. Fitting the linearized forms of the Langmuir, Freundlich, Temkin, and H-J models to the P adsorption data for the alum and iron sludges are shown in Appendix A (Figure A.1 to A.8). The results as presented in Table 4.3 indicate that the fitting of the experimental data exhibited a linear relationship to a few models across the range of initial pH values. The linear correlation coefficients (R^2) were found to be highest for the Freundlich isotherm model for most of the dewatered sludges except the GU sludge. The constant parameters obtained from the regression plots of the linear forms of the four models used for the fourteen dewatered sludges are summarized in Table 4.3. The results are further discussed below.

4.3.2.2.1 Langmuir model

The Langmuir model was used to determine the maximum adsorption capacities of the sludges at different pHs. The results, as presented in Table 4.3, show that pH significantly influences the adsorption capacity with the highest maximum adsorption capacities obtained at pH 4. In addition, the adsorption capacities were found to decrease as the pH increases, indicating that the adsorption process is more favoured under acidic conditions. Furthermore, it can be seen from the model fitting for selected Al- and Fe-based sludges (Figure 4.1 a-f), that Langmuir model fitted the P uptake data quite well across the three initial pHs for only the GU sludge.

Based on these results (Figure 4.1 and Table 4.2), the sludges were categorized into three groups: the first group included the GU, MO, WD and OS dewatered sludges which had the best fitting across the three pH levels ($R^2 > 0.9$); the second group included the CA, FO, AR, WY and BU sludges, which have low R^2 with approximately the same adsorption capacities at pH 7 and 9; and the third group which included the BS, HO, HH, HU and WA sludges, which gave better fit with increase in pH from 4 to 9. A possible explanation for these might be that surface complexation by the inner or outer sphere is the dominant P retention mechanism for the GU, MO, WD and OS sludges; whereas for the third group of sludges, the

observed behaviour could be due to a different P retention mechanism which is favoured under alkaline conditions.

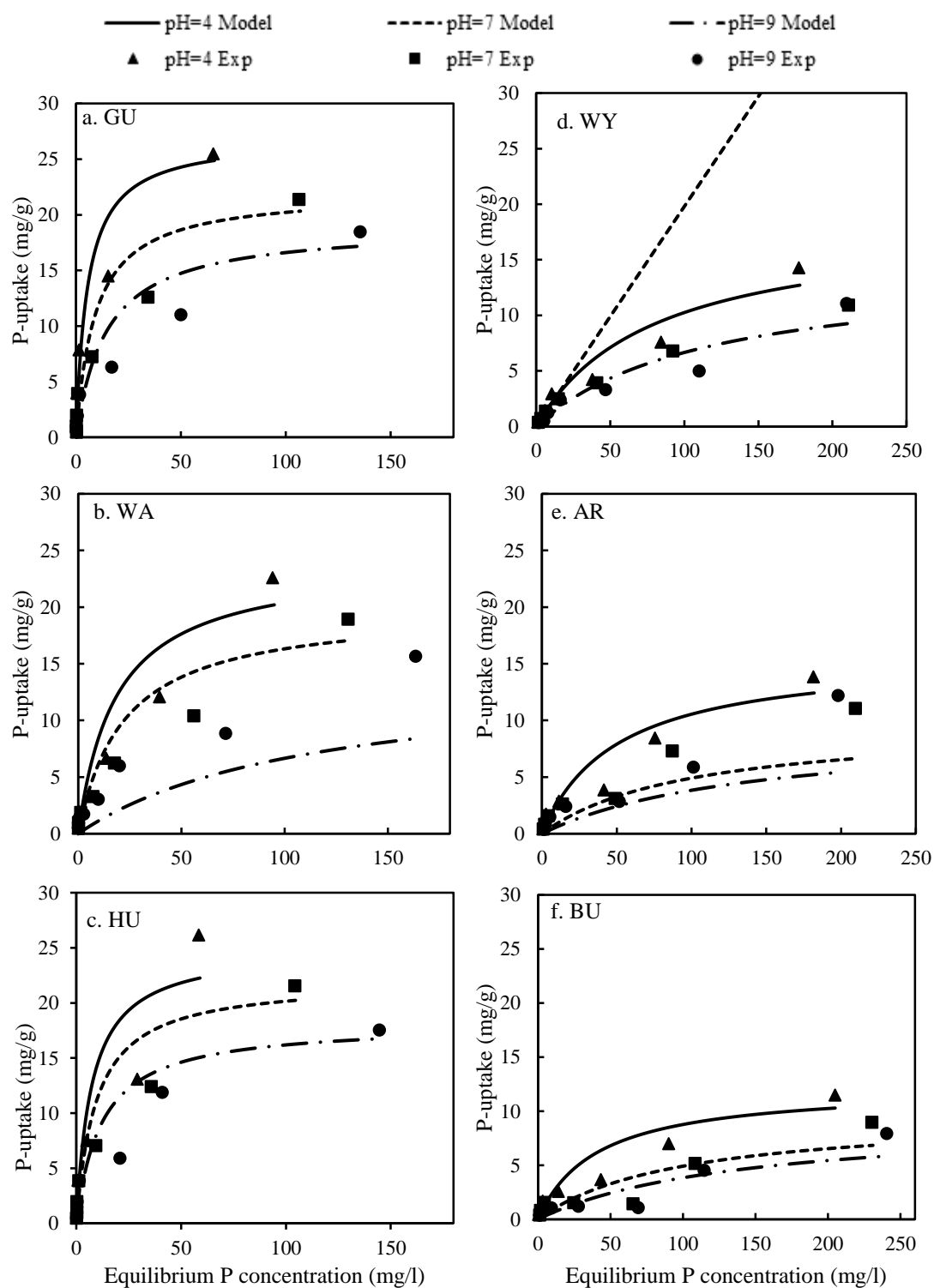


Figure 4.1 P-uptake of Al-based sludges (a-c) and Fe-based sludges (d-f) at three pH values with seven levels of initial P concentration; and their corresponding fitting

with the Langmuir isotherm model. (*Exp* = experimental data; *Model* = Langmuir model data).

Table 4.2 Adsorption isotherm model equations and their linearized expression.

Isotherm	Equation	Linear expression	Plot
Langmuir	$q_e = \frac{Q_0 b C_e}{1 + b C_e}$	$\frac{C_e}{q_e} = \frac{C_e}{Q_0} + \frac{1}{Q_0 b}$	C_e/q_e vs. C_e
Freundlich	$q_e = K_F C_e^{1/n}$	$\log q_e = \log K_F + \frac{1}{n} \log C_e$	$\log q_e$ vs. $\log C_e$
Temkin	$q_e = \frac{RT}{b} \ln(k_T C_e)$	$q_e = B_1 \ln k_T + B_1 \ln C_e$	q_e vs. $\ln C_e$
H-J	$\frac{1}{q_e^2} = \left(\frac{B}{A}\right) - \left(\frac{1}{A}\right) \log C_e$	$\frac{1}{q_e^2} = \left(\frac{B}{A}\right) - \left(\frac{1}{A}\right) \log C_e$	$1/q_e^2$ vs. $\log C_e$

In comparison with other adsorbents studied for P removal, the adsorption capacities of the DWTSs determined in this study can be seen to be comparable and generally high. For instance, Baker et al. (2014) evaluated thirteen light-weight aggregates for their ability to retain P in batch experiments and obtained maximum adsorption capacity of 0.702 mg-P/g. Furthermore, Babatunde et al. (2009), Ippolito et al. (2003), and Yang et al. (2006b) determined, respectively maximum P adsorption capacities of 31.9 mg-P/g, 10.4 to 37 mg-P/g and 3.5 mg-P/g for waterworks sludges.

The mean values of P adsorbed normalised to either Al or Fe content of the sludges are presented in Figure 4.2; in addition to those reported in other studies. In the current study, the maximum P adsorption capacities normalised to the Al and Fe contents of the sludges across the three pHs were 156-217 mg/g-Al and 55-66 mg/g-Fe, respectively. These were higher than the values obtained for other studies as presented in Figure 4.2, except the sludges from China which have the highest P loading for Fe-based sludge at initial pH 5 and 7; and with the lowest variance for Al-based sludge. These differences are likely related to the characteristics of the sludges.

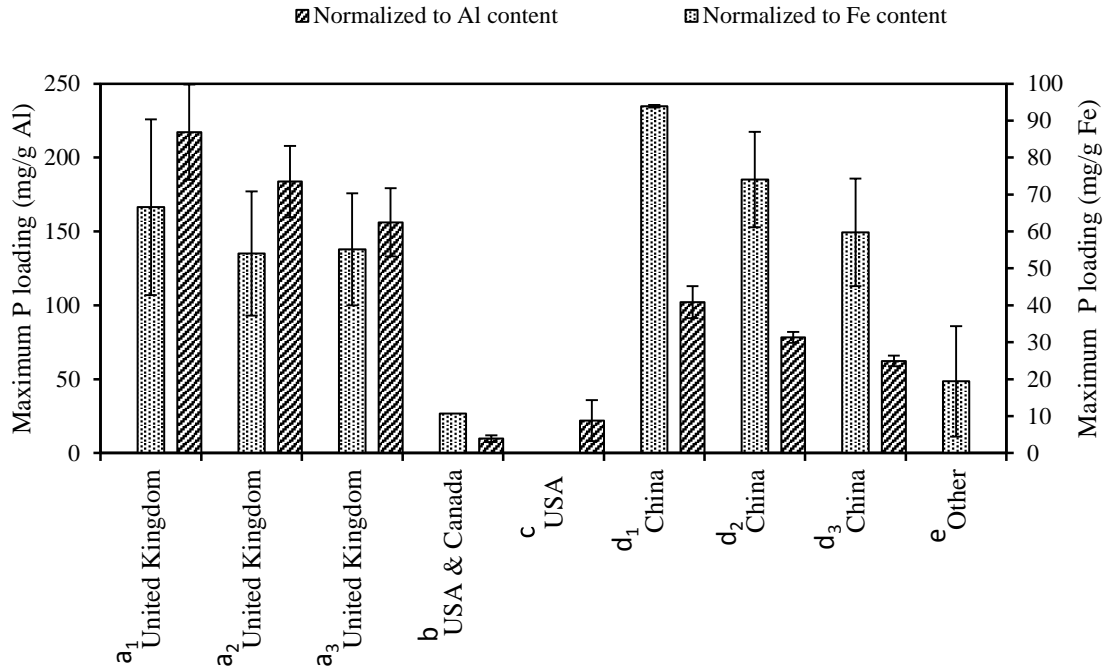


Figure 4.2 Maximum P loadings (calculated from Langmuir model) for different Al- and Fe- based sludges. a₁, a₂, and a₃ represent, respectively the mean results obtained in the current study at initial pH solution 4, 7 and 9 for five Al-based and eight Fe-based sludges. Only sludges fitted well with the Langmuir model were used. b represents values of two Al- and one Fe-based sludges at initial pH 6.2 (Gibbons and Gagnon 2011). c represents mean values of 21 Al-based sludge (Dayton et al. 2003). d₁, d₂ and d₃ represent, respectively mean values at three initial pH solution 5, 7 and 9 for three Al-based and two Fe-based sludges (Bai et al. 2014). e represents mean values of thirteen sands with mainly iron content and with initial pH equal to equilibrium pH (Del Bubba et al. 2003).

4.3.2.2.2 Freundlich model

The results of selected DWTs are presented in Figure 4.3, and it shows that the equilibrium adsorption data were generally well fitted with the Freundlich model (except GU at pH 4 and BU at pH 7 and 9). Furthermore, the K_f values for all the sludges decreased with increasing pH values from 4 to 9 (Table 4.2); whilst the Freundlich n constant was larger than 1 in all cases, increasing with pH increase from 4 to 9 for most sludges. When $n > 1$, it indicates that P adsorption onto the waterworks sludges is heterogeneous. The K_f constant relates to the bonding affinity

of the adsorbent for P. Thus; the sludges exhibit higher affinity for P binding in the acidic conditions.

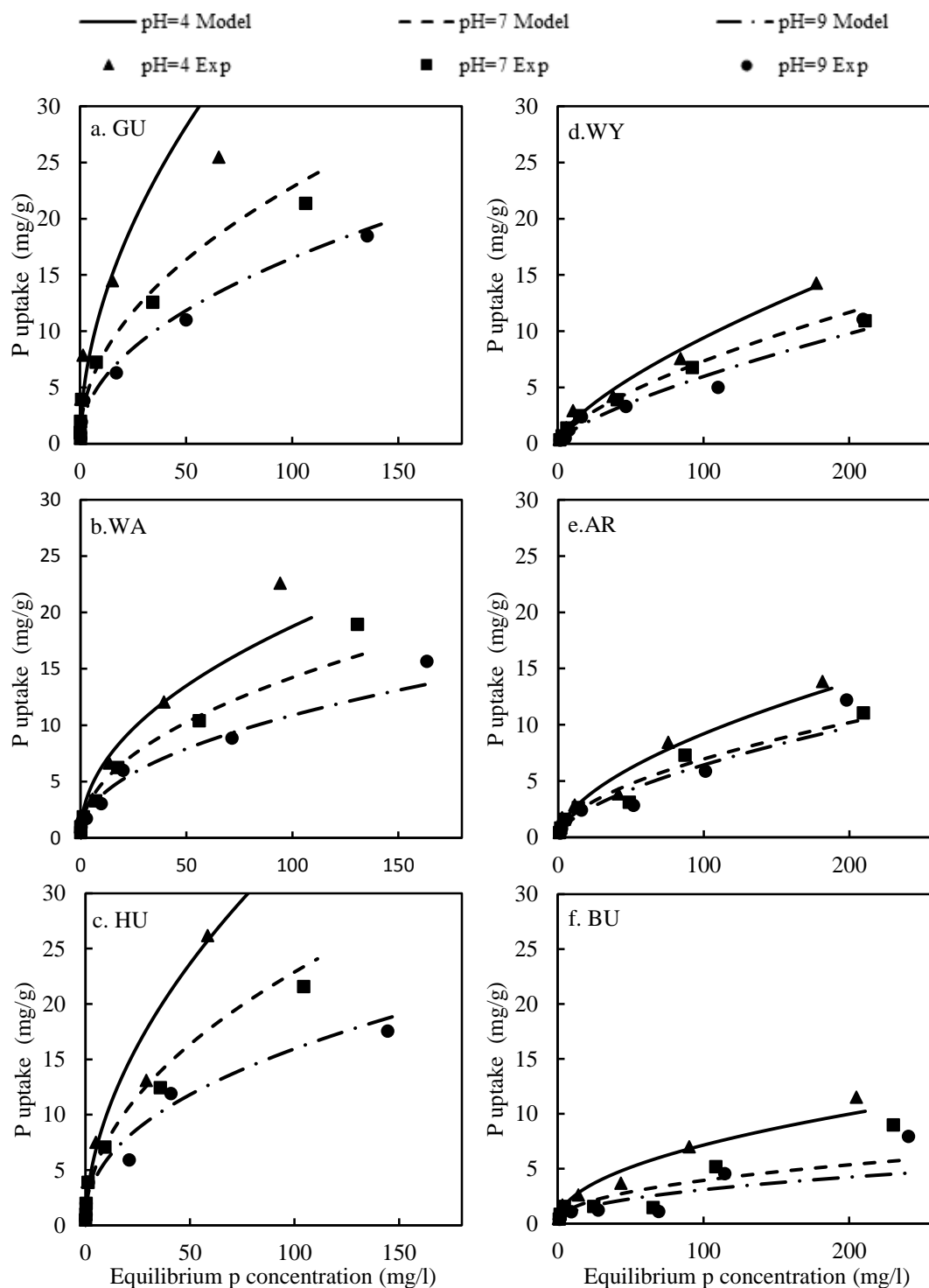


Figure 4.3(a-f) P-uptake of three Al-based (a-c) and Fe-based (d-f) dewatered sludges at three pH values with seven initial P concentration; and their

corresponding fitting with the Freundlich isotherm model. (Exp = experimental adsorption data; Model = Freundlich model data).

4.3.2.2.3 Temkin and H-J model

A good fitting of the experimental data with the Temkin model was obtained at initial pH 4 ($R^2 = 0.733 - 0.955$); whereas the data less fitted with the model as the solution pH increased ($R^2 = 0.581 - 0.876$). The constants of the Temkin isotherm model are presented in Table 4.2. The data indicate that the heat of adsorption (BI) and the equilibrium binding constants (K_T) decrease with an increase in initial pH except for the AR sludge. The decline of adsorption heat and equilibrium constant with increasing pH indicates that P retention is pH dependent, and more favoured in the acidic condition. Furthermore, it can be seen from Table 4.2 that Al-based sludges had higher BI and K_T than Fe-based sludges across the three initial pH values; and this also supports earlier findings in the study which shows variability in P retention between the two main sludge types. For the AR sludge which had the highest Ca content, the heat of adsorption (BI) increased at initial pH 9. This might indicate that the additional P uptake is by precipitation.

The J-H model did not produce a good fit with the adsorption data across the three initial pH values ($R^2 = 0.191 - 0.651$); it was therefore not analysed further.

Table 4.3 Constant parameters, adsorption capacity and correlation coefficients calculated for the five-adsorption models at three different pHs.

Isotherm model	Iron-based sludges								Aluminium-based sludges						
	BS	MO	CA	FO	HH	AR	WY	BU	GU	HO	WD	OS	HU	WA	
Langmuir Isotherm Parameters															
pH= 4	Q _o (mg-P/g)	16.50	18.38	11.47	14.35	23.75	15.85	18.38	12.32	26.95	22.17	25.84	22.37	25.06	24.10
	b(L/mg)	0.01	0.05	0.02	0.01	0.03	0.02	0.01	0.02	0.18	0.06	0.16	0.08	0.13	0.05
	R ²	0.654	0.906	0.816	0.644	0.694	0.751	0.801	0.819	0.965	0.824	0.942	0.947	0.851	0.808
pH= 7	Q _o (mg-P/g)	15.02	14.01	9.27	11.48	20.00	12.50	13.64	9.76	22.08	17.24	21.94	19.42	22.08	19.92
	b(L/mg)	0.01	0.04	0.02	0.01	0.02	0.02	0.01	0.01	0.11	0.06	0.10	0.05	0.11	0.05
	R ²	0.672	0.907	0.759	0.703	0.793	0.747	0.935	0.296	0.952	0.908	0.937	0.903	0.937	0.862
pH= 9	Q _o (mg-P/g)	12.14	13.25	9.30	11.36	16.98	13.70	14.31	9.30	19.01	15.55	18.76	17.01	18.15	16.45
	b(L/mg)	0.01	0.04	0.01	0.01	0.02	0.01	0.01	0.01	0.07	0.05	0.07	0.03	0.08	0.04
	R ²	0.672	0.867	0.665	0.570	0.804	0.574	0.677	0.191	0.923	0.916	0.927	0.924	0.924	0.886
Freundlich Isotherm Parameters															
pH= 4	n	1.54	1.96	1.87	1.48	1.59	1.73	1.44	2.08	1.90	2.12	1.90	1.86	1.86	2.11
	K _f (L/g)	0.37	1.36	0.54	0.23	0.98	0.64	0.39	0.78	3.58	2.01	3.14	1.94	2.87	2.11
	R ²	0.979	0.969	0.972	0.941	0.963	0.958	0.976	0.972	0.819	0.920	0.908	0.933	0.955	0.942
pH= 7	n	1.55	2.05	2.05	1.52	1.66	1.82	1.49	2.24	2.09	2.29	2.05	1.94	2.06	2.11
	K _f (L/g)	0.33	1.07	0.49	0.21	0.83	0.55	0.34	0.50	2.51	1.77	2.33	1.43	2.45	1.61
	R ²	0.979	0.946	0.960	0.947	0.964	0.959	0.986	0.794	0.874	0.916	0.944	0.970	0.960	0.963
pH= 9	n	1.56	2.06	1.96	1.53	1.77	1.66	1.40	2.19	2.09	2.16	2.11	1.73	2.30	2.18
	K _f (L/g)	0.25	0.98	0.38	0.17	0.77	0.40	0.23	0.38	1.82	1.35	1.85	0.85	2.16	1.31
	R ²	0.931	0.935	0.952	0.941	0.959	0.946	0.958	0.774	0.915	0.939	0.938	0.978	0.936	0.963

Chapter 4: Experimental and theoretical investigation of P adsorption by DWTSSs

Isotherm model	Iron-based sludges								Aluminium-based sludges						
	BS	MO	CA	FO	HH	AR	WY	BU	GU	HO	WD	OS	HU	WA	
Temkin parameters															
pH=4	B1	2.07	2.28	1.54	1.76	3.10	2.09	2.43	1.52	3.63	2.43	3.34	2.92	3.27	2.45
	$K_T(L/mg)$	0.43	2.43	0.74	0.30	1.19	0.80	0.45	0.79	8.01	5.07	7.29	3.46	6.62	5.89
	R^2	0.757	0.842	0.793	0.776	0.761	0.797	0.811	0.784	0.955	0.758	0.912	0.902	0.831	0.733
pH= 7	B1	1.92	1.83	1.20	1.48	2.60	1.70	1.98	1.16	2.72	1.95	2.64	2.36	2.61	2.14
	$K_T(L/mg)$	0.39	1.87	0.71	0.29	1.01	0.71	0.41	0.71	6.20	4.88	5.75	2.59	6.61	3.87
	R^2	0.753	0.862	0.764	0.802	0.802	0.801	0.88	0.615	0.908	0.827	0.884	0.831	0.875	0.758
pH= 9	B1	1.56	1.75	1.17	1.33	2.19	1.84	1.91	1.05	2.33	1.86	2.28	2.32	2.04	1.81
	$K_T(L/mg)$	0.33	1.62	0.52	0.25	0.99	0.47	0.30	0.50	3.96	2.91	4.28	1.13	7.29	3.08
	R^2	0.76	0.838	0.722	0.749	0.798	0.722	0.777	0.581	0.876	0.842	0.875	0.861	0.864	0.768
Harkins–Jura (H-J) parameters															
pH=4	A	2.345	1.016	1.72	4.207	1.32	1.59	2.313	1.313	0.65	0.808	0.779	0.901	0.879	0.827
	B	9.848	1.605	5.326	33.324	2.654	4.35	9.252	3.041	0.547	0.974	0.703	1.135	0.85	0.97
	R^2	0.552	0.44	0.617	0.413	0.439	0.506	0.588	0.541	0.191	0.374	0.321	0.357	0.421	0.423
pH= 7	A	2.567	1.103	1.83	4.517	1.396	1.752	2.702	1.776	0.697	0.8	0.804	1.026	0.833	0.923
	B	11.99	2.067	6.306	38.989	3.18	5.495	13.107	6.219	0.728	1.035	0.88	1.578	0.886	1.297
	R^2	0.602	0.418	0.578	0.446	0.438	0.522	0.519	0.481	0.251	0.37	0.37	0.485	0.431	0.48
pH= 9	A	3.348	1.163	2.184	5.198	1.412	2.319	3.7	2.109	0.829	0.957	0.855	1.388	0.798	1.004
	B	21.495	2.356	9.19	52.691	3.399	9.827	25.389	9.112	1.072	1.504	1.091	3.084	0.907	1.618
	R^2	0.651	0.4	0.626	0.488	0.441	0.484	0.623	0.566	0.331	0.43	0.396	0.564	0.438	0.539

4.3.3 Phosphorus adsorption kinetics differentiation

The results of the kinetics test are presented in Figure 4.4a (showing one Al-based sludge) and Figure 4.4b (showing one Fe-based sludge). The figures present the amount of P-uptake (q_t) in mg/g onto the sludges plotted against agitation time (min) at initial pH values of 4, 7 and 9; and with 10 mg-P/l concentration. For both Al- and Fe-based sludges, it can be seen that P adsorption was biphasic, characterised by an initial fast rate followed by a slow rate. This is thought to be related to the amount of reactive aluminium or iron, specific surface area, exchangeable anions, and cations and total carbon or organic carbon of the sludges (Ippolito et al. 2003; Makris et al. 2004a; Yang et al. 2006b).

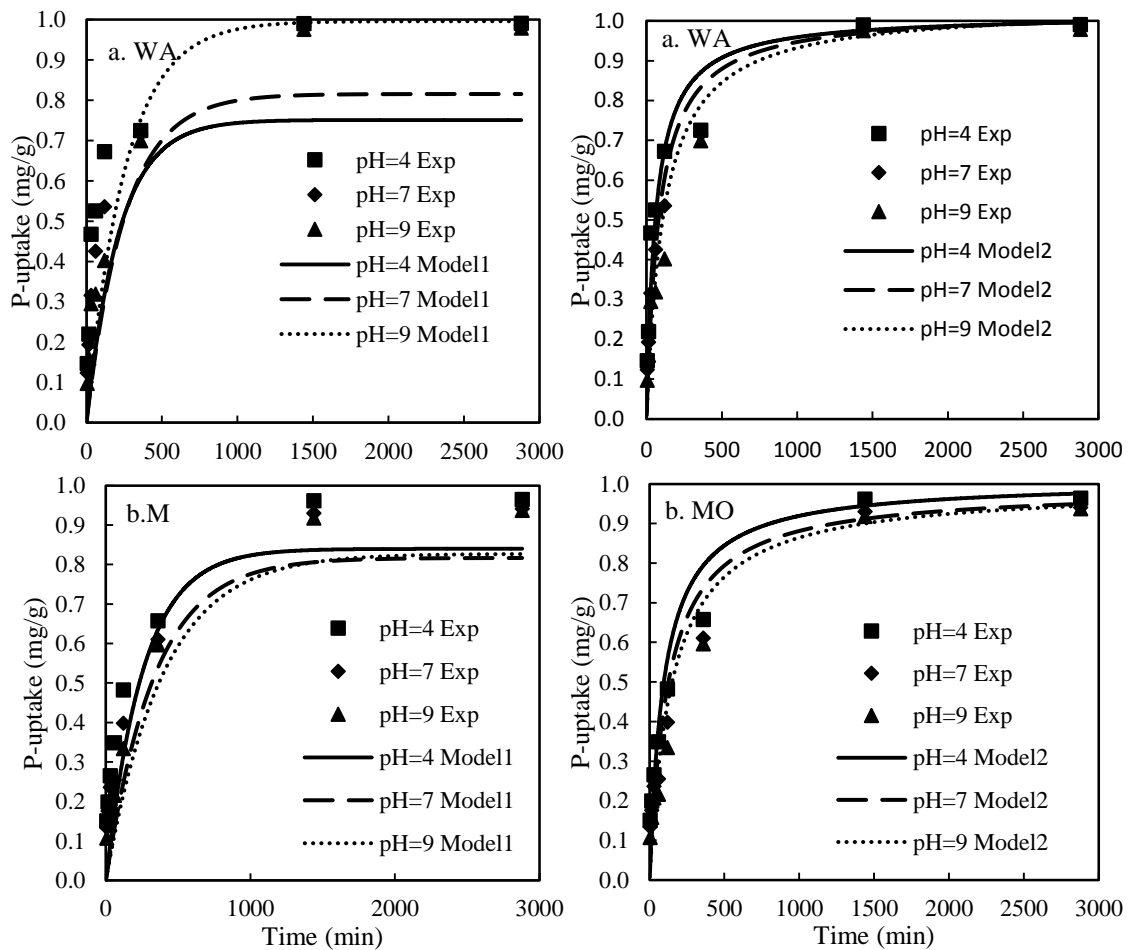


Figure 4.4 Kinetics of P adsorption onto dewatered water treatment sludges with initial P concentration = 10 mg/L and initial pH solution of 4, 7 and 9. Lines represent modelled results using pseudo-first-order (model1) and pseudo-second-order (model 2) models. (a = Al-based sludges and b = Fe-based sludges).

The experimental data of P adsorption rate across the three-initial pH solution were well fitted with the pseudo-first order and pseudo-second order models, with correlation coefficients for both models ranging from 0.88 to 1.0 (Table 4.3). Figures of fitting of the P adsorption kinetic data with the kinetic and intraparticle diffusion models for both sludge types are given in Appendix A (Figure A.9 to A.14). The fitting of the models to the experimental data for selected Al- and Fe-based sludges is shown in Figure 4.4. It can be seen from the figure that the pseudo-second order model fitted the experimental data for the WA and MO sludges quite well. However, with a view to finding out which of the two kinetic models gave the best fit, SSE, NSD, and correlation coefficient (R^2) were used. The results, as presented in Table 4.4, show that the kinetics of P adsorption across the three levels of pH is best fitted with the pseudo-second-order model. This implies that chemisorption is the rate-controlling step of P adsorption onto the waterworks sludges.

The pseudo-second-order rate constant (K_2) was found to decrease with increasing pH from 4 to 9 for all the sludges, except for the BS sludge (Table 4.4). It can also be seen from Table 4.4 that at pH 9, the K_2 value increased in the case of FO, OS and WY sludges. The P retention rate is pH dependent, being more favoured by acidic conditions. In the case of FO, OS and WY sludges, which showed an increase in the rate of P uptake under alkaline conditions, this might be due to the release of cations (Fe, Al, Ca and Mg), thereby increasing P retention rate through adsorption to metal precipitates or precipitation mechanism. Del Bubba et al. (2003) found that P uptake as calcium phosphate mineral is the dominant mechanism when the pH solution higher than 7.7.

The kinetics of P adsorption is initially fast through the attractive force between positive and negative charges. Thereafter, it becomes slower through intraparticle diffusion into meso- and micro-pores of the adsorbent. Therefore, to further probe the rate of internal mass transfer, data fitted with the intraparticle diffusion model (see Supplementary data – Appendix B). From Equation 4.10, the fitting of the kinetic data to the intraparticle diffusion model, should result in a strong linear relationship. The correlation coefficients (R^2), the rate constants of the intraparticle diffusion model, and the intercept of boundary layer thickness indicator are presented in Table 4.4. Whereas good R^2 were obtained from the model fitting at the initial P

concentration of 10 mg/L and at the three pH levels, which in most cases increased as pH increased. However, the correlation coefficients and the constant rate K_d were between 0.71 - 0.949 and 0.007 – 0.018 g/mg min^{1/2} respectively, and these values increased with increasing pH for most sludges, while the contrary trend for intercept values was observed. This indicates that the particle diffusion model may not be the rate limiting mechanism for P adsorption at the fast stage. These results are consistent with those of Babatunde and Zhao (2010), who found the same behaviour for Al-based sludge. The exchangeable cations and anions of the sludge in addition to the organic carbon may be promoting other sites for P diffusion into the meso- and micro-pores of the sludge during the slow reaction phase. This P diffusion would be highly influenced by the internal surface area within the micro pores, as well as the organic carbon content which restricts this diffusion (Makris et al. 2004a).

Chapter 4: Experimental and theoretical investigation of P adsorption by DWTSSs

Table 4.4 Adsorption rate constants and correlation coefficients for adsorption of phosphorus on dewatered waterworks sludges at initial P concentrations of 10 mg/L in three levels of initial pH solution.

Kinetic Model	Iron-based sludges								Aluminium-based sludges						
	BS	MO	CA	FO	HH	AR	WY	BU	GU	HO	WD	OS	HU	WA	
pH 4	q _e (mg/g)	0.604	0.840	0.699	0.538	0.794	0.796	0.469	0.751	0.448	0.712	0.502	0.669	0.462	0.751
	K ₁ * 10 ⁻² (min ⁻¹)	0.345	0.392	0.322	0.253	0.345	0.461	0.438	0.461	0.230	0.392	0.345	0.322	0.276	0.461
	R ²	1.000	0.993	0.988	0.943	0.999	0.995	0.877	0.983	0.949	0.984	0.966	0.986	0.980	0.983
	SSE	0.153	0.164	0.145	0.172	0.165	0.085	0.234	0.304	0.381	0.189	0.534	0.352	0.584	0.304
	NSD	0.710	0.663	0.706	0.769	0.689	0.549	0.891	0.755	0.751	0.471	0.974	0.858	1.002	0.755
pH 7	q _e (mg/g)	0.512	0.817	0.719	0.580	0.820	0.796	0.469	0.751	0.612	0.804	0.637	0.669	0.462	0.751
	K ₁ * 10 ⁻² (min ⁻¹)	0.276	0.299	0.276	0.299	0.322	0.461	0.438	0.461	0.253	0.345	0.415	0.322	0.276	0.461
	R ²	0.991	0.998	0.990	0.986	0.998	0.995	0.877	0.983	0.985	0.987	0.990	0.986	0.980	0.983
	SSE	0.163	0.163	0.118	0.105	0.118	0.158	0.181	0.212	0.430	0.225	0.386	0.254	0.469	0.212
	NSD	0.776	0.776	0.690	0.644	0.641	0.729	0.830	0.702	0.937	0.745	0.848	0.808	0.935	0.702
pH 9	q _e (mg/g)	0.267	0.827	0.742	0.524	0.861	0.997	0.998	0.996	0.612	0.796	0.684	0.998	0.997	0.996
	K ₁ * 10 ⁻² (min ⁻¹)	0.230	0.253	0.322	0.184	0.345	0.276	0.184	0.392	0.253	0.253	0.345	0.184	0.345	0.392
	R ²	0.887	1.000	0.983	0.920	0.997	0.995	0.968	0.996	0.983	0.997	0.990	0.999	0.982	0.996
	SSE	0.191	0.133	0.092	0.145	0.076	0.273	0.592	0.055	0.363	0.193	0.321	0.179	0.093	0.055
	NSD	0.943	0.687	0.621	0.768	0.561	1.643	4.736	0.191	0.902	0.761	0.821	0.712	0.261	0.191
Pseudo second order equation Parameters															
pH 4	q _e (mg/g)	0.779	1.009	0.835	0.737	0.974	0.887	0.693	0.980	0.336	0.161	0.999	0.986	0.984	1.017
	K ₂ * 10 ⁻¹ (g/mg.min)	0.131	0.102	0.107	0.107	0.100	0.098	0.166	0.065	0.998	0.991	0.302	0.156	0.300	0.163
	R ²	0.992	0.990	0.976	0.973	0.989	0.987	0.989	0.976	0.106	0.104	0.999	0.989	0.997	0.994
	SSE	0.066	0.083	0.090	0.077	0.085	0.077	0.073	0.079	0.279	0.349	0.091	0.133	0.173	0.085
	NSD	0.399	0.359	0.428	0.505	0.402	0.420	0.424	0.461	0.991	1.008	0.288	0.416	0.386	0.262

Chapter 4: Experimental and theoretical investigation of P adsorption by DWTs

Kinetic Model	Iron-based sludges								Aluminium-based sludges					
	BS	MO	CA	FO	HH	AR	WY	BU	GU	HO	WD	OS	HU	WA
q _e (mg/g)	0.689	0.990	0.840	0.735	0.970	0.868	0.685	0.909	0.187	0.108	1.006	0.968	0.994	1.026
K ₂ * 10 ⁻¹ (g/mg.min)	0.144	0.082	0.083	0.082	0.076	0.087	0.126	0.061	0.995	0.981	0.207	0.112	0.230	0.117
pH 7 R ²	0.991	0.983	0.963	0.951	0.977	0.982	0.978	0.969	0.104	0.118	0.999	0.982	0.996	0.994
SSE	0.057	0.086	0.092	0.071	0.089	0.074	0.072	0.068	0.342	0.423	0.077	0.119	0.116	0.067
NSD	0.417	0.415	0.468	0.555	0.459	0.449	0.490	0.446	0.993	0.991	0.307	0.442	0.349	0.275
q _e (mg/g)	0.450	0.993	0.820	0.681	0.986	0.824	0.489	0.876	0.115	0.086	1.003	0.840	0.999	1.039
K ₂ * 10 ⁻¹ (g/mg.min)	0.365	0.067	0.075	0.084	0.062	0.082	0.216	0.045	0.974	0.977	0.152	0.121	0.179	0.084
pH 9 R ²	0.996	0.977	0.950	0.952	0.971	0.974	0.989	0.921	0.156	0.104	0.997	0.984	0.996	0.990
SSE	0.045	0.082	0.091	0.064	0.078	0.072	0.050	0.061	0.490	0.443	0.074	0.107	0.106	0.079
NSD	0.395	0.435	0.489	0.535	0.445	0.477	0.428	0.547	0.336	0.161	0.331	0.468	0.363	0.338
Particle diffusion model Parameters														
K _d (mg/g.min ^{1/2})	0.013	0.017	0.014	0.013	0.016	0.015	0.012	0.0171	0.011	0.014	0.013	0.014	0.010	0.015
pH 4 C (intercept)	0.161	0.898	0.163	0.121	0.193	0.157	0.156	0.123	0.499	0.333	0.443	0.336	0.515	0.329
R ²	0.873	0.899	0.930	0.842	0.898	0.893	0.837	0.9132	0.712	0.842	0.710	0.890	0.849	0.774
K _d (mg/g.min ^{1/2})	0.012	0.017	0.015	0.013	0.017	0.015	0.012	0.0161	0.014	0.016	0.014	0.015	0.013	0.017
pH 7 C (intercept)	0.137	0.162	0.122	0.091	0.145	0.13	0.122	0.089	0.357	0.146	0.356	0.240	0.415	0.242
R ²	0.859	0.921	0.946	0.853	0.912	0.891	0.867	0.9209	0.848	0.918	0.791	0.933	0.805	0.857
K _d (mg/g.min ^{1/2})	0.007	0.018	0.014	0.012	0.017	0.014	0.008	0.016	0.015	0.017	0.016	0.014	0.014	0.018
pH 9 C (intercept)	0.135	0.126	0.102	0.075	0.111	0.112	0.104	0.048	0.282	0.178	0.285	0.192	0.345	0.179
R ²	0.782	0.927	0.949	0.862	0.912	0.882	0.901	0.923	0.920	0.934	0.794	0.945	0.803	0.888

4.3.4 Effect of competing anions on P uptake by Al- and Fe-based sludge

The results of P-uptake with and without the competing anions for selected Al- and Fe-based sludges are presented in Figure 4.5. As shown in Figure 4.5 a and b, P-uptakes with the competing anions present at five concentrations deviated from their values at zero anions concentration across the three pHs (see error bars); especially for the Fe-based sludge. However, one-way ANOVA test was used to check the statistical significance of these deviations. The results showed that there is no significant effect of the competing anions on P-uptake ($p > 0.05$). This result is in agreement with the study of Yang et al. (2006b). Therefore, Al-based and Fe-based sludges could adsorb P efficiently with no significant effect of competing anions.

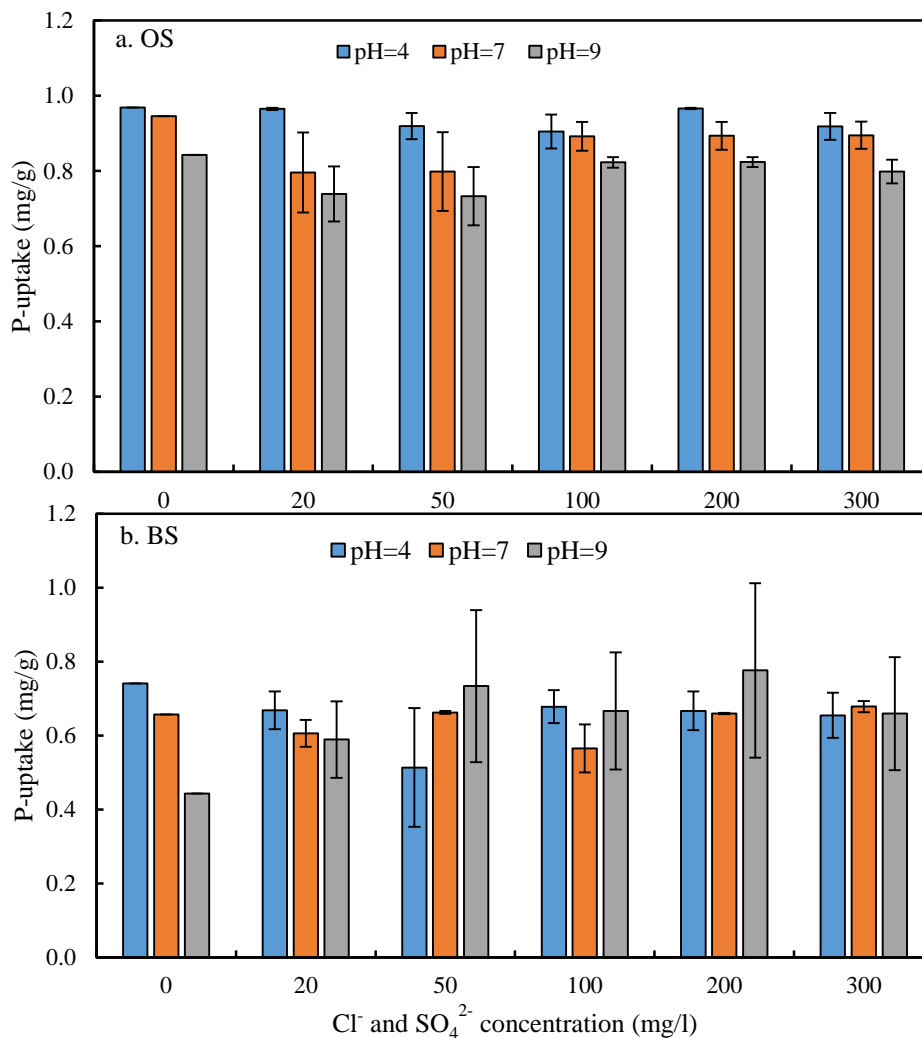


Figure 4.5 Effect of coexisting anions (Cl^- and SO_4^{2-}) on the phosphorus uptake of Al-based (a) and Fe-based (b) sludges with initial P concentration = 10 mg/L and 1g of sludge.

4.4 Summary

This chapter presents experimental and theoretical investigation of P adsorption. Maximum P adsorption capacities calculated from fitting the experimental adsorption data were influenced positively by the decreasing initial pH solution for only GU, WD, and OS Al-based sludges and MO Fe-based sludge ($R^2 > 0.9$), indicates that a monolayer of phosphate molecules is formed on their surfaces and their reactivity increases with increasing pH. Whereas the pH effect was not clearly evidenced either maximum adsorption capacity did not change or it is increased with increased pH for the other sludges, confirming that a homogenous P adsorption is not the dominant process for the majority of DWTSs. For metals affinity, the means values of maximum P adsorption capacities normalised to Al and Fe contents across the three pHs were (156 – 217 mg/g Al) and (55 – 66 mg/g Fe) respectively.

Freundlich model fitted adsorption data for most of the sludges with correlation coefficient range from 0.908 to 0.986. The surface of DWTSs is characterised heterogeneous surface with n values > 1 . The P binding affinity of these surfaces increased in the acidic conditions (K_f constant). Good fittings of the experimental data for Temkin model results at pH 4 ($R^2 = 0.733 - 0.955$) and this degree of fitting decreased with increased pH solution ($R^2 = 0.581 - 0.876$). The heat of adsorption (B_1) constant and equilibrium binding constants (K_T) obtained from the model related negatively with the pH increasing except AR sludge case, which might indicate additional P removal by precipitation.

Results of kinetic P adsorption into the sludge shows that the rate of P transformation from the liquid phase to the solid phase was biphasic, described by fast rate within 2 h followed by slow phase until equilibrium with 26 h. Correlation coefficients (R^2), and error functions of NSD and SSE identified that pseudo-second-order was the best fitting kinetic model for the data across the three pHs. Therefore, chemisorption is the rate-limiting step of P adsorption into DWTSs. The pseudo-second-order rate constant (K_2) was found pH dependent in a negative relationship as the pH increased except in cases of FO, OS, and WY sludges, which might be other precipitation or co-precipitation mechanism being dominant in alkaline conditions. The intraparticle diffusion model is not the dominant controlling process in the fast stage where the

chemisorption occurs. Diffusion process into meso- and micro-pores of DWTS improved when the initial pH solution increased.

Next chapter investigates the differences between the short-term experiments for both batch and continuous feeding system and in addition modelling P adsorption to predict life expectancy for two Al- and Fe-based sludges.

5 Chapter 5: Modelling phosphorus uptake by dewatered water treatment sludges under continuous feeding conditions

5.1 Introduction

Inlet P concentration and hydraulic retention time (HRT) have significant influence on passive treatment performance (Brooks et al. 2000; Kadlec and Wallace 2009). Field operating usually varies depending on influent wastewater characteristics. For example, typical P concentration in domestic wastewater varies from 4 to 12 mg/l (Metcalf and Eddy 2003). With this variation in influent wastewater characteristics, it can lead to unstable performance in systems utilising the adsorption process. In addition, another issue that is generating much research interest is the variation of P uptake and the longevity of the substrate used as the primary media.

Constructed wetland treatment systems are a passive green treatment technology that are engineered to treat and purify wastewater, in most cases by using substrates to remove contaminants from the wastewater stream (Zhao et al. 2009). In the case of the use of DWTS in constructed wetlands, the P uptake depends on the influent P concentration and hydraulic retention time. In order to estimate the effectiveness and longevity of DWTS for P uptake, it is necessary to examine the effect of inlet P concentration and HRT on P uptake and model this effect. Therefore, the main objectives of this study are to demonstrate and investigate the difference in P uptake between batch and continuous feeding experiments; examine the interaction effect of inlet P concentration and HRT on P uptake; model the combined effect through generalization of different control conditions to predict P uptake; and predict the life expectancy of used substrate or quantity of the passed volume at the required P saturation degree (PSD) under different operation conditions of inlet P concentration and HRT. The DWTSs employed in this study were collected from various water treatment works in the UK. By predicting their P uptake, the model can be used to resolve longevity questions which include: (1) what is the maximum accumulated P retained by the sludge?; (2) what is the highest amount of P loaded to sludge at

particular P saturation degree? and (3) how long does it take to reach the specific P saturation level or what volume of influent is passed to reach the required PSD?

5.2 Materials and methods

5.2.1 Characterisation of dewatered water treatment sludge

Two iron and two alum based sludges were obtained from different water treatment plants in the UK. The sludges were air-dried and grounded to pass a 2mm sieve size and then analysed for their chemical and physical properties. Their characteristics and analytical procedures are detailed in chapter three using the coding MO and FO for iron-based sludges; and GU and WD for the alum-based sludges.

5.2.2 Continuous feeding system, setup and experiment conditions

Figure 5.1 shows the schematic diagram of the continuous feeding system (CFS) set-up to evaluate the impact of the hydraulic retention time and initial P concentration on P adsorption by the DWTSs. The CFS set up followed the construction details described by DeSutter et al. (2006). The CFS setup was chosen because it prompts continuous interaction of P loading and a small amount of sludge to reach the saturation level within a short time of operation. A 150 ml column capacity provided with inlet and outlet closure and filter grid support (bought from QMX laboratories limited) was used. In order to keep a constant head inside the column, a flask fitted with two-hole stopper was used as Mariotte bottle. The holes were equipped with vent and solution supply tubes. The solution supply was routed inside the column. Due to the high adsorption capacity of the DWTS, and in order to achieve a representative P removal behaviour during the short-term experiment, a mass of DWTS mixed with acid-washed sand (Garside sand, 16/30 sand, 98.29% silica content, 38% porosity) was used. The ratio of sludge to sand was determined by trial and error until P removal percentages between 0 and 100% within 48 h operation time were achieved. To do this, the sand was firstly washed three times with tap water, and then later soaked with 2% of HCl acid to remove any dissolved ions. Thereafter, it was rinsed three times with tap and deionized water. The pH of the rinsed water was measured each time to assure that it is free of residual acid. After each operation condition, the exhausted mixed mass of acid-washed sand and sludge

was replaced with fresh mixture for the next new inlet P concentration and HRT. The used masses of sludge and acid-washed sand at different operation conditions of RTs and inlet P concentrations in CFS are given in the supplementary data (see Appendix B, Table B.1).

A 0.45 μ m filter was placed below the mixture of acid-washed sand and DWTS, and the effluent from the cell was connected to a peristaltic pump with variable flow rate. Four different HRTs (0.5, 1, 2 and 4 h) and five inlet P concentration (2.5, 5, 10, 20 and 50 mg/l) were used to mimic the P removal behaviour of DWTSs experimentally as a substrate in passive treatment systems. The P stock solution was prepared using deionized water and analytical grade of potassium dihydrogen phosphate (KH_2PO_4). Potassium chloride was added to keep the electrical conductivity around 1000 $\mu\text{s}/\text{cm}$, in order to control the ionic strength of the stock solution at different P concentration, and to also be comparable with the conductivity of real wastewater. The pH of the stock solution was adjusted to 7 by adding drops of 0.01M NaOH or HCl. The amount of volume passed through the media at a particular time is called the flow rate. To obtain the proposed retention times, a variable speed peristaltic pump was used, and known pore volumes of acid-washed sand and sludge mixture were measured. The mass of the mixture was determined as approximately 10 ml pore size. Hence, the pump flow rates were set to 0.33, 0.16, 0.08 and 0.04 (ml/min).

Adsorption experiments were run for 48 hours, during which the effluent solution from the cell was collected every 4 hours using a fraction collector. The collected samples were analysed directly for pH using a Mettler Toledo Seven Multi, and an InLab Expert Pro ISM pH probe. P, Fe, Ca and Al were analysed using inductively coupled plasma atomic emission spectroscopy (ICP-AES/ Perkin Elmer Optima 2100D), SO_4^{2-} using spectrophotometer (HACH DR-3900), and TC using Total Organic Carbon Analyzer (TOC-V CSH (Shimadzu)).

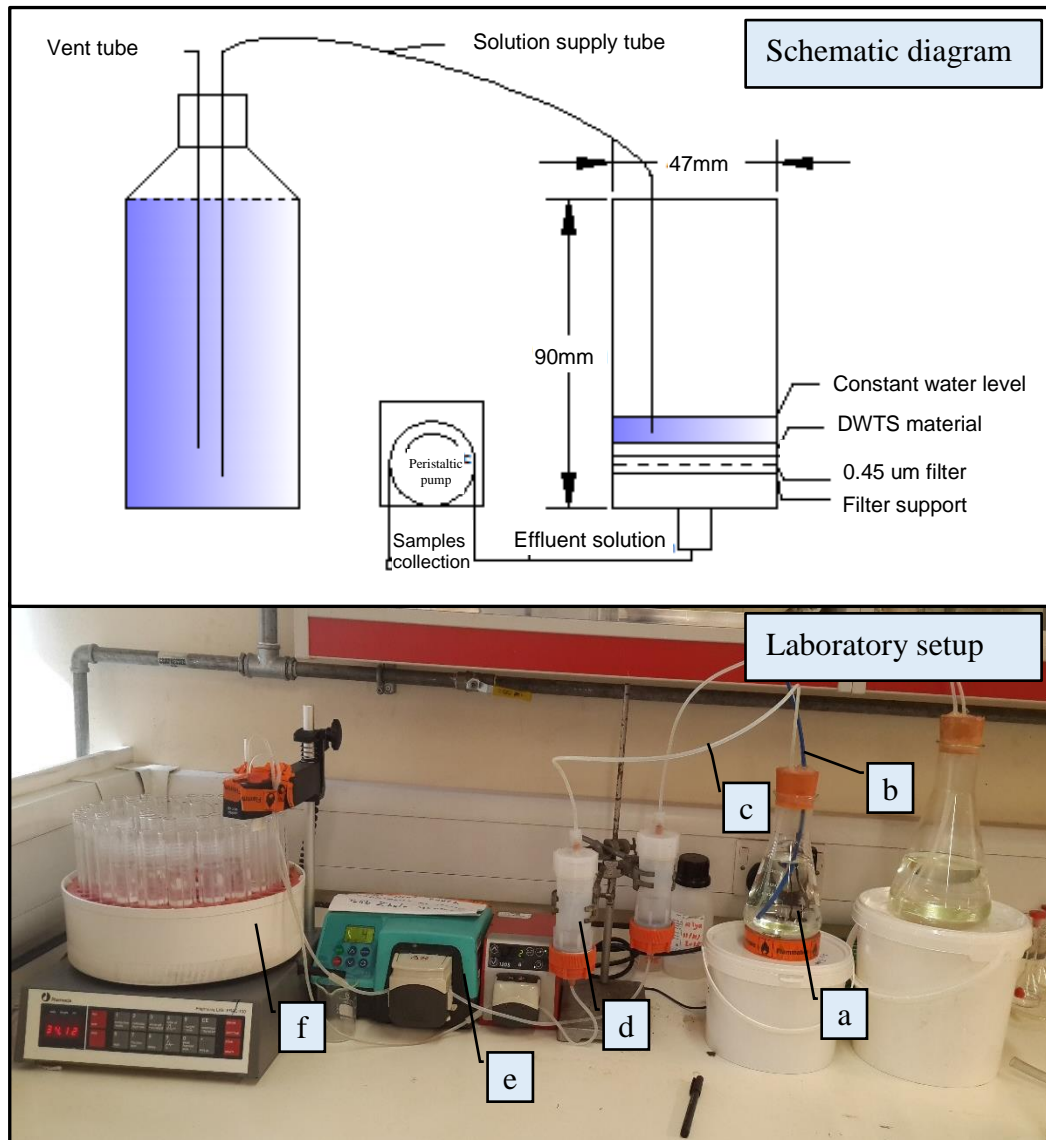


Figure 5.1 Schematic and laboratory setup of the continuous feeding system used to obtain P uptake at various combination of hydraulic retention time and influent concentration. a, b, c, d, e and f refers to the Mariotte bottle, vent tube, supplying tube, column, peristaltic pump and samples collection respectively.

5.2.3 Phosphorus adsorption – batch experiments

To thoroughly understand the combined effect, and also to compare with batch experiments, batch tests were conducted using 1g of each sludge, shaken for 48 h with P stock solution at five initial P concentrations (2.5, 5, 10, 20 and 50 mg/l). After the set time had elapsed, 0.45 µm filters were used to filter the suspension and the supernatants were analysed for Fe, Al, Ca, P, SO_4^{2-} and TC.

5.2.4 Data analysis and P removal modelling

To investigate the impact of HRT and inlet P concentration on the P uptake using different sludges, P uptake (unit mg-P.g⁻¹) was calculated using Equation 5.1.

$$P \text{ uptake} = \frac{(C_o - C_{ei}) * FR * t_i}{m} \quad (5.1)$$

where C_o is the inlet P concentration (mg/l); C_{ei} is the outlet P concentration (mg/l) at collection time (t_i) in an hour for the number of collected sample (i) from 1 to 12. FR is the flow rate (l/h) and m is the mass of sludge used (g). The amount of P loaded to the sludge (mg/g) during the operation period was calculated using Equation 5.2.

$$P \text{ loading} = \frac{C_o * FR * t_i}{m} \quad (5.2)$$

Stoner et al. (2012) suggested that P sorption is exponentially correlated with the amount of P loading to the material (x). Similarly in this study, exponential fittings were found to give the best explanation for the experimental data ($p = 0.000$). This correlation can be expressed as in Equation 5.3 to describe P uptake during the period of P loading to the sludge.

$$P \text{ uptake} = b_{0*} e^{-b_{1*}x} \quad (5.3)$$

In each combination of inlet P concentration and HRT, the y-axis intercept (b_0) and the slope (b_1) of Equation 5.3 either increased when HRT is constant and inlet P concentration is changed, or decreased when the inlet P concentration is constant and HRT is changed. To examine the effect of HRT and inlet P concentration on the intercept and slope of P uptake curve for each sludge type, and more importantly to generalize the various operation conditions of HRTs and P levels into sequential prediction steps, multiple linear regression models were used to predict the slope and intercept as dependent variables, and using the HRTs and inlet P concentrations as independent variables. The multi-linear model can be expressed as in Equation 5.4a and 5.4b. IBM SPSS Statistics 23 software was used. The slope and intercept values were normalised using one of the normalisation functions (i.e. logarithmic, square root inverse functions) when the non-normal distribution of residual values with the predicted values from the model was observed in histogram and probability plots.

$$\bar{b}_0 = a_1 * RT + a_2 * C_o + a_3 \quad (5.4a)$$

$$\bar{b}_1 = c_1 * RT + c_2 * C_o + c_3 \quad (5.4b)$$

where a_1 , a_2 , a_3 and c_1 , c_2 , c_3 are constants obtained from fitting multiple linear regression models with intercepts (b_0) and slopes (b_1). Substituting the predicted intercept (\bar{b}_0) and slope (\bar{b}_1) from Equations 5.4a and 5.4b into Equation 5.3 gives the generalized predicted P uptake Equation 5.5.

$$\text{General P uptake} = \bar{b}_0 * e^{-\bar{b}_1 x} \quad (5.5)$$

The total amount of accumulative P removal can be calculated during the time of P loading as in Equation 5.6 at any given level of P loading.

$$\text{Cumulative P uptake} = \frac{1}{x} \int_0^x \bar{b}_0 * e^{-\bar{b}_1 * x} dx \quad (5.6)$$

When the sludge reached its exhaustion point, the outlet P concentration is equal to 95 percent of inlet P concentration ($C_e=0.95*C_o$). While at P saturation degree (PSD) of 50 percent, the outlet P concentration is equal to 50 percent of inlet P concentration and so on. Substituting PSD into Equation 5.1 yields Equation 5.7 which can be used to calculate the P uptake at any PSD.

$$\text{P uptake (at different saturation level)} = \frac{(1-PSD)*C_o*FR*t_i}{m} \quad (5.7)$$

The P uptake and P loading calculations were based on using the determined amount of sludge and the sample collection period, and then the predicted P loaded to the sludge at different PSDs can be calculated using Equation 5.8 after substituting Equation 5.7 into Equation 5.5.

$$\text{predicted P loading } (x_p) = \frac{1}{\bar{b}_1} \ln \left(\frac{m*\bar{b}_0}{C_o*FR*t_i*(1-PSD)} \right) \quad (5.8)$$

By substituting Equation 5.8 into Equation 5.5 yields the maximum accumulative amount of P uptake by the sludge at the predicted P loading rate.

Moreover, the time required to reach the different degree of P saturation can be calculated by substituting the X_p obtained from Equation 5.8 into Equation 5.2 to yield Equation 5.9.

$$t_{PSD} = \frac{x_p * m}{C_o * FR} \quad (5.9)$$

Equation 5.9 can be expressed in terms of the total volume passed through the sludge at different PSDs as in Equation 5.10.

$$V_{PSD} = \frac{x_p * m}{C_o} \quad (5.10)$$

The procedure of the P uptake model followed the same steps as used in Stoner et al. (2012) to derive Equations 5.3 to 5.6. Life expectancy of the sludge for P uptake was clearly explained, and prediction equations were added in the current study as to enhance the P uptake prediction model.

5.3 Results and discussion

5.3.1 Comparison of P adsorption under continuous feeding and batch experiments

It is necessary to understand the differences in P uptake of DWTS under batch and continuous feeding systems. In the case of batch tests, the P uptake correlated positively with increase in the initial P concentration, where the contact time was constant at 48 h (Figure 5.2); this indicates that P uptake is a function of initial P concentration. The dissolution rate of sulphate and TC for both iron and aluminium based sludge increased in most cases as the initial P concentration increased as shown in Figure 5.2. This effect of initial P concentration was clearly demonstrated as the primary factor causing dissolution rate, and then affecting the P uptake behaviour. However, the variation of the inherent characteristics of the studied materials has a significant influence on the P uptake. Drizo et al. (1999) attempted to link the effect of physical and chemical properties (pH, cation exchange capacity, hydraulic conductivity, porosity, specific surface area and particle size distribution) of seven potential adsorbents (bauxite, shale, burnt oil shale, limestone, zeolite, light expanded clay aggregates and fly ash) to P adsorption capacity. It was found that the physicochemical properties of the materials were not strongly correlated with the observed P adsorption capacity, and direct laboratory experiments were better used to examine the differences in their P removal. In chapter three, experiments were conducted to find which of physicochemical characteristics of the 17 DWTSs

controlled P uptake using batch experiments. The content of Al and Fe, their reactive forms and the total surface area had the highest explanation percentage of the variation in P uptakes, followed by calcium and organic carbon content as the second group, and sulphate ion and pH as the third group.

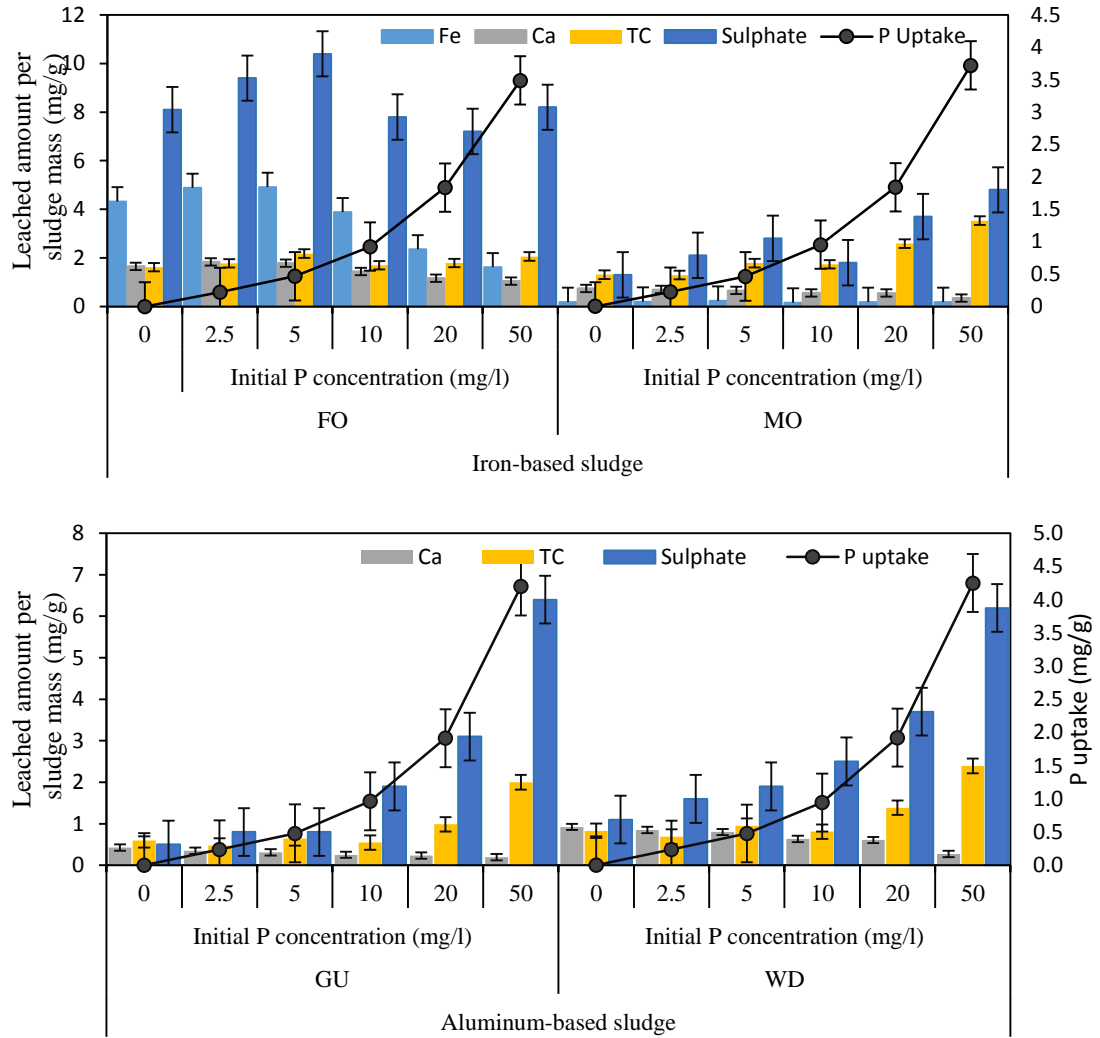


Figure 5.2 Elemental dissolution at different initial P concentration in the batch experiments for two iron- and aluminium based sludges with contact time 48h.

However, the interaction between the continuous P feeding and dissolution rates are critical factors for P uptake mechanisms which were not clearly understood in the batch experiment. Figure 5.3 illustrates this interaction between sulphate and TC dissolution and P loading rate at HRT of 4h and inlet P concentration of 5 mg/l. The sulphate and TC release were, respectively 1.4 and 1.3 mg/g for aluminium sludge

during the first four hours of P loading, matching the highest P uptake during the P loading time. These values of both elements releasing and up-taking P decreased with the progress in P loading, indicating that the ligand exchange mechanism is most likely to be the key factor in P uptake by the DWTSs under constant P loading. The comparison between the batch and the CFS in terms of P uptake, at the same P loading volume of 1.2 and 2.3 mg/g of accumulated P uptake using CFS, were much higher than 0.46 and 0.48 mg/g with using batch test for iron (MO) and aluminium (WD) sludge respectively in case of 5 mg/l initial P concentration. The reason for these differences could be due to the uninterrupted P loading in the case of CFS as a result of the continuous reciprocal action between HRT and influent P concentration, leading to increase in the exchangeable ions with P ions, or providing more places for P adsorption, which is probably the main contribution to these differences in P uptakes.

5.3.2 Combined effect of hydraulic retention time and inflow P concentration on P uptake

P is removed continuously under CFS as it continually exchanges with sulphate ion and TC, and it adsorbs into the metal hydroxide of Fe and Al or co-precipitates with the released metals. The release and exchange or adsorption mostly depends on inlet P concentration and HRT. Figure 5.4 shows the combined effect of both factors on the accumulative P uptake within 48 h operation time. The accumulative P removal represented the summation of the P uptake of 12 collection samples. In general, Al-based sludge showed higher values than Fe-based sludge, which apparently reflected the number of exchanged elements with P during the experimental period (see Figure 5.3), and also for the high percentage of amorphous aluminum associated with the Al-sludge. Although the accumulative P uptake increased with increasing inlet P concentration, the effect of HRT was not clearly demonstrated in Figure 5.4. The reason for this is that with the lower HRT, a higher amount of P loaded to the sludge and higher accumulated P uptake is obtained. For example, at inlet 2.5 mg-P/l of the Fe-based sludge, the cumulative P removed decreased from 0.84 to 0.57 mg-P.mg⁻¹ when the HRT increased from 0.5 to 4 h. While at HRT of 4 h, the P uptake increased from 0.57 to 3.31 mg-P.mg⁻¹ when the inlet P concentration rose from 2.5

to 50 mg/l respectively. Similar behaviour of the interaction of these three parameters was found with the Al-based sludge.

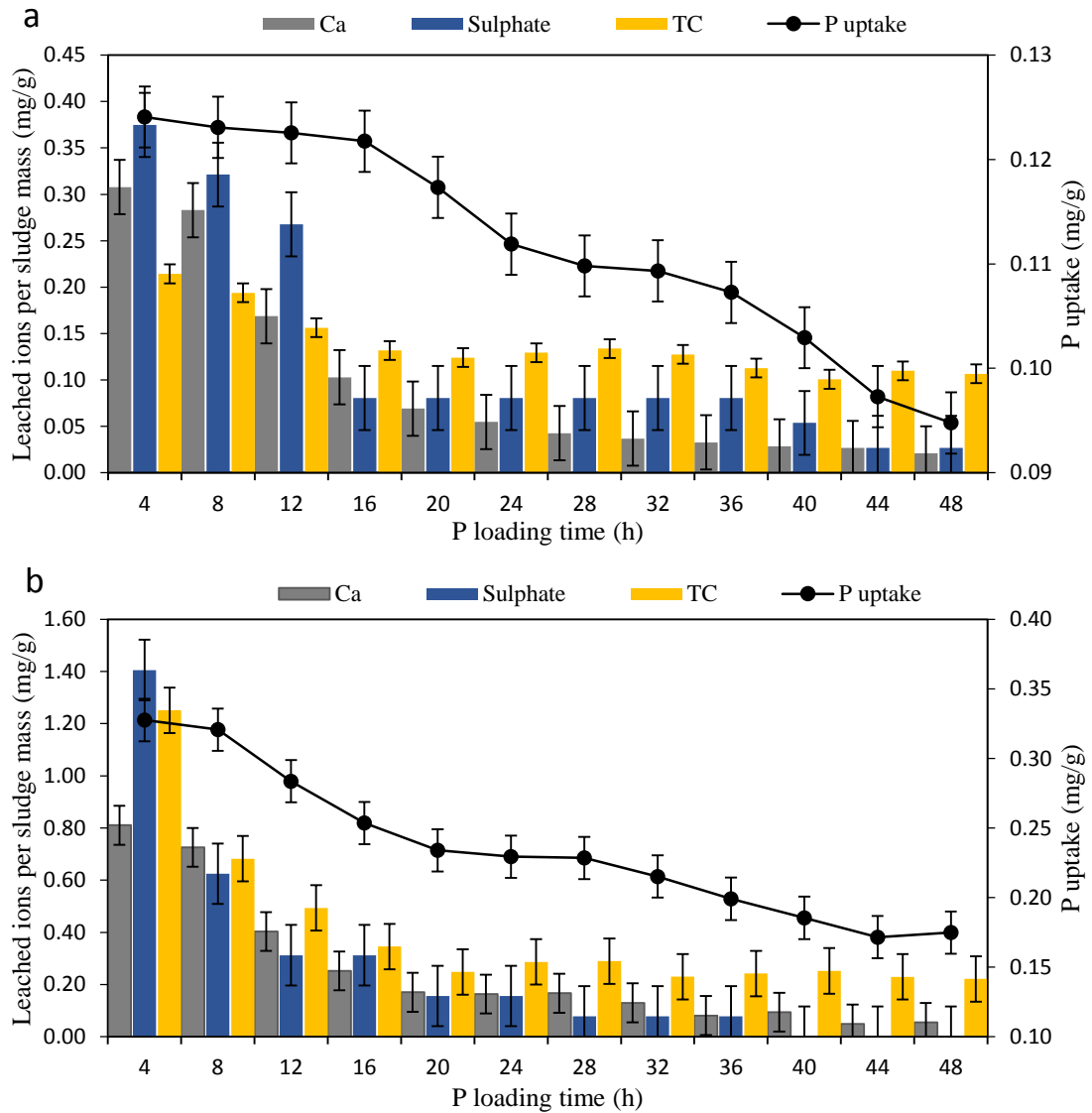


Figure 5.3 Leached ions and P uptake of: (a) iron- and (b) aluminium based sludge with retention time of 4 h and inflow P concentration of 5 mg/l under short-term continuous feeding system.

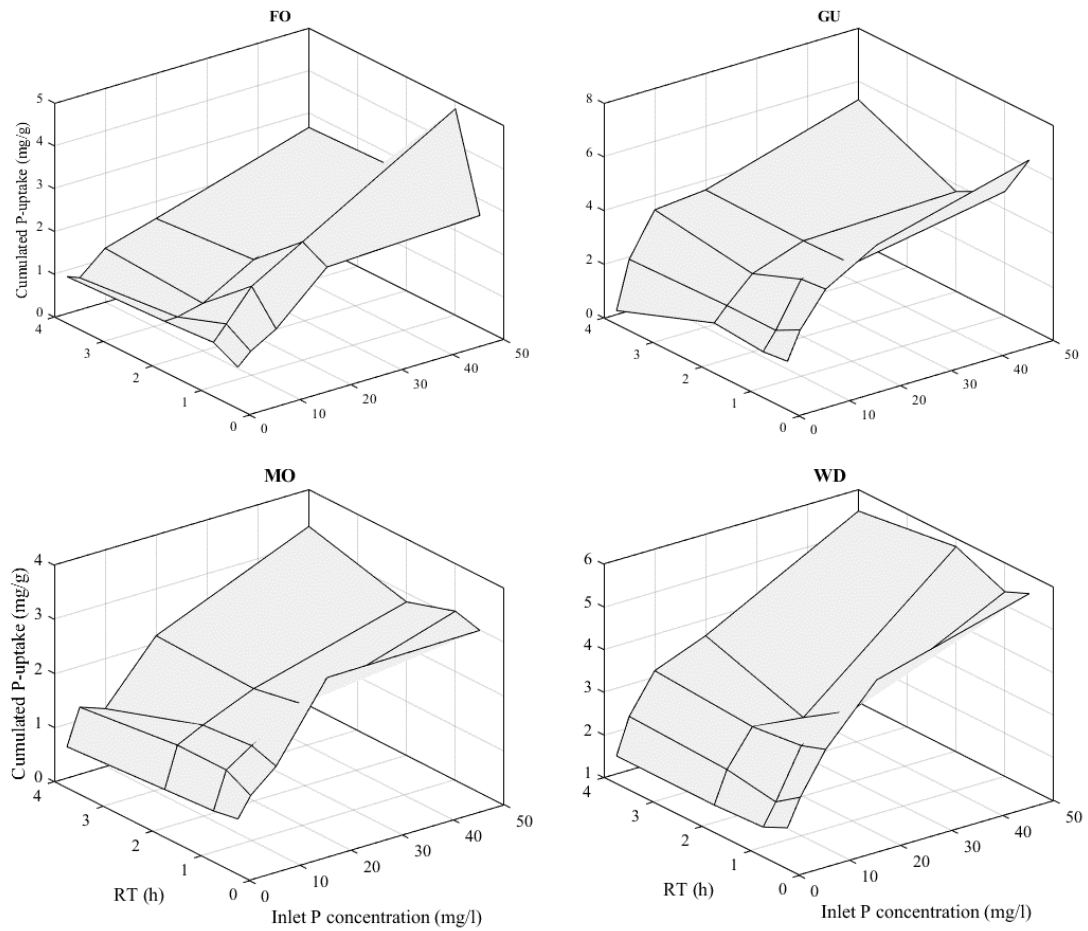


Figure 5.4 Accumulative P uptake after 48 h operation time for two iron- (FO and MO) and two aluminium (GU and WD) based sludges at different conditions of five inlet P concentrations and four hydraulic retention times.

To display the effect of HRT on P uptake, normalisation of P uptake to the P loading rate (influent P concentration multiplies by flow rate) was done. Figure 5.5 shows the impact of HRT on P uptakes at inlet P concentration of 10 mg/l and RTs of 0.5, 1, 2 and 4h. It can be seen from this figure that HRT positively affects P uptake, and this effect was decreased when the sludge reached its P exhaustion point. It also confirms that Al-sludge has higher adsorption capacity than Fe-sludge. The positive effect of HRT is due to increase in the dissolved ions level coupled with the P ligand exchange mechanism. HRT is a crucial design factor for achieving optimal removal efficiency in treatment systems. Long HRT permits vast interaction between P and DWTR. Whilst with a high hydraulic loading rate (HLR) or low HRT, the contact time with the substrate is shortened and leads to reducing this interaction (Zhang et al. 2014; Wu et al. 2015). Previous studies have evaluated the long-term operation of

field systems, in this case constructed wetland systems in order to determine the effect of HLR on P removal efficiency. Dzakpasu et al. (2015) observed lower and highly varied P removal with high HLR, and higher and more stable P removal with low HLR. In another study, HRT was noted as a significant factor for increasing P removal efficiency, through enhancing the formation of hydroxyapatites precipitates when electric arc furnace material was used in a continuous flow column, with 20 mg/l and 400 mg/l initial P concentration, and flow rate of 2.1 – 2.8 ml/min (Drizo et al. 2006). In another study using continuous flow experiments, Bowden et al. (2009) found that the percentage of P removal efficiency increased from 35% to 62% when the HRT was increased from 8 to 22 h across the range of initial P concentration from 1 to 50 mg/l; however, this percentage decreased as initial P level increased. In general, HRT and influent P concentration play a vital role in P adsorption mechanisms, driving higher P uptake values from continuous feeding system than that from batch experiments.

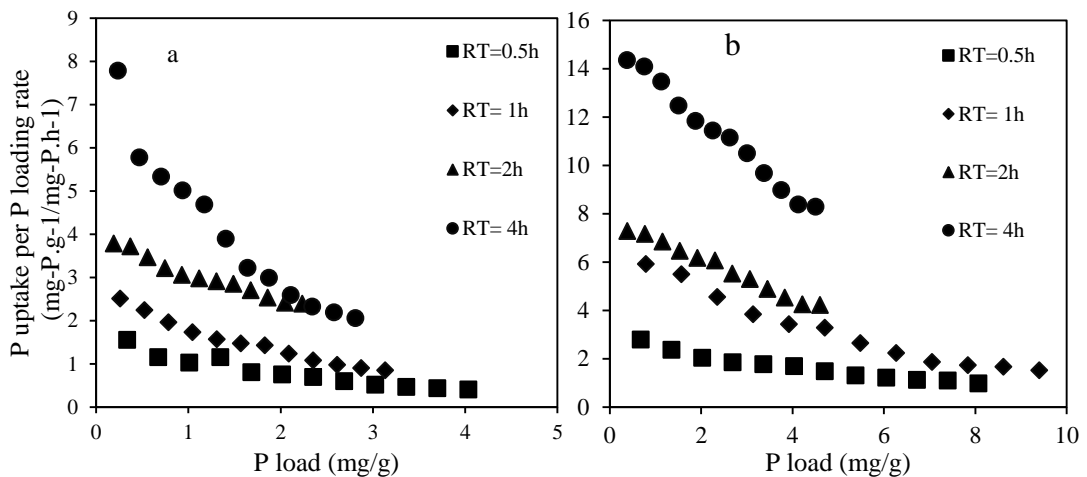


Figure 5.5 Effect of HRT on P uptake for (a) Fe- (MO) and (b) Al- (WD) based sludges at influent P concentration of 10 (mg/l).

5.3.3 P adsorption modelling

The P uptake of DWTSs depends on the HRT and inlet P concentration as explained in the previous section. Figure 5.6 presents the modelling of P removal by the Fe- and Al-based sludges. The exponential correlation gave the best fit for all the sludges with the different operation conditions of RTs and inlet P concentrations (R^2 range from 0.910 to 0.995), see Table 5.1 for more details of intercept (b_0), slope (b_1), and

R^2 for the four DWTRs (Appendix B includes all the figures showing the relationship between P uptake and P loading, as can be seen in Figure B.1 and B.2). It can be seen from Figure 5.6 a and d for Fe- and Al-based sludge respectively, that P uptake decreased exponentially with more P loading to the sludge, while the differences between the curves resulted from the effect of retention time. The weight values and the significance of the predictors and total weight of the multiple linear regression models are listed in Table 5.2. The intercept of P uptake curve was significantly explained by the inlet P concentration with weight percentage ranging from 60 to 87% for all the sludge ($p < 0.05$). The inlet P concentration coefficient (a_2) had a positive impact on the P uptake curve intercept, this indicates that the more influent P loading, the larger the y-intercept. The HRT constant (a_1) was statistically significant in estimating the intercept for the Fe-based sludges only, with weighing values of 25% and 8% for FO and MO sludge, respectively. The overall multiple linear models were significant in predicting the intercept of the generalised P uptake curve for all the sludges.

For estimating the slope of the P uptake, HRT had no statistically significant effect on the slope prediction of P uptake curve, while the inlet P concentration was the primary parameter explaining the variation of the slope in percentage range from 43 to 63. Overall, the models fitting were statistically significant ($P < 0.05$) with R^2 ranging from 0.43 to 0.63 (Table 5.2).

The purpose of predicting the intercept and slope of the fitting of P uptake is to generalise the correlation of different HRT and inlet P concentration conditions. This generalisation procedure gives Equation 5.5, which can be utilised in predicting P uptake for particular HRT and P concentration. The cumulative P uptake can then be calculated using Equation 5.6. More importantly is to find the maximum amount of P that can be loaded to the sludge at the point of the media becoming exhausted, or the outlet P concentration being equal to 95% of the inlet P concentration ($C_o = 0.95 * C_e$). This can be calculated using Equation 5.8. The maximum amount of cumulative P uptake can then be determined by substituting the maximum P loaded (obtaining from Equation 5.8) to the media into Equation 5.6.

The extrapolated values of intercept and slope in Table 5.2 can be utilised to predict the P uptake curve for a particular sludge at any given HRT and inlet P

concentration. An example is shown in Figure 5.6 b and e, respectively for MO- and WD-based sludges. These curves are generated by taking the coefficient parameters of RT and inlet P concentration from Table 5.2 to obtain the intercept (\bar{b}_0) and slope (\bar{b}_1) from Equation 5.4a and 5.4b at RT of 2 h, and inlet P concentration of 10 mg/l (see Figure 5.6 b and e). The curves can be used to size the P removal system, predict the amount of P uptake and how long it takes before the media is used up. This can be done by the integrating the modelled P uptake curve using Equation 5.6 to generate the accumulative P uptake curve (see Figure 5.6 c and f). By calculating the maximum amount of P that can be loaded to the sludge from Equation 5.8, it can be determined that a maximum of 8.6 and 17.4 mg of P can be loaded, respectively to 1g of MO and WD-sludges to reach the P exhaustion point. By applying these values of maximum P loading to the Equation 5.6, a 3.0 and 5.5 (mg-P. g⁻¹) P uptakes can be cumulated to MO-sludge and WD-sludge, respectively at RT of 2 h and inlet P concentration of 10 mg/l.

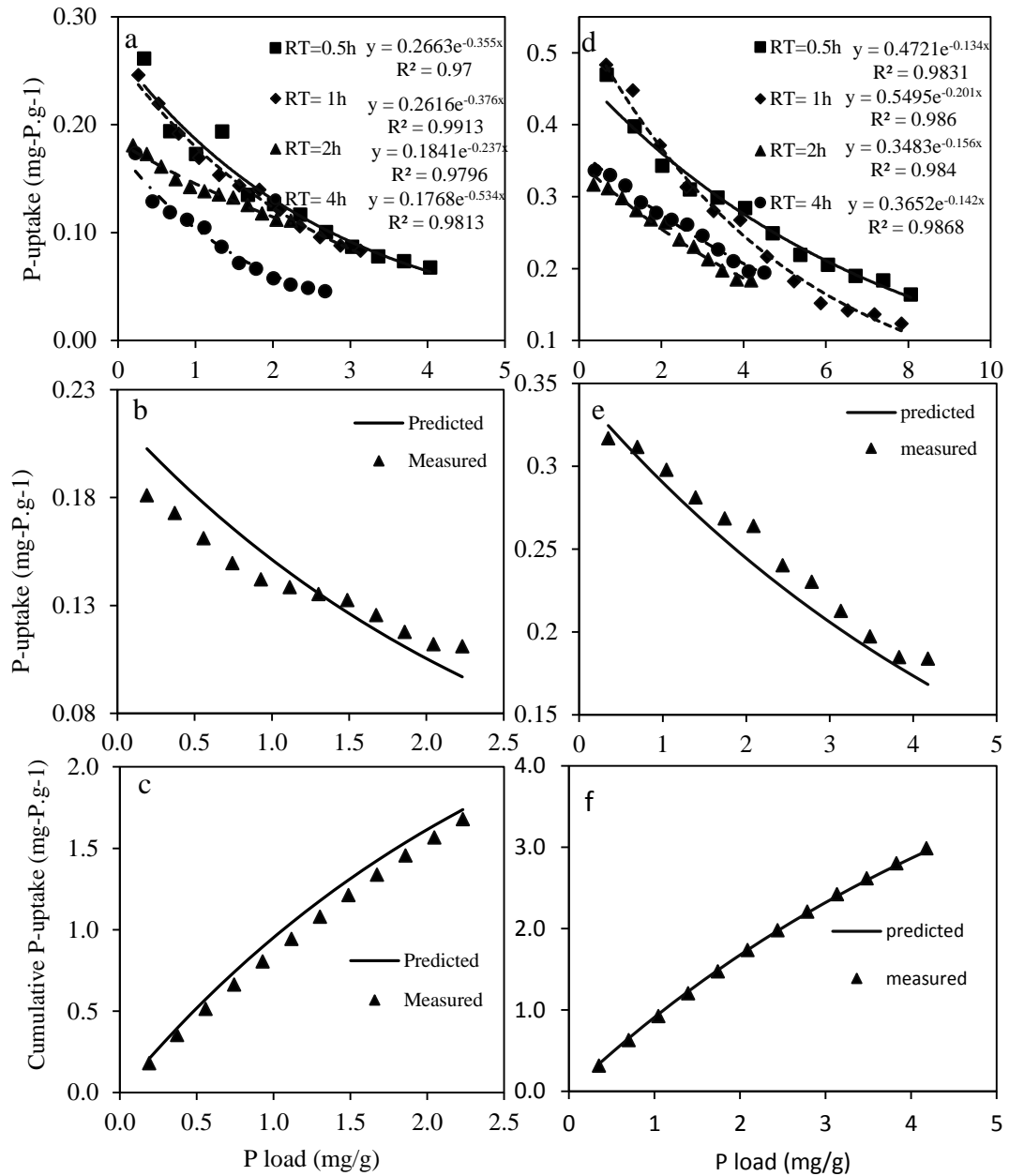


Figure 5.6 Modelling steps of P uptake for iron- (a to c) (MO) and aluminium- (d to f) (WD) based sludges at inflow P concentration of 10 mg/l. a & d represents the exponential correlation between the P uptakes and P loaded to the sludge at inlet P concentration of 10 mg/l and HRT of 0.5, 1,2 and 4 h; b & e represent the experimental P uptake and the modelled P uptake curve at HRT of 2 h and inlet P concentration of 10 mg/l; c & f represent the experimental cumulative and modelled cumulative data of P uptake at HRT of 2 h and inlet P concentration of 10 mg/l.

Table 5.1 The intercept (b_0), slope (b_1) and correlation coefficient at different operation conditions of HRT and inlet P concentrations obtained from fitting P uptake with P loading exponentially for two iron-(FO and MO) and two aluminium- (GU and WD) based sludge.

HRT(h)	P (mg/l)	FO			MO			GU			WD		
		b_0	b_1	R^2	b_0	b_1	R^2	b_0	b_1	R^2	b_0	b_1	R^2
0.5952	2.5	0.1806	-1.059	0.989	0.1409	-0.719	0.984	0.208	-0.384	0.979	0.1849	-0.162	0.912
0.5952	5	0.1714	-0.61	0.966	0.1835	-0.519	0.983	0.2767	-0.155	0.929	0.3213	-0.193	0.954
0.5952	10	0.3333	-0.598	0.982	0.3227	-0.293	0.97	0.4604	-0.131	0.969	0.4721	-0.134	0.983
0.5952	20	0.5225	-0.279	0.979	0.4929	-0.179	0.972	0.6439	-0.118	0.977	0.6434	-0.142	0.961
0.5952	50	0.6055	-0.238	0.986	0.6657	-0.225	0.993	0.7839	-0.083	0.985	0.9374	-0.127	0.991
1.021	2.5	0.2798	-0.792	0.962	0.1121	-0.496	0.935	0.14	-0.181	0.95	0.1459	-0.167	0.956
1.021	5	0.2385	-0.532	0.976	0.1511	-0.409	0.983	0.2706	-0.247	0.99	0.2848	-0.213	0.975
1.021	10	0.325	-0.256	0.986	0.2616	-0.376	0.991	0.4547	-0.137	0.95	0.5494	-0.201	0.986
1.021	20	0.5965	-0.257	0.946	0.3703	-0.301	0.991	0.4558	-0.104	0.975	0.4967	-0.163	0.984
1.021	50	0.8897	-0.128	0.9624	0.5591	-0.22	0.992	0.5517	-0.094	0.947	0.8991	-0.104	0.985
2.089	2.5	0.23	-0.821	0.982	0.125	-0.697	0.961	0.1524	-0.165	0.949	0.1776	-0.28	0.984
2.089	5	0.1454	-0.625	0.976	0.1943	-0.375	0.99	0.1994	-0.13	0.975	0.2726	-0.214	0.983
2.089	10	0.1732	-0.558	0.974	0.1841	-0.237	0.98	0.32	-0.116	0.97	0.3832	-0.142	0.984
2.089	20	0.2174	-0.324	0.955	0.2729	-0.277	0.98	0.3435	-0.058	0.932	0.2976	-0.112	0.99
2.089	50	0.4703	-0.327	0.91	0.3768	-0.195	0.97	0.3609	-0.062	0.948	0.7694	-0.113	0.983
4.269	2.5	0.1533	-1.026	0.979	0.1014	-0.842	0.989	0.2095	-0.445	0.972	0.1433	-0.194	0.954
4.269	5	0.1033	-0.829	0.977	0.1311	-0.187	0.955	0.1864	-0.138	0.912	0.2708	-0.19	0.965
4.269	10	0.1527	-0.395	0.979	0.2476	-0.381	0.981	0.3693	-0.105	0.981	0.3652	-0.142	0.987
4.269	20	0.1675	-0.234	0.962	0.2072	-0.115	0.965	0.447	-0.1	0.945	0.4733	-0.139	0.995
4.269	50	0.4095	-0.266	0.987	0.4333	-0.176	0.963	0.5972	-0.062	0.968	0.7667	-0.097	0.993

Table 5.2 Model coefficients for intercept and slope resulted from multiple linear regressions model, where intercept and slope of exponential correlations as dependent variables and HRTs and inlet P concentrations as independent variables.

Model coefficients for intercept prediction											
	HRT			Inlet P concentration			Intercept		Overall Model		
	a ₁	Sig.	R ²	a ₂	Sig.	R ²	a ₃	Sig.	Std. Error*	Sig.	R ²
FO	-0.088	0.000	0.253	0.011	0.000	0.547	-0.582	0.000	0.120	0.000	0.800
MO	-0.032	0.013	0.083	0.008	0.000	0.734	0.204	0.000	0.073	0.000	0.817
GU	-0.022	0.255	0.033	0.007	0.000	0.564	0.284	0.000	0.118	0.000	0.597
WD	-0.028	0.076	0.026	0.013	0.000	0.848	0.273	0.000	0.093	0.000	0.874

Model coefficients for slope prediction											
	HRT			Inlet P concentration			Intercept		Overall Model		
	c ₁	Sig.	R ²	c ₂	Sig.	R ²	c ₃	Sig.	Std. Error*	Sig.	R ²
FO	0.016	0.563	0.008	-0.011	0.000	0.593	-0.200	0.018	0.171	0.000	0.601
MO	-0.033	0.269	0.044	-0.008	0.003	0.389	-0.293	0.002	0.185	0.008	0.433
GU	0.492	0.262	0.030	0.181	0.000	0.596	4.611	0.001	2.697	0.000	0.625
WD	-0.006	0.620	0.006	-0.005	0.000	0.611	-0.703	0.000	0.078	0.000	0.617

* standard error of the estimate.

5.3.4 Predicting life expectancy of dewatered treatment sludge for P uptake

The primary purpose of this chapter is to propose a statistical prediction model for DWTS longevity when used in a treatment system such as a constructed wetland system, based on various operation conditions of HRTs and influent P concentrations. Long-term operation of treatment systems such as constructed wetlands using DWTS as the substrate can be predicted using the generalised P uptake curve equations. The prediction procedure involves using Equation 5.8 to calculate the maximum amount of P loaded to the sludge at specific PSD, applying this value into Equation 5.6 to determine the accumulative retaining P, and finally predicting the sludge longevity for P uptake up to the required PSD point using Equation 5.9, or estimating the volume that can be treated up to the PSD point using Equation 5.10. The estimated values for maximum P loaded to sludge, accumulative P uptake and time taken to reach 50% and 95% PSD levels are listed in Table 5.3. These values are examples of predicted life expectancy calculated based on influent P concentrations of 5 and 10 mg/l and four different HRTs. At inlet P concentration of 5 and 10 mg/l, the predicted time of 50 and 95% PSDs increased with the increasing HRT in most cases. For example, the longevity of FO- sludge changed from 35 and 117 h to 52 and 188 h at inlet P concentration of 5 mg/l, when the HRT increased from 0.5 h to 4 h for PSD of 50% and 95% respectively. These differences could be explained by the fact that HRT increases the interaction between leachable ions and phosphate ions in sludge structure. In addition, it could also enhance the P-Ca precipitation if the pH and Ca^{2+} concentration rise because of calcium dissolution. The impact of increasing inlet P concentration was apparently noticed from the reduction in the sludge longevity for P uptake with both PSDs between the 5 and 10 mg/l inlet P levels. This impact was lowered as the RT increased, and this could be explained by more places being available for P sorption in the physical and chemical sludge structure. In general, Al-based sludges, showed higher life expectancy for P uptake than Fe-based sludges.

For practical application of the proposed predicted model procedure, if FO-sludge is used to treat wastewater with HRT 6h, and flow rates 190 l/c.d (typical for rural

areas) and 460 l/c.d (typical for urban areas) with influent P dry mass 17.3 and 7.2 g/c.d respectively. The proposed inflow wastewater characteristics of FRs and P concentration were adopted from Metcalf and Eddy (2003) based on individual residences. The required sludge masses for rural and urban FR are 105 and 253 kg per captia respectively, calculating from known sludge porosity (0.49), particle density (2115 kg/m³), and given FRs. From Table 5.2 and Equations 5.4 a and b, the intercepts (\bar{b}_0) and the slopes (\bar{b}_1) were 0.780 and 0.063 for rural inflow and 0.115 and 0.424 for urban inflow. To find the maximum amount of P that can be loaded to FO-sludge and lifespan or total treated water at 50% PSD, Equation 5.8 and 5.9 are used to obtain about 64 and 9 (mg-P loading.g⁻¹) and 388 and 321 days for these two inflow conditions respectively. The predicted lifespan and the amount of outflow volume of proposed operation conditions for FO-sludge at a full range of PSD from 0 to 95% are presented in Figure 5.7 a and b. At 95% PSD, about 609 days (1.67 years), 116,000 l and 512 days (1.4 years), 193,000 l were predicted at the exhausted point for rural and urban flow conditions respectively. The differences in these values are a result of dissimilarity of HRTs and inlet P concentration, which effect on P adsorption characteristics as explained in previous sections.

Previous studies utilised maximum adsorption capacity obtained from the Langmuir model or from P saturation point obtained experimentally of long-term continuous flow column test to estimate the life expectancy of substrates used in constructed wetland (Drizo et al. 1999; Xu et al. 2006; Zhao et al. 2009). This estimation is either over or underestimation because of the arbitrary nature of batch experimental conditions which are influenced by many factors (such as initial pH, initial P concentration, contact time, particle size). Furthermore, critical parameters have not taken in lifetime estimation, which includes the changing of inflow concentration and the hydraulic retention time. Thus, it becomes difficult to compare the result of a recent study with the previous study. The above field applicable example of rural areas flow rate characteristic if the inflow P concentrations are 5 and 10 mg/l, the life expectancy of FO- sludge will be 3.83 and 2 years to reach its exhaustion point respectively. These figures are based on the ideal flow through a constructed wetland and consider the sludge mass used. Drizo et al. (1999) proposed that if a dry weight

of 2.3 g-P/c.d is loaded with 4.5 tonnes of shale material used as wetland substrate, the saturation point is reached after 20 years however when taking into account the limitations of flow through reed beds this figure was more realistically reduced to 7 years. In more recent studies, Callery et al. 2016 and Callery and Healy 2017 developed a model based on the fundamental of Freundlich theory using small-scale column of short term experiments. Their model was successfully able to describe and predict the effluent concentration and then the breakthrough curves which were sufficient to predict the performance of large scale filters.

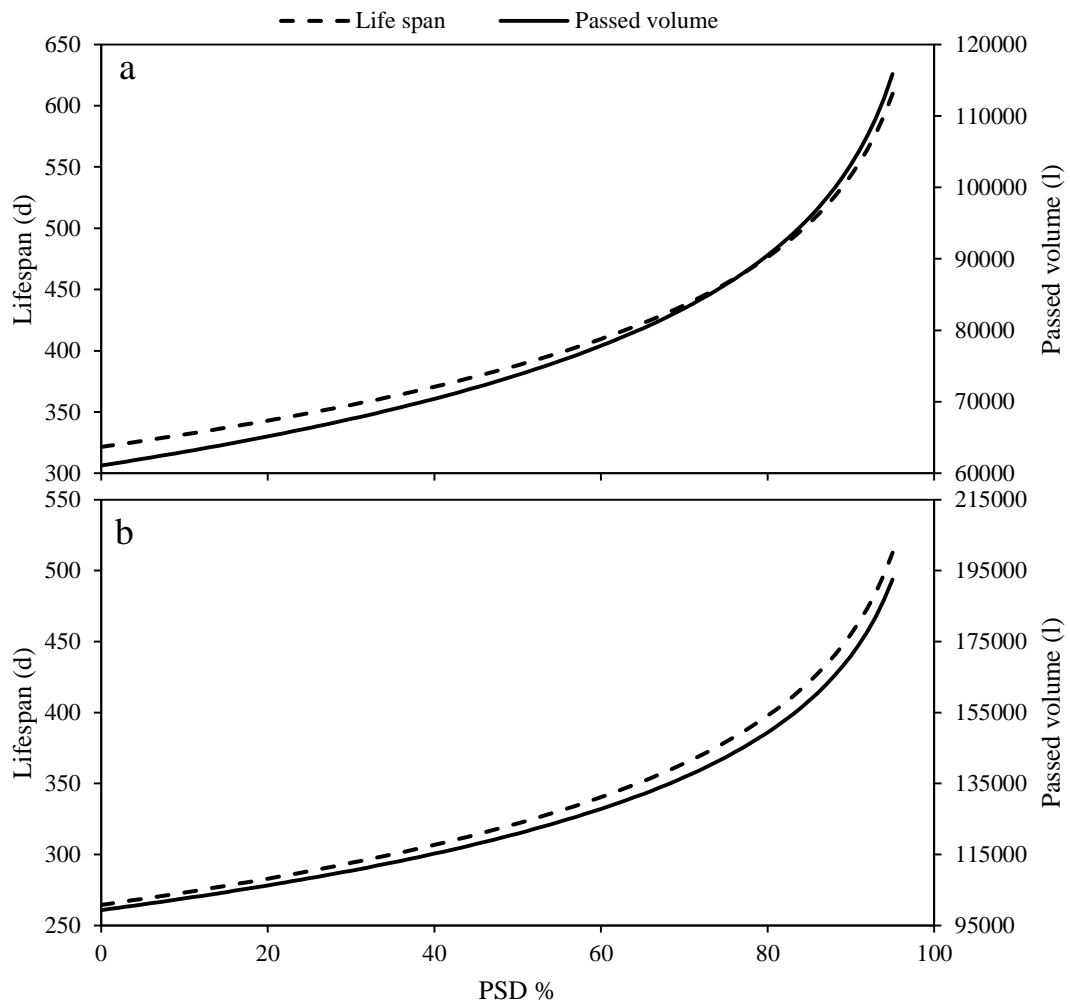


Figure 5.7 Predicted lifespan and the treated wastewater volume at a range of P saturation levels from 0% to 95% for Fe- sludge (FO). a and b refer to flow rates of 190 and 460 (l/c.d), with influent P dry mass weight of 17.3 and 7.2 (g/c.d).

Table 5.3 Parameters for estimation of life expectancy of DWTSs at inlet concentrations of 5 and 10 mg/l and hydraulic retention times of 0.5, 1, 2 and 4 h.

Inlet P concentration =5mg/l

	RT=0.5h						RT=1h						RT=2h						RT=4h					
	50%			95%			50%			95%			50%			95%			50%			95%		
	Xp ^a	MA ^b	t _n ^c	Xp	MA	t _n	Xp	MA	t _n	Xp	MA	t _n	Xp	MA	t _n	Xp	MA	t _n	Xp	MA	t _n	Xp	MA	t _n
FO	1.7	1.5	34.9	5.8	2.3	116.9	2.1	1.2	61.4	6.1	1.7	175.5	1.5	1.2	37.2	5.3	1.9	133.4	1.3	1.08	51.8	4.9	1.77	187.8
MO	1.4	1.0	23.6	6.6	2.0	110.0	1.8	1.3	36.6	7.1	2.4	146.0	1.7	1.2	35.9	7.5	2.3	162.2	1.7	1.1	53.6	8.5	2.4	276.1
GU	4.0	2.9	52.8	17.4	5.5	228.0	3.6	2.5	44.1	17.5	5.2	213.9	6.2	5.1	116.0	21.2	8.1	399.4	6.7	5.3	142.5	24.2	8.8	516.8
WD	2.3	1.4	21.8	14.7	3.9	140.0	1.9	1.1	17.5	14.4	3.6	132.3	3.1	2.1	38.7	15.8	4.5	197.5	1.9	1.1	24.4	15.0	3.7	191.6

Inlet P concentration =10mg/l

FO	1.2	0.8	13.7	5.8	1.7	68.5	1.6	0.7	25.9	6.1	1.2	99.9	1.6	1.2	33.0	5.9	2.1	124.0	1.0	0.7	26.7	5.1	1.5	129.6
MO	1.1	0.7	13.4	6.8	1.8	81.1	1.7	1.2	25.6	7.5	2.3	115.6	2.3	1.8	47.4	8.6	3.0	180.5	0.9	0.5	16.3	8.4	2.0	151.1
GU	2.1	1.2	17.0	17.6	4.3	141.2	2.1	1.2	17.2	18.0	4.3	147.4	4.0	2.9	45.7	17.4	5.5	200.0	2.8	1.7	29.8	22.4	5.5	239.2
WD	0.80	0.43	4.74	13.9	3.0	83.0	0.79	0.42	4.83	14.0	3.0	85.9	3.4	2.3	35.8	16.8	5.0	176.0	2.5	1.5	26.5	16.3	4.2	174.1

^a Maximum amount of P that can be loaded to the sludge, in a unit of (mg/g), to reach 50 or 95 percent P saturation degree.

^b Maximum accumulated P removal by the sludge, in a unit of (mg-P. g⁻¹), at P saturation level of 50% or 95%.

^c The required time in hours for the sludge to reach the 50 or 95 percent P saturation level.

5.4 Summary

The aim of this chapter was to investigate the differences in batch and continuous flow experiments for P uptake, and to construct a P uptake model using CFS, operated at different operation conditions of influent P concentrations and HRTs.

The comparison of the results of P adsorption between batch and CFS showed that P uptake in CFS was more than two- to four-folds of that obtained from batch tests, under the same condition of P loading for both iron and alum-based sludges. These differences can be explained by the continuous interaction between the DWTS and P loading that leads to increasing the exchangeable rate of ions with phosphate ions, or providing more reactive places in case of CFS.

The results of the effect of influent P concentration and HRT on P uptake in CFS showed that both of them played a significant role in the dissolution rate of exchangeable ions, or in providing additional places for phosphate removal from the liquid phase into the solid phase. The effect of influent P concentration was clearly demonstrated while HRT impact was identified after normalising P uptake to the P loading rate.

The exponential correlation between P added to the DWTS and sludge P uptake was found to have the best significant fit for all sludges with various operation conditions (R^2 range from 0.910 to 0.995, $p < 0.001$). The slopes and intercepts resulting from this correlation (dependent variables), and the operation conditions of influent P concentrations and HRTs (independent variables) were modelled to generate linear equations predicting the slope and intercept values at any P concentration and HRT. These predicted values could be used in the exponential function of P uptake curve to produce a general prediction model. Moreover, the maximum cumulative P added to the sludge, and the maximum amount of cumulative P uptake at the point where the sludge is no more removing P could be calculated. The lifespan of DWTS for P removal at any PSD or the amount of treated volume was successfully calculated based on the experimental results. Results from this study indicate that the generalised model can be used to predict the P uptake and life span of DWTS at various operation conditions and saturation degrees in a treatment system.

Next chapter investigates P and coagulant recovery from different degrees of P saturation using electro dialysis technology.

6 Chapter 6: Coagulant and phosphorus recovery from P saturated sludge

6.1 Introduction

Upon saturation with P, finding a new and sustainable source of coagulants and P via recovery from the P-saturated sludge is not only an economic and environment sustainable approach, but it also contributes to reducing the environmental risk generated from the disposal of P saturated sludge (PSS).

DWTS removes P via adsorption mechanisms onto metal hydroxides of Fe or Al, and ligand exchange with sulphate ion and OC as detailed in Chapter 3. This ligand exchange mechanism reduces the OC inherent in sludge simultaneously, resulting in PSS with less OC content. In the acid solubilization step, in addition to extracting both coagulant and P, other trace elements and DOC are also mobilised from the PSS, resulting in solubilized PSS with different degrees of DOC contamination. Utilising such solubilized PSS with high DOC content in water treatment as a coagulant will lead to lower performance in terms of water purification, and a higher potential for the formation of disinfection by-products in the final treated water. Therefore, the development of alternative process with high ionic selectivity and low carryover of DOC and energy consumption is a critical need. Previous studies of metal recovery technologies like pressure driven membrane, ion exchange and electrochemical systems, have only focused on coagulant recovery with low DOC content (Keeley et al. 2014a; Prakash and Sengupta 2003). Consequently, new processes to recover coagulant with high purity and also P at the same time are still required.

Electrodialysis (ED) is a promising process with one-step operation for P and coagulant recovery from PSS. This process operates with the same advantages of ion selectivity, but offers greater control over the separation kinetics and its cost through the applied potential. ED not only lowers the concentration in the feed solution, it also concentrates the beneficial ingredients in the acidified sludge for further reuse (Baker 2012). Different operation modes of ED were used in previous studies to treat surface water, separate monovalent and divalent ions from aqueous solution, extract

heavy metals and recover P from sewage sludge, and to recover cyanide from gold mine effluent (Van Der Bruggen et al. 2003; Van Der Bruggen et al. 2004; Ebbers et al. 2015; Zheng et al. 2015). However, very little is known about using ED process for P and coagulant recovery from PSS at different P saturation degrees.

Therefore, the aim of the study presented in this chapter is to provide understanding of the impact of various saturation degrees of PSS on the recovery of ferric coagulant and P in one step operation; and to give an indication of the purity of the recovered ferric coagulant in terms of DOC contamination and other trace elements. The performance of the recovered ferric coagulant was also evaluated. Furthermore, the interaction between the PSS and the loaded acid was investigated in order to determine the leachability of Fe, P, DOC and other trace elements at different saturation degrees of PSS. Three and five compartments ED cells were used in order to compare the recovered purity with and without presence of the effect of half way reaction of anodic and cathodic compartments respectively.

6.2 Materials and method

6.2.1 P saturation iron-based sludge and solubilization

Iron-based dewatered water treatment sludge which contains 25.5%, 1.2%, 0.4%, 0.04%, and 16.4% of Fe, Al, Ca, P, and TOC respectively, was collected from water treatment work treating reservoir water with the following characteristics: 4.4 (NTU), and 1.81mg/l and 13.96mg/l, respectively, for turbidity and TOC. The sludge cake was air-dried and ground to particle size < 2 mm.

Three columns were packed with 720, 720 and 1000 g of iron-based sludge to prepare 0%, 50% and 100% of PSS (see Appendix C, Figure C1 shows curves of 50% and 100% breakthrough points). The packed amounts of air-dried sludge were loaded with P in a continuous flow. To accelerate the breakthrough point of saturation with P, a high inlet P concentration was used. Similar high inlet P concentration (400 mg-P/l) was used in a previous study to using a continuous feeding system (Drizo et al. 2006). The column effluent P concentration was measured daily, and the P loading was stopped when 50% and 100% of P-saturation degree was reached. The 50% and 100% P saturation were determined, respectively

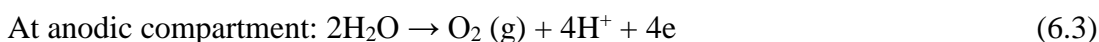
based on P concentration at outlet flow being equal to 50% and 100% of the inlet P concentration. Thereafter, the columns with different percentages of PSS were rinsed with deionized water to obtain homogeneous sludges. The extraction step was then started by directly pumping 5 l of different stoichiometry of 2:1 molar ratios of sulfuric acid:ferric to the three PSSs. Sulfuric acid was used due to its efficiency of P and coagulant extraction, safety and the price as explained elsewhere (Zhao and Zhao 2009). The molar ratio of sulfuric acid to ferric was calculated based on the quantity of iron in the packed sludge and according to Equation 6.1; and most importantly, the extra amount of sulfuric acid required overcoming the buffering capacity of sludge. Low-speed pumping was used to increase the contact time between the acid and sludge. The molar ratio determined based on the amount of iron in the column. After the whole 5 l acid had passed through the sludge, the extracted mixture was recirculated to enable more iron and phosphate to be solubilized. This process of extraction was implemented to study the interaction between PSSs and the sulfuric acid that was continuously added; and more importantly the reaction status in recycling stage, the hypothesis being that more coagulant and P are solubilized, and more acid is consumed in recycling step. Samples were collected periodically, and indirect measurement of pH was conducted every 40 min using a data logger. The recirculation was stopped when the change in the electrical conductivity (EC ms/cm) was low.



6.2.2 Electrodialysis cells

6.2.2.1 Design and operation

The extracted coagulant, P, sulphate and other trace elements from the PSSs were recovered simultaneously in the one-step operation of electrodialysis cell (ED). Two stack modes of ED were setup: the conventional three compartments (mode 1) and a new approach of five compartments (mode 2). The two different modes of ED stacks were used to study the effect of the half-way reaction in the anodic and cathodic compartments (Mode 1) on the recovery efficiency, according to Equations 6.2 and 6.3 (Ottosen et al. 2007; Zito 2011; Ebberts et al. 2015).



The compartments were made from Polyvinyl Chloride (PVC) material to avoid chemical corrosion. The internal dimensions were 10 x 5 x 2 cm and 10 x 5 x 1.2 cm (L x W x H), respectively, for mode 1 and 2. The compartments were combined together by screwing on the corners, and silicone sealant was used to assure waterproof conditions. Nafion 115 was used as cation exchange membrane (CEM), and fumasep® FAS-PK-130 was used as anion exchange membrane (AEM). The ED stack electrodes were made of titanium material. To avoid the passivation problem on the anode electrode, the titanium plate was coated with manganese dioxide.

For mode 1 of the three compartments, the solubilized sludge of PSSs was fed in the dilution compartment (DC), which is separated from the anode (AC) and cathode (CC) compartments by anionic and cationic membranes, respectively. The anionic exchange membrane (AEM) allows P, sulphate (SO_4^{-2}) and any other anionic ions to permeate toward AC, while cationic exchange membrane (CEM) allows Fe and other trace cationic elements to permeate toward CC. Ions flux through the membrane is affected by the membrane type and its capacity, applied voltage, resistance and pH (Baker 2012). To overcome the electrode reaction problem in the anode and cathode compartment as previously stated, five compartments of ED (mode 2) were set-up. Mode 2 consists of the DC (where the diluted solubilized sludge is fed), the anodic concentrated compartment (ACC) (to recover anionic ions), and cathodic concentrated compartment (CCC) (to recover cationic ions). The diluted solubilized PSS is fed into DC separated from the other compartments by AEM and CEM. This organisation of membranes allows anionic ions permeation towards ACC, while the cationic ions permeate towards CCC. In addition, the electrolyte solution of anodic and cathodic compartments is separated completely from the concentration compartment by using CEM and AEM, respectively. Figure 6.1 represents the experimental design scheme for the two modes of ED stack.

It has been reported that membrane fouling in ED is mainly due to organic compounds (Keeley et al. 2014a). Therefore, two different dilution ratios of the solubilized PSS at 0%, 50% and 100% were used to prepare two concentrations. The

concentrations were classified in term of the iron level, into low concentration (LC) and high concentration (HC), in order to investigate if the recovery efficiency and the recovered purity are affected by increasing the DOC level and P concentration. The electrolytes solution was made of 5 wt% sodium sulphate solution for both modes, while ACC and CCC were fed with deionized water only to assure the used electrolyte and the concentrated compartment solutions are free of DOC content, and also to avoid any undesirable reaction e.g. toxic gases generation. The corresponding solution of each compartment was recirculated at 0.25 l/min from 0.5 L beaker using the multichannel head peristaltic pump. The total volume of each solution was 500 ml including the external volume in the recirculation loop. The diluted solubilized sludge, the feeding solution into AC and CC for mode 1, and the feeding solution into ACC and CCC of mode 2 were continuously stirred using a magnetic stirrer to ensure a homogeneous feeding. Three pH probes were placed in the recirculation lines (flow through cells were connected to the outlet of each compartment to insert pH probes) of AC, DC and CC of mode 1, or ACC, DC and CCC of mode 2 to periodically measure the change in the pH value. In addition, the EC probe was connected to the DC outlet to monitor the electrical conductivity of the diluted solubilized sludge. These probes were connected to a 12-channel measuring and recording data logger (EA Instruments, London, UK). The applied voltage was supplied by a regulated DC power supply (KEYSIGHT, Agilent, E3634), and the current was monitored using current logger (IN myDAQ) and LabVIEW software. The schematic plan for the whole experiments of P loading, extraction and recovery is shown in Figure 6.2.

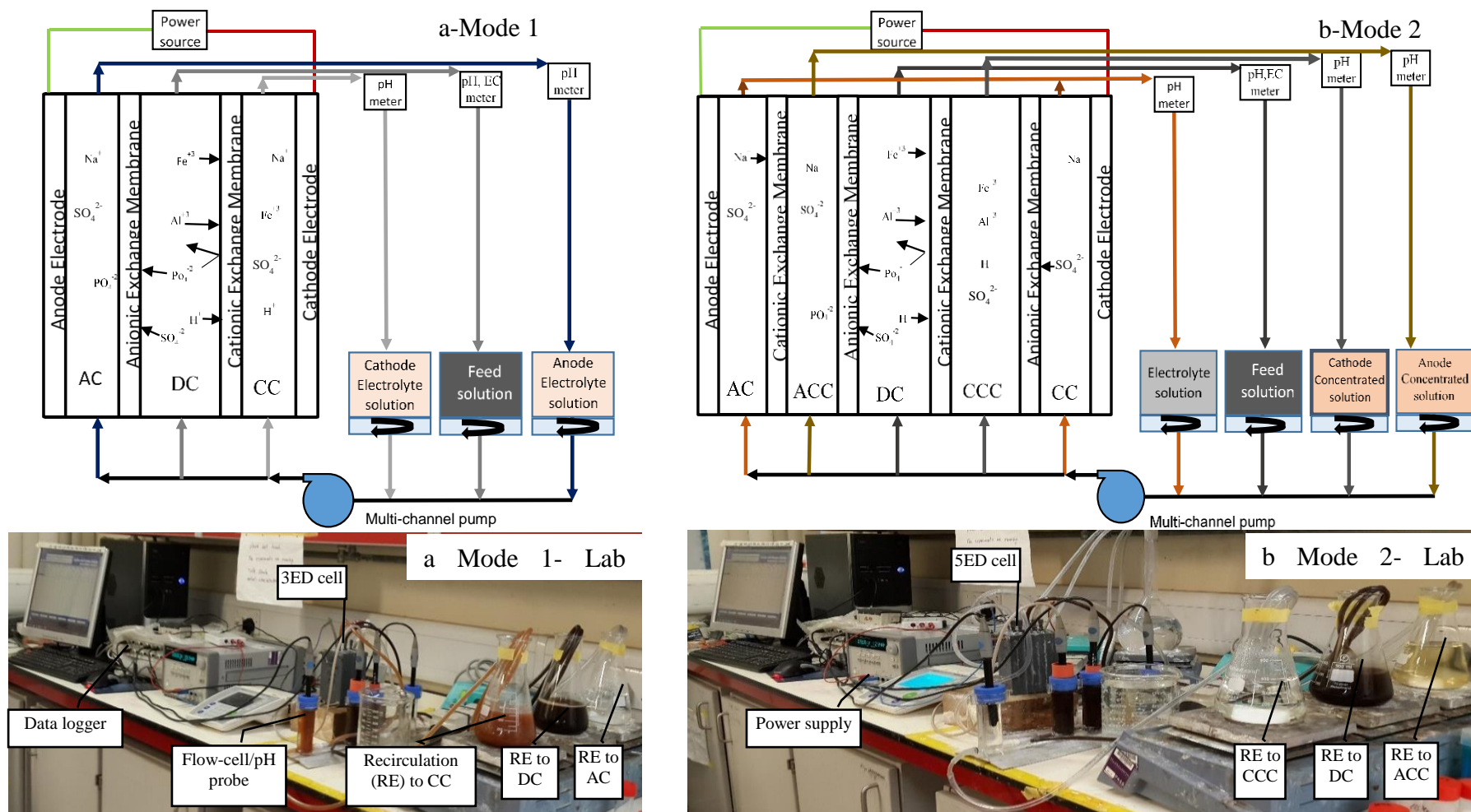


Figure 6.1 Schematic diagram of three compartments (a- mode 1), five compartments electro dialysis (b- mode 2) cells, and their lab setup.

6.2.2.2 Chemical analysis

Liquid samples were collected periodically from the continuously stirred solution in the 500 ml beakers of each compartment of both modes. To represent the collected data thoroughly during the operation time, collection time was set at every 36 min in the case of LC. Meanwhile, with the HC operation condition, samples were collected at the end of operation time, since the purpose of using HC is to evaluate the recovered purity as explained in the previous section. The collected samples of 1 ml volume from DC and CC/CCC were diluted, digested by adding drops of nitric acid, and then analyzed for Fe, Al, Ca, Mg, Mn, K, Na, Zn and P using inductively coupled plasma atomic emission spectroscopy ((ICP – AES), Perkin Elmer Optima 2100D). Hach spectrophotometer (DR 3900) was used to monitor sulphate (SO_4^{2-}) reduction in the dilution compartment (DC). At the end of operation time, samples were taken from the CC (after digestion with nitric acid) and CCC to analyse them for dissolved organic carbon (DOC) using Total Organic Carbon Analyzer (TOC-V CSH (Shimadzu)). For the anodic compartments for both modes (AC and ACC), samples of 5 ml volume were collected at the end of operation time and analysed for P only. These measurements and monitoring procedures were planned, firstly to evaluate the cations and anions mobilization from DC to CC/CCC, and from DC to AC/ACC, and to show how this mobilization changes under different applied voltages. Secondly the measurements were done to study the effect of P saturation degree on the recovery process efficiency in ED of both modes; and thirdly to evaluate the purity of the recovered coagulant in terms of the DOC carryover.

6.2.3 Evaluation of recovered coagulants for water treatment

To assess the efficiency of the recovered coagulants for water treatment; commercial ferric sulphate coagulant (measured as 11.5% Fe) and raw water (collected from River Taff, Cardiff, UK) were prepared. Jar tests (using a Stuart SW6 flocculator) were conducted at room temperature to evaluate the performance based on residual turbidity, Zeta potential, residual DOC and UV254 absorbance. To do this, optimisation of commercial coagulant dose and initial pH were first obtained. Secondly, the optimum conditions were used to evaluate different 12 recovered coagulants; these were recovered coagulants produced from three levels of P saturation degree of LC and HC used in the two modes of ED (see Table 6.3).

UV254 absorbance and zeta potential were measured using a spectrophotometer and Malvern Zetasizer Nano Series respectively.

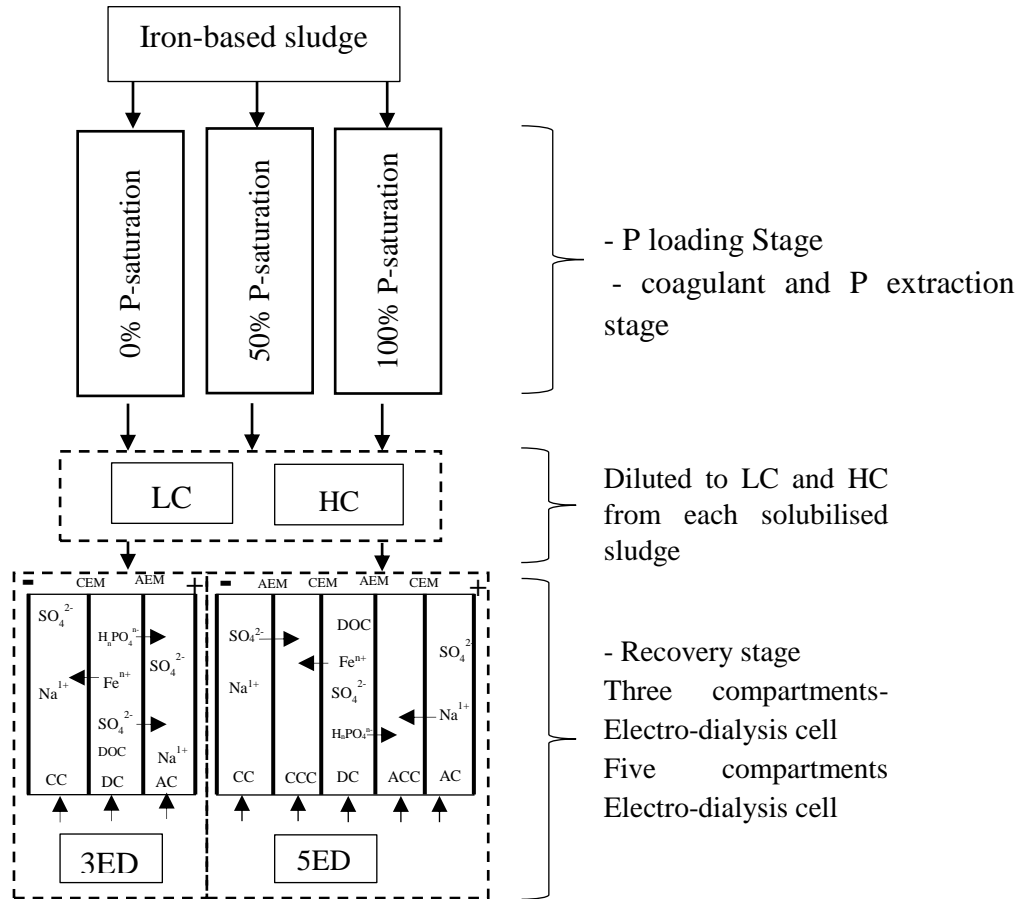


Figure 6.2 Schematic diagram of the experimental processes for P loading, extraction, and recovery.

A series of jar tests with a range of commercial coagulant concentration between 5 and 32 mg/l at constant pH of 5 were conducted to optimise the coagulant dose. The chosen coagulant dosage ranges were determined based on the removal efficiency of turbidity and DOC; while the pH value was selected to be between the optimum iron-based coagulant range of 4.5 to 6 (Matilainen et al. 2010). Another series of tests with constant coagulant dose and a range of pH between 4 and 6.5 was carried out to optimise the pH value (1M of HCl and 5M of NaOH were used for pH adjustment). The mixture was subjected to rapid mixing speed (200 rpm) for 2 min followed by slow mixing (40 rpm) for 20 min. The aggregated flocs were allowed to precipitate for 20 min after the mixing had stopped. The selected jar test procedure was based on

yielding optimum coagulation-flocculation conditions, making the procedure varied with varying raw water characteristics (Rossini et al. 1999; Franceschi et al. 2002; Parsons and Jefferson 2006; Sharp et al. 2006; Zhao et al. 2011). After settling, the purified water was withdrawn carefully with a syringe. A portion of the water sample was filtered using syringe filter with 0.45 μm polyethersulfone membrane, before analysing for DOC and UV254 absorbance to remove the suspended particles. The syringe filter was rinsed with 180 ml of deionized water to give UV254 reading less than 0.01 cm^{-1} according to the APHA procedure. The other portion was analysed for turbidity, zeta potential and chemical analysis was also conducted to determine Fe, Al, Ca, Mg, Mn, P, Cd, Pb, Ni, Cu and Zn, in order to compare the obtained values with the recommend limits for drinking water; whilst also making a comparison between the different coagulants.

6.3 Results and discussion

6.3.1 Solubilization of coagulant and P

After preparing three columns packed with sludge cakes with three levels of P saturation (0%, 50% and 100%, see Appendix C-Figure C.1), acidification with sulfuric acid was achieved in two steps: At the acid loading step, the extracted amount of Fe and P and the DOC carried over started to dissolve in high concentrations as the ionic strength increased after few hours of continuous acid injection. Thereafter, the dissolution decreased as the ionic strength increased, indicating, that more contact time is essential after the first solubilization period. In the recirculation step, the solubilized Fe, P and DOC increased respectively from 14 to 24 (g/l), 0.03 to 0.44 (mg/l), and 3 to 6.5 (g/l) for 0% - P; 7 to 16 (g/l), 0.4 to 0.9 (g/l), and 1.5 to 3.6(g/l) for 50% - P; 9 to 23 (g/l), 1.6 to 4.2 (g/l), and 1.1 to 2.7 (g/l) for 100% - P. With increasing contact time with the acid, the solubilization of Fe, P and DOC, in addition to the other trace elements, was found to also increase with a positive correlation (see Appendix C, Figure C.2). DWTS adsorbs P not only via ferric hydr(oxide), but also via interaction with the complexes of Fe-OM to form organic-Fe -P complexes through ligand exchange mechanism. This explains the changes in the amount of DOC during the extraction when increasing the PSS from 0% to 100%. The metals solubilization with acid and base solution is an unavoidable

step that is needed to commence the recovery process. As expected and reported previously, the undesirable elements that are solubilized are one of the challenges for Fe recovery with high purity from DWTS which is meant to be used again as a coagulant in water treatment (Keeley et al. 2014a). The main concern about the reuse of the recovered Fe coagulant in water purification is its DOC content which might raise the level of Trihalomethane formation potential (THM-fp) after chlorine injection (Keeley et al. 2014b). The Fe/DOC ratio in the final extracted solution increased from 3.78 to 8.83 as the percentage of PSS increased from 0% to 100%, indicating that higher purity of recovered Fe can be achieved with PSS (see Table 6.1).

The extracted amount of Fe, P, dissolved DOC and other ions in acid solutions, and the DWTS chemical characteristics before and after P loading, and after acidification are represented in Table 6.1. It can be seen that 68% and 51% of Fe were solubilized, respectively from 0% and 100% of the PSS. Meanwhile, the extracted percentages of P were 79% and 73% for the 0% and 100% PSS respectively. Similar same trend was found for the dissolved DOC, which decreased from 28% to 8% when P saturation degree increased from 0% to 100%. This pattern of Fe, P and DOC solubilization can be explained by two-steps. Firstly, the sludge buffering capacity of 50% and 100% P loaded are different from 0% P loaded, due to the increasing amounts of P and K during the P loading. Secondly, OC changes with P in the ligand exchange mechanisms; this leads to the loss of more OC from the sludge loaded heavily with P, thus reducing the amount of DOC released as the sludge P loading degree increased during the extraction process. Most of the previous studies conducted the extraction experiments by shaking the P saturated sludge with an acid solution. On the basis of the extraction process efficiency, Zhao and Zhao (2009b) found that the optimal condition for 98% of P extraction is by shaking 0.8g of Al-based sludge and 0.063M in 142ml of sulfuric acid. As mentioned earlier, the extraction process in this study was conducted with a fixed sludge bed to mimic real-life application. Therefore, the yield percentages of P and Fe extraction is reasonable.

Chapter 6: Coagulant and phosphorus recovery from P saturated sludge

Table 6.1 Mass balance of dewatered water treatment sludge constituents before and after P loading, and after acid extraction and the amount of the solubilized elements in the acid solution of three levels of P saturation degree.

Element (mg/g)	Sludge characteristics						Extracted amount		
	Before P loading	After P loading		After Extraction			0%	50%	100%
		50%	100%	0%	50%	100%			
Fe	255.40 ± 25.97	245.26 ± 20.31	232.35 ± 19.35	80.66 ± 13.23	132.50 ± 15.23	115.60 ± 8.97	173.74 ± 0.03	113.89 ± 1.2	118.20 ± 0.89
Al	11.94 ± 2.16	11.75 ± 1.53	11.56 ± 1.64	10.54 ± 1.39	10.84 ± 1.89	10.65 ± 1.56	1.40 ± 0.04	0.91 ± 0.1	0.91 ± 0.06
Ca	4.01 ± 0.64	3.84 ± 0.35	3.45 ± 0.25	1.26 ± 0.32	2.35 ± 0.23	1.98 ± 0.13	2.75 ± 0.27	1.49 ± 0.04	1.47 ± 0.30
K	2.32 ± 0.83	13.65 ± 0.12	24.17 ± 2.31	2.20 ± 0.87	3.54 ± 0.79	6.73 ± 0.56	0.11 ± 0.15	10.11 ± 0.35	17.44 ± 0.12
Mg	0.71 ± 0.15	0.52 ± 0.053	0.51 ± 0.02	0.44 ± 0.09	0.45 ± 0.1	0.44 ± 0.12	0.27 ± 0.10	0.07 ± 0.08	0.07 ± 0.09
Mn	3.16 ± 0.56	2.98 ± 0.64	2.68 ± 0.36	0.64 ± 0.09	1.62 ± 0.36	1.46 ± 0.78	2.52 ± 0.18	1.36 ± 0.2	1.22 ± 0.31
Na	0.65 ± 0.90	2.35 ± 0.51	2.87 ± 0.52	0.57 ± 0.30	0.09 ± 0.03	0.18 ± 0.07	0.08 ± 0.02	2.26 ± 0.05	2.69 ± 0.03
Zn	0.97 ± 0.24	0.85 ± 0.11	0.78 ± 0.02	0.39 ± 0.13	0.62 ± 0.1	0.49 ± 0.2	0.58 ± 0.38	0.23 ± 0.29	0.30 ± 0.01
P	0.39 ± 0.10	15.68 ± 1.59	28.70 ± 3.09	0.08 ± 0.02	10.25 ± 1.01	6.75 ± 1.56	0.31 ± 0.27	6.60 ± 0.41	20.95 ± 0.86
DOC	163.55 ± 3.25	136.56 ± 4.35	108.42 ± 3.65	117.54 ± 3.98	111.37 ± 3.56	95.04 ± 2.89	46.01 ± 1.25	25.19 ± 0.942	13.38 ± 0.45
Fe/DOC	1.56	1.8	2.14	0.69	1.19	1.22	3.78	4.52	8.83

6.3.2 Soluble iron and P in dilution compartment and electrochemistry characteristics

In order to understand the experimental process for anions and cations mobilisation in the electrodialysis system, the changes in the electrochemical characteristics of the diluted feeding solubilized sludge with three levels of P-saturation were determined. Figure 6.3 presents and compares the changes in the iron and P concentrations in the dilution compartment of 3ED and 5ED modes at two applied voltages of 9v and 15v (in the case of LC). The current profiles, pH profiles in CC/CCC, DC, and AC/ACC using HC of solubilized sludge with different degree of P saturation for both modes are presented in Appendix C (see Figure C.3, C.4, and C.5). The current generated and its flux through the different compartment of both modes depend on the solution chemical matrix. In the 3ED mode, high current fluxed from the anode to the cathode electrodes where the high ionic conductivity was provided in all the three compartments. The electrolyte solution in anodic and cathodic compartments of sodium sulphate (where the recovered ions concentrated), in addition to the solution matrix of the feeding at DC leads to the maximum amount of current density flux through the cell at initial operation time. With the continuous reduction in the concentration of iron, P and other trace elements in DC, and the deposit and accumulation of organic foulants on the membrane surface, the current density decreased in an inverse correlation. However, the initial current density in 5ED mode at 9v was not the same as in 3ED mode as shown in Figure 6.3; the difference is due to using just deionized water in the anode and cathode compartments. After approximately 1 hour of operation, the cations (especially Fe) and anions permeated to the cathodic and anodic compartments, thereby building up the necessary connection between the anode and cathode electrodes. As the operation progressed, the ionic permeation increased causing increase in the current density. The more the decrease of ions concentration in DC during the operation time, the lower the conductivity between ED compartments, and higher electrical resistance resulted according to Ohm's law. Ionic depletion in the DC of both modes are not the only reason for the drop in the current, there were also minor losses in the current due to membranes resistance, and also due to accumulation of large and charged organic molecules or colloids such as humic acid on the membrane surface (Baker 2012). At applied voltage of 15V for both modes, the current profile at the end of operation

remained relatively unchanged; this is because the equilibrium of ions migration between the compartments made a minimal difference in solutions conductivities.

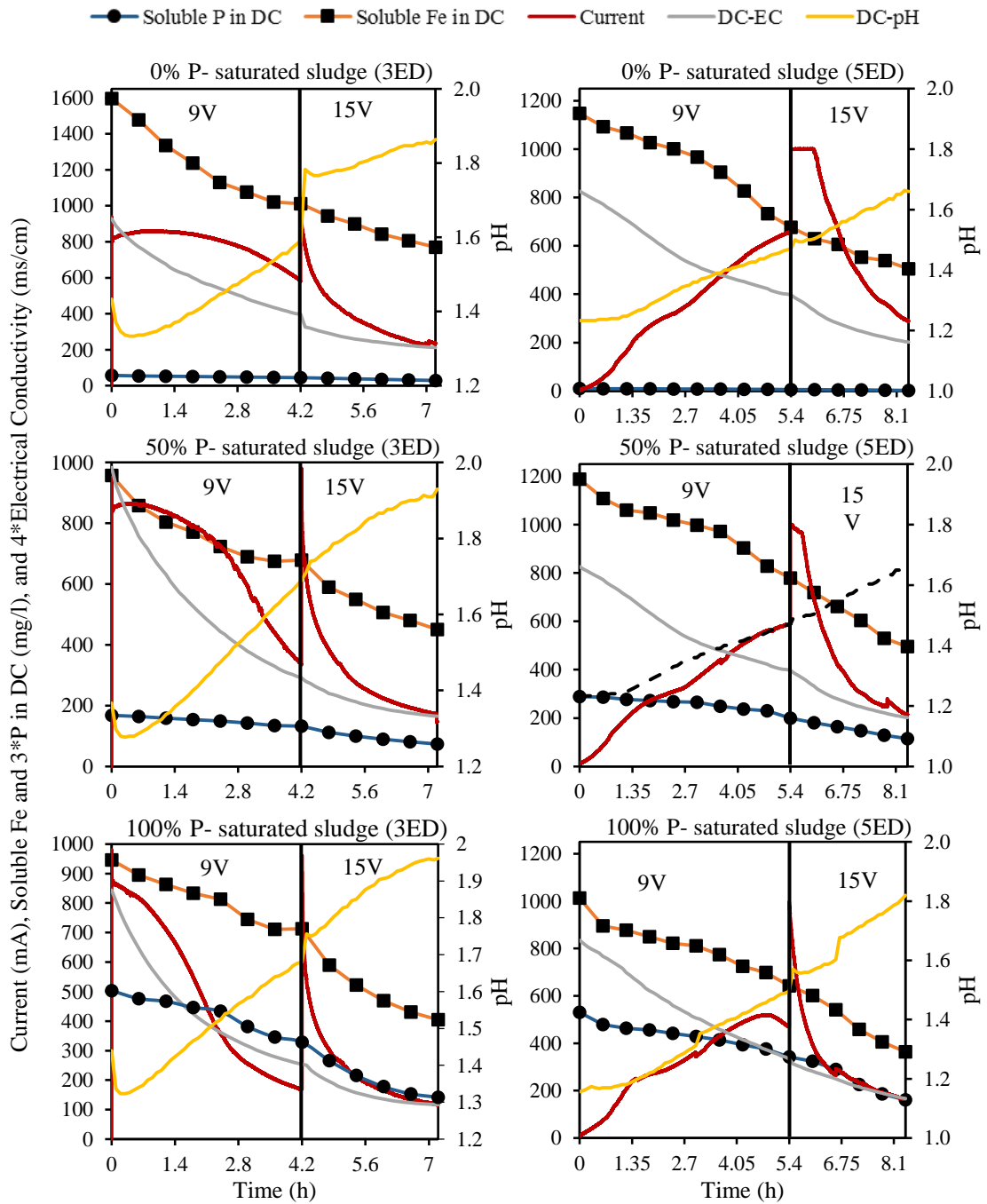


Figure 6.3 Mean value of soluble iron and P, and current profile with acidity and electrical conductivity changes in the dilution compartment (DC) in the 3ED and 5ED modes at three levels of P-saturated dewatered water treatment sludge (0%-P, 50%-P, and 100%-P).

Figure 6.3 also illustrates the changes in Fe and P concentrations with applied voltages of 9 and 15 V as a function of time. It can be seen that at the P saturation degree of 50% and 100% for both modes of ED, the behaviour of iron and P reduction in DC were almost the same, indicating that iron and P correlated and permeated through the membranes in same proportion, working as counterions in the same mixture. This reduction in the concentration of both Fe and P ions increased when higher current fluxed through the compartments of ED in both modes. Also, the acidity of the solubilized sludge decreased with the progress of the ED operation; this indicates that the feeding solution was continuously diluted with more cations and anions flux for the opposite directions (especially H^+ ions). Furthermore, sulphate reduction followed the same trend of Fe and P reduction in different operating conditions as shown in Figure 6.4.

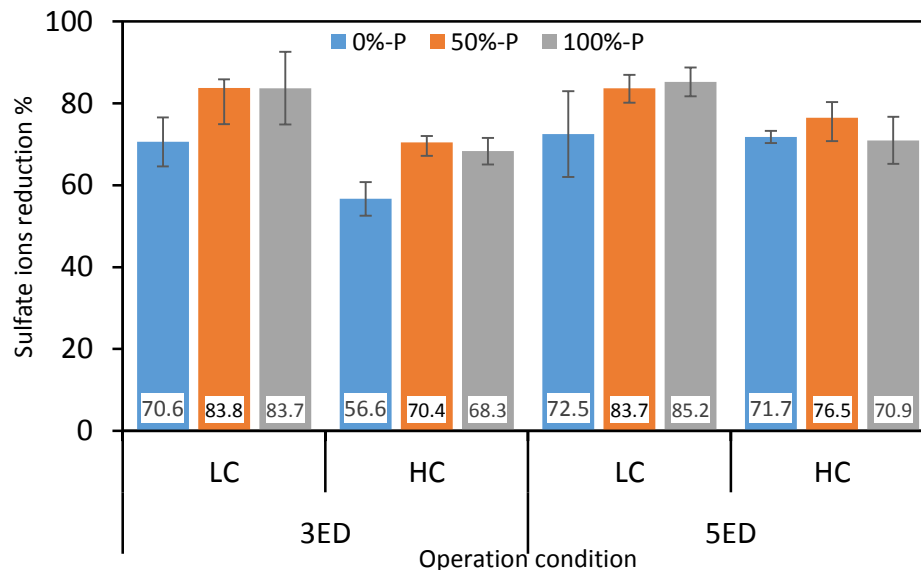


Figure 6.4 Mean values of sulphate ion reduction in dilution compartment for both ED mode at two different initial concentrations ($n=3$).

6.3.3 Effect of P-saturation degree on:

6.3.3.1 P and coagulant recovery

In order to assess the purification process of ED on the separation of iron and P from the solubilized sludge, on the cathodic and anodic compartments respectively, elemental analyses of the collected samples from AC/ACC, DC and CC/CCC for Fe, P and other trace elements was conducted. Interestingly, insignificant amount of

recovered P was found in the AC and ACC compartment. Therefore, the primary focus was on the DC and CC/CCC compartments of both modes. Figure 6.5 gives the overall percentages for Fe and P reduction, lost and recovered in the DC and CC/CCC compartments, respectively, in the ED mode 1 and 2. For 3ED (mode 1), the highest decrease in the amount of Fe in DC was $57 \pm 14\%$ at LC, and $75 \pm 9\%$ at HC using solubilized sludge with 100% PSS. Similarly for P reduction in the DC, $71 \pm 15\%$ and $79 \pm 8\%$ of LC and HC, respectively, were reduced in the solubilized sludge of 100% PSS. For Fe and P mobilisation between DC and CC, $43 \pm 16\%$ and $15 \pm 13\%$; $44 \pm 3\%$ and $63 \pm 3\%$ were recorded as the highest percentages at LC and HC, respectively, when mode 1 was fed with solubilized sludge with 0% PSS. The proportions of Fe and P lost with the rejected DOC (as fouling on the membrane) was highest with 100% PSS feed. For the 5ED (mode 2), the amount of reduction, recovered and loss of Fe and P followed the same behaviour as in mode 1. From Figure 6.5, a clear trend of decrease in the percentages of the recovered Fe and P with increasing P saturation degree of the sludge was observed. For example, in mode 2 with LC operating condition, the percentages of recovered Fe and P decreased from $70 \pm 8\%$, $49 \pm 3\%$ to $17 \pm 2\%$, $6 \pm 1\%$, respectively when the PSS increased from 0% to 100% (P inherent in the sludge of 0%-P originates from the raw water characteristics). The coupled permeation of P ions with Fe ion migration from DC to CC/CCC might be explained by the electro-neutrality status generated in the solution (Van Der Bruggen et al. 2003). The most striking in Figure 6.5 is that the lost percentages of Fe and P in most operation conditions followed the same trend of a positive correlation with increasing P saturation degree (see supporting data in Appendix C, Figure C.6 showing the mass balance). P sorption in water treatment sludge is practically irreversible through multiple chemical bonding. Where the main mechanisms involve P adsorption to metal oxides or hydroxides, P can be exchanged with natural organic compounds as explained in chapter three. During the recovery process using ED, the rejected DOC and high Fe selectivity were the basis of the designed ED, and therefore the rejected percentages of chemically combined Fe, P and DOC increased with increase in the P loaded sludge. This observation can also be explained by the presence of these counterions (complexes of P-Fe-OC) in the same mixture that makes their transport rate through the membrane lower, and therefore the efficiency of separation will be impaired by this mixture of ions (Van

Der Bruggen et al. 2004). A previous study attempted to recover P from solubilized Al-based sludge by precipitation of P as hydroxyapatite via adding different ratios of P:Ca (Zhao et al. 2011). Al ions were still simultaneously co-precipitated with the formed calcium phosphate even at P:Ca molar ratio of 3 and pH 13. Another attempt to recover P from iron phosphate sludge via sulphide addition in solid-liquid extraction process was performed by Mejia Likosova et al. (2013). P separation and FeS precipitation likely depend on colloidal nature of FeS inherent from the sludge characteristics.

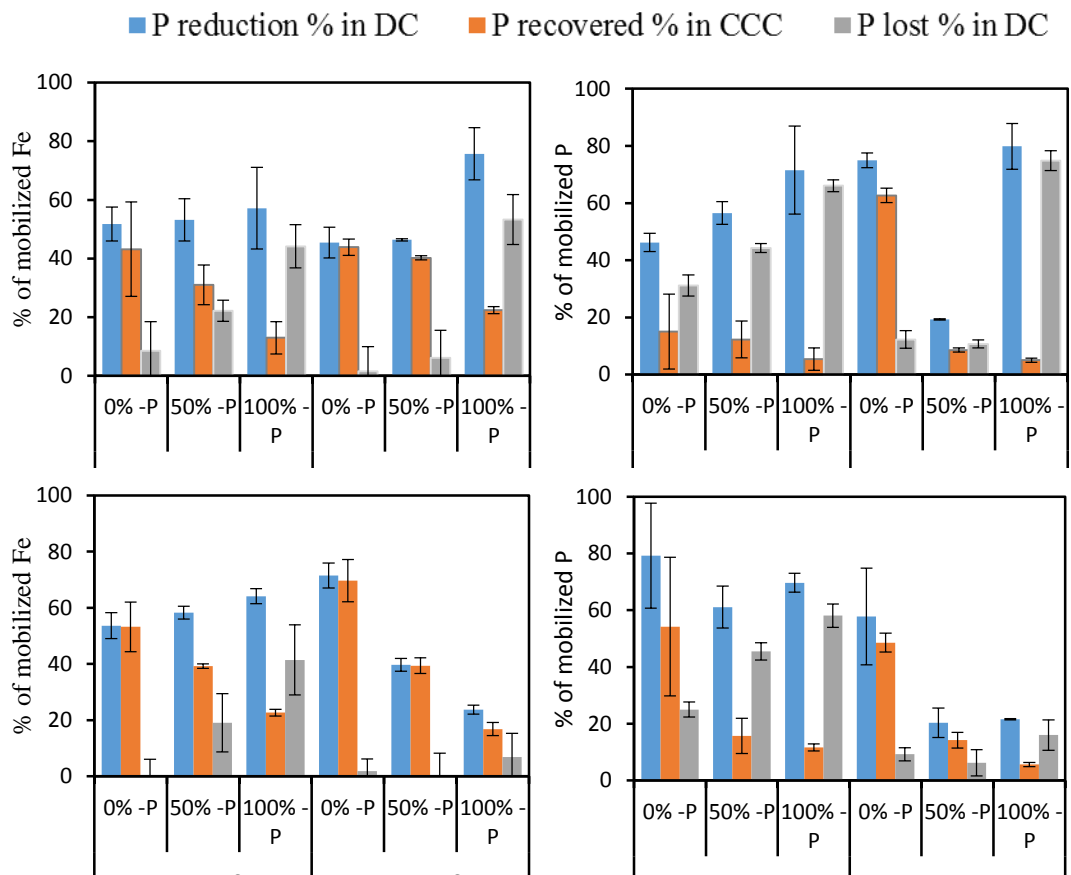


Figure 6.5 Mean values of the mobilised Fe and P ions between DC and CC\CCC of three levels of solubilized P-saturation sludge, with low concentration (LC) and high concentration (HC) applied in two operation modes of electro dialysis cell.

6.3.3.2 Recovered coagulant purity

In order to prove the ability of ED cell to recover coagulant with high purity and in the same time recover P and other anions especially acid used in the solubilization stage, the concentration of permeated Fe together with DOC in CC or CCC of both

modes, and the ratio of Fe to DOC are presented in Table 6.2. The amount of recovered Fe in mode 1 decreased from 690.8 ± 266 mg/l to 122 ± 51 mg/l with increase in the degree of P saturation when using LC of solubilized sludge. Interestingly, the permeated DOC also decreased from 6.7 ± 0.89 to 4.17 ± 0.06 mg/l as the level of P- saturation sludge changed from 0% to 100%, respectively at the same operation condition of mode 1. A possible explanation for this might be that high current density flows between the electrodes, and this makes the counterions in electro-neutralization status causing less effect at 0% PSS, to significant impact at 100%. This explains the effect of P saturation degree on the permeated DOC with recovered Fe: the lower the P concentration in the solubilized sludge, the lesser is its effect on Fe migration to the recovery side, and also more DOC carried over with Fe. For mode 2 at LC operation condition, although the recovered values of Fe and P were almost higher than that found in mode 1, the permeated DOCs with the recovered Fe were less. This observation implies that the gradual increase in current flow within the anode and cathode electrodes reduces the effect of co-existing ion and leachable DOC with the recovered ions. With operation conditions of HC and longer running time in both modes, higher concentrations of recovered Fe and P and almost the same DOC contamination were observed. What is striking about the figures in Table 6.2 is that the purity of recovered Fe in both modes was negatively correlated with the degree of P saturation of the sludge as a result of the influence of counterions in the same mixture.

To validate the efficiency of ED with respect to the purity of the recovered coagulant (carried over DOC), comparison with a very recent study (Keeley et al., 2016) was made by calculating the ratio of the recovered Fe to the permeated DOC. It can be seen from Table 6.2 that the Fe/DOC ratio decreased in most cases with increase in the percentage of PSS. In general, the purities of the recovered coagulants in mode 2 were about twofold those obtained in mode 1. This can be explained by the high ionic conductivity which causes high current flux leading to less Fe migration and high DOC permeation in ED of mode 1. The ratios obtained in this study are comparable with those reported by Keeley et al (2016) with acid solubilized sludge. Maximum Fe/DOC ratio was 290 at running time of 12 h of 5ED for the recovered Fe from acidified sludge. The ED process for coagulant recovery

offers higher kinetic ionic migration and higher selectivity with no pre-and post-treatment processes needed.

Table 6.2 Characterization of recovered coagulant in terms of Fe and DOC concentrations, and Fe/DOC ratios

Recovered coagulant specification			Fe (mg/l)	P (mg/l)	DOC (mg/l)	Fe/DOC Ratio	Study
3ED	LC	0%-P	690.8 ± 266	3.8 ± 5	6.74 ± 0.89	102	Current study
		50%-P	295.5 ± 59	6.6 ± 3	4.98 ± 0.82	59	
		100%-P	122.0 ± 51	9.2 ± 7	4.17 ± 0.06	29	
	HC	0%-P	1232.1 ± 82	5.6 ± 1	8.27 ± 0.16	149	
		50%-P	725.5 ± 17	9.5 ± 1	5.487 ± 0.46	132	
		100%-P	791.6 ± 13	34.4 ± 2	4.66 ± 0.79	170	
5ED	LC	0%-P	676.0 ± 4	1.8 ± 1	3.03 ± 0.24	223	
		50%-P	466.1 ± 5	16 ± 10	2.19 ± 0.64	213	
		100%-P	229.6 ± 10	20.5 ± 2	2.29 ± 0.57	100	
	HC	0%-P	2044.5 ± 178	4.6 ± 0	9.22 ± 1.31	222	
		50%-P	731.7 ± 51	16 ± 3	2.52 ± 0.04	290	
		100%-P	622.2 ± 88	36.0 ± 5	3.13 ± 0.18	199	
Alkali, acidified, UF			874 ± 17	---	61	14	Keeley et al. (2016)
Acidified, UF			1285 ± 34	---	91	14	
Alkali, acidified, DD			1056 ± 28	---	4	264	
Acidified, DD			2555 ± 75	---	29	88	

6.3.3.3 Recovered coagulant performance with respect water treatment

To evaluate the recovered coagulants from the different operation conditions of the two modes of ED for water treatment, and the impact of P saturation degree; a series of jar tests were conducted and this were proceeded by optimization of the commercial coagulant dose and pH. 15 mg-Fe/l of commercial coagulant dose and pH value of 5 were selected based on the optimum removals for turbidity, DOC and the zeta potential (Figure 6.6 a & b,).

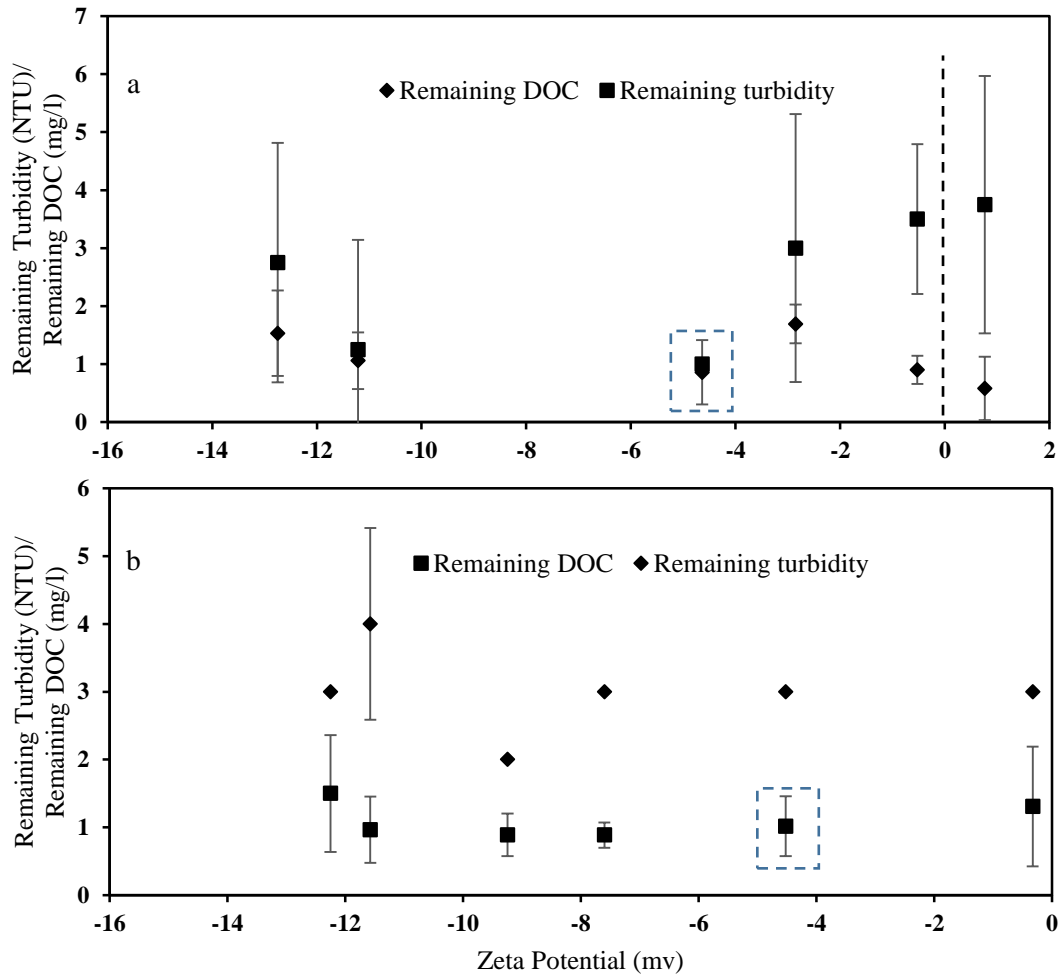


Figure 6.6 Optimisation steps of coagulant dose for commercial coagulant (a) and pH (b) for remaining turbidity, remaining DOC and zeta potential ($n=4$).

The characteristics of raw water and clarified water by 12 recovered and commercial coagulants are listed in Table 6.3. Evaluation of recovered coagulants from different operation conditions of ED based on residual turbidity, DOC, Fe, and P showed no significant trend between these control parameters. The specific UV₂₅₄ values (used as an indicator of THMs precursor) of 0.044, 0.058 and 0.075 were obtained with using recovered coagulants of 0%-P, 50%-P and 100%-P at LC- 3ED, respectively which were much higher than 0.012 for the commercial coagulant. This can be explained by the interference caused by the sulphate ion, giving a great reading of the UV₂₅₄ absorbance since sodium sulphate was used as electrolyte in the AC and CC. Using coagulant content with high concentration of sodium sulphate is undesirable in water treatment, unless this is diminished by concentrated the recovered Fe.

To improve the reduction of the formation of Disinfection By-Products (DBPs) as a result of chlorination of naturally occurring organic precursor, prior chlorination process is required (WHO 2011). The DOC percentage removals were between 41.8 to 58.8% for most recovered coagulants, implying that the performance of the recoveries is comparable with commercial coagulant in term of DOC removal. The lower turbidity removals and higher residual Fe obtained using coagulants of HC-3ED and 5ED in comparison with commercial coagulants, which might imply that more settling time was required or less dose should be applied.

In terms of residual metals contributed by the recovered coagulants, Cu, Pb, Ni, Cd and Cr were not detected from the recovered coagulants. An increase in the concentrations of Fe and Mn after using commercial and recovered coagulants from their original levels in raw water to breach the limit of 0.2 and 0.05 mg/l respectively were found, this suggest that further treatment is required downstream of the coagulation to destabilise the Fe and Mn colloids. In addition, it can be seen from Table 3 that there were no clear trends on the influence of P saturation degrees on elevating the concentrations in the final treated water. Although there is no limitation for the level of Zn in drinking water, Zn concentrations increased from 0 mg/l in raw water to a range between 0.01 and 0.17 mg/l in clarified water. However, no guideline for health impact level has been proposed by WHO for drinking water.

Chapter 6: Coagulant and phosphorus recovery from P saturated sludge

Table 6.3 Purified water quality and percentage removals obtained by commercial and recovered coagulants (n=3).

Recovered coagulant specification	Turbidity (NTU)	DOC (mg/l)	Zeta potential (mv)	DOC % removal	SUV ₂₅₄	Residual concentration (mg/l)											
						Fe	P	Al	Ca	Mg	Mn	Zn	Cu	Pb	Ni	Cd	Cr
Raw Water	5.5	2.37	-12		0.033	0.1	0.21	0.00	28.05	9.19	0.00	0.0	0	0	0	0	0
Commercial ferric sulphate	2.5	0.97	-4.64	58.9	0.012	0.4	0.05	0.00	30.04	10.05	0.08	0.01	0	0	0	0	0
0%-P	2	1.19	-5.04	49.6	0.044	0.4	0.01	0.06	28.68	8.75	0.37	0.12	0	0	0	0	0
LC 50%-P	2	1.02	-8.18	57.1	0.058	0.4	0.02	0.03	27.56	8.45	0.28	0.17	0	0	0	0	0
100%-P	4	1.14	-6.47	51.8	0.075	0.2	0.02	0.06	24.61	7.39	0.39	0.15	0	0	0	0	0
3ED 0%-P	3	0.97	-1.97	58.8	0.025	1.0	0.03	0.04	29.31	9.14	0.32	0.10	0	0	0	0	0
HC 50%-P	3	1.35	-3.5	42.77	0.022	0.6	0.02	0.04	29.06	9.02	0.26	0.09	0	0	0	0	0
100%-P	4	1.25	-2.19	46.97	0.022	0.4	0.04	0.05	29.40	9.05	0.34	0.12	0	0	0	0	0
0%-P	2	1.71	-0.91	27.8	0.01	1.9	0.27	0.04	28.54	8.94	0.31	0.09	0	0	0	0	0
LC 50%-P	1.5	1.12	-1.40	52.8	0.015	1.6	0.18	0.06	28.18	8.79	0.30	0.10	0	0	0	0	0
100%-P	2	1.38	-3.55	41.8	0.013	1.2	0.19	0.05	27.60	8.49	0.33	0.11	0	0	0	0	0
5ED 0%-P	4.5	1.00	-1.09	57.6	0.015	2.6	0.14	0.03	30.36	9.54	0.24	0.08	0	0	0	0	0
HC 50%-P	5	1.00	-1.44	57.5	0.016	2.2	0.06	0.04	29.58	9.16	0.33	0.11	0	0	0	0	0
100%-P	4.5	1.07	-1.91	54.7	0.018	2.0	0.05	0.07	29.61	9.11	0.42	0.15	0	0	0	0	0

6.4 Summary

This chapter investigated P and coagulant recovery from 0%, 50% and 100% phosphorus saturated sludge (PSS) using ion exchange membrane technology (electrodialysis, ED).

A two-step process of sulfuric acid solubilization revealed that the high dissolution rate of Fe, P and DOC during the acid loading step decreased with loading time and increased with ionic strength. In the recirculation step, the dissolution increased with increasing contact time with acid. DOC concentration in acid solubilized sludge correlated negatively with increase in P saturation level; this can be explained by the continuous exchange of OC through ligand exchange mechanisms during the P loading stage. DOC/Fe ratio increased from 3.78 to 8.83 as the percentage of P saturation increased from 0 to 100. The extracted percentages of Fe and P were 68 to 51 and 79 to 73, at P saturation degrees of 0% and 100% respectively.

The effect of P saturation degree on the P and Fe recovery was assessed by analysing the collected samples from DC, CC/CCC and AC/ACC. In the AC/ACC where the anionic ions should be recovered, insignificant amount of P was observed and instead it was recovered with Fe. This can be explained by the electro-neutrality status generated in the solution. The percentage of Fe and P permeation decreased with increase in P saturation degree. In mode 1, the recovered Fe decreased from 690.8 ± 266 mg/l to 122 ± 51 mg/l as the percentage of PSS increased from 0 to 100. The lost amount of P and Fe in all operation conditions followed the same trend of rising in P saturation degree, indicating that the presence of the counterions (Fe, P, and DOC) in the same mixture, impairs their permeation rate through the membrane and then impact on the recovery efficiency.

With regards to the coagulant purity, the contamination of recovered Fe with DOC decreased with increase in the saturation degree. In mode1 with LC operation condition, the DOC contamination changed from 6.7 ± 0.89 to 4.17 ± 0.06 mg/l as the level of saturation increased, indicating that the electro-neutralization charge of the Fe, P and DOC leading to rejecting more DOC with Fe and P in present high current density. While in mode 2, the DOC contamination was reduced because of the gradual increase of the current density, and therefore the charge neutralisation of

counterions was reduced. The range of Fe/DOC ratios were between 29 (100%PSS, LC-3ED) and 299 (50%PSS, HC-5ED).

The treatment performance of the recovered coagulants with respect to meeting drinking water quality requirements was evaluated in comparison with commercial coagulant. The performance of most of the recovered coagulants was comparable with commercial coagulant in terms of turbidity and DOC removal, and UV254 absorbance. It can therefore be concluded that ED is a promising technology, not only for coagulant recovery but also for other essential elements that can be enhanced for further benefits.

Next chapter lists the main conclusions and recommendations for future work.

Chapter 7: Conclusions and recommendations

7.1 Conclusions

This thesis advanced our understanding of P adsorption by drinking water treatment sludges, and also investigated P and coagulant recovery from the P saturated sludge.

The main conclusions from this are presented below:

- Al and Fe based dewatered waterworks sludges have considerable variability in their physicochemical properties; and the difference in their P retention behaviour can be explained by the amount of reactive Al and Fe available, the total specific surface area, and in some cases, the presence of crystalline phases of total carbon and other minerals.
- Al-based sludges tended to have higher total specific surface areas and thus, higher adsorption capacities (6.09 - 26.95 mg-P/g) than Fe-based sludges (5.83 -23.75 mg-P/g).
- Phosphorus retention was shown to be generally through surface complexation, ligand exchange and/or precipitation. In particular, FTIR results indicate that surface complexation of inner and outer sphere played a key role in the adsorption mechanism.
- In almost all cases, adsorption data was well described by the Freundlich model indicating the heterogeneity of P adsorption on the surface of the sludges. However, adsorption data for two of the sludges, which were Al, based were best fitted with the Langmuir model, with minimal leaching of Al, Calcium and sulphate ions observed. This implies that P adsorption by surface complexation is the only possible mechanism for the two sludges.
- Principal component and multiple linear regression analyses revealed that the metal content (Al, Fe, Al_{oxalate} and Fe_{oxalate}) and total specific surface area components had the most significant explanation for the variance of (i) P-uptake at different initial P concentrations; (ii) the adsorption maxima; and (iii) the Freundlich constant (K_f); ($p < 0.001$). Total carbon (TC), organic carbon, Ca content and exchangeable Ca components explained a significant reasonable variance in P-uptake and K_f . This explanation was demonstrated for the role of Ca content in chemical P precipitation mechanism, and also for

exchanging TC sites on the surface of the sludges with phosphate ions via ligand exchange mechanism.

- Overall, giving the combined effect of intrinsic sludge properties and solution chemistry; dewatered waterworks sludges with high reactive metal content (Al and Fe), Ca and SO_4^{2-} ions, and the specific surface area would be the best choice for P retention in practical applications.
- DWTSs were shown to have high variability in their chemical and physical characteristics. Five different Al-based sludges showed considerable variation in their aluminium (Al) (± 22.56) mg/g, iron (Fe) (± 9.23) mg/g, total carbon (TC) (± 36.88) mg/g, and surface areas (± 115.5) m^2/g ; while nine different Fe-based sludge had high deviation from the mean values in their Fe (± 49.8) mg/g, Al (± 20.09) mg/g, Ca (± 7.83) mg/g, TC (± 95.21) mg/g, and surface area (± 95.21) m^2/g . This variation in their characteristics might explain the differences in their P removal equilibrium and kinetic behaviour.
- Average and standard deviation of maximum adsorption capacity for Al and Fe- based sludges were respectively (24.86 ± 1.7) (mg/g) and (15.3 ± 4.1) (mg/g) at initial pH solution of 7. Freundlich, Langmuir and Temkin adsorption isotherm models were well fitted to the adsorption data in that particular ranked order. In most cases, the constant parameters and correlation coefficient increased with decreasing pH.
- The kinetics of P adsorption followed the pseudo-second-order kinetic model, describing that chemisorption was the rate-limiting step for P adsorption onto the waterworks sludges. The average and standard deviation of pseudo-second-order rate constant (K_2) for Al- and Fe-based sludges were respectively ($0.17 \pm 0.05 * 10^{-1}$) and ($0.094 \pm 0.03 * 10^{-1}$) (g/mg.min) at initial pH solution of 7. In most cases, higher rate constants were associated with lower initial solution pH values when surface complexation is the main P retention mechanism.
- Intraparticle diffusion may not be the rate limiting P retention mechanism. However, the diffusion rate constant increased with increasing pH, indicating that diffusion may occur during the long-term P adsorption where both the ligand exchange, and/or precipitation are the dominant mechanisms.

- The combined effects of HRT and influent phosphorus (P) concentration on P adsorption of DWTS were shown to be the key factors that contributed to the differences in P adsorption behaviour between the continuous feed systems and the batch tests.
- In both experiments of short-term experiments of batch and continuous feeding system (CFS), aluminium-based sludge showed higher P adsorption than Fe-based sludge. The results showed that P uptakes obtained from CFS are higher than that from batch experiments, where the constant P feeding with increasing HRT leads to more leachable ions from sludge, thereby promoting more exchange with P or making more adsorption sites available.
- Data from multi-paired HRTs and influent P concentrations obtained from the CFS experiment were modelled and generalized to generate P uptake equations; these can be used to predict with a very good accuracy, P uptake, cumulative P uptakes, maximum amount of P loaded to the sludge at different saturation degrees, and lifetime or effluent volume treated up to the particular saturation point.
- For Fe and P extraction: The extracted Fe, P and DOC increased as the contact time of P saturated sludge (PSS) increased, especially after few hours of the acid loading stage. The P saturation degree affected the amount of DOC released during the loading and recirculating stages; resulting in an elevation of the DOC concentration from 1.5 to 6.5 g/l, 1.5 to 3.6 g/l, and 1.1 to 2.7 g/l, from moving acid loading to recirculating stage of 0%, 50%, and 100% PSS. The final DOC content decreased as the P saturation degree increased.
- Fe and P recovery: The percentage of recovered coagulant and P correlated negatively with increasing P saturation degree because of existence of counterions complexes of P, Fe, and DOC; leading to rejected Fe and P with DOC, and then reducing the percentage from $70 \pm 8\%$, $49 \pm 3\%$ to 17 ± 2 , $6 \pm 1\%$ when P saturation degree increased from 0% to 100%, respectively. Because of the generated electro-neutral charge in ED, and with presence Fe ion and DOC, P permeated toward cationic compartment alongside with Fe.
- In terms of the purity of the recovered coagulant: the Fe/DOC ratios were higher by three to one and a half folds using 5ED (range from 100 to 290),

than that obtained with 3ED (range from 29 to 170). The higher the current flux in the 3ED mode than the 5ED mode, the more the DOC migration with Fe, and the lower the Fe/DOC ratios. ED offered a comparable coagulant recovery in terms of high purity and fast kinetics as a one-step purification process, compared with other technologies such as Donnan Dialysis and ultrafiltration.

- With respect to evaluating the recovered coagulants for water treatment: there was no remarkable differences between the recovered and commercial coagulants for turbidity and DOC removal, and also UV254 absorbance. In most cases, the DOC% removals were between 42 to 59%. The residual Fe and Mn concentrations breached the UK and WHO drinking water limits, therefore suggesting further treatment process.
- ED mode performance: the recovered coagulant in the case of the 3ED mode had high concentration of sodium and sulphate ions, and these might impair the treated water quality. It was also determined that the 5ED mode provided better performance for coagulant purity than the 3ED mode.

7.2 Recommendations for further work

- Physicochemical properties of DWTS are affected by raw water characteristics which in turn are changing with season. Samples of DWTS are needed to be collected at different seasons to investigate the effect of season on the sludge characteristics and its adsorption behaviour.
- Because of high affinity of DWTS for P adsorption, using DWTS in land application as one of recycling options might therefore reduce P availability for plants, increase metal content of the soil, and then impact on ground water quality. Further investigation is required to link and find out the combined influence of these parameters together.
- Long-term experiments at laboratory and pilot scale with real wastewater are needed to investigate the applicability of the proposed P adsorption model (chapter 5) using DWTS. After determining the inflow characteristics of HRT and influent P concentration, and the DWTS physical properties, the required mass of DWTS can be calculated and the lifespan can be predicted at any required P saturation degree.

- Further investigation is needed to characterise fouling and its effect on power dropping (which increases the resistances between the anode and cathode), and to separate the recovered P from the solution containing sulphate ions (where both sulphate and P are recovered in the same direction).
- It has been reported that coagulant recovery using ED technology offers no cost benefit in comparison to conventional practice (Keeley et al. 2012). Therefore, the performance and associated cost would be enhanced through investigating: other ionic exchange membranes, design configuration, considering acids recovery to be reused again in sludge solubilization, concentrating the recoveries and energy generating.

References

- Ádám, K., Krogstad, T., Vråle, L., Søvik, A.K. and Jenssen, P.D. 2007. Phosphorus retention in the filter materials shellsand and Filtralite P®—Batch and column experiment with synthetic P solution and secondary wastewater. *Ecological Engineering* 29(2), pp. 200–208.
- Agyin-Birikorang, S., O'Connor, G. a, Jacobs, L.W., Makris, K.C. and Brinton, S.R. 2001. Long-term phosphorus immobilization by a drinking water treatment residual. *Journal of environmental quality* 36(1), pp. 316–323.
- Apak, R. 2013. Adsorption of heavy metal ions on soil surfaces and similar substances: theoretical aspects. *ChemInform* 44(51)
- Arias, C. a., Del Bubba, M. and Brix, H. 2001. Phosphorus removal by sands for use as media in subsurface flow constructed reed beds. *Water Research* 35(5), pp. 1159–1168.
- Arnell, N.W. 1998. Climate change and water resources in {Britain}. *Climatic Change* 39(1), pp. 83–110.
- Awual, M.R., Jyo, A., El-Safty, S. a, Tamada, M. and Seko, N. 2011. A weak-base fibrous anion exchanger effective for rapid phosphate removal from water. *Journal of hazardous materials* 188(1–3), pp. 164–71.
- Babatunde, A.O. and Zhao, Y.Q. 2007. Constructive Approaches Toward Water Treatment Works Sludge Management: An International Review of Beneficial Reuses. *Critical Reviews in Environmental Science and Technology* 37(2), pp. 129–164.
- Babatunde, A.O. and Zhao, Y.Q. 2009. Phosphorus removal in laboratory-scale unvegetated vertical subsurface flow constructed wetland systems using alum sludge as main substrate. *Water science and technology: a journal of the International Association on Water Pollution Research* 60(2), pp. 483–9.
- Babatunde, A.O. and Zhao, Y.Q. 2010. Equilibrium and kinetic analysis of phosphorus adsorption from aqueous solution using waste alum sludge. *Journal of Hazardous Materials* 184(1–3), pp. 746–752.

References

Babatunde, A.O., Zhao, Y.Q., Burke, a M., Morris, M. a and Hanrahan, J.P. 2009. Characterization of aluminium-based water treatment residual for potential phosphorus removal in engineered wetlands. *Environmental pollution (Barking, Essex : 1987)* 157(10), pp. 2830–6.

Babatunde, A.O., Zhao, Y.Q., Doyle, R.J., Rackard, S.M., Kumar, J.L.G. and Hu, Y.S. 2011. Performance evaluation and prediction for a pilot two-stage on-site constructed wetland system employing dewatered alum sludge as main substrate. *Bioresource technology* 102(10), pp. 5645–52.

Babatunde, A.O., Zhao, Y.Q., Yang, Y. and Kearney, P. 2008. Reuse of dewatered aluminium-coagulated water treatment residual to immobilize phosphorus: Batch and column trials using a condensed phosphate. *Chemical Engineering Journal* 136(2–3), pp. 108–115.

Bai, L., Wang, C., He, L. and Pei, Y. 2014. Influence of the inherent properties of drinking water treatment residuals on their phosphorus adsorption capacities. *Journal of Environmental Sciences* 26(12), pp. 2397–2405.

Baker, M.D., Simkins, S., Spokas, L. a., Veneman, P.L.M. and Xing, B.S. 2014. Comparison of Phosphorus Sorption by Light-Weight Aggregates Produced in the United States. *Pedosphere* 24(6), pp. 808–816.

Baker, R.W. 2012. Ion Exchange Membrane Processes - Electrodialysis. In: *Membrane Technology and Applications*. Chichester, UK: John Wiley & Sons, Ltd., pp. 417–451.

Bal Krishna, K.C., Aryal, A. and Jansen, T. 2016. Comparative study of ground water treatment plants sludges to remove phosphorous from wastewater. *Journal of Environmental Management* 180, pp. 17–23.

Barat, R., Montoya, T., Borrás, L., Ferrer, J. and Seco, a 2008. Interactions between calcium precipitation and the polyphosphate-accumulating bacteria metabolism. *Water research* 42(13), pp. 3415–24.

Başar, C.A. 2006. Applicability of the various adsorption models of three dyes adsorption onto activated carbon prepared waste apricot. *Journal of Hazardous Materials* 135(1–3), pp. 232–241.

References

- Basibuyuk, M. and Kalat, D.G. 2004. The use of waterworks sludge for the treatment of vegetable oil refinery industry wastewater. *Environmental technology* 25(3), pp. 373–80.
- Battistoni, P., Fava, G., Pavan, P., Musacco, A. and Cecchi, F. 1997. Phosphate removal in anaerobic liquors by struvite crystallization without addition of chemicals: Preliminary results. *Water Research* 31(11), pp. 2925–2929.
- Behnamfard, A. and Salarirad, M.M. 2009. Equilibrium and kinetic studies on free cyanide adsorption from aqueous solution by activated carbon. *Journal of Hazardous Materials* 170(1), pp. 127–133.
- Bellier, N., Chazarenc, F. and Comeau, Y. 2006. Phosphorus removal from wastewater by mineral apatite. *Water Research* 40(15), pp. 2965–2971.
- Betancourt, W.Q. and Rose, J.B. 2004. Drinking water treatment processes for removal of *Cryptosporidium* and *Giardia*. *Veterinary Parasitology* 126(1–2 SPEC.ISS.), pp. 219–234.
- Blaney, L.M., Cinar, S. and SenGupta, A.K. 2007. Hybrid anion exchanger for trace phosphate removal from water and wastewater. *Water research* 41(7), pp. 1603–13.
- Bogestrand, J. 2004. *Eutrophication indicators in lakes*. Copenhagen
- Bond, P.L. and Blackall, L.L. 1999. Anaerobic Phosphate Release from Activated Sludge with Enhanced Biological Phosphorus Removal . A Possible Mechanism of Intracellular pH Control.
- Bowden, L.I., Jarvis, A.P., Younger, P.L. and Johnson, K.L. 2009. Phosphorus removal from waste waters using basic oxygen steel slag. *Environmental science & technology* 43(7), pp. 2476–81.
- Bratby, J. 2015. *Coagulation and Flocculation in Water and Wastewater Treatment - Second Edition*
- British Standards Institution 1990. Methods of test for soils for civil engineering purposes (BS 1377). *Part 2: Classification tests*
- Brooks, A.S., Rozenwald, M.N., Geohring, L.D., Lion, L.W. and Steenhuis, T.S.

References

2000. Phosphorus removal by wollastonite: A constructed wetland substrate. *Ecological Engineering* 15(1–2), pp. 121–132.

Van Der Bruggen, B., Koninckx, A. and Vandecasteele, C. 2004. Separation of monovalent and divalent ions from aqueous solution by electrodialysis and nanofiltration. *Water Research* 38(5), pp. 1347–1353.

Van Der Bruggen, B., Milis, R., Vandecasteele, C., Bielen, P., Van San, E. and Huysman, K. 2003. Electrodialysis and nanofiltration of surface water for subsequent use as infiltration water. *Water Research* 37(16), pp. 3867–3874.

Del Bubba, M., Arias, C. a and Brix, H. 2003. Phosphorus adsorption maximum of sands for use as media in subsurface flow constructed reed beds as measured by the Langmuir isotherm. *Water research* 37(14), pp. 3390–400.

Callery, O. and Healy, M.G. 2017. Predicting the propagation of concentration and saturation fronts in fixed-bed filters. 123, pp. 556–568.

Callery, O., Healy, M.G., Rognard, F., Barthelemy, L. and Brennan, R.B. 2016. Evaluating the long-term performance of low-cost adsorbents using small-scale adsorption column experiments. *Water Research* 101, pp. 429–440.

Cao, X. and Harris, W. 2008. Carbonate and magnesium interactive effect on calcium phosphate precipitation. *Environmental science & technology* 42(2), pp. 436–42.

Carliell-Marquet, C., Oikonomidis, I., Wheatley, A. and Smith, J. 2010. Inorganic profiles of chemical phosphorus removal sludge. *Proceedings of the ICE - Water Management* 163(2), pp. 65–77.

Casey, T.J. and Casey, T.J. 1997. *Unit treatment processes in water and wastewater engineering*. Wiley West Sussex, England.

Cerato, A.B. and Lutenecker, A.J. 2002. Determination of surface area of fine-grained soils by the ethylene glycol monoethyl ether (EGME) method. *Geotechnical Testing Journal* 25(3), pp. 315–321.

Chen, Y., Randall, A. a and McCue, T. 2004. The efficiency of enhanced biological phosphorus removal from real wastewater affected by different ratios of acetic to

propionic acid. *Water research* 38(1), pp. 27–36.

Chen, Z., Ma, W. and Han, M. 2008. Biosorption of nickel and copper onto treated alga (*Undaria pinnatifida*): Application of isotherm and kinetic models. *Journal of Hazardous Materials* 155(1–2), pp. 327–333.

Chitrakar, R., Tezuka, S., Sonoda, A., Sakane, K., Ooi, K. and Hirotsu, T. 2006. Phosphate adsorption on synthetic goethite and akaganeite. *Journal of Colloid and Interface Science* 298(2), pp. 602–608.

Choy, K.K.H., McKay, G. and Porter, J.F. 1999. Sorption of acid dyes from effluents using activated carbon. *Resources, Conservation and Recycling* 27(1–2), pp. 57–71.

Cisse, L. and Mrabet, T. 2004. World Phosphate Production: Overview and Prospects. *Phosphorus Research Bulletin* 15, pp. 21–25.

Codling, E.E. 2008. Effects of Soil Acidity and Cropping on Solubility of By-Product-Immobilized Phosphorus and Extractable Aluminum, Calcium, and Iron From Two High-Phosphorus Soils. *Soil Science* 173(8), pp. 552–559.

Conley, D.J., Paerl, H.W., Howarth, R.W., Boesch, D.F., Seitzinger, S.P., Havens, K.E., Lancelot, C. and Likens, G.E. 2009. Controlling eutrophication: nitrogen and phosphorus. *Science (New York, N.Y.)* 323(5917), pp. 1014–1015.

Converti, A., Rovatti, M. and Borghi, M.D.E.L. 1995. WASTEWATERS BY ALTERNATING AEROBIC. 29(1), pp. 263–269.

Cooney, D.O. 1998. *Adsorption design for wastewater treatment*. CRC Press.

Council of the European Union 1991. Council Directive of 21 May 1991 concerning Urban Waste Water Treatment (91/271/EEC). *Official J. Eur. Commun. L* 34(May 1991), pp. 1–16.

Cucarella, V. and Renman, G. 2009. Phosphorus sorption capacity of filter materials used for on-site wastewater treatment determined in batch experiments—a comparative study. *J Environ Qual* 38(2), pp. 381–392.

Dayton, E. a., Basta, N.T., Jakober, C. a. and Hattey, J. a. 2003. Using treatment residuals to reduce phosphorus in agricultural runoff. *Journal (American Water*

Works Association) 95(4), pp. 151–158.

Dayton, E. a and Basta, N.T. 2005. A Method for Determining the Phosphorus Sorption Capacity and Amorphous Aluminum of Aluminum-Based Drinking Water Treatment Residuals. *Journal of Environment Quality* 34(3), p. 1112.

de-Bashan, L.E. and Bashan, Y. 2004. Recent advances in removing phosphorus from wastewater and its future use as fertilizer (1997-2003). *Water research* 38(19), pp. 4222–46.

Delpla, I., Jung, A. V., Baures, E., Clement, M. and Thomas, O. 2009. Impacts of climate change on surface water quality in relation to drinking water production. *Environment International* 35(8), pp. 1225–1233.

Demirbas, E., Dizge, N., Sulak, M.T. and Kobya, M. 2009. Adsorption kinetics and equilibrium of copper from aqueous solutions using hazelnut shell activated carbon. *Chemical Engineering Journal* 148(2–3), pp. 480–487.

DeSutter, T.M., Pierzynski, G.M. and Baker, L.R. 2006. Flow-Through and Batch Methods for Determining Calcium-Magnesium and Magnesium-Calcium Selectivity. *Soil Science Society of America Journal* 70(2), p. 550.

Diaz, R.J. and Rosenberg, R. 2008. Spreading Dead Zones and Consequences for Marine Ecosystems. *Science* 321(5891), pp. 926–929.

Dizge, N., Aydiner, C., Demirbas, E., Kobya, M. and Kara, S. 2008. Adsorption of reactive dyes from aqueous solutions by fly ash: Kinetic and equilibrium studies. *Journal of Hazardous Materials* 150(3), pp. 737–746.

Drizo, A., Comeau, Y., Forget, C. and Chapuis, R.P. 2002. Phosphorus saturation potential: A parameter for estimating the longevity of constructed wetland systems. *Environmental Science and Technology* 36(21), pp. 4642–4648.

Drizo, A., Forget, C., Chapuis, R.P. and Comeau, Y. 2006. Phosphorus removal by electric arc furnace steel slag and serpentinite. *Water Research* 40(8), pp. 1547–1554.

Drizo, A., Frost, C.A., Grace, J. and Smith, K.A. 1999. Physico-Chemical screening of Phosphate removing substrates for use in constructed wetland systems. *Water*

Research 33(17), pp. 3595–3602.

Duley, B. 2001. Recycling phosphorus by recovery from sewage. *Rhodia Consumer Specialties UK Ltd.(for Centre Europeen d'Etudes des Polyphosphates)*

Dzakpasu, M., Scholz, M., McCarthy, V. and Jordan, S.N. 2015. Assessment of long-term phosphorus retention in an integrated constructed wetland treating domestic wastewater. *Environmental Science and Pollution Research* 22(1), pp. 305–313.

Ebbers, B., Ottosen, L.M. and Jensen, P.E. 2015. Electrodialytic treatment of municipal wastewater and sludge for the removal of heavy metals and recovery of phosphorus. *Electrochimica Acta* 181, pp. 90–99.

Eckenfelder, W.W. 1989. *Industrial water pollution control*. McGraw-Hill.

Elliott, H. a, O'Connor, G. a, Lu, P. and Brinton, S. 2002. Influence of water treatment residuals on phosphorus solubility and leaching. *Journal of Environmental Quality* 31(4), pp. 1362–1369.

Erdal, U.G., Erdal, Z.K. and Randall, C.W. 2003. The competition between PAOs (phosphorus accumulating organisms) and GAOs (glycogen accumulating organisms) in EBPR (enhanced biological phosphorus removal) systems at different temperatures and the effects on system performance. *Water Science and Technology* 47(11), p. 1 LP-8.

Foo, K.Y. and Hameed, B.H. 2010. Insights into the modeling of adsorption isotherm systems. *Chemical Engineering Journal* 156(1), pp. 2–10.

Franceschi, M., Girou, A., Carro-Diaz, A.M., Maurette, M.T. and Puech-Costes, E. 2002. Optimisation of the coagulation-flocculation process of raw water by optimal design method. *Water Research* 36(14), pp. 3561–3572.

Fujiwara, M. 2011. Outline of Sludge Treatment & Disposal at Water Purification Plant in Japan What does JWRC do ?

Fytianos, K., Voudrias, E. and Raikos, N. 1998. Modelling of phosphorus removal from aqueous and wastewater samples using ferric iron. *Environmental pollution (Barking, Essex : 1987)* 101(1), pp. 123–30.

References

- Galarneau, E. and Gehr, R. 1997. Phosphorus removal from wastewaters: Experimental and theoretical support for alternative mechanisms. *Water Research* 31(2), pp. 328–338.
- Gao, S., Wang, C. and Pei, Y. 2013. Comparison of different phosphate species adsorption by ferric and alum water treatment residuals. *Journal of Environmental Sciences* 25(5), pp. 986–992.
- Gibbons, M.K. and Gagnon, G. a. 2011. Understanding removal of phosphate or arsenate onto water treatment residual solids. *Journal of Hazardous Materials* 186(2–3), pp. 1916–1923.
- Goldberg, S. and Johnston, C.T. 2001. Mechanisms of Arsenic Adsorption on Amorphous Oxides Evaluated Using Macroscopic Measurements, Vibrational Spectroscopy, and Surface Complexation Modeling. *Journal of colloid and interface science* 234(1), pp. 204–216.
- Goldbold, P., Lewin, K., Graham, A. and Barker, P. 2003. The potential reuse of water utility products as secondary commercial materials. *WRc Report No. UC 6081*
- Gon Kim, J., Hyun Kim, J., Moon, H.-S., Chon, C.-M. and Sung Ahn, J. 2003. Removal capacity of water plant alum sludge for phosphorus in aqueous solutions. *Chemical Speciation & Bioavailability* 14(1–4), pp. 67–73.
- Gray, H., Parker, W. and Smith, S. 2015. *State of Knowledge of the Use of Sorption Technologies for Nutrient Recovery from Municipal Wastewaters*
- Gray, S., Kinross, J., Read, P. and Marland, A. 2000. The nutrient assimilative capacity of maerl as a substrate in constructed wetland systems for waste treatment. *Water Research* 34(8), pp. 2183–2190.
- Gupta, V.K., Gupta, M. and Sharma, S. 2001. Process development for the removal of lead and chromium from aqueous solutions using red mud--an aluminium industry waste. *Water research* 35(5), pp. 1125–34.
- Harkins, W.D. and Jura, G. 1944. The Decrease (π) of Free Surface Energy (γ) as a Basis for the Development of Equations for Adsorption Isotherms; and the Existence of Two Condensed Phases in Films on Solids. *The Journal of Chemical Physics*

12(3), pp. 112–113.

Heal, K., Younger, P.L., Smith, K., Glendinning, S., Quinn, P. and Dobbie, K. 2003. Novel use of ochre from mine water treatment plants to reduce point and diffuse phosphorus pollution. *Land Contamination and Reclamation* 11(2), pp. 145–152.

Henderson, J.L., Raucher, R. and Weicksel, S. 2009. *Supply of Critical Drinking Water and Wastewater Treatment Chemicals—A White Paper for Understanding Recent Chemical Price Increases and Shortages*

Hendricks, D. 2010. *Fundamentals of water treatment unit processes: physical, chemical, and biological*. CRC Press.

Ho, Y.. and McKay, G. 1999. Pseudo-second order model for sorption processes. *Process Biochemistry* 34(5), pp. 451–465.

Horth, H., Gendebien, A., Agg, R. and Cartwright, N. 1994. Treatment and disposal of waterworks sludge in selected European countries. *Foundation for water research technical reports. No. FR 428*

Huang, S.-H. and Chiswell, B. 2000. Phosphate removal from wastewater using spent alum sludge. *Water Science and Technology* 42(3–4), pp. 295–300.

Hurst, A.M., Edwards, M.J., Chipps, M., Jefferson, B. and Parsons, S.A. 2004. The impact of rainstorm events on coagulation and clarifier performance in potable water treatment. *Science of the Total Environment* 321(1–3), pp. 219–230.

Ippolito, J. a, Barbarick, K. a and Elliott, H. a 2011. Drinking water treatment residuals: a review of recent uses. *Journal of environmental quality* 40(1), pp. 1–12.

Ippolito, J. a, Barbarick, K. a, Heil, D.M., Chandler, J.P. and Redente, E.F. 2003. Phosphorus Retention Mechanisms of a Water Treatment Residual. *Journal of Environment Quality* 32(5), p. 1857.

Isherwood, K.F. 2000. *Mineral Fertilizer Use and the Environment, International Fertilizer Industry Association/United Nations Environment Programme*. France

Izquierdo, M., Marzal, P., Gabaldón, C., Silvetti, M. and Castaldi, P. 2012. Study of the Interaction Mechanism in the Biosorption of Copper(II) Ions onto Posidonia

References

oceanica and Peat. *CLEAN - Soil, Air, Water* 40(4), pp. 428–437.

Jarvie, H.P., Neal, C. and Withers, P.J. a 2006. Sewage-effluent phosphorus: a greater risk to river eutrophication than agricultural phosphorus? *The Science of the total environment* 360(1–3), pp. 246–53.

Johansson, L. and Gustafsson, J.P. 2000. Phosphate removal using blast furnace slags and opoka-mechanisms. *Water Research* 34(1), pp. 259–265.

Johansson Westholm, L. 2006. Substrates for phosphorus removal-potential benefits for on-site wastewater treatment? *Water research* 40(1), pp. 23–36.

Kaasik, A., Vohla, C., Mõtlep, R., Mander, U. and Kirsimäe, K. 2008. Hydrated calcareous oil-shale ash as potential filter media for phosphorus removal in constructed wetlands. *Water research* 42(4–5), pp. 1315–23.

Kadlec, R.H. and Wallace, S.D. 2009. *Treatment Wetlands*. Second Edi. CRC Press, Taylor & Francis Group, LLC.

Kagalou, I., Papastergiadou, E. and Leonardos, I. 2008. Long term changes in the eutrophication process in a shallow Mediterranean lake ecosystem of W. Greece: response after the reduction of external load. *Journal of environmental management* 87(3), pp. 497–506.

Kang, S.J., Olmstead, K.P. and Takacs, K.M. 2007. THE PRACTICAL LIMITS OF PHOSPHORUS REMOVAL: HOW LOW CAN YOU RELIABLY GO? In: *Proceedings of the Water Environment Federation*. Water Environment Federation., pp. 1460–1469.

Karaca, S., Gürses, a, Ejder, M. and Açıkyıldız, M. 2006. Adsorptive removal of phosphate from aqueous solutions using raw and calcinated dolomite. *Journal of hazardous materials* 128(2–3), pp. 273–9.

Keeley, J., Jarvis, P. and Judd, S.J. 2012. An economic assessment of coagulant recovery from water treatment residuals. *Desalination* 287, pp. 132–137.

Keeley, J., Jarvis, P. and Judd, S.J. 2014a. Coagulant Recovery from Water Treatment Residuals: A Review of Applicable Technologies. *Critical Reviews in Environmental Science and Technology* 44(24), pp. 2675–2719.

Keeley, J., Jarvis, P., Smith, A.D. and Judd, S.J. 2016. Coagulant recovery and reuse for drinking water treatment. *Water Research* 88, pp. 502–509.

Keeley, J., Smith, A.D., Judd, S.J. and Jarvis, P. 2014b. Reuse of recovered coagulants in water treatment: An investigation on the effect coagulant purity has on treatment performance. *Separation and Purification Technology* 131, pp. 69–78.

Khelifi, O., Kozuki, Y., Murakami, H., Kurata, K. and Nishioka, M. 2002. Nutrients adsorption from seawater by new porous carrier made from zeolitized fly ash and slag. *Marine Pollution Bulletin* 45(1–12), pp. 311–315.

Kim, J.G., Kim, J.H., Moon, H.S., Chon, C.M. and Ahn, J.S. 2003. Removal capacity of water plant alum sludge for phosphorus in aqueous solutions. *Chemical Speciation and Bioavailability* 14(1–4), pp. 67–73.

Kostura, B., Kulveitová, H. and Lesko, J. 2005. Blast furnace slags as sorbents of phosphate from water solutions. *Water research* 39(9), pp. 1795–802.

Kumar, E., Bhatnagar, A., Hogland, W., Marques, M. and Sillanpää, M. 2014a. Interaction of anionic pollutants with Al-based adsorbents in aqueous media - A review. *Chemical Engineering Journal* 241, pp. 443–456.

Kumar, E., Bhatnagar, A., Hogland, W., Marques, M. and Sillanpää, M. 2014b. Interaction of inorganic anions with iron-mineral adsorbents in aqueous media - A review. *Advances in Colloid and Interface Science* 203, pp. 11–21.

Leader, J.W., Dunne, E.J. and Reddy, K.R. 2008. Phosphorus Sorbing Materials: Sorption Dynamics and Physicochemical Characteristics. *Journal of Environment Quality* 37(1), p. 174.

Li, Y., Liu, C., Luan, Z., Peng, X., Zhu, C., Chen, Z., Zhang, Z., Fan, J. and Jia, Z. 2006. Phosphate removal from aqueous solutions using raw and activated red mud and fly ash. *Journal of hazardous materials* 137(1), pp. 374–83.

Li, Z., Jiang, N., Wu, F. and Zhou, Z. 2013. Experimental investigation of phosphorus adsorption capacity of the waterworks sludges from five cities in China. *Ecological Engineering* 53, pp. 165–172.

Li, Z., Tang, X., Chen, Y. and Wang, Y. 2009. Behaviour and mechanism of

enhanced phosphate sorption on loess modified with metals: equilibrium study. *Journal of Chemical Technology & Biotechnology* 84(4), pp. 595–603.

Liu, Y., Chen, Y. and Zhou, Q. 2007. Effect of initial pH control on enhanced biological phosphorus removal from wastewater containing acetic and propionic acids. *Chemosphere* 66(1), pp. 123–9.

Mahdy, A.M., Elkhatib, E.A. and Fathi, N.O. 2008. Drinking water treatment residuals as an amendment to alkaline soils: Effects on bioaccumulation of heavy metals and aluminum in corn plants. *234 PLANT SOIL ENVIRON.* 54(6), pp. 234–246.

Maiden, P., Hearn, M.T.W., Boysen, R.I., Chier, P., Warnecke, M. and Jackson, W.R. 2015. *Alum Sludge Reuse Investigation (100S-42) prepared by GHD and Centre for Green Chemistry (Monash University) for the Smart Water Fund.* Victoria

Mainston, C.P. and Parr, W. 2002. Phosphorus in rivers--ecology and management. *The Science of the total environment* 282–283, pp. 25–47.

Makris, K.C. 2004. Long-Term Stability of Sorbed Phosphorus By Drinking-Water Treatment Residuals: Mechanisms and Implications., p. 198p.

Makris, K.C., El-Shall, H., Harris, W.G., O'Connor, G. a. and Obreza, T. a. 2004a. Intraparticle phosphorus diffusion in a drinking water treatment residual at room temperature. *Journal of Colloid and Interface Science* 277(2), pp. 417–423.

Makris, K.C., Harris, W.G., O'Connor, G. a. and El-Shall, H. 2005a. Long-term phosphorus effects on evolving physicochemical properties of iron and aluminum hydroxides. *Journal of Colloid and Interface Science* 287(2), pp. 552–560.

Makris, K.C., Harris, W.G., O'Connor, G. a. and Obreza, T. a. 2004b. Phosphorus immobilization in micropores of drinking-water treatment residuals: Implications for long-term stability. *Environmental Science and Technology* 38(24), pp. 6590–6596.

Makris, K.C., Harris, W.G., O'Connor, G. a., Obreza, T. a. and Elliott, H. a. 2005b. Physicochemical Properties Related to Long-Term Phosphorus Retention by Drinking-Water Treatment Residuals. *Environmental science & technology* 39(11), pp. 4280–4289.

References

- Makris, K.C., Sarkar, D. and Datta, R. 2006. Evaluating a drinking-water waste by-product as a novel sorbent for arsenic. *Chemosphere* 64(5), pp. 730–741.
- Matilainen, A., Vepsäläinen, M. and Sillanpää, M. 2010. Natural organic matter removal by coagulation during drinking water treatment: A review. *Advances in Colloid and Interface Science* 159(2), pp. 189–197.
- Maurer, M. and Boller, M. 1999. Modelling of phosphorus precipitation in wastewater treatment plants with enhanced biological phosphorus removal. *Water science and technology* 39(1), pp. 147–163.
- Mayer, B.K., Gerrity, D., Rittmann, B.E., Reisinger, D. and Brandt-Williams, S. 2013. Innovative Strategies to Achieve Low Total Phosphorus Concentrations in High Water Flows. *Critical Reviews in Environmental Science and Technology* 43(4), pp. 409–441.
- McClintock, S.A., Randall, C.W. and Pattarkine, V.M. 1993. Effects of temperature and mean cell residence time on biological nutrient removal processes. *Water Environment Research* 65(2), pp. 110–118.
- McCormick, N., Younker, J., Mackie, A. and Walsh, M.E. 2009. Data review from full-scale installations for water treatment plant residuals treatment processes. In: *American Water Works Association Annual Conference (ACE)*. Chicago, USA.
- McGhee, T.J. and Steel, E.W. 1991. *Water supply and sewerage*. McGraw-Hill New York.
- McKeague, J. a. and Day, J.H. 1966. DITHIONITE- AND OXALATE-EXTRACTABLE Fe AND Al AS AIDS IN DIFFERENTIATING VARIOUS CLASSES OF SOILS. *Canadian Journal of Soil Science* 46(1), pp. 13–22.
- Mejia Likosova, E., Keller, J., Poussade, Y. and Freguia, S. 2014. A novel electrochemical process for the recovery and recycling of ferric chloride from precipitation sludge. *Water Research* 51(Iii), pp. 96–103.
- Mejia Likosova, E., Keller, J., Rozendal, R. a., Poussade, Y. and Freguia, S. 2013. Understanding colloidal FeS_x formation from iron phosphate precipitation sludge for optimal phosphorus recovery. *Journal of Colloid and Interface Science* 403, pp. 16–

21.

Metcalf, L. and Eddy, H.P. 2003. *Wastewater engineering: treatment, disposal, and reuse*. New York [etc.]: McGraw-Hill.

Mino, T., Loosdrecht, M.C.M.V.A.N. and Heijnen, J.J. 1998. REVIEW PAPER MICROBIOLOGY AND BIOCHEMISTRY OF THE ENHANCED BIOLOGICAL PHOSPHATE REMOVAL. 32(11)

Morse, G., Brett, S., Guy, J. and Lester, J. 1998. Review: Phosphorus removal and recovery technologies. *The Science of The Total Environment* 212(1), pp. 69–81.

Mortula, M., Gibbons, M. and Gagnon, G.A. 2007. Phosphorus adsorption by naturally-occurring materials and industrial by-products. *Journal of Environmental Engineering and Science* 6(2), pp. 157–164.

Mulkerrins, D., Dobson, a D.W. and Colleran, E. 2004. Parameters affecting biological phosphate removal from wastewaters. *Environment international* 30(2), pp. 249–59.

Oguz, E. 2004. Removal of phosphate from aqueous solution with blast furnace slag. *Journal of hazardous materials* 114(1–3), pp. 131–7.

Ottosen, L.M., Pedersen, A.J., Hansen, H.K. and Ribeiro, A.B. 2007. Screening the possibility for removing cadmium and other heavy metals from wastewater sludge and bio-ashes by an electrodialytic method. *Electrochimica Acta* 52(10 SPEC. ISS.), pp. 3420–3426.

Owen, P.G. 2002. Water Treatment Works' Sludge Management. *CIWEM conference on innovations in Potable Water Sludge Treatment and Disposal*, pp. 282–285.

Ozacar, M. and Sengil, I.A. 2005. Adsorption of metal complex dyes from aqueous solutions by pine sawdust. *Bioresource technology* 96(7), pp. 791–795.

Pan, J.R., Huang, C. and Lin, S. 2004. Reuse of fresh water sludge in cement making. *Water Science and Technology* 50(9), pp. 183–188.

Panswad, T., Doungchai, A. and Anotai, J. 2003. Temperature effect on microbial

References

community of enhanced biological phosphorus removal system. *Water research* 37(2), pp. 409–15.

Parsons, S.A. and Jefferson, B. 2006. *Introduction to Potable Water Treatment Processes*. Blackwell Publishing Ltd.

Persson, P., Persson, P., Nilsson, N., Nilsson, N., Sjöberg, S. and Sjöberg, S. 1996. Structure and Bonding of Orthophosphate Ions at the Iron Oxide-Aqueous Interface. *Journal of colloid and interface science* 177(1), pp. 263–275.

Pradhan, J., Das, J., Das, S. and Thakur, R.S. 1998. Adsorption of Phosphate from Aqueous Solution Using Activated Red Mud. *Journal of Colloid and Interface Science* 204(1), pp. 169–172.

Prakash, P. and Sengupta, A.K. 2003. Selective coagulant recovery from water treatment plant residuals using donnan membrane process. *Environmental Science and Technology* 37(19), pp. 4468–4474.

Pratt, C., Shilton, a, Haverkamp, R.G. and Pratt, S. 2009. Assessment of physical techniques to regenerate active slag filters removing phosphorus from wastewater. *Water research* 43(2), pp. 277–82.

Proudfit, D.P. 1968. Selection of disposal methods for water treatment plant wastes. *Journal (American Water Works Association)* 60(6), pp. 674–680.

Ragsdale, D. 2007. *Advanced wastewater treatment to achieve low concentration of phosphorus*

Ramirez, R., Cerón, O., Cabirol, N., Espejel, F. and Durán, A. 2008. Optimization of the preparation conditions of ceramic products using drinking water treatment sludges. *Journal of environmental science and health. Part A, Toxic/hazardous substances & environmental engineering* 43(13), pp. 1562–1568.

Razali, M., Zhao, Y. and Bruen, M. 2007. Effectiveness of a drinking-water treatment sludge in removing different phosphorus species from aqueous solution. *Separation and Purification Technology* 55(3), pp. 300–306.

Renman, A. and Renman, G. 2010. Chemosphere Long-term phosphate removal by the calcium-silicate material Polonite in wastewater filtration systems. *Chemosphere*

79(6), pp. 659–664.

Rew, T. 2006. *Aluminum Water Treatment Residuals for Reducing Phosphorus Loss from Manure-Impacted, High Watertable Soils.*

Rofe, B.H. 1994. *Wastewater Treatment: Evaluation and Implementation: Proceedings of Water Environment '94, a Joint Institution of Civil Engineers and Institution of Water and Environment Management Conference, Held in London on 9-10 March 1994.* Thomas Telford.

Rossini, M., Garrido, J.G. and Galluzzo, M. 1999. Optimization of the coagulation-flocculation treatment: Influence of rapid mix parameters. *Water Research* 33(8), pp. 1817–1826.

Sansalone, J. and Ma, J. 2011. Parametric Analysis and Breakthrough Modeling of Phosphorus from Al-Oxide Filter Media. *Journal of Environmental Engineering* 137(2), pp. 108–118.

Sansalone, J.J., Asce, M., Ma, J. and Asce, A.M. 2009. Parametric Evaluation of Batch Equilibria for Storm-Water Phosphorus Adsorption on Aluminum Oxide Media. (September), pp. 737–746.

Sengupta, A.K. and Prakash, P. 2004. Alum recovery from water treatment sludges. *Water21* (February), pp. 15–16.

Sharp, E.L., Jarvis, P., Parsons, S.A. and Jefferson, B. 2006. The impact of zeta potential on the physical properties of ferric-NOM flocs. *Environmental Science and Technology* 40(12), pp. 3934–3940.

Shilton, A.N., Elmetri, I., Drizo, A., Pratt, S., Haverkamp, R.G. and Bilby, S.C. 2006. Phosphorus removal by an 'active' slag filter-a decade of full scale experience. *Water Research* 40(1), pp. 113–118.

Simpson, A., Burgess, P. and Coleman, S.J. 2002. The Management of Potable Water Treatment Sludge: Present Situation in the UK. *Water and Environment Journal* 16(4), pp. 260–263.

Sincero, A.P. and Sincero, G.A. 2002. *Physical Chemical Treatment of Water and Wastewater.* Press, C. ed.

Skerratt, G. and Anderson, M. 2003. A COMPARISON OF TWELVE SOURCES OF WATERWORKS SLUDGE IN ENGLAND AND THE REPUBLIC OF IRELAND WITH RESPECT TO THEIR POTENTIAL USE IN FIRED CERAMIC PRODUCTS. In: *Recycling and Reuse of Waste Materials: Proceedings of the International Symposium Held at the University of Dundee, Scotland, UK on 9-11 September 2003.*, p. 67.

Smith, S., Szabó, A., Murthy, S., Lieskó, I. and Daigger, G. 2007. The significance of chemical phosphorus removal theory for engineering practice. *Proceedings of the Water Environment Federation* (2), pp. 1436–1459.

Smith, V.H., Tilman, G.D. and Nekola, J.C. 1999. Eutrophication : Impacts of Excess Nutrient Inputs on Freshwater , Marine , and Terrestrial Ecosystems
Eutrophication : impacts of excess nutrient inputs on freshwater , marine , and terrestrial ecosystems. 7491(FEBRUARY 1999)

Song, X., Pan, Y., Wu, Q., Cheng, Z. and Ma, W. 2011. Phosphate removal from aqueous solutions by adsorption using ferric sludge. *Desalination* 280(1–3), pp. 384–390.

Søvik, a. K. and Kløve, B. 2005. Phosphorus retention processes in shell sand filter systems treating municipal wastewater. *Ecological Engineering* 25(2), pp. 168–182.

Stoner, D., Penn, C., McGrath, J. and Warren, J. 2012. Phosphorus Removal with By-Products in a Flow-Through Setting. *Journal of Environment Quality* 41(3), p. 654.

Stumm, W. and Morgan, J. 2012. *Aquatic chemistry: chemical equilibria and rates in natural water* (Vol. 126). Third Edit. JOHN WILEY & SONS, INC.

Thistleton, J., Clark, T., Pearce, P. and Parsons, S.A. 2001. Mechanisms of Chemical Phosphorus Removal: 1—Iron (II) Salts. *Process Safety and Environmental Protection* 79(11), pp. 339–344.

U.S. Epa 2011. Drinking Water Treatment Plant Residuals. Management Technical Report. Summary of residuals generation, treatment and disposal at large community water systems. (December 2011)

References

Ugurlu, A. and Salman, B. 1998. Phosphorus removal by fly ash. *Environment International* 24(8), pp. 911–918.

Ulmert, H. and Särner, E. 2005. The ReAl Process – A COMBINED MEMBRANE AND PRECIPITATION PROCESS FOR RECOVERY OF., pp. 273–281.

Wagner, D.J., Elliott, H.A., Brandt, R.C. and Jaiswal, D. 2008. Managing biosolids runoff phosphorus using buffer strips enhanced with drinking water treatment residuals. *Journal of Environmental Quality* 37(4), pp. 1567–1574.

Wang, C.-H., Gao, S.-J., Wang, T.-X., Tian, B.-H. and Pei, Y.-S. 2011a. Effectiveness of sequential thermal and acid activation on phosphorus removal by ferric and alum water treatment residuals. *Chemical Engineering Journal* 172(2–3), pp. 885–891.

Wang, C., Gao, S., Pei, Y. and Zhao, Y. 2013. Use of drinking water treatment residuals to control the internal phosphorus loading from lake sediments: Laboratory scale investigation. *Chemical Engineering Journal* 225, pp. 93–99.

Wang, C., Guo, W., Tian, B., Pei, Y. and Zhang, K. 2011b. Characteristics and kinetics of phosphate adsorption on dewatered ferric-alum residuals. *Journal of Environmental Science and Health, Part A* 46(14), pp. 1632–1639.

Wang, C., Wang, Z., Lin, L., Tian, B. and Pei, Y. 2012. Effect of low molecular weight organic acids on phosphorus adsorption by ferric-alum water treatment residuals. *Journal of Hazardous Materials* 203–204(April 2010), pp. 145–150.

WHO 2011. *WHO guidelines for drinking-water quality*.

Wood, E., Fergusson, L., Lowe, M. and Leigh, S. 2007. The Application of ViroFilter Technology at Yorkshire Water. *European Water & Wastewater Management*, p. 16.

Wu, F.C., Tseng, R.L. and Juang, R.S. 2005. Comparisons of porous and adsorption properties of carbons activated by steam and KOH. *Journal of Colloid and Interface Science* 283(1), pp. 49–56.

Wu, H., Zhang, J., Ngo, H.H., Guo, W., Hu, Z., Liang, S., Fan, J. and Liu, H. 2015. A review on the sustainability of constructed wetlands for wastewater treatment:

Design and operation. *Bioresource Technology* 175, pp. 594–601.

Wu, T. and Sansalone, J. 2013. Phosphorus Equilibrium. II: Comparing Filter Media, Models, and Leaching. *Journal of Environmental Engineering* 139(11), pp. 1325–1335.

Xiong, J., He, Z., Mahmood, Q., Liu, D., Yang, X. and Islam, E. 2008. Phosphate removal from solution using steel slag through magnetic separation. *Journal of hazardous materials* 152(1), pp. 211–5.

Xu, D., Xu, J., Wu, J. and Muhammad, A. 2006. Studies on the phosphorus sorption capacity of substrates used in constructed wetland systems. *Chemosphere* 63(2), pp. 344–352.

Yang, Y., Tomlinson, D., Kennedy, S. and Zhao, Y. . 2006a. Dewatered alum sludge: a potential adsorbent for phosphorus removal. *Water Science & Technology* 54(5), p. 207.

Yang, Y., Zhao, Y., Babatunde, a, Wang, L., Ren, Y. and Han, Y. 2006b. Characteristics and mechanisms of phosphate adsorption on dewatered alum sludge. *Separation and Purification Technology* 51(2), pp. 193–200.

Zeng, L., Li, X. and Liu, J. 2004. Adsorptive removal of phosphate from aqueous solutions using iron oxide tailings. *Water research* 38(5), pp. 1318–26.

Zhang, D.Q., Jinadasa, K.B.S.N., Gersberg, R.M., Liu, Y., Ng, W.J. and Tan, S.K. 2014. Application of constructed wetlands for wastewater treatment in developing countries - A review of recent developments (2000-2013). *Journal of Environmental Management* 141, pp. 116–131.

Zhang, G.-S., Qu, J.-H., Liu, H.-J., Liu, R.-P. and Li, G.-T. 2007. Removal Mechanism of As(III) by a Novel Fe–Mn Binary Oxide Adsorbent: Oxidation and Sorption. *Environmental Science & Technology* 41(13), pp. 4613–4619.

Zhao, X.H. and Zhao, Y.Q. 2009. Investigation of phosphorus desorption from P-saturated alum sludge used as a substrate in constructed wetland. *Separation and Purification Technology* 66(1), pp. 71–75.

Zhao, X.H., Zhao, Y.Q. and Kearney, P. 2011. Transformation of beneficially reused

References

aluminium sludge to potential P and Al resource after employing as P-trapping material for wastewater treatment in constructed wetland. *Chemical Engineering Journal* 174(1), pp. 206–212.

Zhao, Y., Razali, M., Babatunde, A., Yang, Y. and Bruen, M. 2000. A multi-pronged approach to using dewatered alum sludge to immobilize a wide range of phosphorus contamination. *IWA Beijing 2000 paper 594 698*, p. 4.

Zhao, Y.Q., Babatunde, A.O., Zhao, X.H. and Li, W.C. 2009a. information Development of alum sludge-based constructed wetland: An innovative and cost-effective system for wastewater treatment. *Journal of Environmental Science and Health, Part A*, 44 (8) , pp. 0–17.

Zhao, Y.Q., Razali, M., Babatunde, A.O., Yang, Y. and Bruen, M. 2007. Reuse of aluminum-based water treatment sludge to immobilize a wide range of phosphorus contamination: Equilibrium study with different isotherm models. *Separation Science and Technology* 42(12), pp. 2705–2721.

Zhao, Y.Q., Zhao, X.H. and Babatunde, a O. 2009. Use of dewatered alum sludge as main substrate in treatment reed bed receiving agricultural wastewater: long-term trial. *Bioresource technology* 100(2), pp. 644–8.

Zhao, Y.X., Gao, B.Y., Shon, H.K., Cao, B.C. and Kim, J.H. 2011b. Coagulation characteristics of titanium (Ti) salt coagulant compared with aluminum (Al) and iron (Fe) salts. *Journal of Hazardous Materials* 185(2–3), pp. 1536–1542.

Zheng, Y., Li, Z., Wang, X., Gao, X. and Gao, C. 2015. The treatment of cyanide from gold mine effluent by a novel five-compartment electro dialysis. *Electrochimica Acta* 169, pp. 150–158.

Zito, R. 2011. Mathematical Analysis & Modeling Electrodialysis Systems. *Electrochemical Water Processing* , pp. 95–175.

Appendices

Appendix A - Supporting Data for Chapter 4

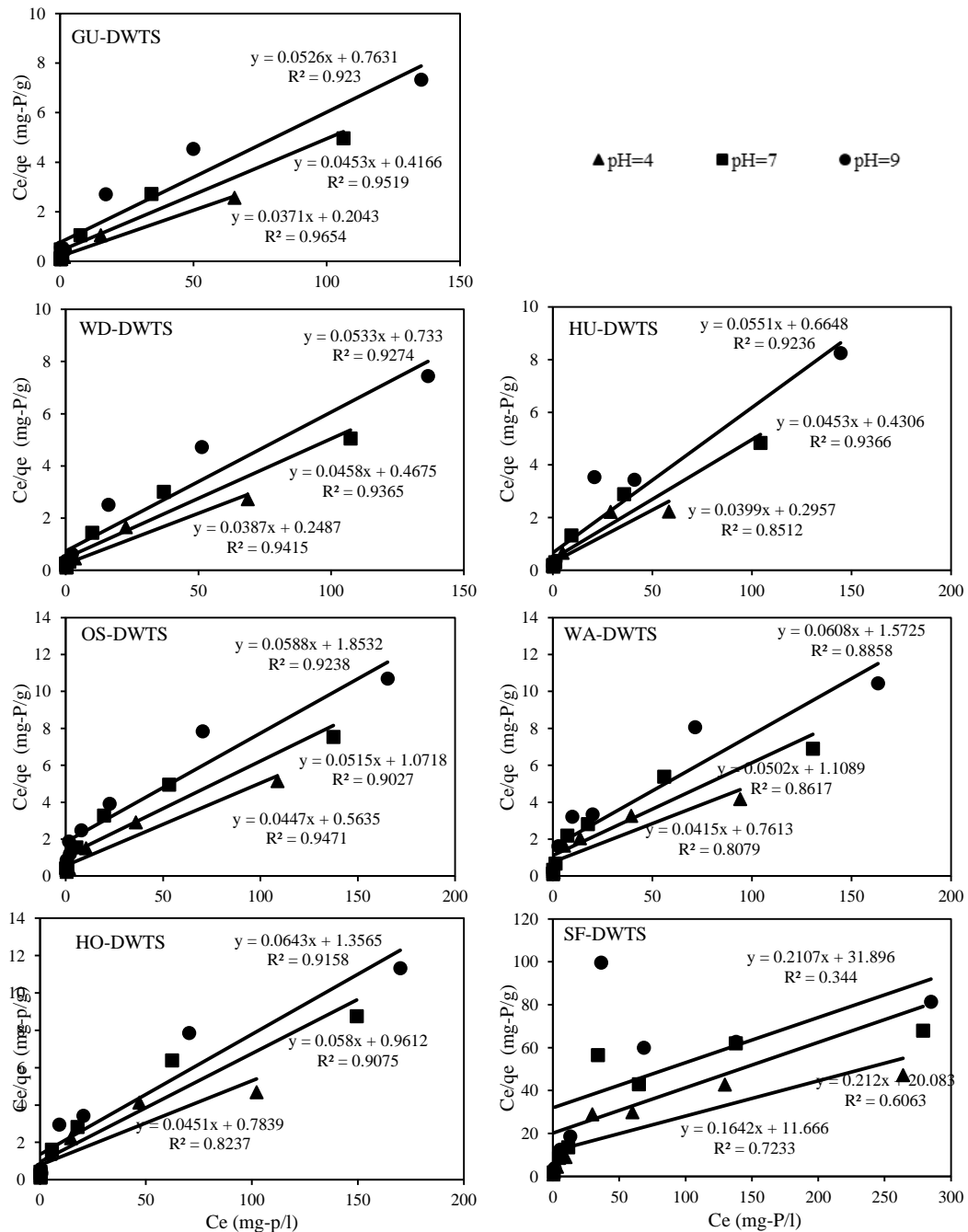


Figure A.1 Fitting P adsorption data of alum-based sludges at three different pH values to the linearized form of Langmuir model.

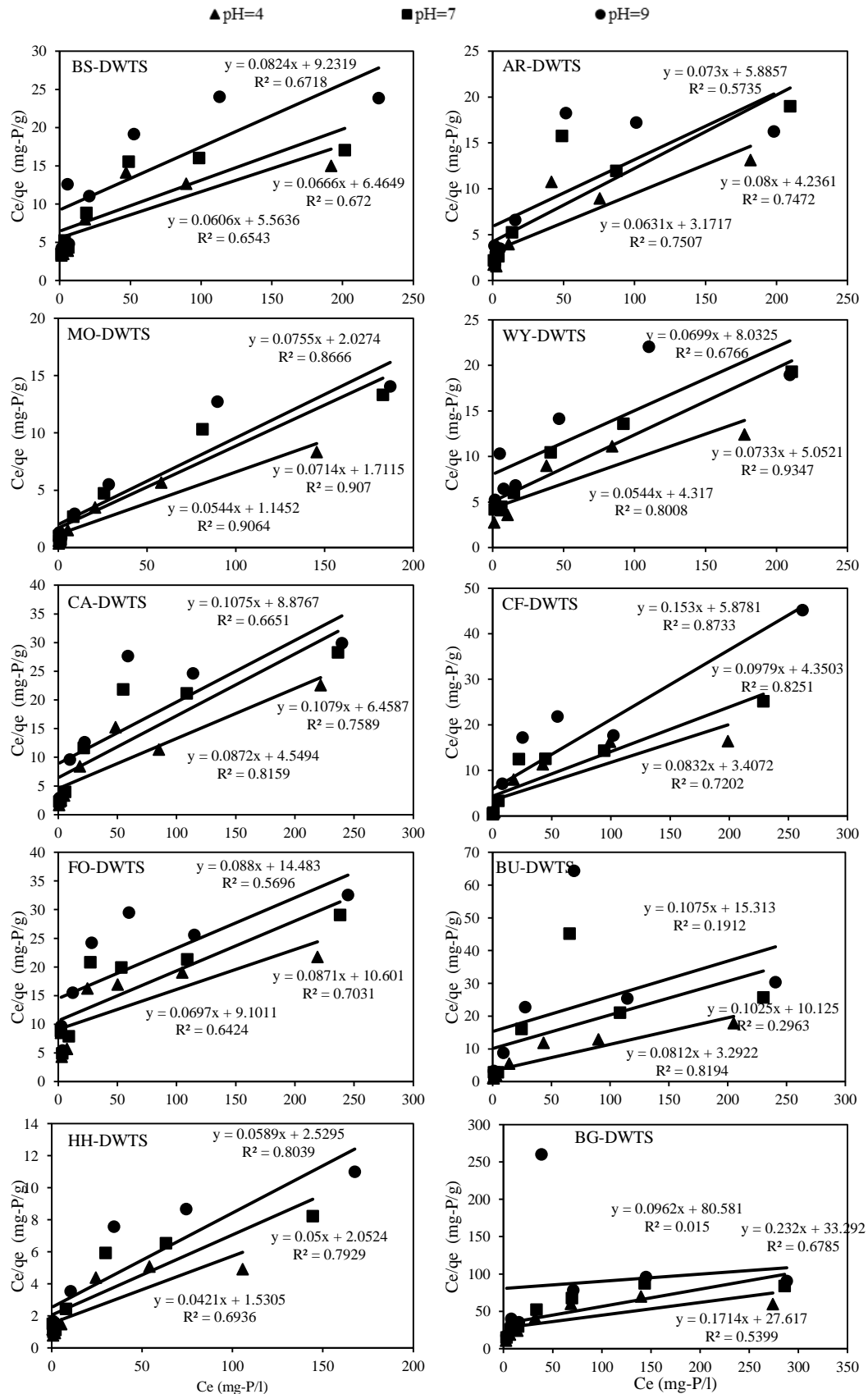


Figure A.2 Fitting *P* adsorption data of iron-based sludges at three different pH values to the linearized form of Langmuir model.

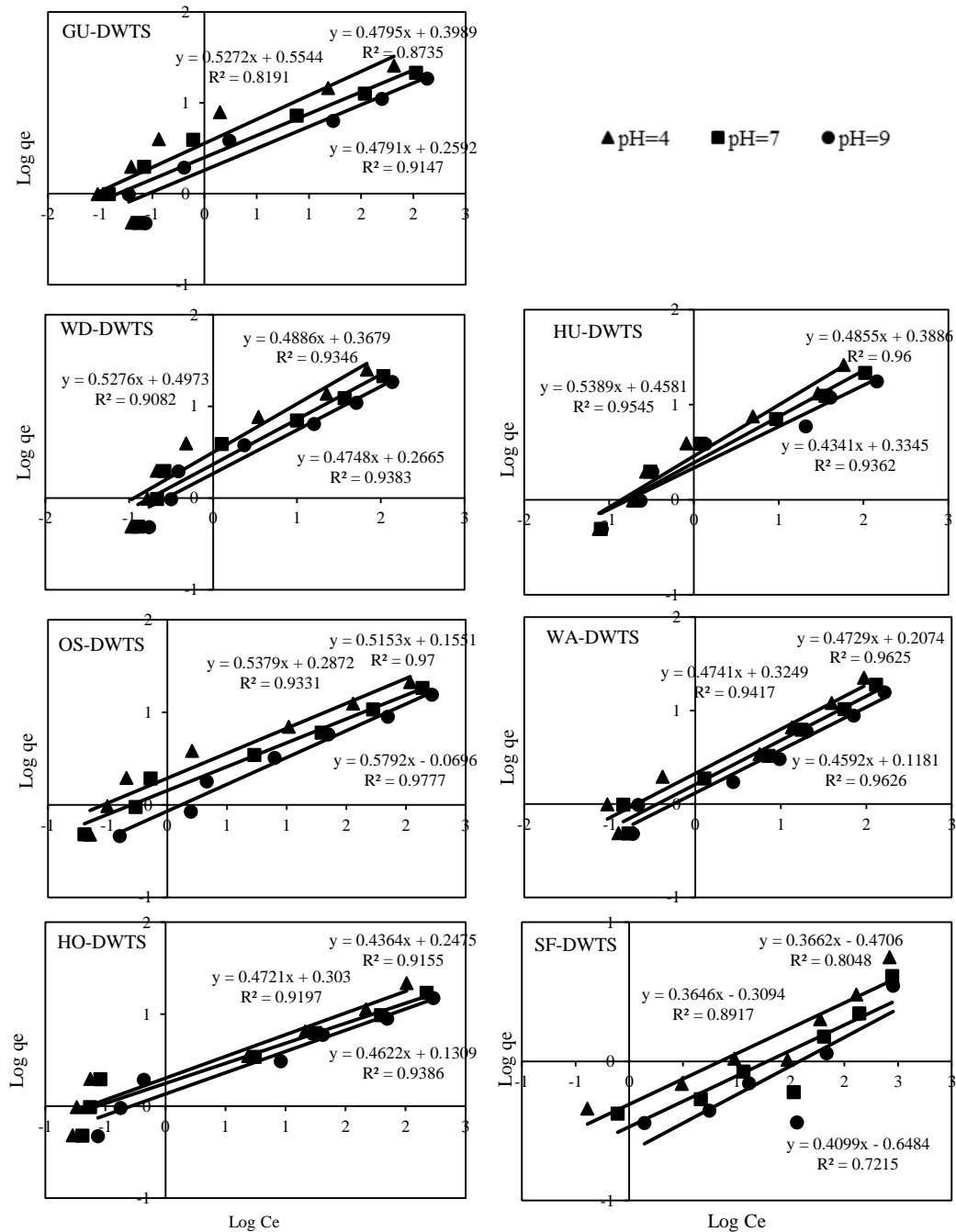


Figure A.3 Fitting P adsorption data of alum-based sludges at three different pH values to the linearized form of Freundlich model.

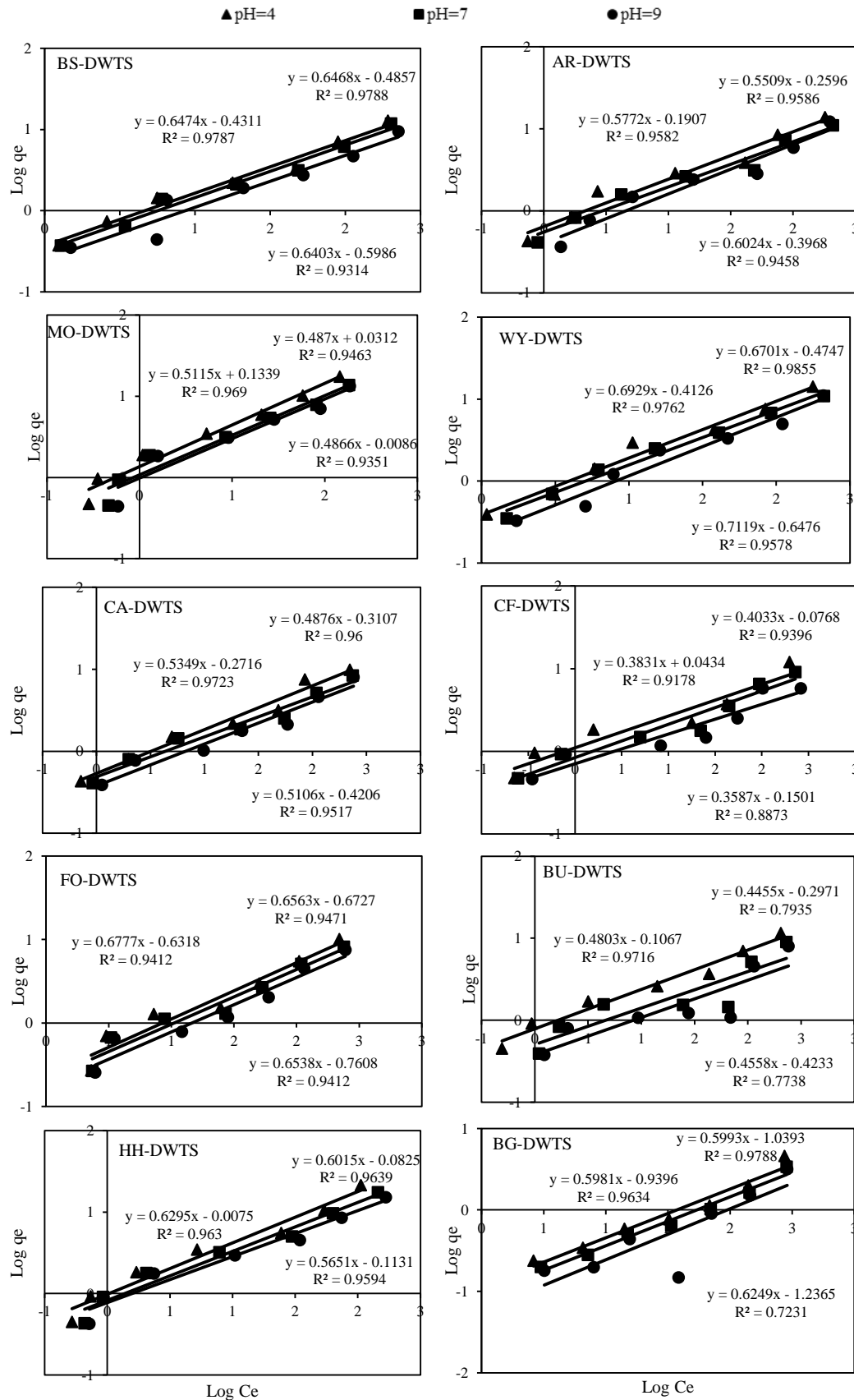


Figure A.4 Fitting P adsorption data of iron-based sludges at three different pH values to the linearized form of Freundlich model.

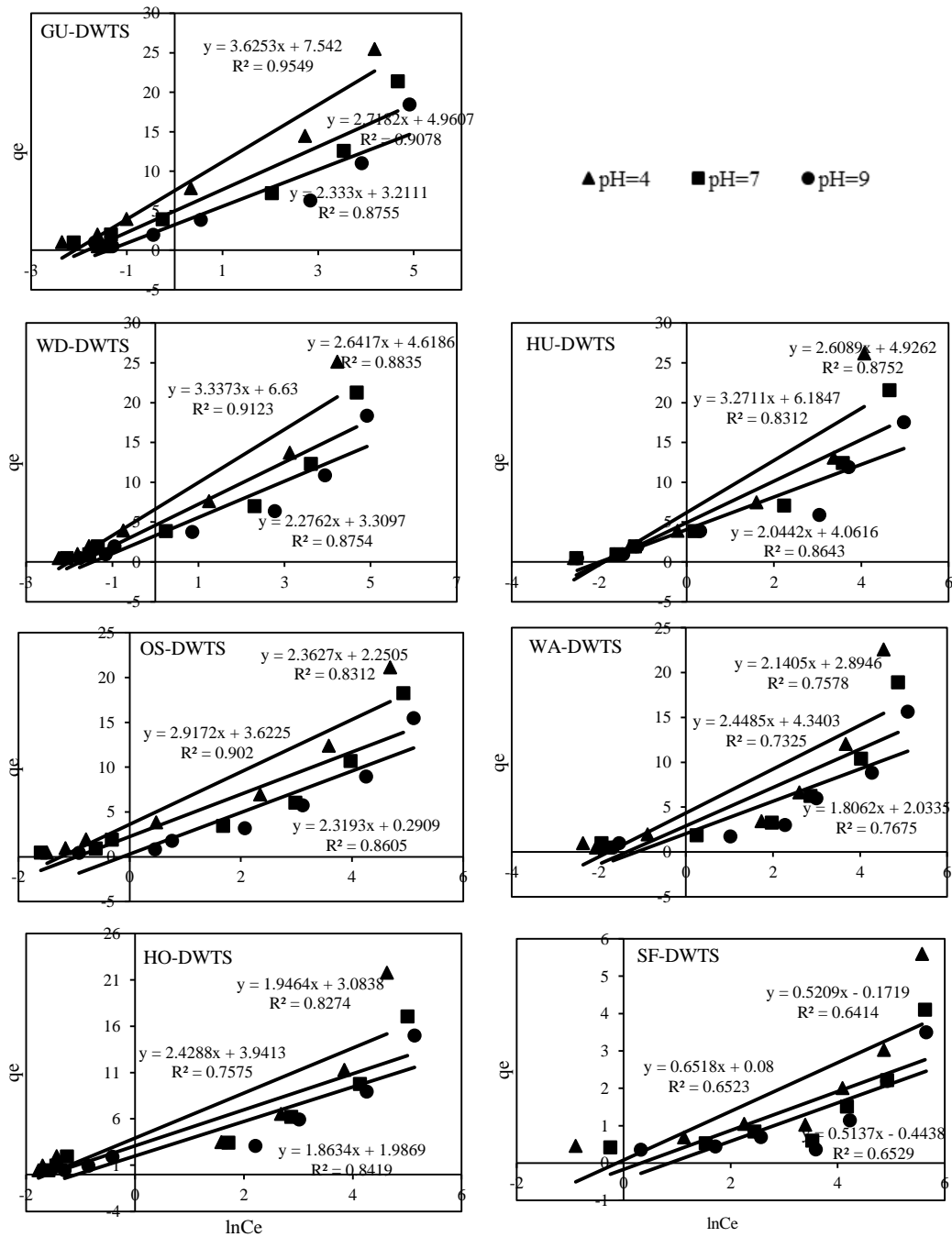


Figure A.5 Fitting P adsorption data of alum-based sludges at three different pH values to the linearized form of Temkin model.

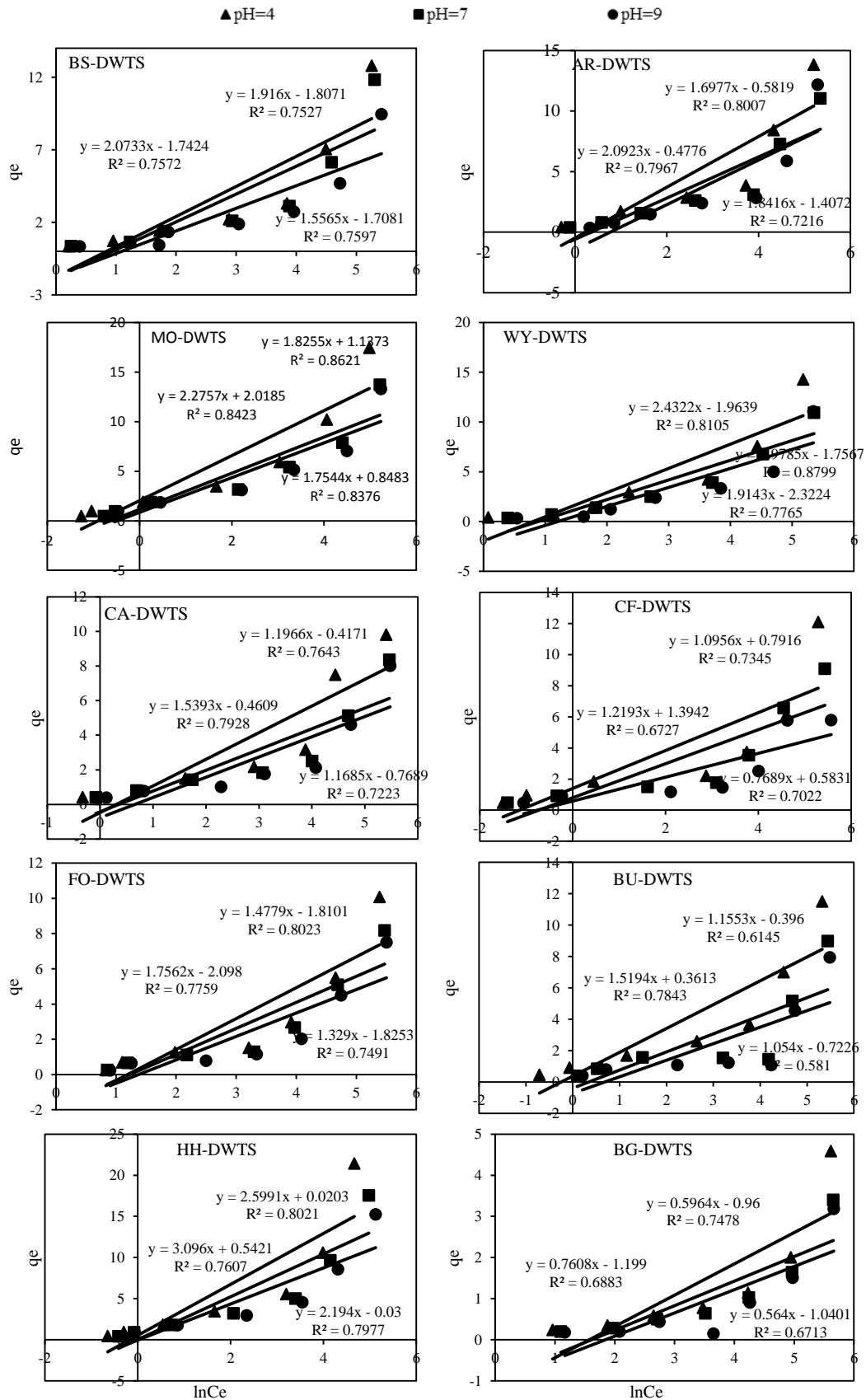


Figure A.6 Fitting P adsorption data of iron-based sludges at three different pH values to the linearized form of Temkin model.

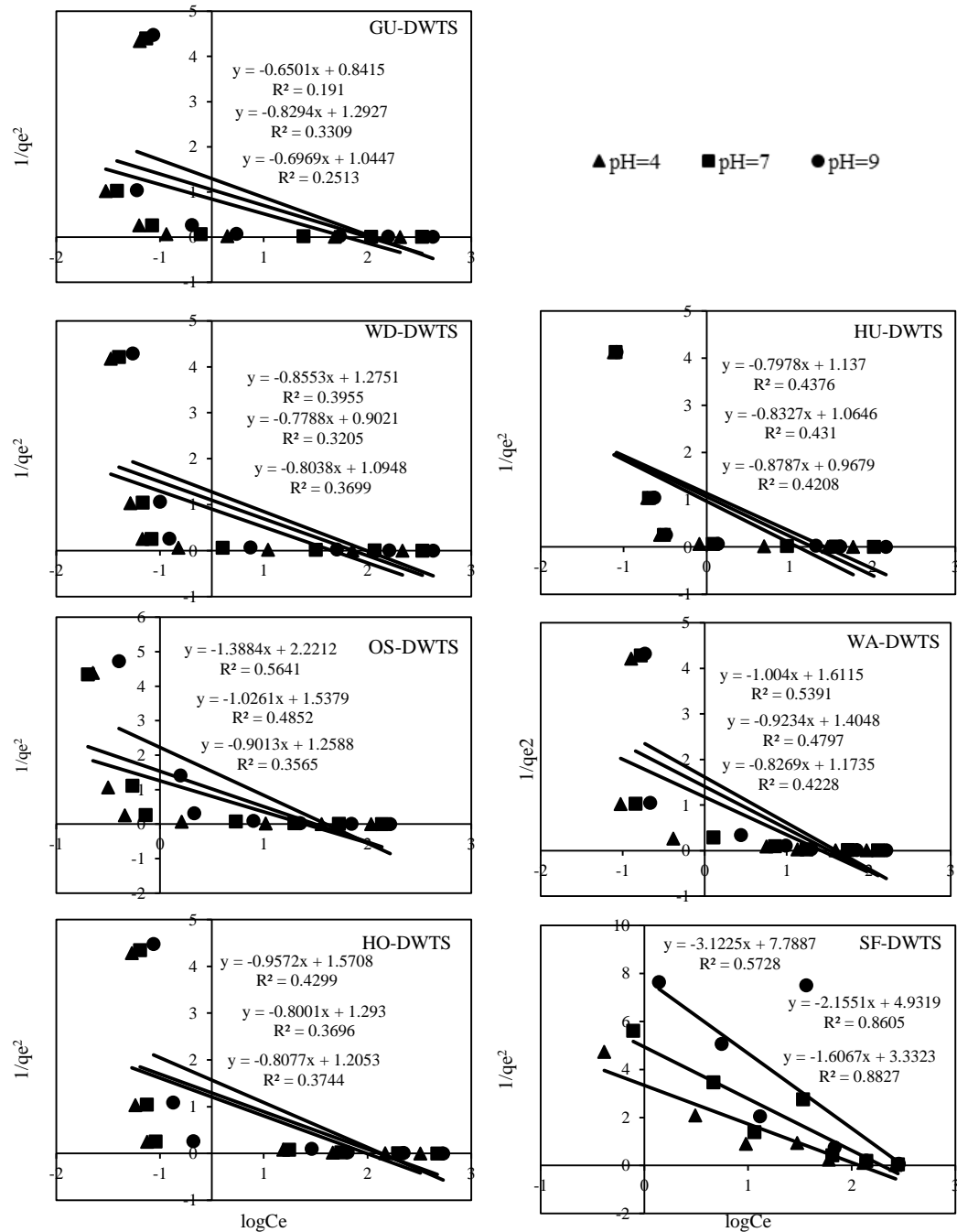


Figure A.7 Fitting P adsorption data of alum-based sludges at three different pH values to the linearized form of Harkins–Jura (H-J) model.

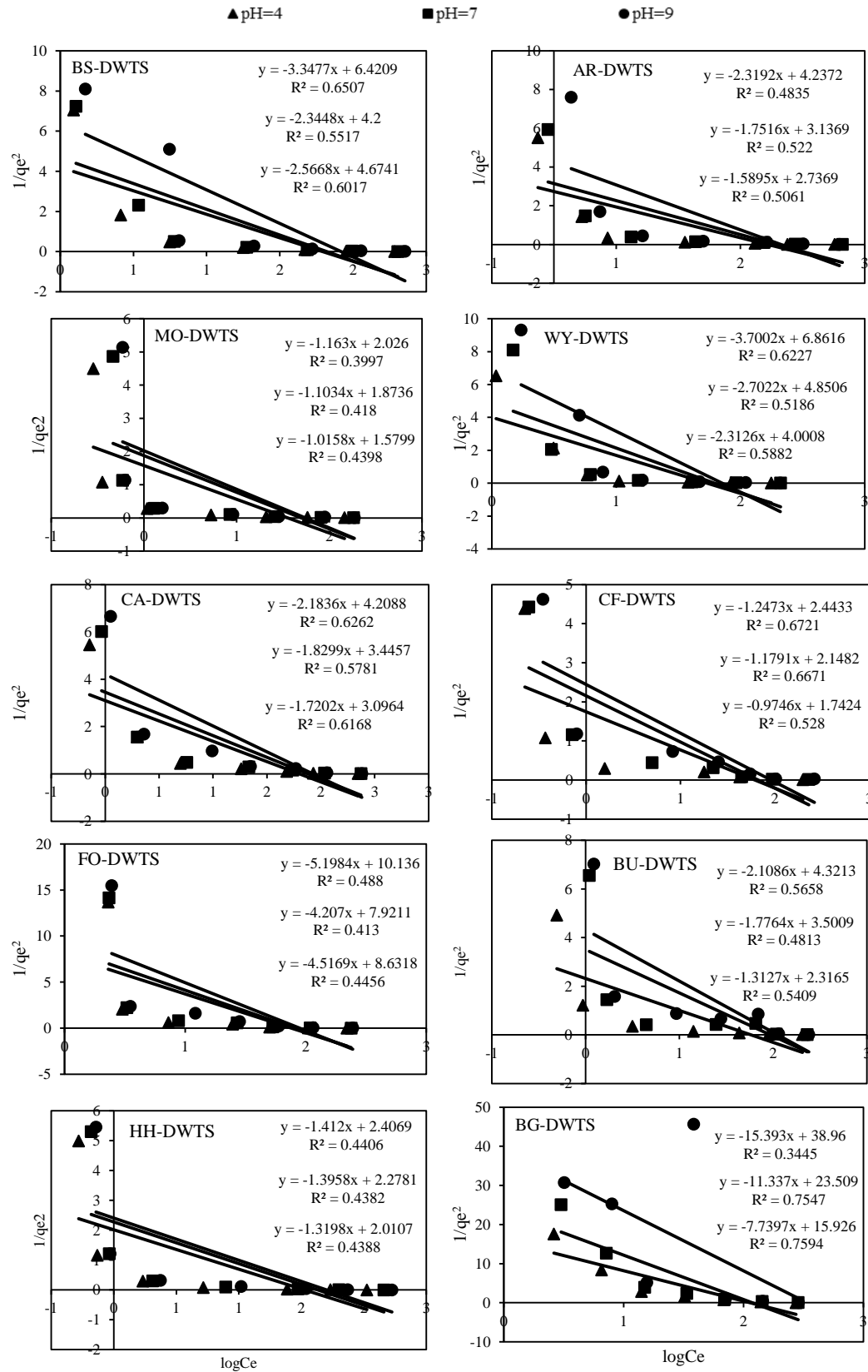


Figure A.8 Fitting P adsorption data of iron-based sludges at three different pH values to the linearized form of Harkins–Jura (H-J) model.

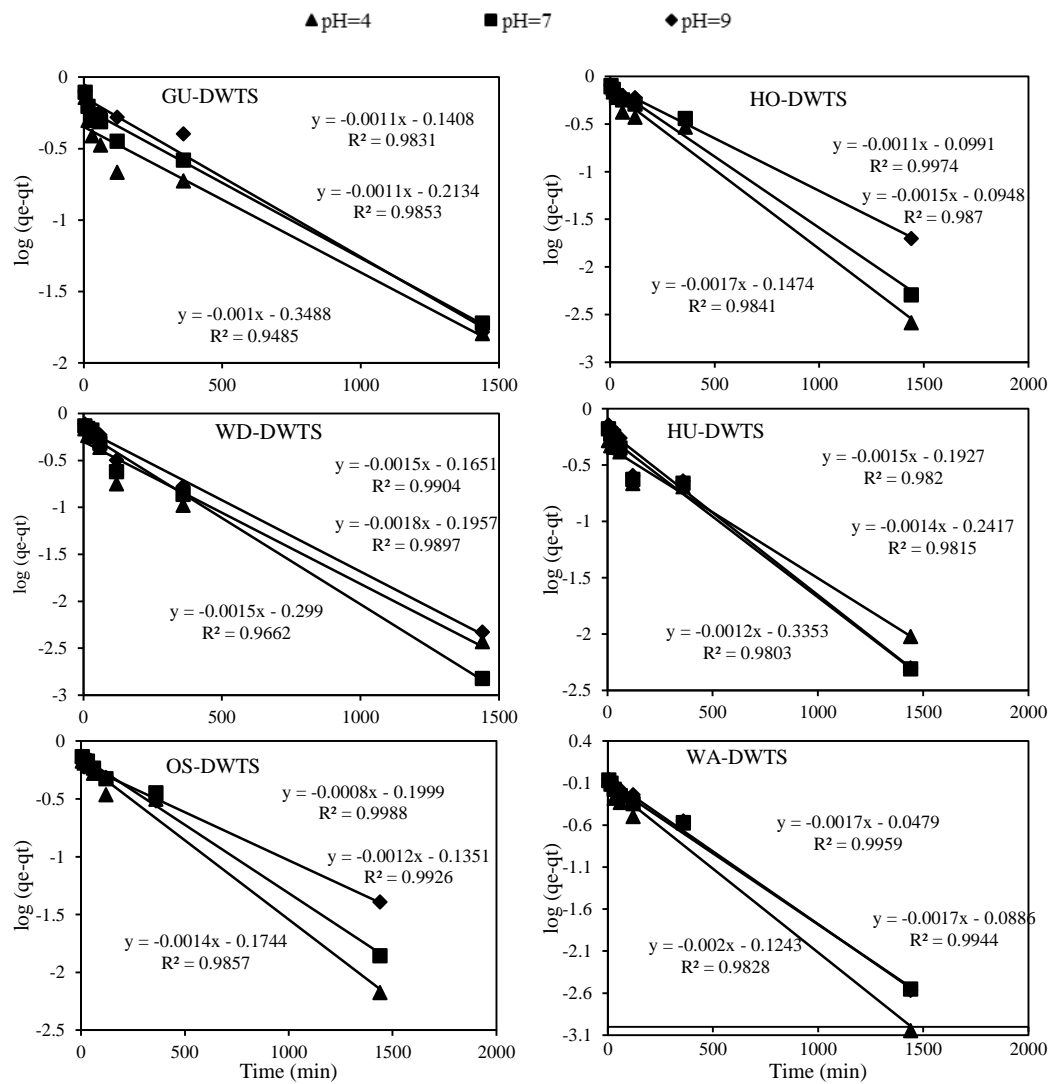


Figure A.9 Fitting P adsorption kinetic data of alum-based sludges at three different pH values and 10 mg/l initial P concentration to the linearized form of Pseudo-first order kinetic model.

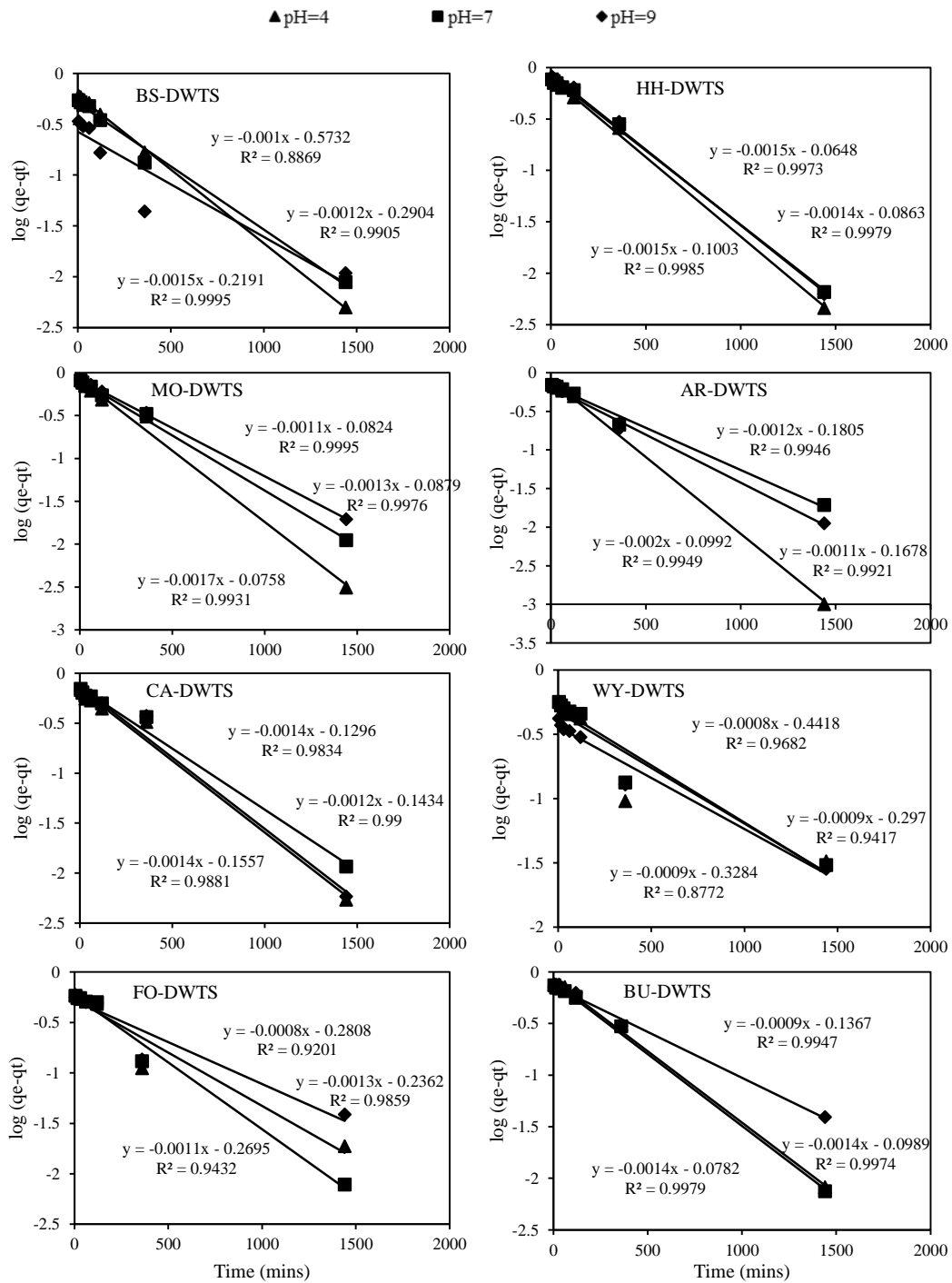


Figure A.10 Fitting P adsorption kinetic data of iron-based sludges at three different pH values and 10 mg/l initial P concentration to the linearized form of Pseudo-first order kinetic model.

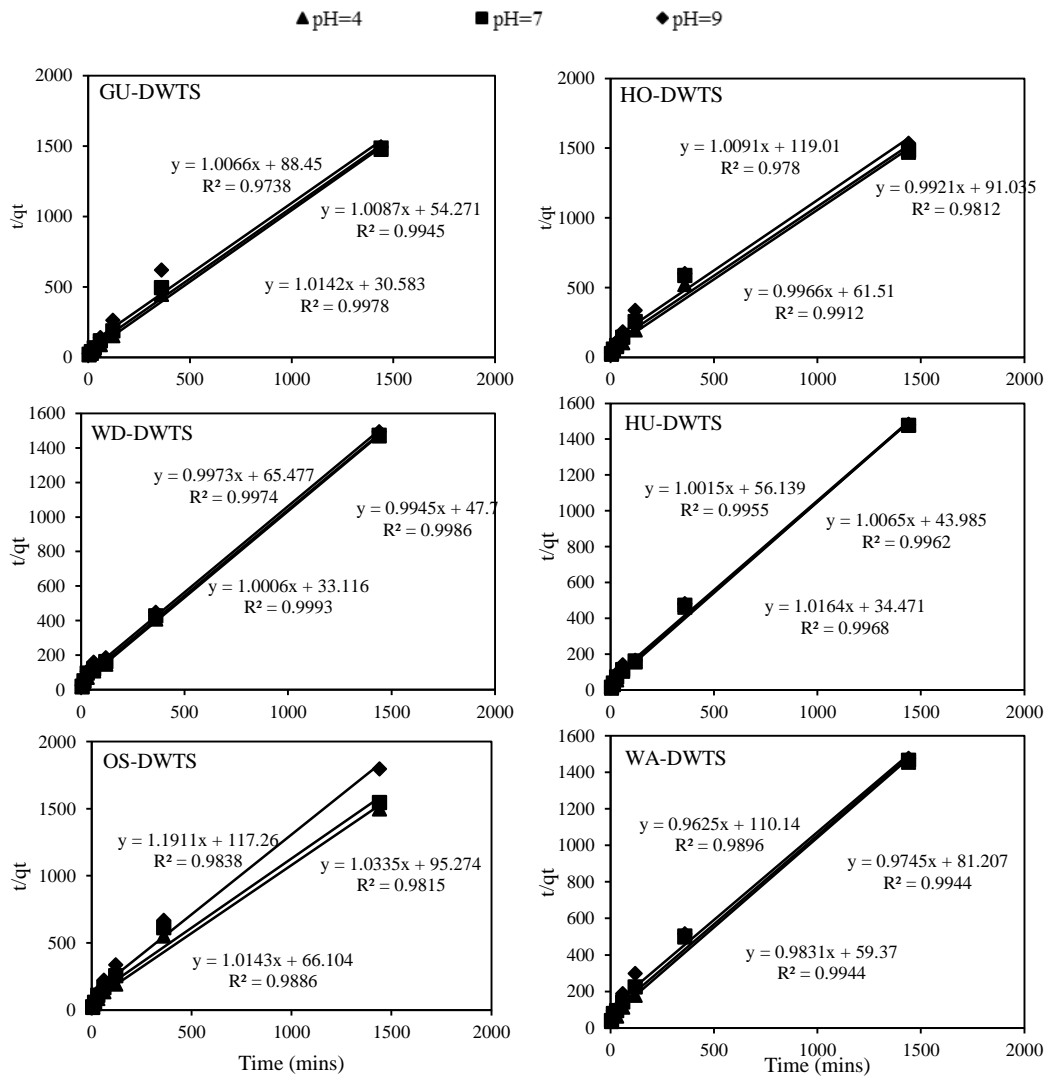


Figure A.11 Fitting P adsorption kinetic data of alum-based sludges at three different pH values and 10 mg/l initial P concentration to the linearized form of Pseudo-second order kinetic model.

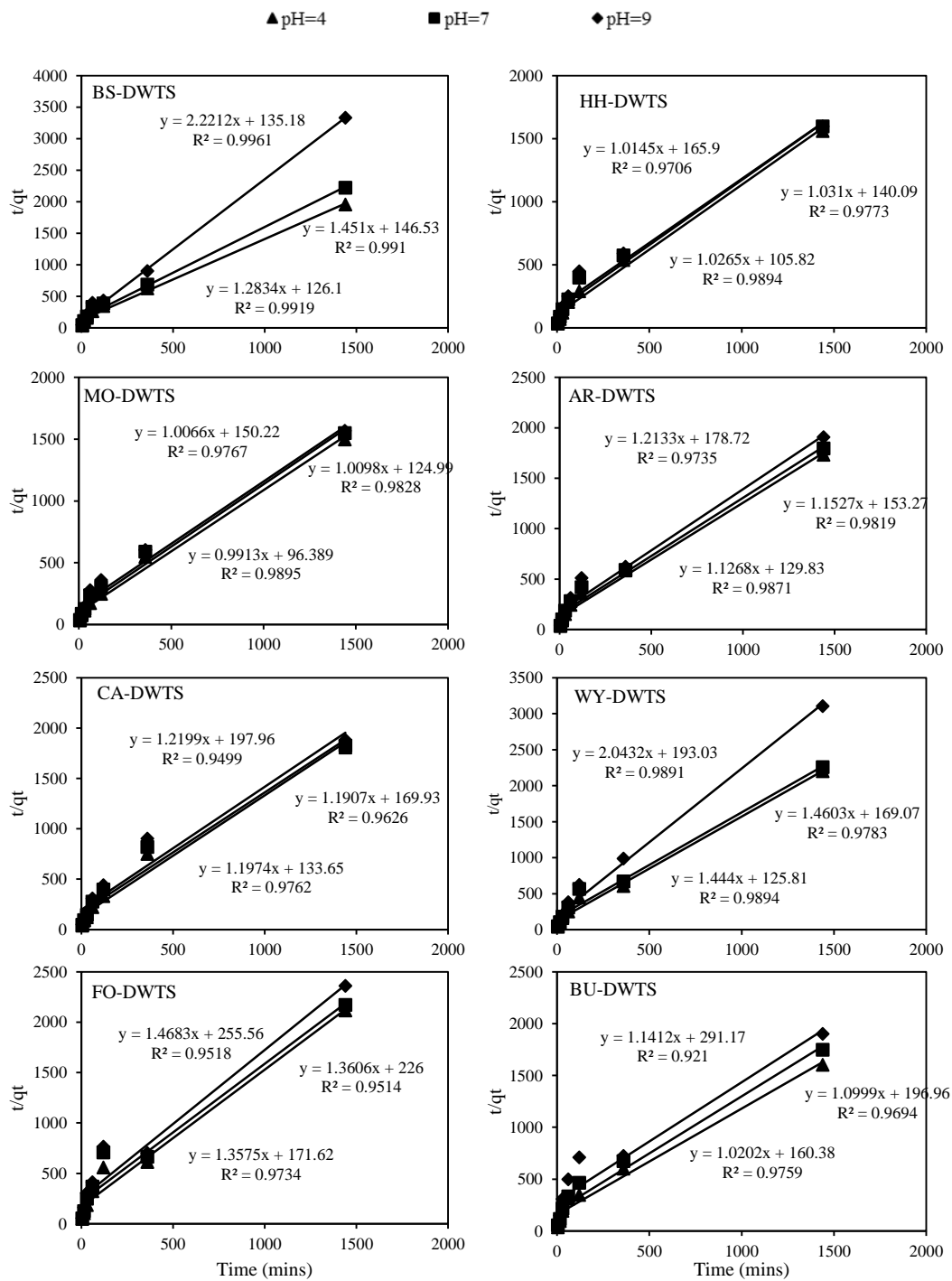


Figure A.12 Fitting P adsorption kinetic data of iron-based sludges at three different pH values and 10 mg/l initial P concentration to the linearized form of Pseudo-second order kinetic model.

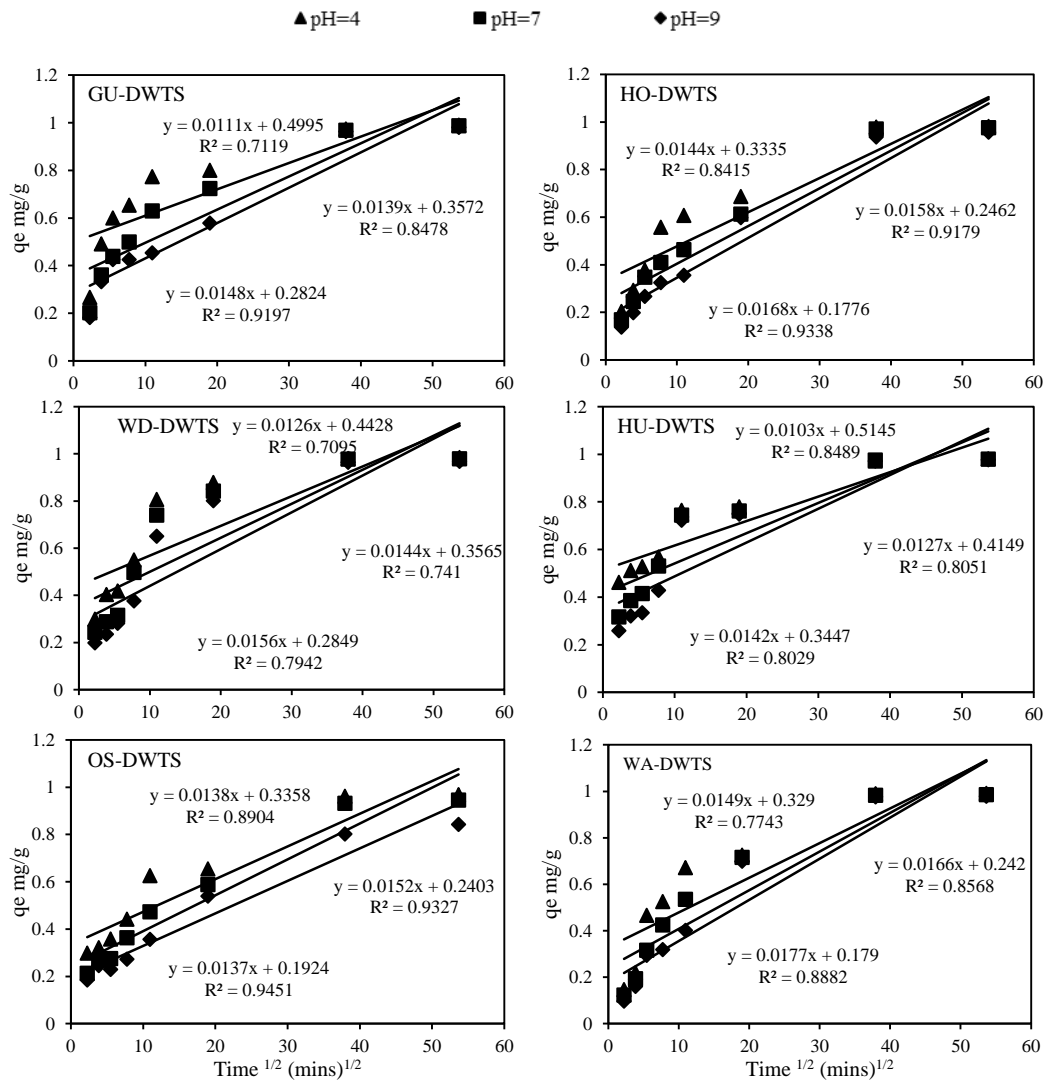


Figure A.13 Fitting *P* adsorption kinetic data of alum-based sludges at three different pH values and 10 mg/l initial *P* concentration to the intraparticle diffusion model model.

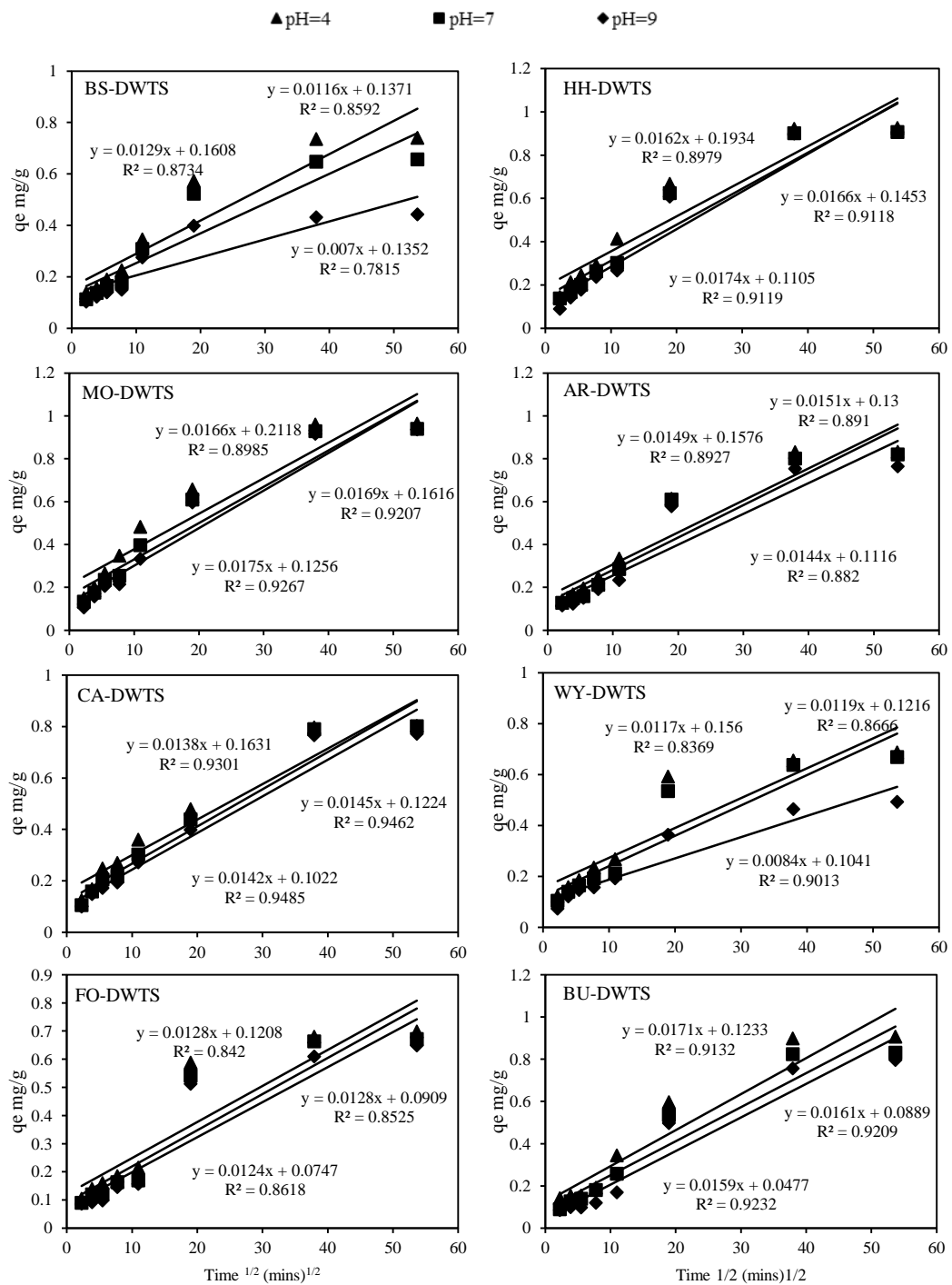


Figure A.14 Fitting P adsorption kinetic data of iron-based sludges at three different pH values and 10 mg/l initial P concentration to the intraparticle diffusion model.

Appendix B –Support data for Chapter 5

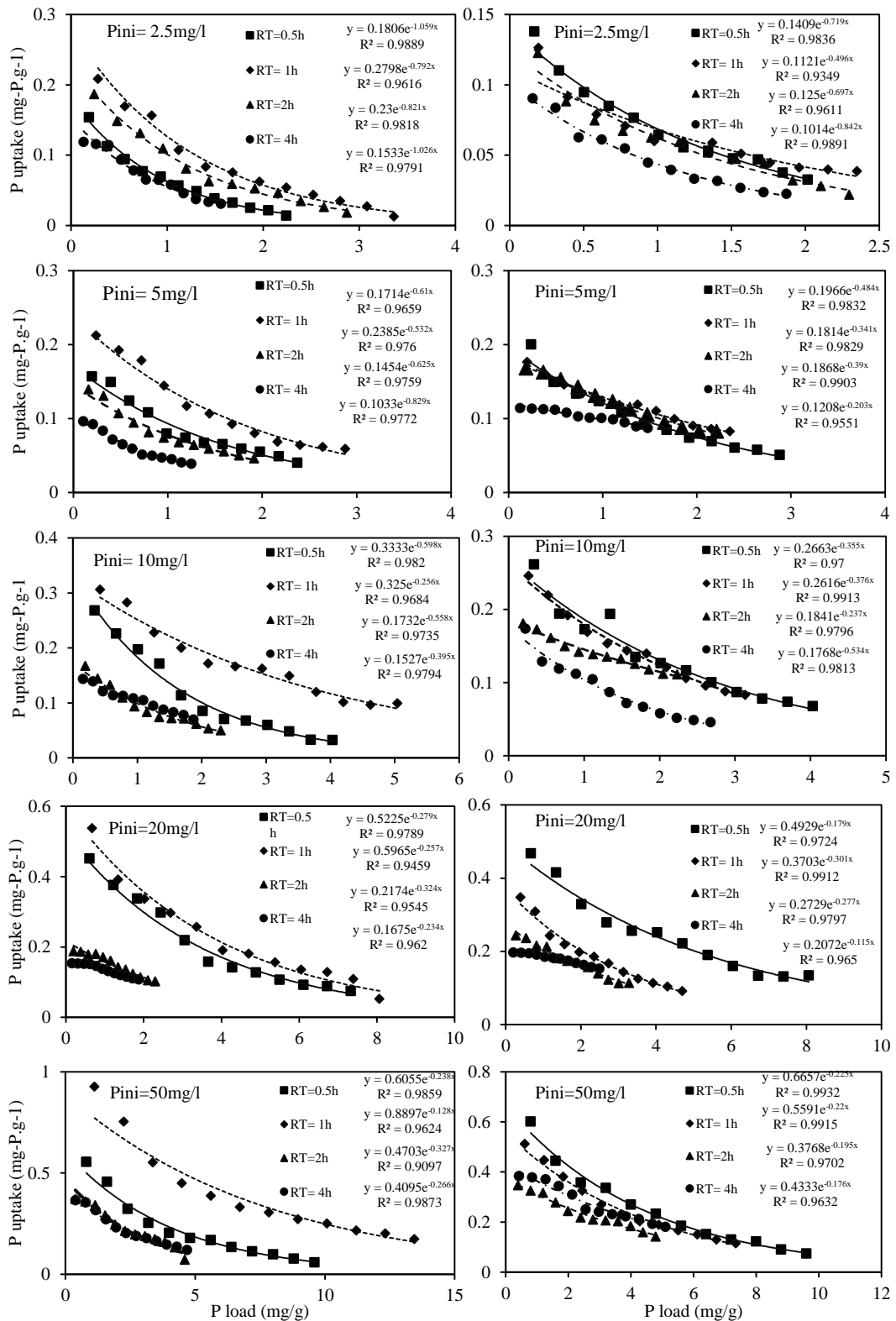


Figure B.1 The exponential relationship between P uptake and amount of P loaded to Fe-sludges (FO-DWTS left side figures, MO-DWTS right side figures). Data obtained from continuous feeding system.

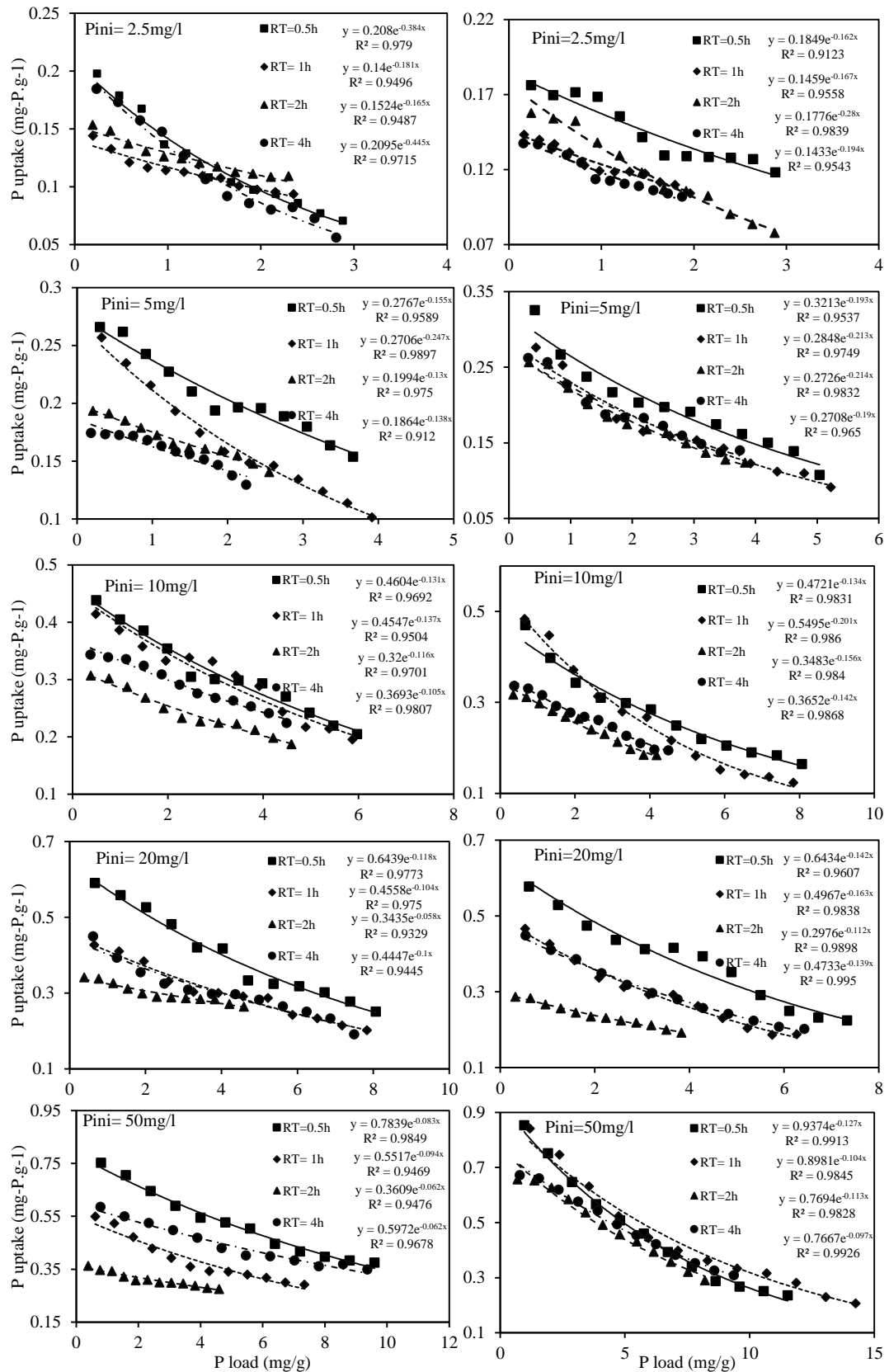


Figure B.2 The exponential relationship between P uptake and amount of P loaded to Al-sludges (GU-DWTS left side figures, WD-DWTS right side figures). Data obtained from continuous feeding system.

Appendices

Table B.1 Masses of acid-washed sand and sludge for two iron (FO and MO) - and aluminium (GU and WD) based sludges at different operation conditions of hydraulic retention time and influent P concentration.

		FO				MO			
		HRT (h)				HRT (h)			
		0.5	1	2	4	0.5	1	2	4
		Weight (g) (sand(sludge))							
P inlet (mg/l)	2.5	41.212(0.9)	41.512(0.6)	41.862(0.25)	41.932(0.18)	41.512(0.8)	41.512(0.6)	41.912(0.2)	41.962(0.15)
	5	40.412(1.7)	40.712(1.4)	41.512(0.6)	41.662(0.45)	40.712(1.4)	41.112(1.0)	41.612(0.5)	41.732(0.38)
	10	40.112(2)	40.512(1.6)	41.112(1)	41.512(0.6)	40.112(2)	40.612(1.5)	41.112(1)	41.692(0.42)
	20	39.912(2.2)	40.112(2)	40.112(2)	40.462(1.2)	40.112(2)	40.112(2)	40.712(1.4)	41.212(0.9)
	50	37.912(4.2)	39.112(3)	39.612(2.5)	40.462(1.2)	37.912(4.2)	38.912(3.2)	39.712(2.4)	41.012(1.1)
		GU				WD			
P inlet (mg/l)	2.5	41.412(0.7)	41.512(0.5)	41.862(0.25)	42.012(0.1)	41.412(0.7)	41.812(0.6)	41.912(0.2)	41.962(0.15)
	5	41.112(1)	41.812(0.6)	41.662(0.45)	41.862(0.25)	41.512(0.8)	41.662(0.45)	41.812(0.3)	41.962(0.15)
	10	40.762(1.35)	41.512(0.8)	41.612(0.5)	41.862(0.25)	41.112(1)	41.512(0.6)	41.612(0.5)	41.862(0.25)
	20	40.112(2)	40.462(1.2)	41.112(1)	41.812(0.3)	39.912(2.2)	40.612(1.5)	40.912(1.2)	41.762(0.35)
	50	37.912(4.2)	38.912 (3.2)	39.612(2.5)	41.812(0.6)	38.912(3.2)	40.462(1.65)	40.712(1.4)	41.512(0.6)

Appendix C – Supporting data for Chapter 6

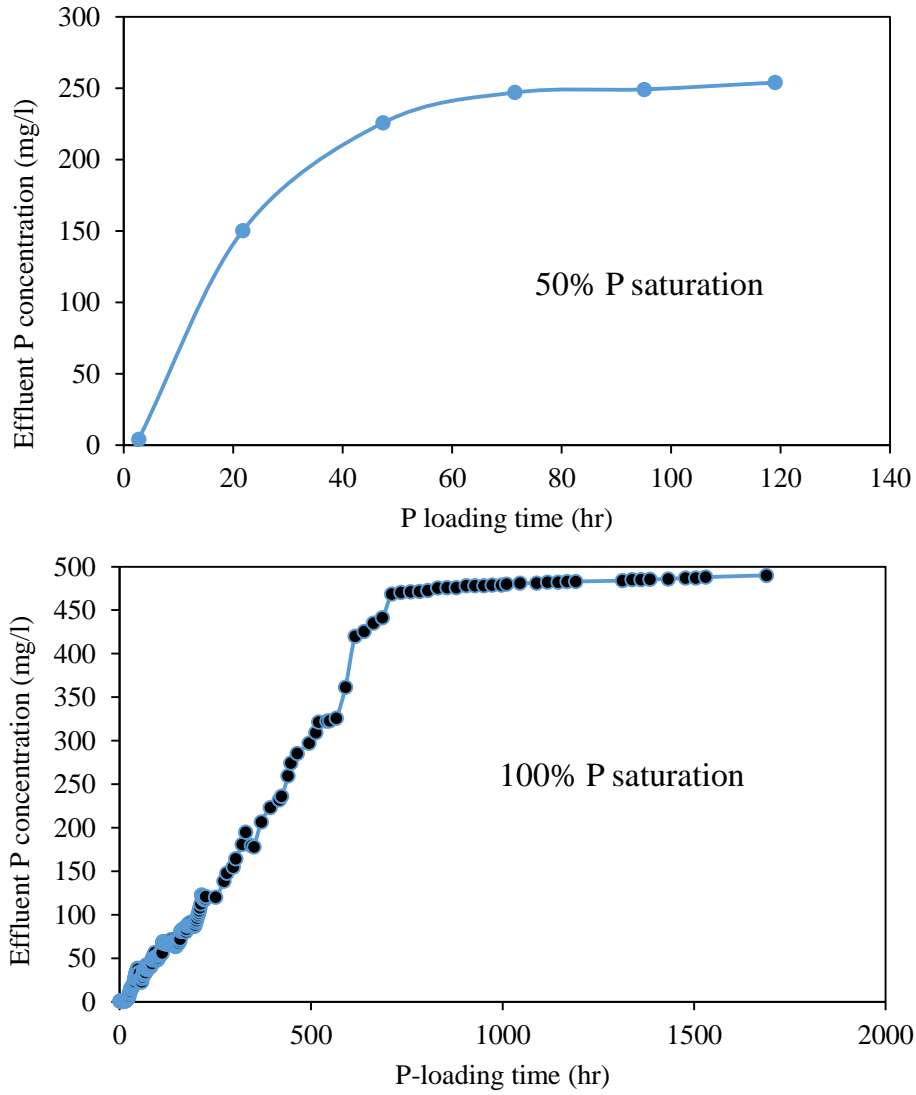


Figure C.1 Breakthrough curves showing the P saturation degrees of 50% and 100% of Fe-based sludge.

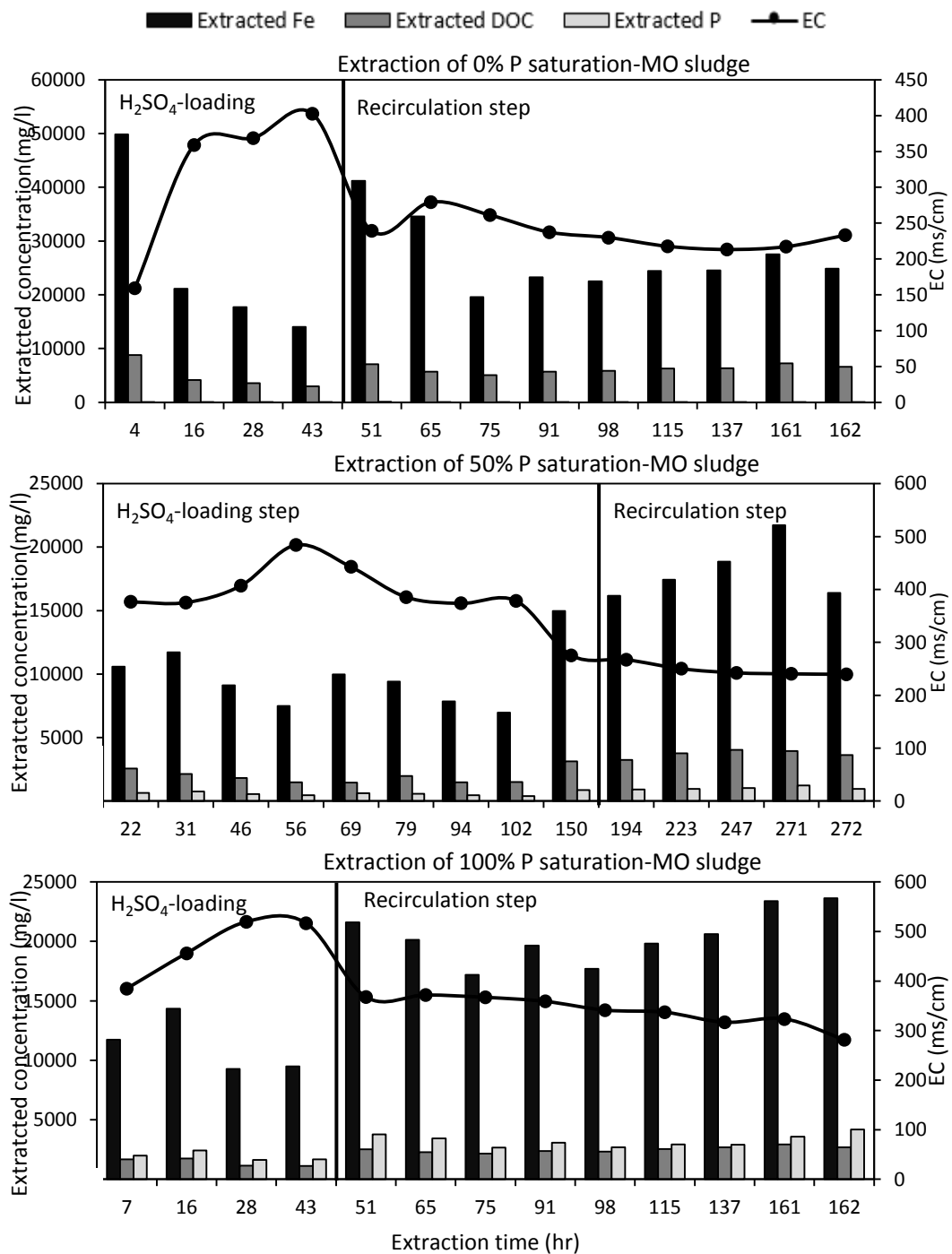


Figure C.2 The extractability of Fe and P and leachability of DOC from the iron-based sludge of three levels of P saturation (0%, 50%, 100%) at two steps of the extraction process.

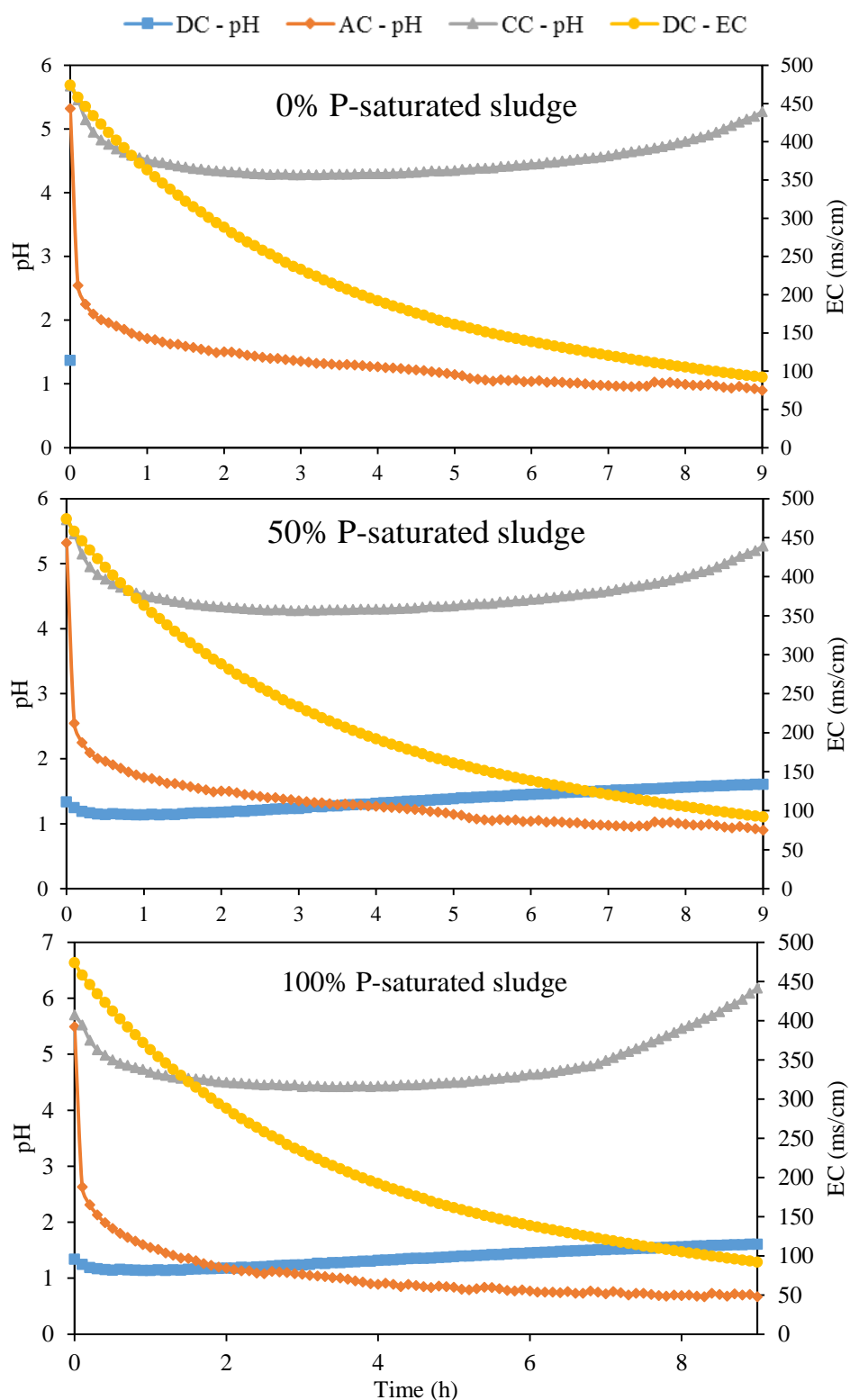


Figure C.3 Profile of pH and electrical conductivity in dilution compartment (DC), anodic compartment (AC), and cathodic compartment (CC) using high concentration (HC) of acid-solubilized sludge 0%, 50%, and 100% P-saturation degrees in 3ED. Please note that pH readings in DC in case 0% P-saturation are lost. (n=3)

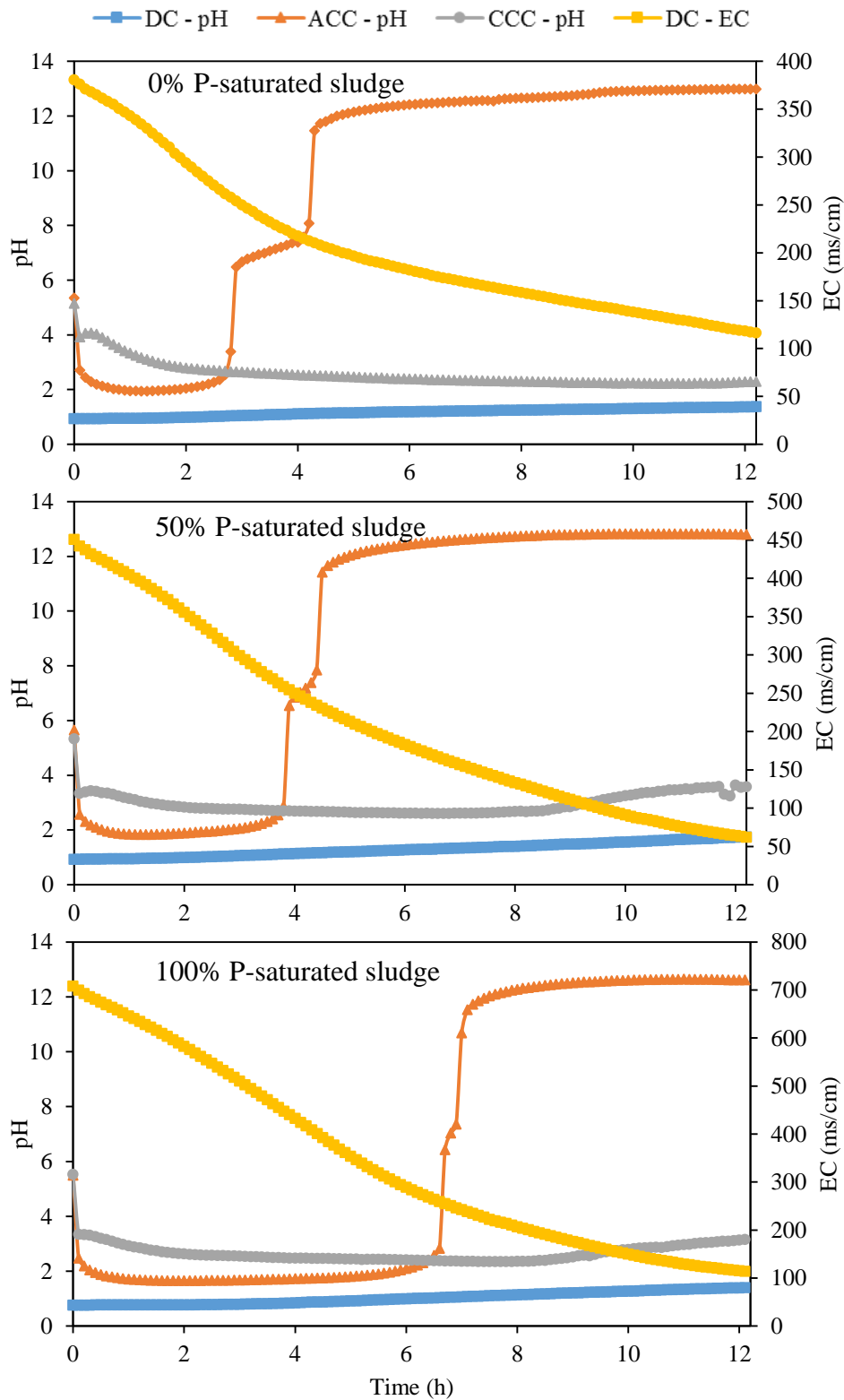


Figure C.4 Profile of pH and electrical conductivity in dilution compartment (DC), anodic concentrated compartment (ACC), and cathodic concentrated compartment (CCC) using high concentration (HC) of acid-solubilized sludge 0%, 50%, and 100% P-saturation degrees in 5ED. (n=3)

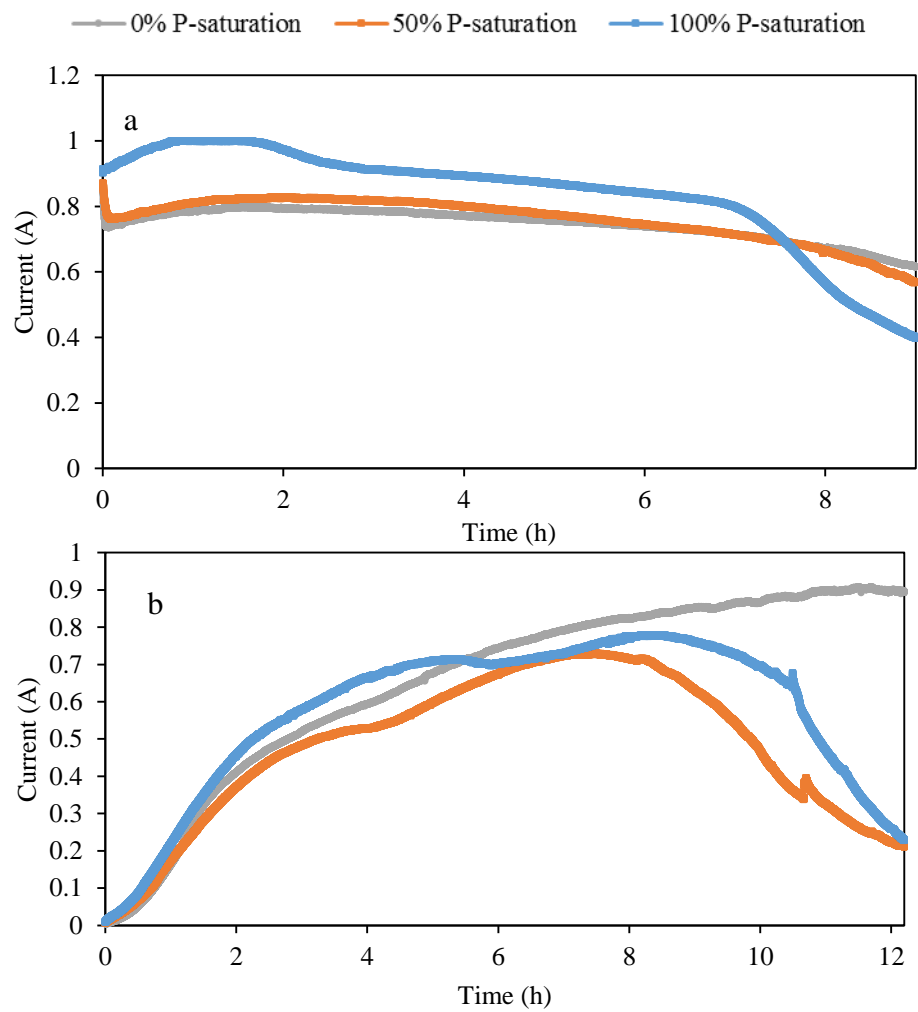
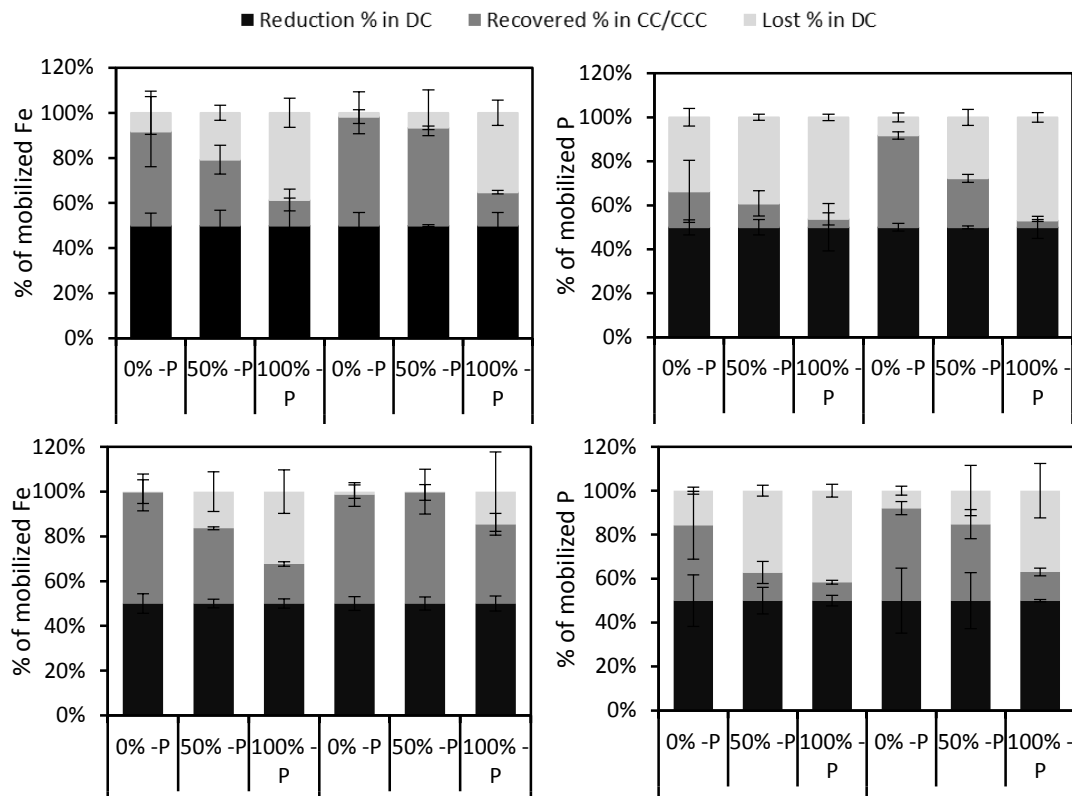


Figure C.5 Current profile of 3ED mode 1 (a) and 5ED mode 2 (b) using high concentration of acid-solubilized of 0%, 50%, and 100% P-saturated sludge. (n=3).



Solubilized sludge details and electro-dialysis mode

Figure C.6 Mass balance of the reduction percentages of Fe and P in DC, and the lost and recovered percentages in DC and CC/CCC respectively.